ISSN 2220-3249 (online)

World Journal of *Virology*

World J Virol 2017 February 12; 6(1): 1-25

Published by Baishideng Publishing Group Inc

WJV World Journal of Virology

A peer-reviewed, online, open-access journal of virology

Editorial Board

2016-2019

The *World Journal of Virology* Editorial Board consists of 370 members, representing a team of worldwide experts in virology. They are from 59 countries, including Argentina (4), Australia (8), Austria (4), Barbados (1), Belgium (1), Brazil (7), Bulgaria (1), Cameroon (1), Canada (12), Chile (2), China (55), Croatia (2), Cuba (1), Czech Republic (1), Denmark (1), Egypt (3), Ethiopia (1), Finland (5), France (10), Gambia(1), Germany (11), Ghana (1), Greece (2), Hungary (1), India (13), Indonesia (1), Iran (2), Ireland (3), Israel (4), Italy (23), Japan (16), Kazakhstan (1), Kenya (1), Kosovo (1), Mexico (2), Netherlands (5), New Zealand (1), Nigeria (1), Pakistan (1), Palestine (1), Poland (1), Portugal (1), Romania (1), Russia (2), Saudi Arabia (1), Singapore (2), Slovakia (2), Slovenia (2), South Africa (2), South Korea (6), Spain (19), Sweden (4), Thailand (8), Tunisia (1), Turkey (4), United Arab Emirates (1), United Kingdom (8), United States (92), and Uruguay (1).

Eiichi N Kodama, *Sendai*
Emoto Masashi, *Gunma*
Hiromitsu Moriyama, *Tokyo*
Kenji Okuda, *Yokohama*
Nobuhiro Suzuki, *Okayama*
Takashi Suzuki, *Shizuoka*
Tetsuro Suzuki, *Hamamatsu*
Yoshiyuki Suzuki, *Nagoya-shi*
Akifumi Takaori-Kondo, *Kyoto*
Tetsuya Toyoda, *Toyohashi*

Kazakhstan

Vladimir E Berezin, *Almaty*

Kenya

George G Maina, *Nairobi*

Kosovo

Lul Raka, *Prishtina*

Mexico

Juan E Ludert, *Mexico City*
Julio Reyes-Leyva, *Mexico*

Netherlands

Kimberley SM Benschop, *Amsterdam*
Benjamin Berkhout, *Amsterdam*
Byron EE Martina, *Rotterdam*
Willem JG Melchers, *Nijmegen*
Monique Nijhuis, *Utrecht*

New Zealand

Olga S Garkavenko, *Auckland*

Nigeria

Olajide A Owolodun, *Plateau State*

Pakistan

Muhammad I Qadir, *Faisalabad*

Palestine

Ahmad Y Amro, *Jerusalem*

Poland

Brygida Knysz, *Wroclaw*

Portugal

Celso Cunha, *Lisbon*

Romania

Anda Baicus, *Bucharest*

Russia

Anton Buzdin, *Moscow*
Elena V Gavrilova, *Novosibirsk*

Saudi Arabia

Ahmed S Abdel-Moneim, *Al-Taif*

Singapore

Sophie Bellanger, *Singapore*
Ding X Liu, *Singapore*

Slovakia

Gabriela Bukovska, *Bratislava*
Julius Rajcani, *Bratislava*

Slovenia

Uros Krapez, *Ljubljana*
Andrej Steyer, *Ljubljana*

South Africa

Janusz T Paweska, *Sandringham*
Dirk Stephan, *Matieland*

South Korea

Sang Hoon Ahn, *Seoul*
Tae-Jin Choi, *Busan*
Young-Ki Choi, *Cheongju*
Kee-Jong Hong, *Cheongwon*
Bum-Joon Kim, *Seoul*
Junsoo Park, *Wonju*

Spain

Alí Alejo, *Valdeolmos*
Alfredo Berzal-Herranz, *Granada*
Rafael Blasco, *Madrid*
Julio Collazos, *Usánsolo-Galdácano*
Juan M Hernández, *Madrid*
Gómez L Jaime, *Córdoba*
Josep M Llibre, *Badalona*
Cecilio López-Galíndez, *Madrid*
F. Xavier López-Labrador, *Valencia*
JoséA Melero, *Madrid*
Luis Menéndez-Arias, *Madrid*
Andrés Moya, *València*
David R Pereda, *Sevilla*
Pilar Perez-Romero, *Sevilla*
Josep Quer, *Barcelona*
Daniel López Rodríguez, *Majadahonda*
Juan-Carlos Saiz, *Madrid*
Noemi Sevilla, *Madrid*
Natalia Soriano-Sarabia, *Madrid*

Sweden

Goran PL Bucht, *Umea*
Ali Mirazimi, *Solna*
Muhammad Munir, *Uppdala*
Bo F Oberg, *Huddinge*

Thailand

Prasert Auewarakul, *Bangkok*
Parin Chaivisuthangkura, *Bangkok*
Wasin Charerntantanakul, *Chiang Mai*
Wansika Kiatpathomchai, *Bangkok*
Sasisopin Kiertiburanakul, *Bangkok*
Winyou Mitarnun, *Chiang Mai*
Yong Poovorawan, *Bangkok*
Viroj Wiwanitkit, *Bangkok*

Tunisia

Olfa Bahri, *Tunis*

Turkey

Omer Coskun, *Ankara*
Iftihar Koksal, *Trabzon*
Aykut Ozdarendeli, *Kayseri*
Ayca A Sayiner, *Izmir*

United Arab Emirates

Tahir A Rizvi, *Al Ain*

United Kingdom

Shiu-Wan Chan, *Manchester*
Simon R Clegg, *Preston*
Chiriva I Maurizio, *Nottingham*
Iain M Morgan, *Glasgow*
Mark R Nelson, *London*
Adrian W Philbey, *Glasgow*
James P Stewart, *Liverpool*
Gavin WG Wilkinson, *Cardiff*

United States

Nafees Ahmad, *Tucson*
Ashok Aiyar, *Los Angeles*
Hizi Amnon, *Bethesda*
Judith M Ball, *Texas*
Igor M Belyakov, *Frederick*
Bradford K Berges, *Provo*
Preeti Bharaj, *Orlando*
Jay C Brown, *Charlottesville*
Victor E Buckwold, *Walkersville*
Alexander A Bukreyev, *Galveston*
Joseph J Carter, *Seattle*
Maria G Castro, *Los Angeles*
Yan-Ping Chen, *Beltsville*

WJV World Journal of Virology

Contents

Quarterly Volume 6 Number 1 February 12, 2017

World Journal of Virology
Volume 6 Number 1 February 12, 2017

Contents

NAME OF JOURNAL
World Journal of Virology

ISSN
ISSN 2220-3249 (online)

LAUNCH DATE
February 12, 2012

FREQUENCY
Quarterly

EDITOR-IN-CHIEF
Ling Lu, MD, PhD, Department of Pathology and Laboratory Medicine, University of Kansas Medical Center, Kansas City, 3901 Rainbow Blvd, WHE 3020, KS 66160, United States

EDITORIAL BOARD MEMBERS
All editorial board members resources online at http://www.wjgnet.com/2220-3249/editorialboard.htm

EDITORIAL OFFICE
Xiu-Xia Song, Director
World Journal of Virology
Baishideng Publishing Group Inc
8226 Regency Drive, Pleasanton, CA 94588, USA
Telephone: +1-925-2238242
Fax: +1-925-2238243
E-mail: editorialoffice@wjgnet.com
Help Desk: http://www.wjgnet.com/esps/helpdesk.aspx
http://www.wjgnet.com

PUBLISHER
Baishideng Publishing Group Inc
8226 Regency Drive,
Pleasanton, CA 94588, USA
Telephone: +1-925-223-8242
Fax: +1-925-223-8243
E-mail: bpgoffice@wjgnet.com
Help Desk: http://www.wjgnet.com/esps/helpdesk.aspx
http://www.wjgnet.com

PUBLICATION DATE
February 12, 2017

INSTRUCTIONS TO AUTHORS
http://www.wjgnet.com/bpg/gerinfo/204

ONLINE SUBMISSION
http://www.wjgnet.com/esps/

World Journal of Virology

Submit a Manuscript: http://www.wjgnet.com/esps/
Help Desk: http://www.wjgnet.com/esps/helpdesk.aspx
DOI: 10.5501/wjv.v6.i1.1

World J Virol 2017 February 12; 6(1): 1-8
ISSN 2220-3249 (online)

MINIREVIEWS

Biological and historical overview of Zika virus

Najealicka Armstrong, Wangheng Hou, Qiyi Tang

Najealicka Armstrong, Wangheng Hou, Qiyi Tang, Deparment of Microbiology, Howard University, College of Medicine, Washington, DC 20059, United States

Author contributions: Armstrong N and Hou W searched most of the references and participated in drafting the manuscript; Armstrong N organized the tables; Tang Q designed the study and drafted the manuscript; all authors read and approved the final manuscript.

Supported by a Charles and Mary Latham Fund (Q.T.), No. NIH/NIAID SC1AI112785 (Q.T.); and National Institute on Minority Health and Health Disparities of the National Institutes of Health, No. G12MD007597.

Conflict-of-interest statement: The authors declare that they have no conflict of interest.

Manuscript source: Unsolicited manuscript

Correspondence to: Qiyi Tang, PhD, Associate Professor, Department of Microbiology, Howard University, College of Medicine, Seeley Mudd Building, Room 315, 520 W Street, NW, Washington, DC 20059, United States. qiyi.tang@howard.edu
Telephone: +1-202-8063915
Fax: +1-202-2388518

Received: May 10, 2016
Peer-review started: May 12, 2016
First decision: June 14, 2016
Revised: June 20, 2016
Accepted: August 11, 2016
Article in press: August 15, 2016
Published online: February 12, 2017

Abstract

The recent outbreak of the Zika virus attracts worldwide attention probably because the most recently affected country (Brazil) will host the 2016 Olympic Game. Zika virus infected cases are now spreading to many other countries and its infection might be linked to some severe medical sequelae. Since its first isolation from the infected monkey in 1947 in Uganda, only a few studies had been taken until recent outbreak. According to the history of referenced publications, there is a 19-year gap from 1989 to 2007. This might be because only mild diseases were diagnosed from Zika virus infected populations. Obviously, the recent reports that Zika virus infection is probably associated with microcephaly of the neonates makes us reevaluate the medical significance of the viral pathogen. It can be transmitted sexually or by mosquito biting. Sexual transmission of the Zika virus distinguishes it from other members of the Genus Flavivirus. Detailed information of the Zika virus is needed through a thorough investigation covering basic, epidemical, subclinical and clinical studies. Here, we reviewed the published information of Zika virus.

Key words: Zika virus; Flavivirus; Congenital infection; Outbreak; Microcephaly

Core tip: Zika virus is gaining new ground with the recent outbreaks that are starting to expand worldwide. While normally transmitted by the mosquito, other routes of transmission are being discovered. Also, other medical complications are being detected with Zika virus infections. These recent findings require the scientific community to thoroughly examine Zika virus to better understand it so that better diagnostic options, treatment, and preventative measures can be developed. In order to beat Zika virus, we must understand its history and outbreak patterns as well as gain a full understanding of

all clinical manifestations associated with this virus.

Armstrong N, Hou W, Tang Q. Biological and historical overview of Zika virus. *World J Virol* 2017; 6(1): 1-8 Available from: URL: http://www.wjgnet.com/2220-3249/full/v6/i1/1.htm DOI: http://dx.doi.org/10.5501/wjv.v6.i1.1

INTRODUCTION

The Zika virus, together with the West Nile virus, Yellow fever virus, Japanese encephalitis virus, Dengue fever virus, and many other classified and unclassified viruses, forms the genus *Flavivirus* that belongs to family Flaviviridae. The family Flaviviridae consists of many other viruses that are summarized in a 2010 review[1]. This family of viruses have enveloped icosahedral capsid that contains a single strand RNA genome (about 11000 nucleotides) with positive sense[2]. Therefore, the infected viral RNA can be directly translated to a large polyprotein precursor, which is co- and post-translationally processed by viral and cellular proteases into structural and non-structural proteins. The three structural proteins are critical for the formation of envelop and capsid, and the seven non-structural (NS) proteins play important roles in virus replication. The three structural proteins are envelope, E; membrane precursor, PrM; and capsid, C. The seven NS proteins include NS1, NS2a, NS2b, NS3, NS4a, NS4b, and NS5 (Figure 1). The names, location in the infected cells, and functions of viral proteins are listed in Table 1. The members of the genus *Flavivirus* are characterized by similarities in genomic structure, viral protein function, pathogenesis and transmission.

The large polyprotein precursor must be cleaved to generate actively functional proteins. The cleavage of the polyprotein precursor is a sophisticated process and is completed collaboratively by cellular proteases of the PACE (Paired basic Amino acid Cleaving Enzyme)-type or other Golgi-localized proteases and the viral serine protease embedded in the N-terminal domain of non-structural protein 3 (NS3Pro), which requires NS2b for its activity[1]. A distinct feature of genus *Flavivirus* from other genera of Flaviviridae is that the 5′-end of the (+)ssRNA genome of genus *Flavivirus* is decorated with an RNA cap structure (N7meGpppA2′Ome-RNA). 5′end capping of the viral RNA is as important as that for eukaryotic mRNAs, not only to initiate the process of translation but also to protect the viral RNA from degradation by endogenous RNA exonucleases. The protein translation happens immediately after the uncoating of viral particle in the cytoplasm. The (+)ssRNA genome is used as a template not only for gene expression but also for viral genome replication. Both viral RNA replication and gene translation occur in the cytoplasm. For RNA replication, viral NS proteins and cellular proteins interact to form a replication compartment (RC). During the period of viral RNA replication in the cytoplasm, the RC consists of morphologically distinct, membrane-bound compartments that also differ with respect to both function and NS proteins composition[3]. The NS3 and NS5 proteins are central to the viral RC, as together, they harbor most, if not all, of the catalytic activities required to both cap and replicate the viral RNA. Following replication, the protected genomic RNA is packaged by the C protein to form a capsid in a host-derived lipid bilayer in which the E protein is embedded and later integrated into viral envelope. The mature particles subsequently exit from the host cell by exocytosis.

REGIONAL ISOLATION OF ZIKA VIRUS

The Zika virus is phylogenetically close to *Spondweni* virus and a member of Flaviviridae family[4]. Comparative genomic analysis revealed that coding regions of pre-epidemic and epidemic strains of the Zika virus were similar with the exception of the NS2B. Bootscan analysis and multiple sequence alignment of the Asian lineage suggested that there may be genetic recombination of a fragment (nucleotides 4237-4528) of NS2B with that of the *Spondweni virus*[5].

African countries

In 1947, a group of scientists from United Kingdom led by Haddow *et al*[4] who were investigating yellow fever isolated Zika virus from a rhesus macaque with fever in the Zika Forest in Uganda[6,7]. The isolated viral strain has been stored in ATCC (ATCC® VR84™, MR 766) and the European Virus Archive (France) and is now still used for studies. The next important step was to find out whether the Zika virus is transmitted by mosquitos. First, Boorman *et al*[8] demonstrated that Zika virus can infect and replicate in mosquitos, providing experimental evidence that Zika virus may be transmitted by mosquitos. Later, the United Kingdom *Flavivirus* research group continued their studies of arboreal mosquitos as virus vectors in Uganda. They isolated 12 strains of Zika virus from *Aedes (Stegomyia) africanus* in the Zika forest[9]. Zika virus is apparently enzootic in Zika forest, and the evidence collected by Hoddow *et al*[9] suggested that *Aedes africanus* is the primary vector and that forest-dwelling monkeys and human are, on occasion, involved. It was not clear whether the mosquito transmitted the virus to other animals because no small mammal trapped in the forest showed serum antibody against the Zika virus. The Zika virus infection in humans was first reported in 1954[10]. It has also been experimentally demonstrated *via* volunteers that the Zika virus is able to infect humans[11]. In summary, results from these investigations suggest that the Zika virus is an arbovirus, transmitted by mosquitos and infects at least monkeys and humans.

Southern Asian countries

The first isolation of Zika virus in South-Eastern Asia was reported in 1969 in Malaysia[12]. Some years later, there was another report that the Zika virus was isolated from patients in Indonesia[13]. The event occurred

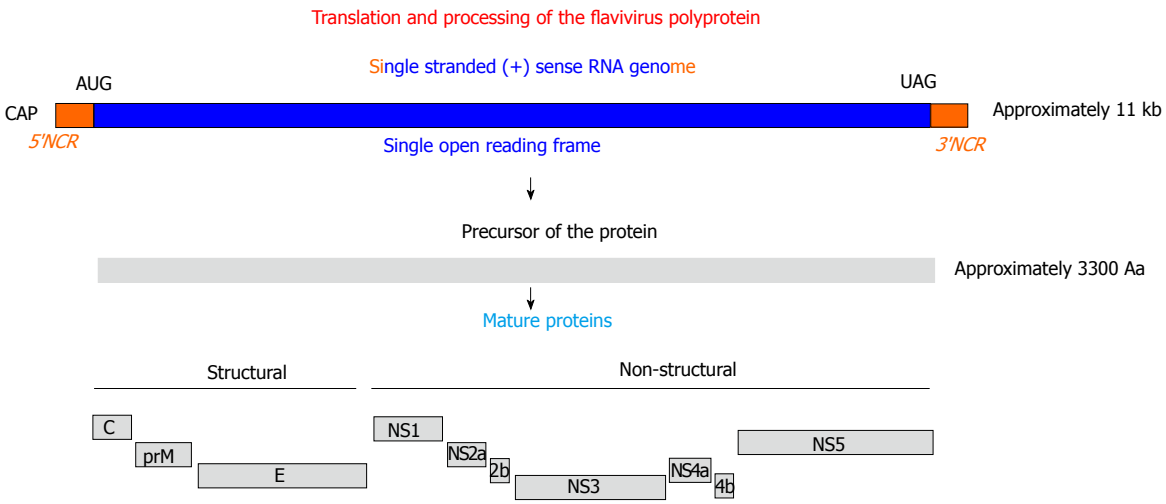

Figure 1 Genomic structure and gene production of Flavivirus. AUG: Translation start codon; UAG: Translation stop codon; NCR: Non coding RNA sequence; kb: Kilo base; Aa: Amino acid.

Table 1 Roles of viral protein and RNA during viral infection in permissive cells

Name of the vital material	Location in cell	Function
Viral genome + ssRNA (approximately 11000 nt)	Cytoplasm	Template for protein translation and for viral genome replication
Envelope, E (53 KDa)[52]	Cell membrane	Viral assembly, budding, attachment to target cells, and viral membrane fusion
Membrane precursor, PrM (20 KDa)[53]	Cell membrane	Facilitating E protein folding and trafficking, and virion maturation
Capsid, C (12 KDa)[54]	Cytoplasm	Virion maturation
NS1 (glycoprotein)[55] (46-55 kDa)	Endoplasmic reticulum vesicular compartments, cell surface	Subverting immune response virus-induced intracellular RNA replication, neurovirulence
NS2a (25 kDa)[56]	Transmembrane	Virus assembly, inhibit IFN-response
NS2b (14 kDa)[1,57]	Cytoplasm, nucleus	Viral protein cleavage
NS3 (69 kDa)[1]	Cytoplasm, nucleus	Viral protein cleavage, RNA triphosphatase, mRNA capping, RNA helicase
NS4a (16 kDa)[58]	Transmembrane	Viral RNA replication
NS4b (21.5 kDa)[59]	Integral membrane	Suppression of (IFN-α/β), suppression of the host RNAi, negatively regulate the helicase function, viral replication
NS5 (103 kDa)[60,61]	Cytoplasm, nucleus	The RNA triphosphatase, RNA-dependent RNA polymerase

during the end of the rainy season of 1977 when *Aedes aegypti* usually flourishes. Seven patients in central Java, Indonesia, appeared in the hospital with high fever, malaise, stomach ache, dizziness and anorexia. Data on these 7 Zika virus cases and several previously reported human infections indicated that clinical characteristics of infection with Zika virus appeared relatively mild, self-limiting, and nonlethal. It was suspected that the virus was transmitted by *Aedes aegypti*, which had been reported to be a probable vector in Malaysia[12]. A later investigation in Sabah, Malaysia, showed that the Zika virus infected 60 semi-captive and 84 free-ranging orangutans (Pongo pygmaeus pygmaeus)[14]. Another study conducted by the United States Naval Medical Research Unit No. 2 (NAMRU-2) isolated Zika virus in Cambodia in 2010[15]. This case was from a 3-year-old boy who had 4 d of fever, sore throat and cough as well a headache that lasted for 3 d. The studies conducted in southern Asia further confirmed that mosquitos are the vector and the primates might be the end host of viral infection.

The Zika virus has been also isolated from animals and human in other African countries. For examples, during the years 1964 to 1970, Moore *et al*[16] isolated 171 arboviruses of 15 different types from humans in Ibadan, Nigeria. Zika virus isolation rates also varied by season, with peaks in rainy seasons (June to August) and lows in dry seasons (January to February). Viruses were isolated from all age groups, with the majority from children one to four years old. The viruses isolated in largest numbers were chikungunya and yellow fever, which caused epidemics in 1969, and dengue types 1 and 2 and Tataguine, which are endemic in Ibadan. The Zika virus was isolated at a low rate. In 1999, three strains of the Zika virus were isolated as part of yellow fever studies in the Ivory Coast[17]. In 2010, it was

reported that the Zika virus was isolated at a high rate in Cameroon. The research group investigated 102 sera from febrile patients (with negative laboratory findings for malaria and typhoid fever) at clinics in the Fako Division of Cameroon. The Zika virus was isolated at a rate of 11.4%, higher than that of any other members of Genus *Flavivirus*[18]. Therefore, following the time, the Zika virus has been spread throughout Africa.

More and more Zika virus strains have been isolated from humans worldwide[17]. Studies conducted in Nigeria during 1971-1975 isolated the Zika virus from humans. Serological experiments showed that 40% of the persons tested had neutralizing antibody to the Zika virus[16,19]. The infected populations were detected in other African countries such as Uganda, Tanzania, Egypt, Central African Republic, Sierra Leone, and Gabon, and in parts of Asia, including India, Malaysia, the Philippines, Thailand, Vietnam, and Indonesia[20]. Table 2 lists the strains that have been sequenced. The data from the viral genomic analysis support the hypothesis that the Zika viruses can be classified by origin into the Southern-Eastern Asian type and African type (Table 2). Other isolates might be derived from these types.

ZIKA VIRUS OUTBREAKS AND CLINICAL COMPLICATIONS

The Zika virus has been considered as a benign pathogen, causing asymptomatic or mild infections. Currently, there is no serological test that can clearly distinguish the Zika virus from other *Flaviviruses*. Diagnostic tests for Zika include RT-PCR, an IgM ELISA, and a plaque reduction neutralization test (PRNT). Some commercial tests have only become recently available[21]. Even a report from Olson *et al*[13] in 1981 that a cluster of 7 people with serologic evidence of the Zika virus illness in Indonesia did not attract serious attention and was not considered an outbreak due to the mildness of the associated illness. Later on, the same arbovirus research group performed a serological study that showed that 9/71 (13%) human volunteers in Lombok, Indonesia, had neutralizing antibodies to the Zika virus[22]. However, no serious cases were reported. The first outbreak of Zika virus-caused diseases was reported in 2007 on Yap Island of Micronesia. In April 2007, physicians on Yap Island characterized the disease with rash, conjunctivitis, arthralgia, arthritis, and fever. The disease affected 99 patients in 2 mo. A comprehensive study that combined analysis of patient samples, serological testing and real-time RT-PCR revealed the genetic and serological properties of the Zika virus epidemic[23]. The studies suggested that the 2007 Yap Island Zika virus is distantly related to African subclades and may be spread from Southeast Asia and the Pacific. Duffy *et al*[24] later conducted an extensive study on the Yap Island Zika virus outbreak. From 185 patients, 49 had been confirmed with the Zika virus illness, only 5 were excluded from Zika virus infection, and all others were suspected of Zika virus infection. They used survey studies in a large population, and estimated that 73% of the population of the Yap Island was infected with the Zika virus during the epidemic outbreak. Therefore, the outbreak on Yap Island in 2007 suggested that Zika virus infection has been spread outside of Africa and Asia[17]. Of course, whether or not the Zika virus was imported from Africa or Asia or other places remains to be verified.

Another Zika outbreak occurred between Oct. 2013 and Feb. 2014 in French Polynesia - like Yap Island, another island in the Pacific Ocean. In the very beginning of the outbreak, a mild dengue-like illness was observed in the patients within a family (consisting of wife, husband and their son-in-law). The symptoms included low fever (< 38 ℃), asthenia, wrist and fingers arthralgia, headache, rash, and conjunctivitis. The RT-PCR test confirmed that it was a Zika virus infection[25]. The epidemic has been spread to a large population as reported by the syndromic surveillance network (6630 suspected Zika virus infection cases), 333 of which were confirmed by real-time RT-PCR as Zika virus infections. Symptoms of most Zika virus infection cases are mild and self-limited (mean duration of symptoms is 3-6 d)[25-27]. No hospitalizations for acute infection have been reported. In contrast to the outbreak in Yap Island, some severe complications were seen in this outbreak: The first case of Guillain-Barré syndrome (GBS) was found immediately after a Zika virus infection[28], and another case of vertical transmission from an infected pregnant woman to the baby was reported in this outbreak[29].

The spread of Zika virus from the outbreak of French Polynesia has been reported. Two Japanese travelers were confirmed to be infected with the Zika virus after they returned from a trip to French Polynesia during the time of the outbreak[30]. In addition, it was found to have spread to other Pacific Islands including New Caledonia, Cook Islands, Easter Island, Vanuatu, and Solomon Islands[31]. The introduction of the Zika virus from French Polynesia into New Caledonia caused another outbreak in New Caledonia in 2014[32]; The first cases of Zika virus infection were confirmed in November 2013, and they were imported from French Polynesia. By the end of 2014, a total of 1383 cases were confirmed in a laboratory[32]. Consequently, an outbreak in New Caledonia was declared. Thus far, introduction of the Zika virus from French Polynesia to other countries has been continuously reported.

Between 1947 and 2006, < 20 cases of Zika virus infection have been reported[5]. There have been recent reports of imported cases of Zika virus infections in 18 travelers returning to the Netherlands from Surinam, which is in South America near the northern border of Brazil, and the Dominican Republic[33], 13 infections were imported from Venezuela, Fiji/Samoa, or Suriname to China[34], and 4 infections were imported from Brazil to Portugal[35]. Autochthonous cases were reported in places such as Mexico[36], Colombia[37], and Easter Island, which was the first outbreak (51 cases) reported in a territory of the Americas in early 2014[38].

Table 2 Origin of the types Zika viruses

Isolation region	Isolation year	Accession #	Strain	Ref.
Malaysia	1966	HQ234499	P6-740	Haddow *et al*[4]
Micronesia	2007	EU545988	N/A	Lanciotti *et al*[23]
Cambodia	2010	JN860885	FSS13025	Haddow *et al*[4]
Thailand	2016	KU681082	H.sapiens-tc/PHL/2012/CPC-0740	unpublished
Philippines	2016	KU681081	H.sapiens-tc/THA/2014/SV0127	unpublished
China	2016	KU744693	VE Ganxian	unpublished
China	2016	KU740184	GD01	unpublished
Nigeria	1968	HQ234500	IBH 30656	Haddow *et al*[4]
Senegal	1984	HQ234501	ArD 41519	Haddow *et al*[4]
Uganda	1947	HQ234498	MR766	Haddow *et al*[4]
Uganda	2004	NC012532	N/A	Kuno *et al*[62]
CAR	2014	KF268948	ARB13565	Berthet *et al*[63]
CAR	2014	KF268949	ARB15076	Berthet *et al*[63]
CAR	2014	KF268950	ARB7701	Berthet *et al*[63]
Senegal	2001	KF383119	ArD158084	Faye *et al*[2]
Senegal	2001	KF383118	ArD157995	Faye *et al*[2]
Senegal	2001	KF383117	ArD128000	Faye *et al*[2]
Senegal	2001	KF383116	ArD7117	Faye *et al*[2]
Brazil	2016	KU497555	Brazil-ZKV2015	Calvet *et al*[64]
Brazil	2016	KU707826	SSABR1	Costa *et al*[65]
Brazil	2016	KU527608	Natal RGN	Mlakar *et al*[48]
Brazil	2016	KU501215	PRVABC59	Lanciotti *et al*[23]
Brazil	2016	KU321639	ZikaSPH2015	Staples *et al*[66]
Brazil	2016	KU312312	Z1106033	Enfissi *et al*[67]
France	2014	KJ776791	H/PF/2013	Baronti *et al*[68]
Martinique	2016	KU647676	Martinique_PaRi_2015	Baronti *et al*[68]
Haiti	2014	KU509998	Haiti/1225/2014	Lednicky *et al*[69]

CAR: Central African Republic; N/A: Not applicable.

The recent outbreak in Brazil has attracted the most attention due to not only its growing infected population but also its likely enhanced severity of the clinical sequelae. In March of 2015, Zanluca *et al*[39] from the Molecular Virology Laboratory of Carlos Chagas Institute, Oswaldo Cruz Institute, state of Paraná, Brazil, detected the Zika virus genome by RT-PCR from 8 out of 21 acute-phase serum specimens from the patients with dengue-like symptoms. This is the first report of Zika virus outbreak in Brazil. Later, another group reported a similar detection of Zika virus cases (8 out 24 samples) by RT-PCR[40]. The virus has been assumed to have been imported from French Polynesia either by the travelers during the time of the World Cup[39] or by the teams from the Va'a World Sprint Championship canoe race that was held in Rio de Janeiro, Brazil[41]. It has been reported that the virus is carried by the travelers to other countries[42]. Genomic sequencing has been conducted to analyze the similarities between different strains isolated historically. Phylogenetic studies showed that the Brazilian strain is closely related to the one from French Polynesia, and the French Polynesia strain is likely derived from Yap Island. These strains all belong to the Asian lineage[41].

The severe clinical sequelae caused by Zika virus infection include the following. First, during the outbreak of the Zika virus in French Polynesia, the Zika virus was detected from the semen of a patient, which brought out the presumption that the Zika virus might be transmitted sexually[43]. Several cases of Zika virus infected patients have been reported to be sexually transmitted[44]. This observation implies another transmission route for the Zika virus other than through mosquito. Secondly, the Zika virus was reported to be transmitted vertically (from the infected mother to the fetus). This is a major problem for patients infected by Zika virus because the virus directly results in birth defects. Again, the first cases of congenital Zika virus infection were found during the French Polynesia outbreak[29]. Thirdly, it was reported to be related to some severe syndromes like GBS[28,45]. In addition, Zika virus infection might have been associated with microcephaly[46-51]. However, after more detailed and accurate experimental studies and clinical analysis, the number of Zika-related microcephaly dropped quickly. Therefore, all the linkages to the severe diseases are still informative not conclusive. Systemic research in different aspects for Zika virus is needed to assure that the clinical findings are explained and understood.

FUTURE DIRECTIONS

Even though the world has noticed the emergence of Zika virus infection, time is needed to achieve understanding of its pathogenesis, prevention, and treatment. A previously systemic study is lacking, so the Zika virus, from now on, will be another member of Genus *Flavivirus* to be the center of virological research. The following aspects may be very important in the near future: Animal model for Zika virus infection: It will help researchers understand

whether and how Zika virus causes neural disorder through interfering with the neural progenitor cell/neural stem cell (NPC/NSC) proliferation and differentiation; vaccine development: Like all other viruses, the best and most effective way to prevent viral infection is by vaccine. Some successful experience in Dengue virus and yellow fever virus may be useful towards developing the Zika vaccine; transmission prevention. Viral transmission needs to be studied, such as whether and how semen components enhance viral infection.

REFERENCES

1 **Bollati M**, Alvarez K, Assenberg R, Baronti C, Canard B, Cook S, Coutard B, Decroly E, de Lamballerie X, Gould EA, Grard G, Grimes JM, Hilgenfeld R, Jansson AM, Malet H, Mancini EJ, Mastrangelo E, Mattevi A, Milani M, Moureau G, Neyts J, Owens RJ, Ren J, Selisko B, Speroni S, Steuber H, Stuart DI, Unge T, Bolognesi M. Structure and functionality in flavivirus NS-proteins: perspectives for drug design. *Antiviral Res* 2010; **87**: 125-148 [PMID: 19945487 DOI: 10.1016/j.antiviral.2009.11.009]

2 **Faye O**, Freire CC, Iamarino A, Faye O, de Oliveira JV, Diallo M, Zanotto PM, Sall AA. Molecular evolution of Zika virus during its emergence in the 20(th) century. *PLoS Negl Trop Dis* 2014; **8**: e2636 [PMID: 24421913 DOI: 10.1371/journal.pntd.0002636]

3 **Mackenzie J**. Wrapping things up about virus RNA replication. *Traffic* 2005; **6**: 967-977 [PMID: 16190978 DOI: 10.1111/j.1600-0854.2005.00339.x]

4 **Haddow AD**, Schuh AJ, Yasuda CY, Kasper MR, Heang V, Huy R, Guzman H, Tesh RB, Weaver SC. Genetic characterization of Zika virus strains: geographic expansion of the Asian lineage. *PLoS Negl Trop Dis* 2012; **6**: e1477 [PMID: 22389730 DOI: 10.1371/journal.pntd.0001477]

5 **Zhu Z**, Chan JF, Tee KM, Choi GK, Lau SK, Woo PC, Tse H, Yuen KY. Comparative genomic analysis of pre-epidemic and epidemic Zika virus strains for virological factors potentially associated with the rapidly expanding epidemic. *Emerg Microbes Infect* 2016; **5**: e22 [PMID: 26980239]

6 **Dick GW**. Zika virus. II. Pathogenicity and physical properties. *Trans R Soc Trop Med Hyg* 1952; **46**: 521-534 [PMID: 12995441]

7 **Dick GW**, Kitchen SF, Haddow AJ. Zika virus. I. Isolations and serological specificity. *Trans R Soc Trop Med Hyg* 1952; **46**: 509-520 [PMID: 12995440]

8 **Boorman JP**, Porterfield JS. A simple technique for infection of mosquitoes with viruses; transmission of Zika virus. *Trans R Soc Trop Med Hyg* 1956; **50**: 238-242 [PMID: 13337908]

9 **Haddow AJ**, Williams MC, Woodall JP, Simpson DI, Goma LK. Twelve isolations of zika virus from aedes (stegomyia) africanus (theobald) taken in and above a uganda forest. *Bull World Health Organ* 1964; **31**: 57-69 [PMID: 14230895]

10 **Macnamara FN**. Zika virus: a report on three cases of human infection during an epidemic of jaundice in Nigeria. *Trans R Soc Trop Med Hyg* 1954; **48**: 139-145 [PMID: 13157159]

11 **Bearcroft WG**. Zika virus infection experimentally induced in a human volunteer. *Trans R Soc Trop Med Hyg* 1956; **50**: 442-448 [PMID: 13380987]

12 **Marchette NJ**, Garcia R, Rudnick A. Isolation of Zika virus from Aedes aegypti mosquitoes in Malaysia. *Am J Trop Med Hyg* 1969; **18**: 411-415 [PMID: 4976739]

13 **Olson JG**, Ksiazek TG. Zika virus, a cause of fever in Central Java, Indonesia. *Trans R Soc Trop Med Hyg* 1981; **75**: 389-393 [PMID: 6275577]

14 **Kilbourn AM**, Karesh WB, Wolfe ND, Bosi EJ, Cook RA, Andau M. Health evaluation of free-ranging and semi-captive orangutans (Pongo pygmaeus pygmaeus) in Sabah, Malaysia. *J Wildl Dis* 2003; **39**: 73-83 [PMID: 12685070 DOI: 10.7589/0090-3558-39.1.73]

15 **Heang V**, Yasuda CY, Sovann L, Haddow AD, Travassos da Rosa AP, Tesh RB, Kasper MR. Zika virus infection, Cambodia, 2010. *Emerg Infect Dis* 2012; **18**: 349-351 [PMID: 22305269 DOI: 10.3201/eid1802.111224]

16 **Moore DL**, Causey OR, Carey DE, Reddy S, Cooke AR, Akinkugbe FM, David-West TS, Kemp GE. Arthropod-borne viral infections of man in Nigeria, 1964-1970. *Ann Trop Med Parasitol* 1975; **69**: 49-64 [PMID: 1124969]

17 **Hayes EB**. Zika virus outside Africa. *Emerg Infect Dis* 2009; **15**: 1347-1350 [PMID: 19788800 DOI: 10.3201/eid1509.090442]

18 **Fokam EB**, Levai LD, Guzman H, Amelia PA, Titanji VP, Tesh RB, Weaver SC. Silent circulation of arboviruses in Cameroon. *East Afr Med J* 2010; **87**: 262-268 [PMID: 23057269]

19 **Fagbami AH**. Zika virus infections in Nigeria: virological and seroepidemiological investigations in Oyo State. *J Hyg* (Lond) 1979; **83**: 213-219 [PMID: 489960]

20 **Saluzzo JF**, Ivanoff B, Languillat G, Georges AJ. [Serological survey for arbovirus antibodies in the human and simian populations of the South-East of Gabon (author's transl)]. *Bull Soc Pathol Exot Filiales* 1982; **75**: 262-266 [PMID: 6809352]

21 **Saiz JC**, Vázquez-Calvo Á, Blázquez AB, Merino-Ramos T, Escribano-Romero E, Martín-Acebes MA. Zika Virus: the Latest Newcomer. *Front Microbiol* 2016; **7**: 496 [PMID: 27148186 DOI: 10.3389/fmicb.2016.00496]

22 **Olson JG**, Ksiazek TG, Gubler DJ, Lubis SI, Simanjuntak G, Lee VH, Nalim S, Juslis K, See R. A survey for arboviral antibodies in sera of humans and animals in Lombok, Republic of Indonesia. *Ann Trop Med Parasitol* 1983; **77**: 131-137 [PMID: 6309104]

23 **Lanciotti RS**, Kosoy OL, Laven JJ, Velez JO, Lambert AJ, Johnson AJ, Stanfield SM, Duffy MR. Genetic and serologic properties of Zika virus associated with an epidemic, Yap State, Micronesia, 2007. *Emerg Infect Dis* 2008; **14**: 1232-1239 [PMID: 18680646 DOI: 10.3201/eid1408.080287]

24 **Duffy MR**, Chen TH, Hancock WT, Powers AM, Kool JL, Lanciotti RS, Pretrick M, Marfel M, Holzbauer S, Dubray C, Guillaumot L, Griggs A, Bel M, Lambert AJ, Laven J, Kosoy O, Panella A, Biggerstaff BJ, Fischer M, Hayes EB. Zika virus outbreak on Yap Island, Federated States of Micronesia. *N Engl J Med* 2009; **360**: 2536-2543 [PMID: 19516034 DOI: 10.1056/NEJMoa0805715]

25 **Cao-Lormeau VM**, Roche C, Teissier A, Robin E, Berry AL, Mallet HP, Sall AA, Musso D. Zika virus, French polynesia, South pacific, 2013. *Emerg Infect Dis* 2014; **20**: 1085-1086 [PMID: 24856001 DOI: 10.3201/eid2006.140138]

26 **Musso D**, Nilles EJ, Cao-Lormeau VM. Rapid spread of emerging Zika virus in the Pacific area. *Clin Microbiol Infect* 2014; **20**: O595-O596 [PMID: 24909208 DOI: 10.1111/1469-0691.12707]

27 **Musso D**, Nhan T, Robin E, Roche C, Bierlaire D, Zisou K, Shan Yan A, Cao-Lormeau VM, Broult J. Potential for Zika virus transmission through blood transfusion demonstrated during an outbreak in French Polynesia, November 2013 to February 2014. *Euro Surveill* 2014; **19**: [PMID: 24739982]

28 **Oehler E**, Watrin L, Larre P, Leparc-Goffart I, Lastere S, Valour F, Baudouin L, Mallet H, Musso D, Ghawche F. Zika virus infection complicated by Guillain-Barre syndrome--case report, French Polynesia, December 2013. *Euro Surveill* 2014; **19**: [PMID: 24626205]

29 **Besnard M**, Lastere S, Teissier A, Cao-Lormeau V, Musso D. Evidence of perinatal transmission of Zika virus, French Polynesia, December 2013 and February 2014. *Euro Surveill* 2014; **19**: pii: 20751 [PMID: 24721538]

30 **Kutsuna S**, Kato Y, Takasaki T, Moi M, Kotaki A, Uemura H, Matono T, Fujiya Y, Mawatari M, Takeshita N, Hayakawa K, Kanagawa S, Ohmagari N. Two cases of Zika fever imported from French Polynesia to Japan, December 2013 to January 2014 [corrected]. *Euro Surveill* 2014; **19**: pii: 20683 [PMID: 24507466]

31 **Musso D**, Cao-Lormeau VM, Gubler DJ. Zika virus: following the path of dengue and chikungunya? *Lancet* 2015; **386**: 243-244 [PMID: 26194519 DOI: 10.1016/S0140-6736(15)61273-9]

32 **Dupont-Rouzeyrol M**, O'Connor O, Calvez E, Daurès M, John M, Grangeon JP, Gourinat AC. Co-infection with Zika and dengue viruses in 2 patients, New Caledonia, 2014. *Emerg Infect Dis* 2015; **21**: 381-382 [PMID: 25625687 DOI: 10.3201/eid2102.141553]

33 **Duijster JW**, Goorhuis A, van Genderen PJ, Visser LG, Koopmans

MP, Reimerink JH, Grobusch MP, van der Eijk AA, van den Kerkhof JH, Reusken CB, Hahne SJ. Zika virus infection in 18 travellers returning from Surinam and the Dominican Republic, The Netherlands, November 2015-March 2016. *Infection* 2016; **44**: 797-802 [PMID: 27209175 DOI: 10.1007/s15010-016-0906-y]

34 **Zhang Y**, Chen W, Wong G, Bi Y, Yan J, Sun Y, Chen E, Yan H, Lou X, Mao H, Xia S, Gao GF, Shi W, Chen Z. Highly diversified Zika viruses imported to China, 2016. *Protein Cell* 2016; **7**: 461-464 [PMID: 27209301 DOI: 10.1007/s13238-016-0274-5]

35 **Zé-Zé L**, Prata MB, Teixeira T, Marques N, Mondragão A, Fernandes R, Saraiva da Cunha J, Alves MJ. Zika virus infections imported from Brazil to Portugal, 2015. *IDCases* 2016; **4**: 46-49 [PMID: 27134823 DOI: 10.1016/j.idcr.2016.03.004]

36 **Jimenez Corona ME**, De la Garza Barroso AL, Rodriguez Martínez JC, Luna Guzmán NI, Ruiz Matus C, Díaz Quiñonez JA, Lopez Martinez I, Kuri Morales PA. Clinical and Epidemiological Characterization of Laboratory-Confirmed Autochthonous Cases of Zika Virus Disease in Mexico. *PLoS Curr* 2016; **8**: pii: ecurrents.outbreaks.a2fe1b3d6d71e24ad2b5afe982824053 [PMID: 27158557 DOI: 10.1371/currents.outbreaks.a2fe1b3d6d71e24ad2b5afe982824053]

37 **Camacho E**, Paternina-Gomez M, Blanco PJ, Osorio JE, Aliota MT. Detection of Autochthonous Zika Virus Transmission in Sincelejo, Colombia. *Emerg Infect Dis* 2016; **22**: 927-929 [PMID: 27089253 DOI: 10.3201/eid2205.160023]

38 **Zanluca C**, Dos Santos CN. Zika virus - an overview. *Microbes Infect* 2016; **18**: 295-301 [PMID: 26993028]

39 **Zanluca C**, Melo VC, Mosimann AL, Santos GI, Santos CN, Luz K. First report of autochthonous transmission of Zika virus in Brazil. *Mem Inst Oswaldo Cruz* 2015; **110**: 569-572 [PMID: 26061233 DOI: 10.1590/0074-02760150192]

40 **Campos GS**, Bandeira AC, Sardi SI. Zika Virus Outbreak, Bahia, Brazil. *Emerg Infect Dis* 2015; **21**: 1885-1886 [PMID: 26401719 DOI: 10.3201/eid2110.150847]

41 **Musso D**. Zika Virus Transmission from French Polynesia to Brazil. *Emerg Infect Dis* 2015; **21**: 1887 [PMID: 26403318 DOI: 10.3201/eid2110.151125]

42 **Zammarchi L**, Tappe D, Fortuna C, Remoli ME, Günther S, Venturi G, Bartoloni A, Schmidt-Chanasit J. Zika virus infection in a traveller returning to Europe from Brazil, March 2015. *Euro Surveill* 2015; **20**: [PMID: 26084316]

43 **Musso D**, Roche C, Robin E, Nhan T, Teissier A, Cao-Lormeau VM. Potential sexual transmission of Zika virus. *Emerg Infect Dis* 2015; **21**: 359-361 [PMID: 25625872 DOI: 10.3201/eid2102.141363]

44 **Hills SL**, Russell K, Hennessey M, Williams C, Oster AM, Fischer M, Mead P. Transmission of Zika Virus Through Sexual Contact with Travelers to Areas of Ongoing Transmission - Continental United States, 2016. *MMWR Morb Mortal Wkly Rep* 2016; **65**: 215-216 [PMID: 26937739 DOI: 10.15585/mmwr.mm6508e2]

45 **Wise J**. Study links Zika virus to Guillain-Barré syndrome. *BMJ* 2016; **352**: i1242 [PMID: 26932976 DOI: 10.1136/bmj.i1242]

46 **Barreto ML**, Barral-Netto M, Stabeli R, Almeida-Filho N, Vasconcelos PF, Teixeira M, Buss P, Gadelha PE. Zika virus and microcephaly in Brazil: a scientific agenda. *Lancet* 2016; **387**: 919-921 [PMID: 26921913 DOI: 10.1016/S0140-6736(16)00545-6]

47 **de Paula Freitas B**, de Oliveira Dias JR, Prazeres J, Sacramento GA, Ko AI, Maia M, Belfort RJr. Ocular Findings in Infants With Microcephaly Associated With Presumed Zika Virus Congenital Infection in Salvador, Brazil. *JAMA Ophthalmol* 2016 Feb 9; Epub ahead of print [PMID: 26865554 DOI: 10.1001/jamaophthalmol.2016.0267]

48 **Mlakar J**, Korva M, Tul N, Popović M, Poljšak-Prijatelj M, Mraz J, Kolenc M, Resman Rus K, Vesnaver Vipotnik T, Fabjan Vodušek V, Vizjak A, Pižem J, Petrovec M, Avšič Županc T. Zika Virus Associated with Microcephaly. *N Engl J Med* 2016; **374**: 951-958 [PMID: 26862926 DOI: 10.1056/NEJMoa1600651]

49 **Stratton SJ**. Zika Virus Association with Microcephaly: The Power for Population Statistics to Identify Public Health Emergencies. *Prehosp Disaster Med* 2016; **31**: 119-120 [PMID: 26940218 DOI: 10.1017/S1049023X16000170]

50 **Ventura CV**, Maia M, Bravo-Filho V, Góis AL, Belfort R. Zika virus in Brazil and macular atrophy in a child with microcephaly. *Lancet* 2016; **387**: 228 [PMID: 26775125 DOI: 10.1016/S0140-6 736(16)00006-4]

51 **Werner H**, Fazecas T, Guedes B, Lopes Dos Santos J, Daltro P, Tonni G, Campbell S, Araujo Júnior E. Intrauterine Zika virus infection and microcephaly: correlation of perinatal imaging and three-dimensional virtual physical models. *Ultrasound Obstet Gynecol* 2016; **47**: 657-660 [PMID: 26923098 DOI: 10.1002/uog.15901]

52 **Heinz FX**, Mandl CW, Holzmann H, Kunz C, Harris BA, Rey F, Harrison SC. The flavivirus envelope protein E: isolation of a soluble form from tick-borne encephalitis virus and its crystallization. *J Virol* 1991; **65**: 5579-5583 [PMID: 1716695]

53 **Li L**, Lok SM, Yu IM, Zhang Y, Kuhn RJ, Chen J, Rossmann MG. The flavivirus precursor membrane-envelope protein complex: structure and maturation. *Science* 2008; **319**: 1830-1834 [PMID: 18369147 DOI: 10.1126/science.1153263]

54 **Jones CT**, Ma L, Burgner JW, Groesch TD, Post CB, Kuhn RJ. Flavivirus capsid is a dimeric alpha-helical protein. *J Virol* 2003; **77**: 7143-7149 [PMID: 12768036]

55 **Muller DA**, Young PR. The flavivirus NS1 protein: molecular and structural biology, immunology, role in pathogenesis and application as a diagnostic biomarker. *Antiviral Res* 2013; **98**: 192-208 [PMID: 23523765 DOI: 10.1016/j.antiviral.2013.03.008]

56 **Leung JY**, Pijlman GP, Kondratieva N, Hyde J, Mackenzie JM, Khromykh AA. Role of nonstructural protein NS2A in flavivirus assembly. *J Virol* 2008; **82**: 4731-4741 [PMID: 18337583 DOI: 10.1128/JVI.00002-08]

57 **Pastorino BA**, Peyrefitte CN, Grandadam M, Thill MC, Tolou HJ, Bessaud M. Mutagenesis analysis of the NS2B determinants of the Alkhurma virus NS2B-NS3 protease activation. *J Gen Virol* 2006; **87**: 3279-3283 [PMID: 17030861 DOI: 10.1099/vir.0.82088-0]

58 **McLean JE**, Wudzinska A, Datan E, Quaglino D, Zakeri Z. Flavivirus NS4A-induced autophagy protects cells against death and enhances virus replication. *J Biol Chem* 2011; **286**: 22147-22159 [PMID: 21511946 DOI: 10.1074/jbc.M110.192500]

59 **Zou J**, Xie X, Lee le T, Chandrasekaran R, Reynaud A, Yap L, Wang QY, Dong H, Kang C, Yuan Z, Lescar J, Shi PY. Dimerization of flavivirus NS4B protein. *J Virol* 2014; **88**: 3379-3391 [PMID: 24390334 DOI: 10.1128/JVI.02782-13]

60 **Grun JB**, Brinton MA. Dissociation of NS5 from cell fractions containing West Nile virus-specific polymerase activity. *J Virol* 1987; **61**: 3641-3644 [PMID: 2959795]

61 **Laurent-Rolle M**, Morrison J, Rajsbaum R, Macleod JM, Pisanelli G, Pham A, Ayllon J, Miorin L, Martínez-Romero C, tenOever BR, García-Sastre A. The interferon signaling antagonist function of yellow fever virus NS5 protein is activated by type I interferon. *Cell Host Microbe* 2014; **16**: 314-327 [PMID: 25211074 DOI: 10.1016/j.cho m.2014.07.015]

62 **Kuno G**, Chang GJ. Full-length sequencing and genomic characterization of Bagaza, Kedougou, and Zika viruses. *Arch Virol* 2007; **152**: 687-696 [PMID: 17195954 DOI: 10.1007/s00705-006-0903-z]

63 **Berthet N**, Nakouné E, Kamgang B, Selekon B, Descorps-Declère S, Gessain A, Manuguerra JC, Kazanji M. Molecular characterization of three Zika flaviviruses obtained from sylvatic mosquitoes in the Central African Republic. *Vector Borne Zoonotic Dis* 2014; **14**: 862-865 [PMID: 25514122 DOI: 10.1089/vbz.2014.1607]

64 **Calvet G**, Aguiar RS, Melo AS, Sampaio SA, de Filippis I, Fabri A, Araujo ES, de Sequeira PC, de Mendonça MC, de Oliveira L, Tschoeke DA, Schrago CG, Thompson FL, Brasil P, Dos Santos FB, Nogueira RM, Tanuri A, de Filippis AM. Detection and sequencing of Zika virus from amniotic fluid of fetuses with microcephaly in Brazil: a case study. *Lancet Infect Dis* 2016; **16**: 653-660 [PMID: 26897108 DOI: 10.1016/S1473-3099(16)00095-5]

65 **Costa F**, Sarno M, Khouri R, de Paula Freitas B, Siqueira I, Ribeiro GS, Ribeiro HC, Campos GS, Alcântara LC, Reis MG, Weaver SC, Vasilakis N, Ko AI, Almeida AR. Emergence of Congenital Zika Syndrome: Viewpoint From the Front Lines. *Ann Intern Med* 2016; **164**: 689-691 [PMID: 26914810 DOI: 10.7326/M16-0332]

66 **Staples JE**, Dziuban EJ, Fischer M, Cragan JD, Rasmussen SA, Cannon MJ, Frey MT, Renquist CM, Lanciotti RS, Muñoz JL, Powers AM, Honein MA, Moore CA. Interim Guidelines for the Evaluation

and Testing of Infants with Possible Congenital Zika Virus Infection - United States, 2016. *MMWR Morb Mortal Wkly Rep* 2016; **65**: 63-67 [PMID: 26820387 DOI: 10.15585/mmwr.mm6503e3]

67 **Enfissi A**, Codrington J, Roosblad J, Kazanji M, Rousset D. Zika virus genome from the Americas. *Lancet* 2016; **387**: 227-228 [PMID: 26775124 DOI: 10.1016/S0140-6736(16)00003-9]

68 **Baronti C**, Piorkowski G, Charrel RN, Boubis L, Leparc-Goffart I, de Lamballerie X. Complete coding sequence of zika virus from a French polynesia outbreak in 2013. *Genome Announc* 2014 Jun 5; **2**: [PMID: 24903869 DOI: 10.1128/genomeA.00500-14]

69 **Lednicky JA**, Butel JS, Luetke MC, Loeb JC. Complete genomic sequence of a new Human polyomavirus 9 strain with an altered noncoding control region. *Virus Genes* 2014; **49**: 490-492 [PMID: 25260554 DOI: 10.1007/s11262-014-1119-z]

P- Reviewer: Arriagada GL, Cunha C, De Berardinis P, Ghiringhelli PD, Giannecchini S **S- Editor**: Qiu S **L- Editor**: A
E- Editor: Lu YJ

World Journal of Virology

Submit a Manuscript: http://www.wjgnet.com/esps/
Help Desk: http://www.wjgnet.com/esps/helpdesk.aspx
DOI: 10.5501/wjv.v6.i1.9

World J Virol 2017 February 12; 6(1): 9-16
ISSN 2220-3249 (online)

MINIREVIEWS

Value of routine dengue diagnosis in endemic countries

James Ayukepi Ayukekbong, Olufunmilayo G Oyero, Samuel Ekpesu Nnukwu, Henry Nzike Mesumbe, Cajetang Nkong Fobisong

James Ayukepi Ayukekbong, Centre for Continuing and Online Learning, Algonquin College, Ottawa, ON K2G 1V8, Canada

Olufunmilayo G Oyero, Institute for Advanced Medical Research and Training, College of Medicine, University of Ibadan, Ibadan PB200005, Nigeria

Samuel Ekpesu Nnukwu, Department of Medical Laboratory Science, Faculty of Allied Medical Sciences, University of Calabar, Calabar PB3651, Nigeria

Henry Nzike Mesumbe, Cajetang Nkong Fobisong, Section for Clinical Virology, Redeem Biomedical Buea, Buea SWR MILE 16, Cameroon

Author contributions: Ayukekbong JA performed the majority of the writing, prepared the figures and tables; Oyero OG performed data accusation and writing; Nnukwu SE and Mesumbe HN provided the relevant input in writing the paper; Fobisong CN designed the outline and coordinated the writing of the paper.

Conflict-of-interest statement: The authors whose names are listed below certify that they have NO affiliations with or involvement in any organization or entity with any financial interest (such as honoraria; educational grants; participation in speaker' bureaus; membership, employment, consultancies, stock ownership, or other equity interest; and expert testimony or patent-licensing arrangements), or non-financial interest (such as personal or professional relationships, affiliations, knowledge or beliefs) in the subject matter or materials discussed in this manuscript.

Manuscript source: Invited manuscript

Correspondence to: Dr. James Ayukepi Ayukekbong, Centre for Continuing and Online Learning, Algonquin College, 1385 Woodroffe Avenue, Ottawa, ON K2G 1V8, Canada. ja.algonquin@gmail.com
Telephone: +1-819-6391160

Received: October 10, 2016
Peer-review started: October 11, 2016
First decision: November 14, 2016
Revised: November 24, 2016
Accepted: December 7, 2016
Article in press: December 9, 2016
Published online: February 12, 2017

Abstract

Dengue is one of the most common arthropod-borne viral diseases in humans and it is a leading cause of illness and death in the tropical and subtropical regions of the world. It is thought to account for 400 million cases annually among approximately 3.97 billion people at risk of infection in 128 endemic countries. Despite the global prevalence of the disease, the availability of a vaccine is limited in most countries in the endemic areas. Most endemic countries in South America, South East Asia and Africa serve as attractive touristic sites for people from non-endemic countries who become infected and export the virus to dengue-free regions. Dengue fever typically resembles malaria and in endemic countries most cases of dengue are treated as presumptive malaria. Consequently, routine dengue diagnosis among persons with fever will offer early treatment and reduce the burden of the disease. Also, routine testing among travellers from endemic countries will reduce importation and prevent the geographical expansion of dengue. In this essay, we seek to highlight the usefulness of routine dengue testing in endemic countries.

Key words: Dengue virus; Endemic; Mosquito; Vector-borne

Core tip: Dengue is an emerging arborvirus infection currently endemic in 128 countries in the world. In the absence of routine vaccination and specific antivirals, the main method to reduce the burden of dengue is to reduce the vector population, educate people on protective measures and timely laboratory identification. Unfortunately this routine laboratory investigation is currently neglected in most endemic countries and most cases of fevers are often misconstrued as malaria. This review provides a comprehensive summary of dengue infection and highlights the fact that routine dengue diagnosis will reduce the burden and global expansion of dengue.

Ayukekbong JA, Oyero OG, Nnukwu SE, Mesumbe HN, Fobisong CN. Value of routine dengue diagnosis in endemic countries. *World J Virol* 2017; 6(1): 9-16 Available from: URL: http://www.wjgnet.com/2220-3249/full/v6/i1/9.htm DOI: http://dx.doi.org/10.5501/wjv.v6.i1.9

INTRODUCTION

Dengue virus (DENV) is the most common arthropod-borne viral disease in humans and it is endemic in most tropical and sub-tropical countries[1]. It has been designated a major international public health concern by the World health Organization (WHO) as it accounts for 400 million cases annually among 3.97 billion people at risk of infection[1,2]. Previous phylogenetic analysis suggests that there are four distinct DENV serotypes (DENV 1 to 4)[3,4]. However, a 5th serotype associated with milder disease was isolated in 2013 in Malaysia[5]. Over the years, DENV has spread from less than 9 endemic countries to presently about 128 endemic countries[6,7]. Factors such as unrestricted large-scale international travel and trade, urbanization, global warming, virus and vector evolution contributed to its rapid spread to other regions of the World[8].

The main arthropod vectors for the transmission of DENVs are *Aedes aegypti* and *Aedes albopictus mosquitoes* are predominant in both tropical and sub-tropical regions of the world[9,10]. Infected individuals may be asymptomatic or may present with dengue fever (DF) - a mild febrile illness, dengue hemorrhagic fever (DHF) - a life-threatening complication, or dengue shock syndrome (DSS). The incubation period is between 3-15 d following an infected blood meal. Rare cases of human - human transmission *via* needle stick injuries, contaminated blood products, donor organs and vertical transmission from infected mother to an unborn child have been documented[11]. Dengue endemicity in 128 countries makes it a year round occurrence with peak prevalence during the rainy season when environmental conditions are optimal for the *Aedes* vector breeding[12]. As a result, epidemics are common during the rainy season when the vector population is high and the chances for human exposure to mosquito bites is increased[13]. In the absence of routine vaccination and specific antivirals, the main method to reduce the burden of dengue is to reduce the vector population, educate people on protective measures such as spraying of insecticides and wearing protective clothing[7,8,14]. DF typically resembles malaria and in endemic countries most cases of dengue are treated as presumptive malaria. Therefore, routine and differential diagnosis of dengue will provide a basis for evidence-based treatment and reduce the irrational use of antimalarial or antibiotics to treat febrile diseases. Routine screening in endemic countries will provide a better estimate on the burden of dengue disease for public health action.

DENGUE EPIDEMIOLOGY

Dengue is currently regarded as the most important arboviral disease internationally as over half of the world's population lives in dengue endemic countries[7]. A global estimate suggests about 50-200 million cases of dengue with 500000 episodes of DHF/DSS occur annually culminating in about 20000 dengue related deaths[15,16]. The determining factors of dengue epidemiology trends include, but not limited to: (1) rapid urban population growth and density due to rural to urban migration; (2) poor sewage disposal system and land use pattern; (3) global warming; and (4) trade necessitating movement of people[17]. It is now known that every WHO region has evidence of dengue transmission[18]. Almost 75% of the world's population at risk of dengue, live in South East Asia (SEA) and the Western Pacific region and the disease is the leading cause of hospitalization and death in children from these regions (Figure 1)[18]. Dengue is also recognized as an emerging infection in the Eastern Mediterranean region with multiple outbreaks occurring in Pakistan, Yemen, and Saudi Arabia[19]. Almost all countries in the Americas are now hyperendemic for dengue with epidemics occurring every three-to-five years especially in Latin America[16,18]. Due to the significant endemicity of malaria throughout Africa, the majority of "febrile illnesses" including dengue is likely to be mistreated as malaria. This negatively affects our understanding of the epidemiology of dengue in the region. Dengue is indeed underreported in Africa and is not a notifiable disease to WHO by most countries from the continent. A review of the subject by Amarasinghe *et al*[20] suggested that dengue is endemic in 34 countries in Africa and that the four main dengue serotypes circulate in Africa with serotype 2 responsible for most epidemics. Although the threat of dengue is rare in Europe, imported cases by European travellers to and from endemic countries continue to rise (Table 1). A report suggests the importation of dengue to 13 European countries by returning travellers[8].

CLINICAL ASPECTS OF DENGUE INFECTION

Dengue infection may present as a mild asymptomatic

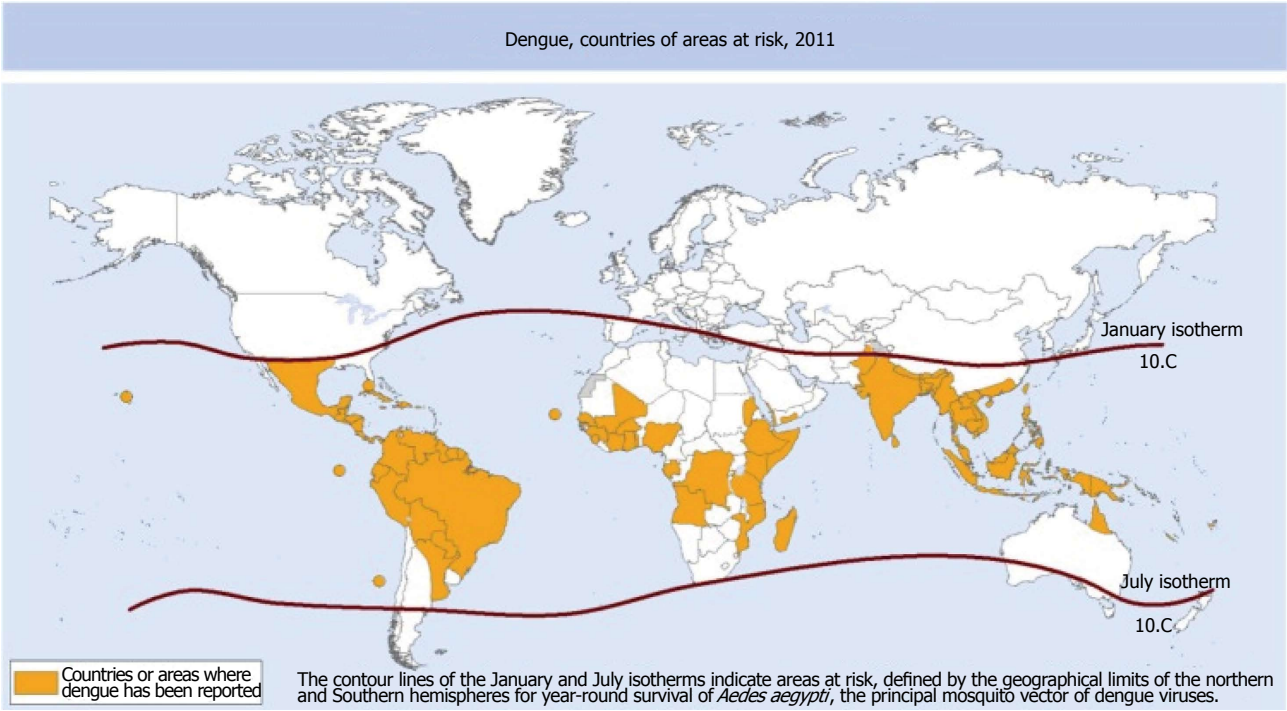

Figure 1 Countries or areas of the world where dengue was reported in 2011, as per data collected by the World Health Organization. Reprinted with permission from Murray *et al*[8]. The boundaries and names shown and the designations used on this map do not imply the expression of any opinion whatsoever on the part of the World Health Organization concerning the legal status of any country, territory, city or area or of its authorities, or concerning the delimitation of its frontiers or boundaries. Dotted and dashed lines on maps represent approximate borderlines for which there may not yet be full agreement.

infection to severe illness that may lead to death in some cases. The disease may start as an undifferentiated febrile illness (UF), which may culminate to a diverse and complicated clinical condition such as: DF, DHF, DSS[21]. Clinically, UF illness mimics malaria and other tropical fevers and in the absence of specific serological testing, UF illness could easily be misdiagnosed or labeled as fever of unknown origin. DF is considered to be a mild disease because death is rarely reported, but may be associated with high fever, severe headache, pain behind the eyes, muscle and bone or joint pains, nausea, vomiting, rash and skin haemorrhages. Leukopenia and thrombocytopenia may also occur. The clinical presentation of DHF is similar to DF but the latter is characterized by plasma leakage resulting from alteration in microvascular permeability. The plasma leakage occurs into the pleural and peritoneal cavities that may result in pleural effusion and ascites. Typical presentation of DHF includes high fever, haemorrhagic phenomena, thrombocytopenia, hepatomegaly and circulatory failure. On the other hand, the clinical features of DSS are also similar to those of DHF but the plasma leakage is so severe that the patient develops shock[21,22]. Other signs of circulatory failure such as the skin becoming cool, blotchy, and congested; circumoral cyanosis may be observed. Also, the patients may initially be lethargic, then become restless and then rapidly enter a critical stage of shock. DSS is usually characterized by weak pulse with narrowing of the pulse, hypotension with cold, clammy skin and restlessness. Death may occur in the absence of appropriate treatment.

DENGUE AMONG TRAVELLERS TO ENDEMIC COUNTRIES

The contribution of dengue expansion through international travel and intercontinental movement of goods is on the rise[23]. As the global community trades and travel more and more, so too do communicable and vector-borne diseases. Most dengue-endemic countries are popular touristic destinations and the frequency of international travel to these regions plays a role in the infection and transmission of the disease. With increasing growing markets and international trade in Africa, Asia and Latin America, the risk of dengue infection by travelers is high. It was observed in 2011 that air travel frequency was 40-times higher compared to the frequency during mid 20th century[24]. Human travel to endemic areas as well as travel of infected persons to non-endemic areas is the main driver in the global transmission and expansion of the disease. Overcrowded airports located in most tropical countries serve as ideal breeding ground and distribution source of dengue viruses and travelers contribute in the importation of the disease (Table 1)[25]. Other globalization factors such as international transport of cargo and goods, especially *via* commercial sea shipment also contribute in the importation or exportation of the dengue's primary and secondary vectors, *Aedes aegypti* and *Aedes albopictus*, respectively[26]. The transatlantic transport of used cars and tires has been linked with the introduction of exotic mosquitoes from America to Europe, which contributed to other vector-borne disease epidemics[27,28].

Table 1 Randomly selected articles revealing dengue importation by travelers from endemic countries

Year	Import country	Source country	No. of cases	Age group	Serotype	Assay	Ref.
2010	France	Benin	1	40s	Unknown	IgG/IgM seology	Gautret *et al*[54]
2001-2009	Denmark	Southeast Asia, South Asia, Central America, Africa, Caribbean, South America	114	6-79	DENV 1, 2, 3 and 4	IgG/IgM serology, PCR	Vinner *et al*[55]
2010	Italy	Caribbean, India, Indonesia, Brazil, Thailand, Venezuela, Nicaragua-Honduras	17	16-63	DENV 1, 3	IgG/IgM immunofluorescence, PCR	Pierro *et al*[56]
2013	France	Guadeloupe	1	50s	DENV 2	PCR	Marchand *et al*[57]
2010	France, Sweden	Tanzania	5	41-69	DENV 3	PCR	Gautret *et al*[58]
2012	Germany, United Kingdom	Madeira	42	20-73	Unknown	Unknown	Frank *et al*[59]
2007-2009	Sweden	Thailand	100	Unknown	DENV 2	Unknown	Heddini *et al*[60]
2009	Italy	Senegal	1	40s	DENV 3	PCR	Nisii *et al*[61]
2012	Finland	Madeira	5	50-60	DENV 3	IgG/IgM, NS1 and PCR	Huhtamo *et al*[62]
2013	Germany	Japan	1	50s	Unknown	IgG/IgM, NS1 and PCR	Schmidt-Chanasit *et al*[63]
2010	Germany	Croatia	1	72	Unknown	IgG/IgM, NS1 and PCR	Schmidt-Chanasit *et al*[64]

DENV: Dengue virus; PCR: Polymerase chain reaction.

ASSESSING DENGUE DISEASE BURDEN IN ENDEMIC COUNTRIES

While geographical expansion of dengue and its vector are evident, the true burden of the disease is underestimated due to lack of an efficient public health surveillance system for dengue. Dengue diagnosis is not routinely performed in endemic countries and most febrile illnesses are treated as presumptive malaria or fever of unknown origin. Also, most dengue cases are asymptomatic and go undetected and infected persons do not seek medical attention. Consequently, the number of dengue cases is underreported and the disease burden is grossly underestimated. However, DF, DHF and DSS cause significant humanitarian and economic hardship and it is suggested that about 3.97 billion people living in 128 endemic countries globally are at risk of dengue[7,29]. The disability adjusted life year (DALY) lost due to dengue infection globally was 700000 per year in 2009 while an estimate of aggregate annual cost of dengue was USD 2.1 billion in the Americas in 2000-2007[15,30-32]. Prior to 1990, dengue was endemic in only 9 countries but the disease is currently endemic in 128 countries across Africa, the Americas, the Eastern Mediterranean, SEA and the Western Pacific regions. A study involving twelve countries in the SEA region from 2001 to 2010 suggest an annual economic burden of US $950 million amongst the studied nation[8]. Overall, due to inadequate disease surveillance, low level of reporting, low case fatality rate, lack of routine diagnosis, the true incidence and burden of the disease is unclear.

DENGUE AND MALARIA ENDEMICITY

Mosquitoes are widespread in most tropical and sub-tropical regions of the world. Dengue vectors as well as those responsible for the transmission of yellow fever, chikungunya (*Aedes spp*) and those responsible for malaria (*Plasmodium spp*,) are known to be well established in these regions. Dengue - malaria co-infection has been recognized as an important clinical problem in endemic regions[33]. Vector expansion is driven partly by population growth, unplanned urbanization, crowded humans settlements and inadequate water, sewage and waste management[24]. These factors with the lack of effective vector control programs increase the exposure of humans to the disease vectors. Concurrent dengue and malaria co-infection has been reported in many areas of the world with predominance in the Americas, Asian tropical and sub-Saharan Africa regions[34-36]. The profound endemicity of both diseases and similar and overlapping clinical presentations often lead to misdiagnosis or misinterpretation as mono infections[37]. We previously reported that 10% of malaria patients in Ibadan, Nigeria had active dengue infection. Also, all malaria patients were positive for dengue IgG antibodies which is suggestive of a previous infection[33]. This concomitant dengue/malaria co-infection is consistent with the endemicity of both infections in the region. Despite this endemicity, routine diagnosis of dengue is often neglected and more focus is on malaria. Dengue misdiagnosis or under-diagnosis poses a great risk of increased morbidity and mortality in endemic countries[38]. Therefore, routine dengue diagnosis is very essential in endemic countries as misdiagnosis or lack of diagnosis is likely to have tremendous public health consequences in the general management of febrile conditions in these regions.

DENGUE DIAGNOSTIC METHODS

Dengue diagnosis is relevant in epidemiological sur-

veillance, outbreak control, routine diagnosis in endemic countries among people with febrile diseases as well as diagnosis among travellers visiting or returning from endemic countries. There are several diagnostic assays such as virus culture, RNA detection, antigen detection and serology. These assays are associated with many advantages and disadvantages as well as different level of specificity and sensitivity.

Virus culture

This is usually done by inoculation of samples (serum, plasma or buffy coat) into mosquitoes cell lines such as C6/36 and AP61 or mammalian cell lines such as Vero and LLC-MK2 cells[39]. Sucking mice inoculated intra-cerebrally have also been used for the isolation of DENV[40]. Autopsy tissues from spleen, liver, thymus and lymph nodes have been used to isolate the virus from fatal cases[3]. After virus isolation, serotype identification is achieved by immunofluorescence using serotype-specific monoclonal antibodies. Despite the sensitivity of this method, the routine use is limited in endemic countries due to the fact that it requires improved laboratory safety capacity. The assay is also labor intensive and time consuming requiring adequate professional training. Also, virus detection is effective mostly during the early stages of the infection. It is therefore thought that, for better results, cultures should be performed using patient sample collected during the acute phase of the infection that may contain high viral copies. Acute infection is associated with rapid viral replication with high viral load that peaks before the onset of symptoms[3]. Therefore, timing of sample collection is very important for reliable test results.

Virus RNA detection

Dengue RNA can be detected by polymerase chain reaction (PCR) from tissues, blood or sera collected during the acute phase of the infection using primers directed to serotype-specific regions of the genome[41,42]. Common genomic regions for PCR include; E, NS1, E/NS1, prM/E, NS5 and NS5/3. Viral load may be quantified by RT-PCR while strain typing could be performed by nucleotide sequencing and phylogenetic analysis[43]. However, it is essential that laboratories performing nested PCR take every precaution to prevent false-positive results that can occur as a result of contamination[40]. A recent development of real-time PCR enables a simpler and faster assay with less exposure to contamination during concurrent dengue detection and typing. The assay utilizes oligonucleotide primers and dual-labeled hydrolysis probes for *in vitro* qualitative detection of DENV serotypes in a singleplex or multiplex reactions. However, this method is hampered by late sample collection (> 5 d after onset of symptoms). Therefore a negative result does not preclude dengue diagnosis and samples should be subjected to an anti-IgM ELISA for laboratory confirmation of infection. Although highly sensitive, the method is financially prohibitive as most dengue endemic countries lack the capacity to perform such nucleic acid amplification test.

Antigen detection

The detection of viral antigen has emerged as a potential alternative to PCR and virus culture. The main antigen target is the non-structural protein 1 (NS1). The NS1 antigen is produced during viral replication and can be detected in patients with primary and secondary dengue infections up to 9 d after the onset of disease[44]. NS1 is secreted in all infected cells during the acute phase of the infection and the presence in blood stimulates a strong humoral response. Quantification of the NS1 is a prognostic maker for dengue disease and higher levels have been linked to progression to DHF[45]. A recent study that evaluates a rapid NS1 assay in both Vietnam and Malaysia revealed the following; in Vietnam the sensitivity and specificity of the test was 69.2% (95%CI: 62.8% to 75.6%) and 96% (95%CI: 92.2% to 99.8%) respectively. In Malaysia the performance was similar with 68.9% sensitivity (95%CI: 61.8% to 76.1%) and 96.7% specificity (95%CI: 82.8% to 99.9%) compared to RT-PCR[46].

Serological methods

Serology is based on screening for dengue IgG/IgM antibodies. It is suggested that IgM production occurs 4-8 d after the onset of fever and last for a couple of weeks. On the other IgG production is low after primary infection but matures slowly within weeks and months and may last for several years[47]. ELISA-based IgM assays have become an important tool for the surveillance of dengue. Although these IgM-based assays are a useful diagnostic tool, results from these tests should be interpreted with caution. In addition, there is cross reactivity with other flaviviruses including West Nile virus (WNV), St. Louis encephalitis virus (SLE), Japanese encephalitis virus (JEV) and yellow fever virus (YFV). Therefore, during interpretation of results, patient's past medical history, recent travel history, and vaccination record (especially yellow fever vaccination) should be reviewed in order to determine the likelihood that the current acute febrile illness is due to an infection with DENV. There may also be false-negative results due to an extended seroconversion period[48]. The presence of anti-dengue IgM suggests recent infection while IgG antibody detection may be used for the classification of both primary and secondary infection[49]. That is a ratio of IgM/IgG greater than 1.78 represents primary infection and lesser than 1.78 represents secondary infections[48]. Also, the diagnostic value of IgA has been suggested and it has been shown that significantly higher levels of IgA antibodies occur in DHF/DSS than in DF cases[50]. The sensitivity and specificity of IgM-based assays is influenced by the quality of the antigen used and can vary greatly between commercially available products.

ROUTINE DENGUE DIAGNOSIS IN ENDEMIC COUNTRIES

In spite of the methods listed above, their routine use

in dengue endemic countries is limited due to either lack of laboratory capacity or skilled personnel. An ideal routine diagnostic test in endemic countries would fulfill the ASSURED criteria: (1) Affordable by those at risk of infection; (2) Sensitive; (3) Specific; (4) User-friendly; (5) Rapid and robust; (6) Equipment-free; and (7) Delivered to those who need it. The recent developments in rapid point-of-care (POC) immunochromatograhic tests (ICT) offer hopes for improved diagnosis of early dengue infection[51]. ICT for the detection of DENV NS1 antigen, IgG, IgM, and IgA antibodies promises to offer tremendous opportunities for the rapid detection of DENV in clinical samples. These ICT are manufactured in lateral flow cassettes and strips and allows the flow of sample by capillary action[52]. Considering that the majority of patients in developing countries are treated in primary health centers without the availability of a laboratory, POC testing may offer a unique advantage in the routine diagnosis of DENV among febrile patients. The tests can be performed in approximately 10-15 min and requires no specialized equipment or training.

PREVENTION AND CONTROL OF DENGUE

In the absence of specific antivirals and a vaccine, the main method of dengue control is to reduce the vector population and to educate people in endemic countries as well as travellers to these regions on basic protection measures such as wearing protective clothing and the use of anti-insecticide sprays.

Effective dengue control in endemic countries also requires more governmental, public and other stakeholder commitment and intervention at all levels. We recommend the following areas for action: Institution of policies for dengue to be a notifiable disease and the provision of POC diagnosis of dengue in febrile patients in endemic regions. Vector reduction activities by sustained environment and space spraying with larvicide as complementary measure. Unfortunately, there is lack of key indicator measurements for vector control programs at national surveillance systems in most tropical countries. Mobilization for public awareness on dengue control and the need to establish a sustained and integrated disease surveillance-response information and knowledge generation programs in vulnerable countries[53]. Effective waste disposal and water supply system management to reduce vector breeding grounds. Operational research is needed to generate evidence-based and cost-effective knowledge for innovative policies to outwit dengue from the region. Innovative approach on genetically modified mosquitoes to reduce vector population and interrupt transmission. Availability of the dengue vaccine, Dengvaxia (Sanofi Pasteur) for use in 9 to 45 years old persons in hotspots areas as well as accelerating dengue drug discovery and the availability of treatment.

CONCLUSION

This review outlined some of the basic public health issues associated with dengue control in endemic countries. Despite the increasing contribution of DENV as a major cause of febrile disease in developing countries, there is a high rate of misdiagnosis and underreporting from endemic countries, as well as lack of routine surveillance and public health prioritization. In summary, we suggest the need for public health commitment to include dengue as a notifiable disease, implement routine laboratory diagnosis and personnel training in endemic countries. Also, dengue NS1 ICTs or IgM antibody tests should be available at all primary health care centers to enable early detection of cases. Travellers visiting dengue endemic countries should be fully informed on symptoms of dengue and strongly urged to do a dengue test prior to departure or immediately after entering their own country, if they suspect infection by the virus, to reduce the risk of importation of the disease.

REFERENCES

1 **Bhatt S**, Gething PW, Brady OJ, Messina JP, Farlow AW, Moyes CL, Drake JM, Brownstein JS, Hoen AG, Sankoh O, Myers MF, George DB, Jaenisch T, Wint GR, Simmons CP, Scott TW, Farrar JJ, Hay SI. The global distribution and burden of dengue. *Nature* 2013; **496**: 504-507 [PMID: 23563266 DOI: 10.1038/nature12060]

2 **Gubler DJ**. The global emergence/resurgence of arboviral diseases as public health problems. *Arch Med Res* 2002; **33**: 330-342 [PMID: 12234522 DOI: 10.1016/S0188-4409(02)00378-8]

3 **Bäck AT**, Lundkvist A. Dengue viruses - an overview. *Infect Ecol Epidemiol* 2013; **3** [PMID: 24003364 DOI: 10.3402/iee.v3i0.19839]

4 **Mustafa MS**, Agrawal VK. Dengue Vaccine: The Current Status. *Med J Armed Forces India* 2008; **64**: 161-164 [PMID: 27408122 DOI: 10.1016/S0377-1237(08)80065-2]

5 **Mustafa MS**, Rasotgi V, Jain S, Gupta V. Discovery of fifth serotype of dengue virus (DENV-5): A new public health dilemma in dengue control. *Med J Armed Forces India* 2015; **71**: 67-70 [PMID: 25609867 DOI: 10.1016/j.mjafi.2014.09.011]

6 **Ebi KL**, Nealon J. Dengue in a changing climate. *Environ Res* 2016; **151**: 115-123 [PMID: 27475051 DOI: 10.1016/j.envres.2016.07.026]

7 **Brady OJ**, Gething PW, Bhatt S, Messina JP, Brownstein JS, Hoen AG, Moyes CL, Farlow AW, Scott TW, Hay SI. Refining the global spatial limits of dengue virus transmission by evidence-based consensus. *PLoS Negl Trop Dis* 2012; **6**: e1760 [PMID: 22880140 DOI: 10.1371/journal.pntd.0001760]

8 **Murray NE**, Quam MB, Wilder-Smith A. Epidemiology of dengue: past, present and future prospects. *Clin Epidemiol* 2013; **5**: 299-309 [PMID: 23990732 DOI: 10.2147/CLEP.S34440]

9 **McCall PJ**, Lenhart A. Dengue control. *Lancet Infect Dis* 2008; **8**: 7-9 [PMID: 18156083 DOI: 10.1016/S1473-3099(07)70298-0]

10 **Murray JV**, Jansen CC, De Barro P. Risk Associated with the Release of Wolbachia-Infected Aedes aegypti Mosquitoes into the Environment in an Effort to Control Dengue. *Front Public Health* 2016; **4**: 43 [PMID: 27047911 DOI: 10.3389/fpubh.2016.00043]

11 **Wagner D**, de With K, Huzly D, Hufert F, Weidmann M, Breisinger S, Eppinger S, Kern WV, Bauer TM. Nosocomial acquisition of dengue. *Emerg Infect Dis* 2004; **10**: 1872-1873 [PMID: 15504282 DOI: 10.3201/eid1010.031037]

12 **de Wet N**, Ye W, Hales S, Warrick R, Woodward A, Weinstein P. Use of a computer model to identify potential hotspots for dengue fever in New Zealand. *N Z Med J* 2001; **114**: 420-422 [PMID: 11700749]

13 **Hales S**, de Wet N, Maindonald J, Woodward A. Potential effect of population and climate changes on global distribution of dengue fever: an empirical model. *Lancet* 2002; **360**: 830-834 [PMID: 12243917 DOI: 10.1016/S0140-6736(02)09964-6]

14 **Ooi EE**, Goh KT, Gubler DJ. Dengue prevention and 35 years of vector control in Singapore. *Emerg Infect Dis* 2006; **12**: 887-893 [PMID: 16707042 DOI: 10.3201/eid1206.051210]

15 **Shepard DS**, Coudeville L, Halasa YA, Zambrano B, Dayan GH. Economic impact of dengue illness in the Americas. *Am J Trop Med Hyg* 2011; **84**: 200-207 [PMID: 21292885 DOI: 10.4269/ajtmh.2011.10-0503]

16 **Shepard DS**, Undurraga EA, Halasa YA, Stanaway JD. The global economic burden of dengue: a systematic analysis. *Lancet Infect Dis* 2016; **16**: 935-941 [PMID: 27091092 DOI: 10.1016/S1473-3099(16)00146-8]

17 **Brady OJ**, Smith DL, Scott TW, Hay SI. Dengue disease outbreak definitions are implicitly variable. *Epidemics* 2015; **11**: 92-102 [PMID: 25979287 DOI: 10.1016/j.epidem.2015.03.002]

18 **Ferreira GL**. Global dengue epidemiology trends. *Rev Inst Med Trop Sao Paulo* 2012; **54** Suppl 18: S5-S6 [PMID: 23011450 DOI: 10.1590/S0036-46652012000700003]

19 **Rasheed SB**, Butlin RK, Boots M. A review of dengue as an emerging disease in Pakistan. *Public Health* 2013; **127**: 11-17 [PMID: 23219263 DOI: 10.1016/j.puhe.2012.09.006]

20 **Amarasinghe A**, Kuritsk JN, Letson GW, Margolis HS. Dengue virus infection in Africa. *Emerg Infect Dis* 2011; **17**: 1349-1354 [PMID: 21801609 DOI: 10.3201/eid1708.101515]

21 **Kalayanarooj S**. Dengue classification: current WHO vs. the newly suggested classification for better clinical application? *J Med Assoc Thai* 2011; **94** Suppl 3: S74-S84 [PMID: 22043757]

22 **Kalayanarooj S**. Clinical Manifestations and Management of Dengue/DHF/DSS. *Trop Med Health* 2011; **39**: 83-87 [PMID: 22500140 DOI: 10.2149/tmh.2011-S10]

23 **Wilder-Smith A**, Gubler DJ. Geographic expansion of dengue: the impact of international travel. *Med Clin North Am* 2008; **92**: 1377-1390, x [PMID: 19061757 DOI: 10.1016/j.mcna.2008.07]

24 **Gubler DJ**. Dengue, Urbanization and Globalization: The Unholy Trinity of the 21(st) Century. *Trop Med Health* 2011; **39**: 3-11 [PMID: 22500131 DOI: 10.2149/tmh.2011-S05]

25 **Gardner LM**, Fajardo D, Waller ST, Wang O, Sarkar S. A predictive spatial model to quantify the risk of air-travel-associated dengue importation into the United States and europe. *J Trop Med* 2012; **2012**: 103679 [PMID: 22523497 DOI: 10.1155/2012/103679]

26 **Banu S**, Hu W, Hurst C, Tong S. Dengue transmission in the Asia-Pacific region: impact of climate change and socio-environmental factors. *Trop Med Int Health* 2011; **16**: 598-607 [PMID: 21320241 DOI: 10.1111/j.1365-3156.2011.02734.x]

27 **Napoli C**, Salcuni P, Pompa MG, Declich S, Rizzo C. Estimated imported infections of Chikungunya and Dengue in Italy, 2008 to 2011. *J Travel Med* 2012; **19**: 294-297 [PMID: 22943269 DOI: 10.1111/j.1708-8305.2012.00640.x]

28 **Sutherst RW**. Global change and human vulnerability to vector-borne diseases. *Clin Microbiol Rev* 2004; **17**: 136-173 [PMID: 14726459 DOI: 10.1128/CMR.17.1.136-173.2004]

29 **Senn N**, Luang-Suarkia D, Manong D, Siba PM, McBride WJ. Contribution of dengue fever to the burden of acute febrile illnesses in Papua New Guinea: an age-specific prospective study. *Am J Trop Med Hyg* 2011; **85**: 132-137 [PMID: 21734138 DOI: 10.4269/ajtmh.2011.10-0482]

30 **Cattand P**, Desjeux P, Guzman MG, Jannin J, Kroeger A, Medici A, Musgrove P, Nathan MB, Shaw A, Schofield CJ. Tropical Diseases Lacking Adequate Control Measures: Dengue, Leishmaniasis, and African Trypanosomiasis. In: Jamison DT, Breman JG, Measham AR, Alleyne G, Claeson M, Evans DB, Jha P, Mills A, Musgrove P, editors. Disease Control Priorities in Developing Countries. 2nd edition. Washington (DC): World Bank, 2006: Chapter 23 [PMID: 21250331]

31 **Hotez PJ**, Fenwick A, Savioli L, Molyneux DH. Rescuing the bottom billion through control of neglected tropical diseases. *Lancet* 2009; **373**: 1570-1575 [PMID: 19410718 DOI: 10.1016/S0140-6736(09)60233-6]

32 **Hotez PJ**. The neglected tropical diseases and their devastating health and economic impact on the member nations of the Organisation of the Islamic Conference. *PLoS Negl Trop Dis* 2009; **3**: e539 [PMID: 19859530 DOI: 10.1371/journal.pntd.0000539]

33 **Oyero OG**, Ayukekbong JA. High dengue NS1 antigenemia in febrile patients in Ibadan, Nigeria. *Virus Res* 2014; **191**: 59-61 [PMID: 25087878 DOI: 10.1016/j.virusres.2014.07.023]

34 **Deresinski S**. Concurrent plasmodium vivax malaria and dengue. *Emerg Infect Dis* 2006; **12**: 1802 [PMID: 17283647 DOI: 10.3201/eid1211.060341]

35 **Kaushik RM**, Varma A, Kaushik R, Gaur KJ. Concurrent dengue and malaria due to Plasmodium falciparum and P. vivax. *Trans R Soc Trop Med Hyg* 2007; **101**: 1048-1050 [PMID: 17568646 DOI: 10.1016/j.trstmh.2007.04.017]

36 **Charrel RN**, Brouqui P, Foucault C, de Lamballerie X. Concurrent dengue and malaria. *Emerg Infect Dis* 2005; **11**: 1153-1154 [PMID: 16032797 DOI: 10.3201/eid1107.041352]

37 **Yong LS**, Koh KC. A case of mixed infections in a patient presenting with acute febrile illness in the tropics. *Case Rep Infect Dis* 2013; **2013**: 562175 [PMID: 23533853 DOI: 10.1155/2013/562175]

38 **Zaki SA**. Malaria and dengue co-infection. *Ann Indian Acad Neurol* 2011; **14**: 141-142 [PMID: 21808485 DOI: 10.4103/0972-2327.82821]

39 **Rosen L**, Gubler D. The use of mosquitoes to detect and propagate dengue viruses. *Am J Trop Med Hyg* 1974; **23**: 1153-1160 [PMID: 4429185]

40 **Peeling RW**, Artsob H, Pelegrino JL, Buchy P, Cardosa MJ, Devi S, Enria DA, Farrar J, Gubler DJ, Guzman MG, Halstead SB, Hunsperger E, Kliks S, Margolis HS, Nathanson CM, Nguyen VC, Rizzo N, Vázquez S, Yoksan S. Evaluation of diagnostic tests: dengue. *Nat Rev Microbiol* 2010; **8**: S30-S38 [PMID: 21548185 DOI: 10.1038/nrmicro2459]

41 **Johnson BW**, Russell BJ, Lanciotti RS. Serotype-specific detection of dengue viruses in a fourplex real-time reverse transcriptase PCR assay. *J Clin Microbiol* 2005; **43**: 4977-4983 [PMID: 16207951 DOI: 10.1128/JCM.43.10.4977-4983.2005]

42 **Wu SJ**, Lee EM, Putvatana R, Shurtliff RN, Porter KR, Suharyono W, Watts DM, King CC, Murphy GS, Hayes CG, Romano JW. Detection of dengue viral RNA using a nucleic acid sequence-based amplification assay. *J Clin Microbiol* 2001; **39**: 2794-2798 [PMID: 11473994 DOI: 10.1128/JCM.39.8.2794-2798.2001]

43 **Chow VT**, Chan YC, Yong R, Lee KM, Lim LK, Chung YK, Lam-Phua SG, Tan BT. Monitoring of dengue viruses in field-caught Aedes aegypti and Aedes albopictus mosquitoes by a type-specific polymerase chain reaction and cycle sequencing. *Am J Trop Med Hyg* 1998; **58**: 578-586 [PMID: 9598444]

44 **Dussart P**, Labeau B, Lagathu G, Louis P, Nunes MR, Rodrigues SG, Storck-Herrmann C, Cesaire R, Morvan J, Flamand M, Baril L. Evaluation of an enzyme immunoassay for detection of dengue virus NS1 antigen in human serum. *Clin Vaccine Immunol* 2006; **13**: 1185-1189 [PMID: 16988003 DOI: 10.1128/CVI.00229-06]

45 **Libraty DH**, Young PR, Pickering D, Endy TP, Kalayanarooj S, Green S, Vaughn DW, Nisalak A, Ennis FA, Rothman AL. High circulating levels of the dengue virus nonstructural protein NS1 early in dengue illness correlate with the development of dengue hemorrhagic fever. *J Infect Dis* 2002; **186**: 1165-1168 [PMID: 12355369 DOI: 10.1086/343813]

46 **Fry SR**, Meyer M, Semple MG, Simmons CP, Sekaran SD, Huang JX, McElnea C, Huang CY, Valks A, Young PR, Cooper MA. The diagnostic sensitivity of dengue rapid test assays is significantly enhanced by using a combined antigen and antibody testing approach. *PLoS Negl Trop Dis* 2011; **5**: e1199 [PMID: 21713023 DOI: 10.1371/journal.pntd.0001199]

47 **Rubens Costa Lima J**, Rouquayrol MZ, Monteiro Callado MR, Florindo Guedes MI, Pessoa C. Interpretation of the presence of IgM and IgG antibodies in a rapid test for dengue: analysis of dengue antibody prevalence in Fortaleza City in the 20th year of the epidemic. *Rev Soc Bras Med Trop* 2012; **45**: 163-167 [PMID: 22534985 DOI: 10.1590/S0037-86822012000200005]

48 **Schwartz E**, Mileguir F, Grossman Z, Mendelson E. Evaluation of ELISA-based sero-diagnosis of dengue fever in travelers. *J Clin*

Virol 2000; **19**: 169-173 [PMID: 11090753 DOI: 10.1016/S1386-6532(00)00114-1]

49 **Blacksell SD**, Jarman RG, Gibbons RV, Tanganuchitcharnchai A, Mammen MP, Nisalak A, Kalayanarooj S, Bailey MS, Premaratna R, de Silva HJ, Day NP, Lalloo DG. Comparison of seven commercial antigen and antibody enzyme-linked immunosorbent assays for detection of acute dengue infection. *Clin Vaccine Immunol* 2012; **19**: 804-810 [PMID: 22441389 DOI: 10.1128/CVI.05717-11]

50 **Koraka P**, Murgue B, Deparis X, Setiati TE, Suharti C, van Gorp EC, Hack CE, Osterhaus AD, Groen J. Elevated levels of total and dengue virus-specific immunoglobulin E in patients with varying disease severity. *J Med Virol* 2003; **70**: 91-98 [PMID: 12629649 DOI: 10.1002/jmv.10358]

51 **Peeling RW**, Mabey D. Point-of-care tests for diagnosing infections in the developing world. *Clin Microbiol Infect* 2010; **16**: 1062-1069 [PMID: 20670288 DOI: 10.1111/j.1469-0691.2010.03279.x]

52 **Blacksell SD**. Commercial dengue rapid diagnostic tests for point-of-care application: recent evaluations and future needs? *J Biomed Biotechnol* 2012; **2012**: 151967 [PMID: 22654479 DOI: 10.1155/2012/151967]

53 **Badurdeen S**, Valladares DB, Farrar J, Gozzer E, Kroeger A, Kuswara N, Ranzinger SR, Tinh HT, Leite P, Mahendradhata Y, Skewes R, Verrall A. Sharing experiences: towards an evidence based model of dengue surveillance and outbreak response in Latin America and Asia. *BMC Public Health* 2013; **13**: 607 [PMID: 23800243 DOI: 10.1186/1471-2458-13-607]

54 **Gautret P**, Simon F, Hervius Askling H, Bouchaud O, Leparc-Goffart I, Ninove L, Parola P. Dengue type 3 virus infections in European travellers returning from the Comoros and Zanzibar, February-April 2010. *Euro Surveill* 2010; **15**: 19541 [PMID: 20429996]

55 **Vinner L**, Domingo C, Ostby AC, Rosenberg K, Fomsgaard A. Cases of travel-acquired dengue fever in Denmark 2001-2009. *Clin Microbiol Infect* 2012; **18**: 171-176 [PMID: 21745259 DOI: 10.1111/j.1469-0691.2011.03543.x]

56 **Pierro A**, Varani S, Rossini G, Gaibani P, Cavrini F, Finarelli AC, Macini P, Cagarelli R, Mattivi A, Angelini P, Landini MP, Sambri V. Imported cases of dengue virus infection: Emilia-Romagna, Italy, 2010. *Clin Microbiol Infect* 2011; **17**: 1349-1352 [PMID: 21745260 DOI: 10.1111/j.1469-0691.2011.03544.x]

57 **Marchand E**, Prat C, Jeannin C, Lafont E, Bergmann T, Flusin O, Rizzi J, Roux N, Busso V, Deniau J, Noel H, Vaillant V, Leparc-Goffart I, Six C, Paty MC. Autochthonous case of dengue in France, October 2013. *Euro Surveill* 2013; **18**: 20661 [PMID: 24342514 DOI: 10.2807/1560-7917.ES2013.18.50.20661]

58 **Gautret P**, Botelho-Nevers E, Charrel RN, Parola P. Dengue virus infections in travellers returning from Benin to France, July-August 2010. *Euro Surveill* 2010; **15**: pii: 19657 [PMID: 20843471]

59 **Frank C**, Höhle M, Stark K, Lawrence J. More reasons to dread rain on vacation? Dengue fever in 42 German and United Kingdom Madeira tourists during autumn 2012. *Euro Surveill* 2013; **18**: 20446 [PMID: 23594519 DOI: 10.2807/1560-7917.ES2013.18.14.20446]

60 **Heddini A**, Janzon R, Linde A. Increased number of dengue cases in Swedish travellers to Thailand. *Euro Surveill* 2009; **14**: pii: 19111 [PMID: 19215716]

61 **Nisii C**, Carletti F, Castilletti C, Bordi L, Meschi S, Selleri M, Chiappini R, Travaglini D, Antonini M, Castorina S, Lauria FN, Narciso P, Gentile M, Martini L, Di Perri G, Audagnotto S, Biselli R, Lastilla M, Di Caro A, Capobianchi M, Ippolito G. A case of dengue type 3 virus infection imported from Africa to Italy, October 2009. *Euro Surveill* 2010; **15**: pii: 19487 [PMID: 20184855]

62 **Huhtamo E**, Korhonen E, Vapalahti O. Imported dengue virus serotype 1 from Madeira to Finland 2012. *Euro Surveill* 2013; **18**: pii: 20405 [PMID: 23449230]

63 **Schmidt-Chanasit J**, Emmerich P, Tappe D, Gunther S, Schmidt S, Wolff D, Hentschel K, Sagebiel D, Schoneberg I, Stark K, Frank C. Autochthonous dengue virus infection in Japan imported into Germany, September 2013. *Euro Surveill* 2014; **19**: pii: 20681 [PMID: 24480059 DOI: 10.2807/1560-7917.ES2014.19.3.20681]

64 **Schmidt-Chanasit J**, Haditsch M, Schoneberg I, Gunther S, Stark K, Frank C. Dengue virus infection in a traveller returning from Croatia to Germany. *Euro Surveill* 2010; **15**: pii: 19677 [PMID: 20946759]

P- Reviewer: Bonilauri P, Garg RK, Kim ST, Santos-Lopez G
S- Editor: Ji FF **L- Editor**: A **E- Editor**: Lu YJ

World Journal of Virology

Submit a Manuscript: http://www.wjgnet.com/esps/
Help Desk: http://www.wjgnet.com/esps/helpdesk.aspx
DOI: 10.5501/wjv.v6.i1.17

World J Virol 2017 February 12; 6(1): 17-25
ISSN 2220-3249 (online)

ORIGINAL ARTICLE

Basic Study

Expression of hepatitis B virus surface antigens induces defective gonad phenotypes in *Caenorhabditis elegans*

Yi-Yin Chen, Li-Wei Lee, Wei-Ning Hong, Szecheng J Lo

Yi-Yin Chen, Li-Wei Lee, Szecheng J Lo, Department of Biomedical Science, College of Medicine, Chang Gung University, Tao Yuan 333, Taiwan

Yi-Yin Chen, Wei-Ning Hong, Szecheng J Lo, Graduate Institute of Biomedical Science, College of Medicine, Chang Gung University, Tao Yuan 333, Taiwan

Author contributions: Chen YY, Lee LW and Lo SJ conceived and designed experiments; Chen YY, Lee LW and Hong WN performed the experiments; Chen YY and Lo SJ analyzed data; Lee LW and Lo SJ wrote the paper.

Supported by Chang Gung Memorial Hospital, grants Nos. CMRPD1C0812, CMRPD1C0813 and BMRP742 (to Lo SJ).

Institutional review board statement: No.

Informed consent statement: No.

Conflict-of-interest statement: The authors declare no conflict of interest.

Data sharing statement: No.

Manuscript source: Invited manuscript

Correspondence to: Szecheng J Lo, PhD, Professor, Department of Biomedical Science, College of Medicine, Chang Gung University, #259 Wen-Hwa 1st Road, Tao Yuan 333, Taiwan. losj@mail.cgu.edu.tw
Telephone: +886-3-2118800-3259
Fax: +886-3-2118392

Received: June 24, 2016
Peer-review started: June 27, 2016
First decision: September 5, 2016
Revised: October 9, 2016
Accepted: November 27, 2016
Article in press: November 29, 2016
Published online: February 12, 2017

Abstract

AIM

To test whether a simple animal, *Caenorhabditis elegans* (*C. elegans*), can be used as an alternative model to study the interaction between hepatitis B virus antigens (HBsAg) and host factors.

METHODS

Three plasmids that were able to express the large, middle and small forms of HBsAgs (LHBsAg, MHBsAg, and SHBsAg, respectively) driven by a ubiquitous promoter (*fib-1*) and three that were able to express SHBsAg driven by different tissue-specific promoters were constructed and microinjected into worms. The brood size, egg-laying rate, and gonad development of transgenic worms were analyzed using microscopy. Levels of mRNA related to endoplasmic reticulum stress, *enpl-1*, *hsp-4*, *pdi-3* and *xbp-1*, were determined using reverse transcription polymerase reaction (RT-PCRs) in three lines of transgenic worms and dithiothreitol (DTT)-treated wild-type worms.

RESULTS

Severe defects in egg-laying, decreases in brood size, and gonad retardation were observed in transgenic worms expressing SHBsAg whereas moderate defects were observed in transgenic worms expressing LHBsAg and MHBsAg. RT-PCR analysis revealed that *enpl-1*, *hsp-4* and *pdi-3* transcripts were significantly elevated in worms expressing LHBsAg and MHBsAg and in wild-

type worms pretreated with DTT. By contrast, only *pdi-3* was increased in worms expressing SHBsAg. To further determine which tissue expressing SHBsAg could induce gonad retardation, we substituted the *fib-1* promoter with three tissue-specific promoters (*myo-2* for the pharynx, *est-1* for the intestines and *mec-7* for the neurons) and generated corresponding transgenic animals. Moderate defective phenotypes were observed in worms expressing SHBsAg in the pharynx and intestines but not in worms expressing SHBsAg in the neurons, suggesting that the secreted SHBsAg may trigger a cross-talk signal between the digestive track and the gonad resulting in defective phenotypes.

CONCLUSION
Ectopic expression of three forms of HBsAg that causes recognizable phenotypes in transgenic worms suggests that *C. elegans* can be used as an alternative model for studying virus-host interactions because the resulting phenotype is easily detected through microscopy.

Key words: Hepatitis B virus; *Caenorhabditis elegans*; Green fluorescence proteins; Endoplasmic reticulum stress; Gonad retardation; Surface antigens

Core tip: In the past, mouse and cell culture models have been used for studying the effects of hepatitis B virus antigens (HBsAg) on hosts. Both models have advantages and disadvantages in terms of economic and time concerns. In this study, we provide an alternative animal model, *Caenorhabditis elegans (C. elegans)*, to demonstrate that SHBsAg can induce observable phenotypes which has never been reported in mouse and cell culture models. We suggest that *C. elegans* can serve as a new plateform for studying various viral pathogenesis.

Chen YY, Lee LW, Hong WN, Lo SJ. Expression of hepatitis B virus surface antigens induces defective gonad phenotypes in *Caenorhabditis elegans*. *World J Virol* 2017; 6(1): 17-25 Available from: URL: http://www.wjgnet.com/2220-3249/full/v6/i1/17.htm DOI: http://dx.doi.org/10.5501/wjv.v6.i1.17

INTRODUCTION

Human hepatitis B virus (HBV), a member of the family *Hepadnaviride*, is a partially double-stranded DNA virus. The genome of HBV contains approximately 3200 nucleotides that encodes four open reading frames, namely surface (S), core (C), polymerase (P) and X in an overlapping but frame-shifted manner[1-3]. Infection with HBV inducers a broad range of clinical outcomes, from asymptomatic hepatitis to fulminant hepatitis. Chronic hepatitis B carriers are highly associated with the development of liver cirrhosis and hepatocellular carcinoma[4,5]. Molecular biology analyses from tumor samples have revealed that HBV DNA integration could activate genes associated with the cell cycles, leading to abnormal cell proliferation[6,7]. Pathogenesis and etiology studies have found that X and truncated preS proteins play oncogenic roles[8-10].

Woodchucks were the first animal model for studying liver carcinogenesis caused by natural woodchuck hepatitis virus (WHV) infection[11,12]. A high incidence of liver tumor formation occurs in newborn woodchucks infected with WHV. Molecular dissection has revealed that *c-myc* oncogene level are highly elevated in liver tumors[13,14]. Later, the transgenic mouse model was applied to express an individual viral protein, such as the large hepatitis B surface antigen (LHBsAg) and X protein, which are driven by the albumin promoter for specific expression in the liver, to study the mechanisms of liver carcinogenesis induced by viral proteins[15,16]. In combining molecular biology analyses of the HBV X (HBx) gene in transfected cells, numerous studies have elucidated that the X protein is multifunctional and induces transactivation activity, signal transduction and cell death[9,17,18]. Recently, Geng *et al*[19] employed *Caenorhabditis elegans* (*C. elegans*), a soil nematode, to express HBx under a heat shock control and found that HBx induced cell apoptosis and necrosis through the interaction of HBx and CED-9, a human homolog of Bcl-2.

C. elegans was first used as a model organism for studying development and the nervous system because the species is transparent throughout its life span and in its adult form, possesses approximately 300 neurons out of 1000 somatic cells[20,21]. Because of its short-life cycle, simplicity, numerous available mutated forms, and ease of handling for knocking-down specific gene, *C. elegans* is now a model for studying various biological topics, such as aging, human diseases, host-pathogen interaction and viral pathogenesis[22-25]. Because of a high percentage of genes in numerous cellular pathways is conserved across nematodes to vertebrates, a study of PEG-mediated *Poxviridae* infection in *C. elegans* revealed that the core genes of apoptosis (*ced-3* and *ced-4*) control vaccinia virus replication in worms[26,27]. Therefore, *C. elegans* could serve as a new platform for virologists to study virus-host interaction and pathogenesis in addition to the currently used cell culture and mammalian models. In this study, we expressed three forms of HBsAg in *C. elegans* to determine different degrees of defects in gonad development.

MATERIALS AND METHODS

Plasmid constructions

P_{fib-1}::gfp::icr::SHBsAg: A 1.5 kb fragment excised from the P_{fib-1}::gfp::LD plasmid[28] by cutting with *Hind*Ⅲ and *Age* Ⅰ and was isolated and then inserted into the *Hind*Ⅲ and *Age* Ⅰ sites of pPD95.75 to generate P_{fib-1}::gfp. P_{fib-1}::gfp was then cut with *EcoR* Ⅰ and ligated with a 0.8 kb of icr::SHBsAg fragment which was isolated from P_{fib-1}::LD::icr::SHBsAg to generate a 6.8 kb of P_{fib-1}::

gfp::icr::SHBsAg. When microinjection of $P_{fib-1::}$gfp::icr::SHBsAg into N2 strain, worms expressed green fluorescence proteins (GFP) and HBV small surface antigens (SHBsAg).

$P_{fib-1::}$gfp::icr::linker: A linker was designed to contain *EcoR* Ⅰ, *Not* Ⅰ, *Bgl* Ⅱ, *Sal* Ⅰ, *Nsi* Ⅰ and *Sac* Ⅰ cutting sites. This linker was ligated to $P_{fib-1::}$gfp and generated plasmid $P_{fib-1::}$gfp::linker. $P_{fib-1::}$gfp::linker was cut with *EcoR* Ⅰ *and Not* Ⅰ and ligated with an icr fragment which was isolated from $P_{fib-1::}$gfp::icr::SHBsAg to generate a 6.2 kb of $P_{fib-1::}$gfp::icr::linker plasmid.

$P_{fib-1::}$gfp::icr::MHBsAg: A 680 bp of MHBsAg DNA fragment was amplified from pMH3/3097[29] using primers HBVs(M)-Not Ⅰ-F and HBVs-Sal Ⅰ-R. This fragment was ligated with $P_{fib-1::}$gfp::icr::linker to generate a 7.0 kb of $P_{fib-1::}$gfp::icr::MHBsAg. Transgenic worm carrying $P_{fib-1::}$gfp::icr::MHBsAg expressed GFP and MHBsAg.

$P_{fib-1::}$gfp::icr::LHBsAg: A 1.1 kb of LHBsAg DNA fragment was amplified from pMH3/3097[29] using primers HBVs(L)-NotI-F and HBVs-Sal Ⅰ-R. This fragment was ligated with $P_{fib-1::}$gfp::icr::linker to generate a 7.3 kb of $P_{fib-1::}$gfp::icr::LHBsAg. When microinjection of $P_{fib-1::}$gfp::icr::LHBsAg into N2 strain, worms expressed GFP and LHBsAg.

$P_{myo-2::}$gfp::icr::SHBsAg: The fragment of *fib-1* promoter was cut from P_{fib-1}GFP-icr-SHBsAg by digestion with *Hind* Ⅲ and *Age*I, and replaced with the *myo-2* promoter which was isolated from $P_{myo-2::}$gfp::icr::DsRed::LD[28] to create a 6.6 kb of $P_{myo-2::}$gfp::icr::SHBsAg. Transgenic worms carrying this plasmid expressed both GFP and SHBsAg in pharynx.

$P_{mec-7::}$gfp::icr::SHBsAg: The plasmid was generated by substitution of the *fib-1* promoter of $P_{fib-1::}$gfp::icr::SHBsAg with the *mec-7* promoter which was isolated from $P_{mec-7::}$gfp::icr::DsRed::LD[28] to create a 6.3 kb of $P_{mec-7::}$GFP::icr::SHBsAg. Transgenic worms carrying this plasmid expressed GFP and SHBsAg in neurons.

$P_{ges-1::}$gfp::icr::SHBsAg: The plasmid was generated by substitution of the *fib-1* promoter of $P_{fib-1::}$gfp::icr::SHBsAg with the *ges-1* promoter which was isolated from $P_{ges-1::}$gfp::icr::DsRed::LD[28] to create a 6.6 kb of $P_{ges-1::}$gfp::icr::SHBsAg. Transgenic worms carrying this plasmid expressed GFP and SHBsAg in intestinal cells.

Primers used in this study

For plasmid constructions and RT-PCR analyses, the following paired primers were used: linker-F: 5′-aat tcaaaaagcggccgcagatctgtcgacatgcatgagctc-3′; linker-R: 5′-gtttttcgccggcgtctagacagctgtacg tactcgagttaa-3′; HBVs(L)+Not Ⅰ-F: 5′-gggaacaagag cggccgcatggggcag-3′; HBVs(M)+Not Ⅰ-F: 5′-acactc atcgcggccgcatgcagtgg-3′; HBVs+Sal Ⅰ-R: 5′-gttttgtgtcgacttaaatgtataccc-3′; eft-2-F: 5′-ggtggtcaaatcatcccaac-3′; eft-2-R: 5′-tcc-tcgaaaacgtgtcctct-3′; endoplasmin-F: 5′-t gaaaa cctccaacagcaca-3′; endoplasmin-R: 5′-gcagtttccttg agccagtc-3′; hsp-4-F: 5′-ttttcgaggttcttgccact-3′; hsp-4-R: 5′-tctccggtattttcgacacc-3′; PDI-F: 5′-gccgtttcca aca aagaaga-3′; PDI-R: 5′-cccttgagc ccatcagtaga-3′; xbp-1-F: 5′-cgtcgtcta cgaagaagaagtcgtc-3′; xbp-1-R: 5′-gatg ata gttagatacatatccacactg-3′.

Worm strains and culture

N2 (wild-type) worm was obtained from the *Caenorhabditis* Genetics Center (CGC, University of Minnesota) and cultured on Nematode Growth Medium (NGM) following standard methods[20]. Images of transgenic worms were acquired using Leica DM2500 equipped with CoolSNAP K4 (photometrics) and processed with a MetaMorph (version 6.1).

Microinjection

Plasmid DNA was prepared by using QIAprep spin miniprep kit and the concentration was adjusted at 100 ng/μL in injection buffer (20 mmol/L potassium phosphate, pH 7.5, 3 mmol/L potassium citrate, pH 7.5, 2% polyethylene glycol, M.W. 6000). The injection mixture also contained pRF-4 which was included as a screening marker. Worm was placed onto 2% agarose pads and injected by capillary needle loaded with DNA mixture using a FemtoJet system (Eppendorf AG, Hamburg, Germany). The glass capillaries were purchased from World Precision Instruments (Kwik-Fil™, borosilicate 16 glass capillaries, item number 1B100F-6, United States) and pull by Flaming/Brown micropipette puller (MODEL P-97, Sutter Instrument Co., United States).

Measurement of egg-laying activity and brood size

Worms were first synchronized and placed one worm per a single plate. The offspring in each plate were counted every day.

Microscopy

For visualization of GFP expression in transgenic worms, an upright fluorescence microscope (Leica DM2500) was used. For visualization of gonad structure and development a differential interference contrast (DIC) microscope was used and images were captured using a cool CCD (CoolSNAP K4).

Reverse transcription

The total RNA was extracted from transgenic worms expressed both GFP and HBsAgs with TRIzol reagent. The reverse transcription reaction was first carried out with 4 μg of RNA, 2 μL of dNTP (10 mmol/L), 2 μL of Oligo-dT (10 mmol/L), and added DEPC H_2O to 12 μL. After incubated at 68 ℃ for 5 min, the mixture was then added 4 μL of 5 × first-strand buffer (invitrogen), 2 μL of DTT (0.1 mmol/L, invitrogen), 1 μL of RNase inhibitor (invitrogen) and 1 μL of Reverse Transcriptase (invitrogen) and incubated at 42 ℃ for 50 min, and then 70 ℃ for

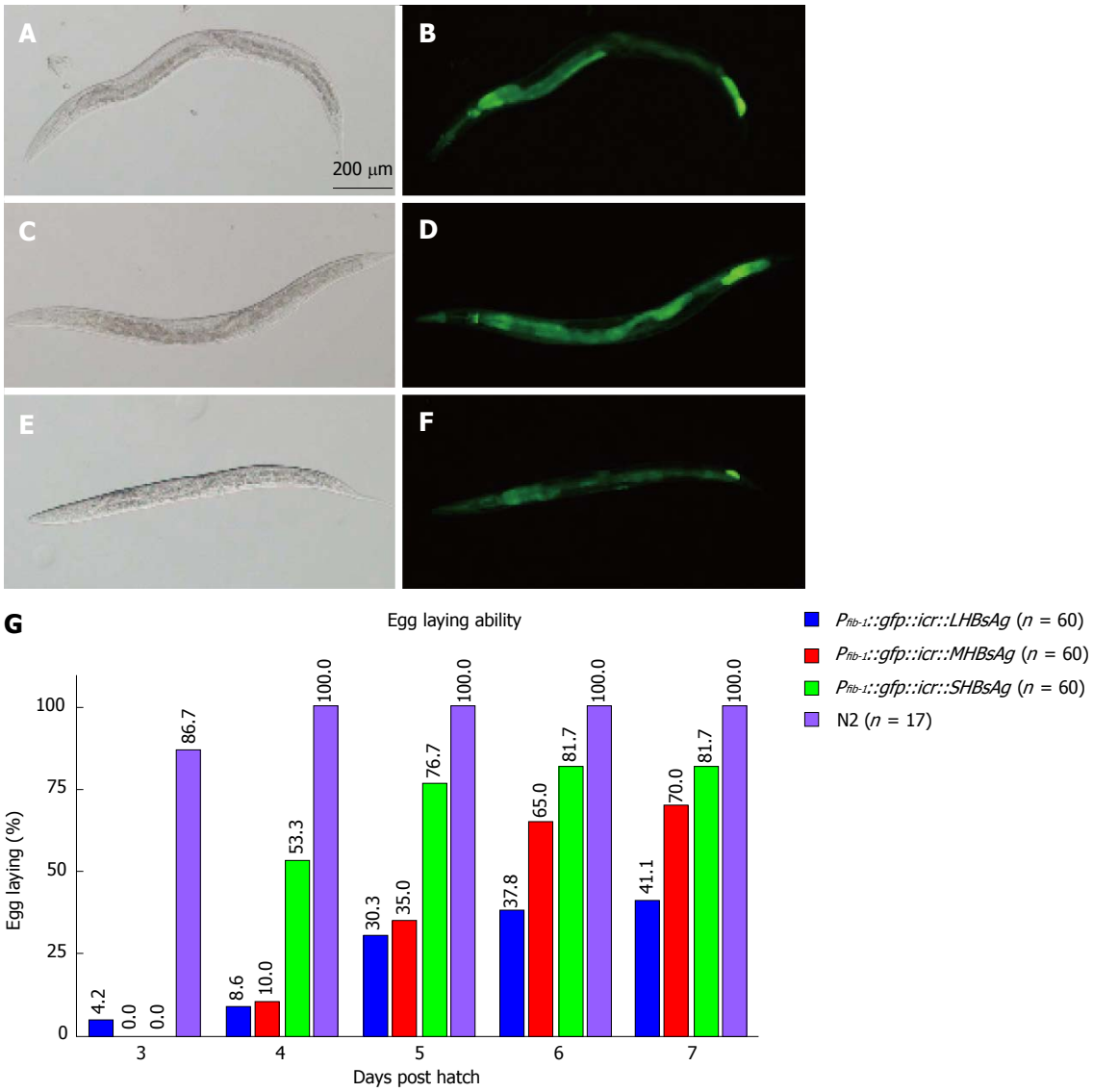

Figure 1 Expression of various lengths of hepatitis B virus antigens in whole worms induced defects in the rate of egg-laying. A-F: Micrographs of transgenic worms expressing LHBsAg (A and B), MHBsAg (C and D), and SHBsAg (E and F) were captured under a bright-field microscope (A, C, and E) and a fluorescence microscope (B, D, and F). The heads of the worms are shown toward the left. The scale bar indicates 200 μm. G: Egg-laying capability of three lines of transgenic worms and wild-type worms (N2) shown using various color bars. The rate of egg-laying in 3 to 7 d post-hatching is shown above the bar. HBsAgs: Hepatitis B virus antigens.

15 min. The primers used in PCR analyses were listed as above.

RESULTS

Expression of three forms of HBsAg reduces egg-laying capability

To determine whether *C. elegans* can be a new platform for studying virus-host interaction we ectopically expressed three lengths of HBsAg (SHBsAg, MHBsAg, and LHBsAg) in worms under the control of the ubiquitous promoter fibrillarin (*fib-1*). Three HBsAg gene sequences were individually placed in a bicistronic vector behind a reporter gene, green fluorescence protein (GFP), which was used as a selection marker[30]. Transgenic worms were selected for the expression of GFP (Figure 1A-F) and maintained to characterize phenotypes. After synchronization, transgenic worms were singled out and placed on single plates, and the numbers of eggs produced by individual worms were counted every day. The results showed different egg-laying averages in a total of 60 transgenic animals in three groups expressing SHBsAg, MHBsAg, and LHBsAg (Figure 1G). On the fourth day after hatching, the wild-type worms (N2) displayed an egg-laying rate of 100% whereas those worms expressing SHBsAg, MHBsAg, and LHBsAg demonstrated laying-egg rates of approximately 8.6%, 10%, and 53.3%, respectively. Although the egg-laying rates of the three lines of transgenic worms increased in the following days, the maximum egg-laying rate was 41.1% for worms expressing SHBsAg, 70% for worms expressing MHBsAg and 81.7% for worms expressing LHBsAg at 7 d post-hatching (Figure 1B). The reduced rate of egg-laying in the three lines of HBsAg-expressing

Table 1 Comparison of egg-laying ability and brood size among various transgenic worms

Construct	Strain	Ecotopic proteins	Protein expression site	Egg-laying ability (%)	Brood size
	N2			100 (n = 17)	290 ± 15 (n = 17)
Pfib-1::gfp::icr	N2	GFP	Whole worm	100 (n = 10)	268 ± 29 (n = 18)
Pfib-1::gfp::icr::SHBsAg	N2	GFP, SHBsAg	Whole worm	9 (n = 60)	66 ± 15 (n = 14)
Pfib-1::gfp::icr::MHBsAg	N2	GFP, MHBsAg	Whole worm	10 (n = 60)	175 ± 50 (n = 15)
Pfib-1::gfp::icr::LHBsAg	N2	GFP, LHBsAg	Whole worm	54 (n = 60)	239 ± 14 (n = 15)
Pmyo-2::gfp::icr::SHBsAg	N2	GFP, SHBsAg	Pharynx	83 (n = 60)	163 ± 20 (n = 26)
Pges-1::gfp::icr::SHBsAg	N2	GFP, SHBsAg	Intestine	97 (n = 60)	203 ± 50 (n = 32)
Pmec-7::gfp::icr::SHBsAg	N2	GFP, SHBsAg	Neuron	100 (n = 60)	270 ± 42 (n = 26)

HBsAgs: Hepatitis B virus antigens; GFP: Green fluorescence proteins; SHBsAg: Human hepatitis B virus small surface antigens; MHBsAg: Human hepatitis B virus middle surface antigens; LHBsAg: Human hepatitis B virus large surface antigens.

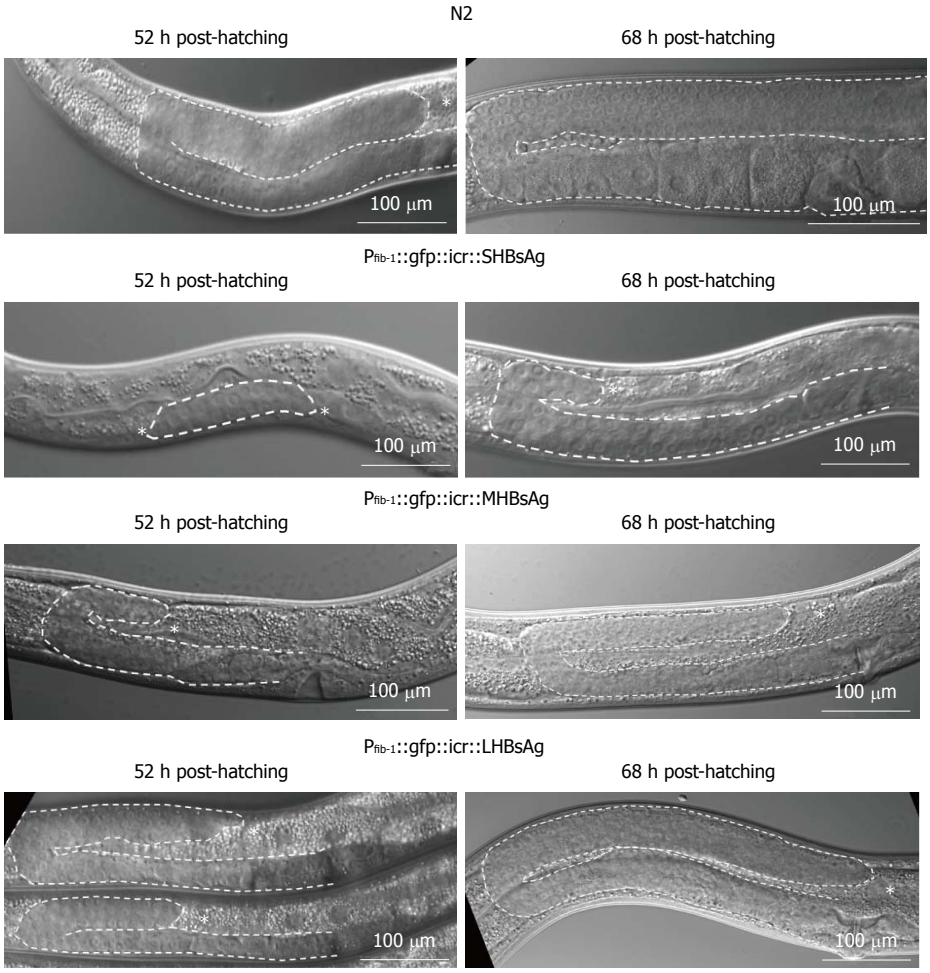

Figure 2 Differential interference contrast micrographs of gonad development in transgenic worms at various post-hatching times. The upper row shows a wild-type worm (N2); the second row shows a transgenic worm expressing SHBsAg; the third row shows a transgenic worm expressing MHBsAg; and the bottom row shows a transgenic worm expressing LHBsAg. The right column shows the gonads at 52 h post-hatching and the left column at shows gonads at 68 h post-hatching expect the worm expressing SHBsAg is at 72 h post-hatching. The gonad contour is indicated with dotted lines and the tip (distal end) is marked by asterisk.

worms was unlikely to have caused by the ectopic expression of GFP because worms carrying a plasmid with the sole function of expressing GFP throughout the body exhibited egg-laying capability of 100% (Table 1).

Expression of SHBsAg causes the most severe gonad retardation

To understand why the expression of various lengths of HBsAg in transgenic worms caused a reduction in egg-laying capability, we examined the gonad development of the three types of transgenic worms under a DIC microscope. As shown in Figure 2 (upper two rows), at 52 h after hatching, wild-type worms had nearly completed the gonad development; by contrast, worms expressing SHBsAg exhibited a dramatic retardation of gonad development in larval stage 3 (L3). The process of oogenesis was observed in N2 worms 68 h post hatching whereas the gonads of worms expressing SHBsAg were

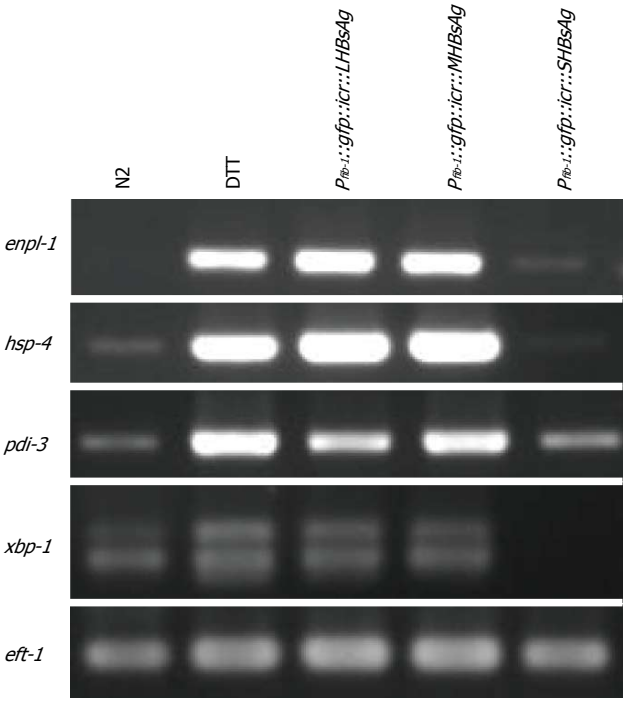

Figure 3 Reverse transcription polymerase reaction analyses of mRNA levels in various transgenic worms. The four transcripts (*enpl-1*, *hsp-4*, *pdi-3*, and *xbp-1*), ER-stress markers, from wild-type worms (N2) with or without DTT pretreatment, an ER stress inducer, and three lines of transgenic worms were analyzed using RT-PCR and gel-electrophoresis. The transcript of the translation factor (*eft-2*) served as a loading control. N2 worms treated with and without DTT and transgenic worms are indicated above the gel. DTT-treated worms severed as positive controls of ER-stress responses. DTT: Dithiothreitol; RT-PCR: Reverse transcription polymerase reaction.

only just beginning to turn as mid-stage of larva 4 as 72 h post-hatching. Oogenesis was observed in some worms expressing SHBsAg until 96 h post-hatching (data not shown). Worms expressing MHBsAg and LHBsAg at 52 h and 68 h post-hatching showed a retardation of gonad development that was less severe than that observed in worms expressing SHBsAg at a similar stage (Figure 2, lower two rows). The severity of gonad retardation clearly reflected the reduced percentage of egg-laying (9%, 10%, and 54%, respectively) and average brood size (66, 175, and 239, respectively) in the three lines of transgenic worms, as shown in Table 1.

Gonad retardation caused by SHBsAg may operate through unknown pathways

A previous study reported that endoplasmic reticulum (ER) stress could cause retardation of gonad development[31]. To determine whether the defective phenotypes of the three lines of transgenic worms resulted from ER stress, we performed RT-PCR analysis of ER stress markers. Total RNA from the three lines of transgenic worms and N2 worms with or without DTT treatment was isolated and analyzed for the expression levels of *enpl-1*, *hsp-4*, *pdi-3* and *xbp-1* through RT-PCR. The results of the gel-electrophoresis of RT-PCR products indicated that the levels of *enpl-1, hsp-4* and *pdi-3* were substantially elevated in worms expressing LHBsAg and MHBsAg, being similar to those N2 worms pretreated with the ER stress-inducer DTT whereas the *xbp-1* level had increased only slightly (Figure 3). Only a slight increase in the level of *pdi-3* was observed in worms expressing SHBsAg compared with that of wild-type worms, and no obvious elevation of other ER stress-related transcripts was detected. We concluded that the defective phenotypes caused by the expression of LHBsAg and MHBsAg were likely attributable to ER stress signals. By contrast, the defect induced by the expression of SHBsAg might have been caused by other unknown pathways.

Expression of SHBsAg in the pharynx and intestines induces defective phenotypes

To determine which tissues expressing SHBsAg were responsible for gonad retardation, we substituted the *fib-1* promoter with *myo-2*, *ges-1*, and *mec-7*, to express SHBsAg in the pharynx, intestines, and neurons, respectively. Transgenic worms expressing GFP in the pharynx, intestines, and neurons were selected (Figure 4A) and analyzed for egg-laying capability and gonad development. As shown in Table 1, 100% and 97% egg-laying capability were found in worms expressing SHBsAg in the neurons and intestines, respectively, compared with 83% egg-laying capability in worms expressing SHBsAg through *myo-2*. When examining the gonad development of the three lines of transgenic worms using DIC, we found no obvious retardation in worms expressing SHBsAg in neuron at 52 h and 68 h post-hatching and a moderate level of gonad retardation in worms expressing SHBsAg in the pharynx and intestines (Figure 4B). This suggested that cross-talk between the digestive and reproductive system may be triggered by secreted SHBsAg, causing defects in a small portion of the population.

DISCUSSION

In this study, we demonstrated that transgenic worms expressing three forms of HBsAgs throughout the body exhibited lower rates of egg-laying, reduced brood sizes and retardation of gonad development to various degrees. Unexpectedly, worms expressing SHBsAg displayed the most severe defects (Table 1). No study has yet reported that the expression of SHBsAg can induce detectable phenotypes in cultured cells or animals; however, ER-stress and tumor formation have been observed in cells and animals expressing LHBsAg and MHBsAg[16,32]. Consistent with previous studies, worms expressing LHBsAg and MHBsAg were found to possess higher levels of *enpl-1*, *hsp-4*, *pdi-3* and *xbp-1* transcripts as did N2 worms pretreated with DTT (Figure 3). Because the gonad is the organ most sensitive to environmental changes[33], we suggest that ER-stress signal occurring autonomously or non-autonomously in the gonad can lead to gonad retardation, a reduced rate of egg-laying, and a smaller brood sizes in transgenic worms expressing LHBsAg and MHBsAg.

The unexpected results of the most severe pheno-

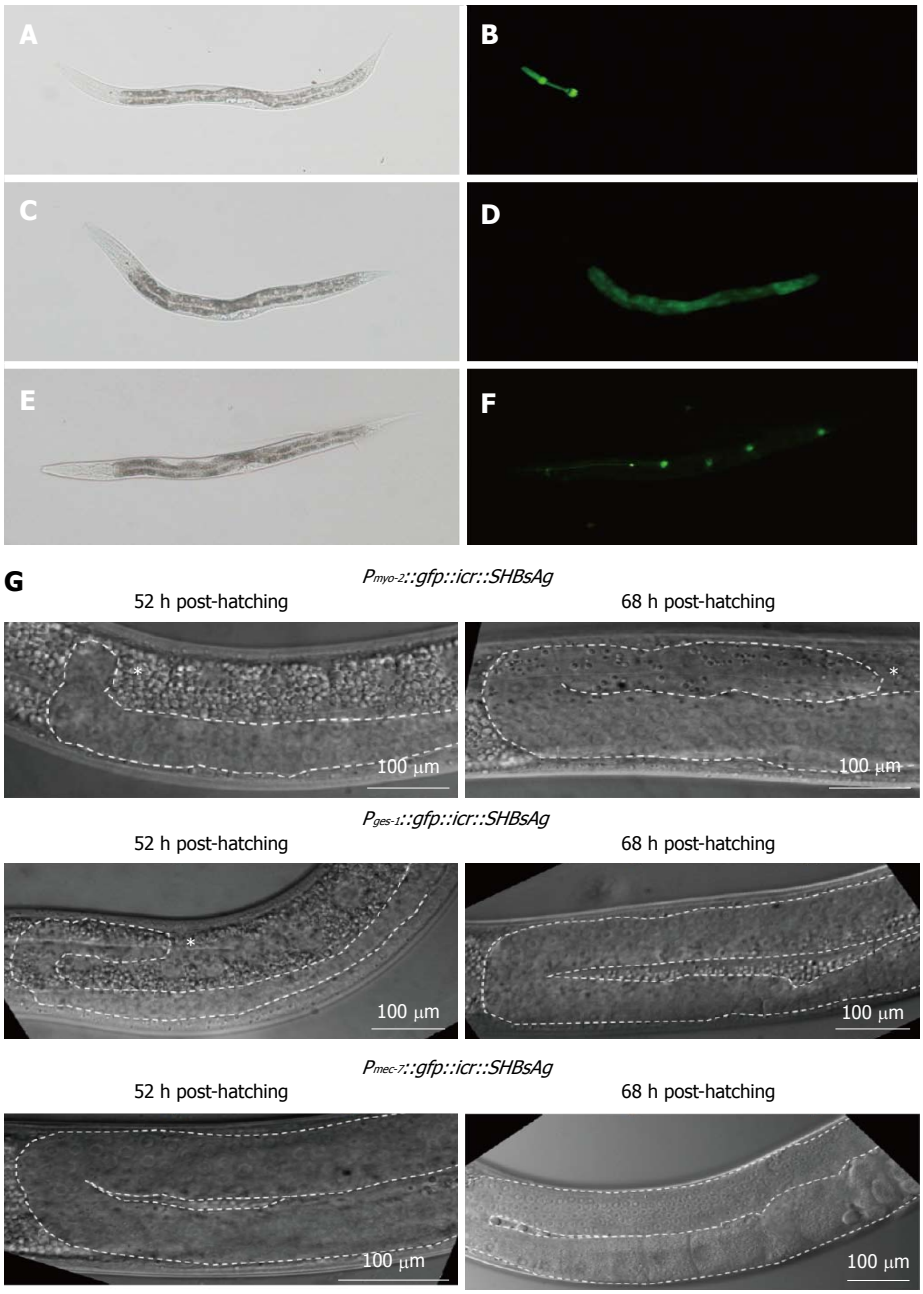

Figure 4 Features of transgenic worms expressing SHBsAgs in different tissues. A-F: Micrographs of transgenic worms expressing SHBsAgs in the pharynx (A, and B), intestinal cells (C and D), and neurons (E and F) were captured under a bright-field microscope (A, C, and E) and a fluorescence microscope (B, D, and F). The heads of the worms are shown toward the left. The scale bar indicates 200 μm; G: Gonad development in transgenic worms: The upper row is a transgenic worm expressing SHBsAg in the pharynx; the middle row is a transgenic worm expressing SHBsAg in intestinal cells; and the lower row is a transgenic worm expressing SHBsAg in neurons. Images were captured under a DIC microscope. The right column shows the gonads at 52 h post-hatching and the left column at 68 h post-hatching. The gonad contour is outlined by dotted lines and the tip (distal end) is marked by asterisk. HBsAgs: Hepatitis B virus antigens.

types induced by the expression of SHBsAg might be explained by the different nature of the three forms of HBsAg. In general, SHBsAg can form subviral particles of approximately 22 nm and be constantly secreted outside of cells whereas MHBsAg is less efficiently secreted and LHBsAg is usually retained in the ER[29,32]. This hypothesis is supported by the results shown in Figure 3, namely that four ER-stress related transcripts (*enpl-1*, *hsp-4*, *pdi-3* and *xbp-1*) were substantially elevated in worms expressing LHBsAg and MHBsAg but only one transcript (*pdi-3*) displayed a slight elevation in worms expressing SHBsAg. The secretion of SHBsAg might either trigger signals inhibiting gonad development or titrate out secretion factors that are required for gonad development, although ER-stress signals might also play a minor role (Figure 4). Nevertheless, the underlying mechanism that leads to the most severe phenotypes in worms expressing SHBsAg remains unknown and will be elucidated by performing rescue and genetic cross experiments in the future.

C. elegans has been used for studying viral pathogenesis and virus-host interaction for more than a

decade[27,34]. In comparison with the number of publications using *C. elegans* study viral, bacterial and fungal pathogenesis, relatively few papers have focused on viral pathogenesis and virus-host interaction in the past 10 years. The bottleneck could be due to the difficulty of creating transgenic worms expressing viral antigens. Currently, two methods for delivering ectopic genes into *C. elegans* are microinjection and gene bombardment, neither of which are easily achievable in general biology laboratories. To use *C. elegans* as a platform for studying virus-host interaction, virologists must collaborate with worm scientists. Alternatively, virologists could engineer the three viruses (Orsay, Santeui, and Le Blanc virus[35,36]), that naturally infect *C. elegans* to become versatile vectors for the easy deliver of different viral genes into worms through infection.

ACKNOWLEDGMENTS

We would like to thank Wallace Academic Editing for editing the manuscript, the *Caenorhabditis* Genetics Center for providing worm strains, and Kuei-Ching Hsiung for preparing the figures. This work is supported by grants from the Chang Gung Memorial Hospital (CMRPD1C0812, CMRPD1C0813 and BMRP742) to to Lo SJ.

COMMENTS

Background

The purpose of this research was to develop a model for human hepatitis B viral antigen interaction with host factors in the standard model animal *Caenorhabditis elegans* (*C. elegans*).

Research frontiers

The hepatitis B viral surface proteins (large, small and middle sized) (LHBsAg, MHBsAg, SHBsAg) are essential in viral assembly and infection. Here the three viral surface proteins were synthesized in *C. elegans* after microinjection of bacterial plasmids containing the genes for the proteins expressed under the control of a ubiquitous animal promoter. Severe reduction in egg laying and brood size as well as gonad retardation occurred with expression of the small hepatitis B virus (HBV) surface antigen in the worm. Smaller effects were found with the middle and larger sized surface antigens.

Innovations and breakthroughs

The specific effects of human HBV surface antigen expression of the *C. elegans* worm demonstrates the worm as a useful model for understanding viral infection and its effects on animal tissues.

Applications

Simple and rapid animal cell and model animal systems are essential for understanding of the infection process and disruptions caused by important human disease agents such as HBV. Here a new and useful model is established and its characteristics presented.

Terminology

HBV is the familiar abbreviation for human hepatitis B virus, although with HAV and HCV, a major cause of liver damage and morbidity. LHBsAg, MHBsAg and SHBsAg are the abbreviations for the large, middle-sized and small versions of the viral surface antigen, the proteins involved in the initial phase of virus surface attachment and infection.

Peer-review

The paper is well written.

REFERENCES

1 **Tiollais P**, Pourcel C, Dejean A. The hepatitis B virus. *Nature* 1985; **317**: 489-495 [PMID: 2995835 DOI: 10.1038/317489a0]

2 **Ganem D**, Varmus HE. The molecular biology of the hepatitis B viruses. *Annu Rev Biochem* 1987; **56**: 651-693 [PMID: 3039907 DOI: 10.1146/annurev.bi.56.070187.003251]

3 **Locarnini S**, Littlejohn M, Aziz MN, Yuen L. Possible origins and evolution of the hepatitis B virus (HBV). *Semin Cancer Biol* 2013; **23**: 561-575 [PMID: 24013024 DOI: 10.1016/j.semcancer.2013.08.006]

4 **Brechot C**, Kremsdorf D, Soussan P, Pineau P, Dejean A, Paterlini-Brechot P, Tiollais P. Hepatitis B virus (HBV)-related hepatocellular carcinoma (HCC): molecular mechanisms and novel paradigms. *Pathol Biol* (Paris) 2010; **58**: 278-287 [PMID: 20667665 DOI: 10.1016/j.patbio.2010.05.001]

5 **Beasley RP**, Hwang LY, Lin CC, Chien CS. Hepatocellular carcinoma and hepatitis B virus. A prospective study of 22 707 men in Taiwan. *Lancet* 1981; **2**: 1129-1133 [PMID: 6118576 DOI: 10.1016/S0140-6736(81)90585-7]

6 **Wang J**, Chenivesse X, Henglein B, Bréchot C. Hepatitis B virus integration in a cyclin A gene in a hepatocellular carcinoma. *Nature* 1990; **343**: 555-557 [PMID: 1967822 DOI: 10.1038/343555a0]

7 **Wang J**, Zindy F, Chenivesse X, Lamas E, Henglein B, Bréchot C. Modification of cyclin A expression by hepatitis B virus DNA integration in a hepatocellular carcinoma. *Oncogene* 1992; **7**: 1653-1656 [PMID: 1321406]

8 **Wang HC**, Chang WT, Chang WW, Wu HC, Huang W, Lei HY, Lai MD, Fausto N, Su IJ. Hepatitis B virus pre-S2 mutant upregulates cyclin A expression and induces nodular proliferation of hepatocytes. *Hepatology* 2005; **41**: 761-770 [PMID: 15726643 DOI: 10.1002/hep.20615]

9 **Bouchard MJ**, Schneider RJ. The enigmatic X gene of hepatitis B virus. *J Virol* 2004; **78**: 12725-12734 [PMID: 15542625 DOI: 10.1128/JVI.78.23.12725-12734.2004]

10 **Yen TT**, Yang A, Chiu WT, Li TN, Wang LH, Wu YH, Wang HC, Chen L, Wang WC, Huang W, Chang CW, Chang MD, Shen MR, Su IJ, Wang LH. Hepatitis B virus PreS2-mutant large surface antigen activates store-operated calcium entry and promotes chromosome instability. *Oncotarget* 2016; **7**: 23346-23360 [PMID: 26992221 DOI: 10.18632/oncotarget.8109]

11 **Tennant BC**, Toshkov IA, Peek SF, Jacob JR, Menne S, Hornbuckle WE, Schinazi RD, Korba BE, Cote PJ, Gerin JL. Hepatocellular carcinoma in the woodchuck model of hepatitis B virus infection. *Gastroenterology* 2004; **127**: S283-S293 [PMID: 15508096 DOI: 10.1053/j.gastro.2004.09.043]

12 **Gerin JL**, Cote PJ, Korba BE, Tennant BC. Hepadnavirus-induced liver cancer in woodchucks. *Cancer Detect Prev* 1989; **14**: 227-229 [PMID: 2695243]

13 **Transy C**, Fourel G, Robinson WS, Tiollais P, Marion PL, Buendia MA. Frequent amplification of c-myc in ground squirrel liver tumors associated with past or ongoing infection with a hepadnavirus. *Proc Natl Acad Sci USA* 1992; **89**: 3874-3878 [PMID: 1570307 DOI: 10.1073/pnas.89.9.3874]

14 **Hsu T**, Möröy T, Etiemble J, Louise A, Trépo C, Tiollais P, Buendia MA. Activation of c-myc by woodchuck hepatitis virus insertion in hepatocellular carcinoma. *Cell* 1988; **55**: 627-635 [PMID: 3180223 DOI: 10.1016/0092-8674(88)90221-8]

15 **Wu BK**, Li CC, Chen HJ, Chang JL, Jeng KS, Chou CK, Hsu MT, Tsai TF. Blocking of G1/S transition and cell death in the regenerating liver of Hepatitis B virus X protein transgenic mice. *Biochem Biophys Res Commun* 2006; **340**: 916-928 [PMID: 16403455 DOI: 10.1016/j.bbrc.2005.12.089]

16 **Chisari FV**, Klopchin K, Moriyama T, Pasquinelli C, Dunsford HA, Sell S, Pinkert CA, Brinster RL, Palmiter RD. Molecular pathogenesis of hepatocellular carcinoma in hepatitis B virus transgenic mice. *Cell* 1989; **59**: 1145-1156 [PMID: 2598264 DOI: 10.1016/0092-8674(89)90770-8]

17 **Kim A**, Kwon OS, Kim SO, He L, Bae EY, Lee MS, Jeong SJ, Shim JH, Yoon DY, Kim CH, Moon A, Kim KE, Ahn JS, Kim BY. Caspase-3 activation as a key factor for HBx-transformed cell death.

Cell Prolif 2008; **41**: 755-774 [PMID: 18700866 DOI: 10.1111/j.1365-2184.2008.00550.x]

18 **Zhang XD**, Wang Y, Ye LH. Hepatitis B virus X protein accelerates the development of hepatoma. *Cancer Biol Med* 2014; **11**: 182-190 [PMID: 25364579]

19 **Geng X**, Harry BL, Zhou Q, Skeen-Gaar RR, Ge X, Lee ES, Mitani S, Xue D. Hepatitis B virus X protein targets the Bcl-2 protein CED-9 to induce intracellular Ca2+ increase and cell death in Caenorhabditis elegans. *Proc Natl Acad Sci USA* 2012; **109**: 18465-18470 [PMID: 23091037 DOI: 10.1073/pnas.1204668109]

20 **Brenner S**. The genetics of Caenorhabditis elegans. *Genetics* 1974; **77**: 71-94 [PMID: 4366476]

21 **Ankeny RA**. The natural history of Caenorhabditis elegans research. *Nat Rev Genet* 2001; **2**: 474-479 [PMID: 11389464 DOI: 10.1038/35076538]

22 **Diogo J**, Bratanich A. The nematode Caenorhabditis elegans as a model to study viruses. *Arch Virol* 2014; **159**: 2843-2851 [PMID: 25000902 DOI: 10.1007/s00705-014-2168-2]

23 **Kurz CL**, Ewbank JJ. Caenorhabditis elegans: an emerging genetic model for the study of innate immunity. *Nat Rev Genet* 2003; **4**: 380-390 [PMID: 12728280 DOI: 10.1038/nrg1067]

24 **Culetto E**, Sattelle DB. A role for Caenorhabditis elegans in understanding the function and interactions of human disease genes. *Hum Mol Genet* 2000; **9**: 869-877 [PMID: 10767309 DOI: 10.1093/hmg/9.6.869]

25 **Olsen A**, Vantipalli MC, Lithgow GJ. Using Caenorhabditis elegans as a model for aging and age-related diseases. *Ann N Y Acad Sci* 2006; **1067**: 120-128 [PMID: 16803977 DOI: 10.1196/annals.1354.015]

26 **Zarski JP**, Kuhns M, Berck L, Degos F, Schalm SW, Tiollais P, Bréchot C. Comparison of a quantitative standardized HBV-DNA assay and a classical spot hybridization test in chronic active hepatitis B patients undergoing antiviral therapy. *Res Virol* 1989; **140**: 283-291 [PMID: 2772413 DOI: 10.1016/S0923-2516(89)80108-6]

27 **Liu WH**, Lin YL, Wang JP, Liou W, Hou RF, Wu YC, Liao CL. Restriction of vaccinia virus replication by a ced-3 and ced-4-dependent pathway in Caenorhabditis elegans. *Proc Natl Acad Sci USA* 2006; **103**: 4174-4179 [PMID: 16537504 DOI: 10.1073/pnas.0506442103]

28 **Lee LW**, Chang TY, Lo HW, Lo SJ. Hepatitis D antigens cause growth retardation and brood-size reduction in C. elegans. *Front Biosci* (Elite Ed) 2011; **3**: 380-390 [PMID: 21196318]

29 **Sheu SY**, Lo SJ. Biogenesis of the hepatitis B viral middle (M) surface protein in a human hepatoma cell line: demonstration of an alternative secretion pathway. *J Gen Virol* 1994; **75** (Pt 11): 3031-3039 [PMID: 7964612 DOI: 10.1099/0022-1317-75-11-3031]

30 **Lee LW**, Lo HW, Lo SJ. Vectors for co-expression of two genes in Caenorhabditis elegans. *Gene* 2010; **455**: 16-21 [PMID: 20149852 DOI: 10.1016/j.gene.2010.06.007]

31 **Safra M**, Ben-Hamo S, Kenyon C, Henis-Korenblit S. The ire-1 ER stress-response pathway is required for normal secretory-protein metabolism in C. elegans. *J Cell Sci* 2013; **126**: 4136-4146 [PMID: 23843615 DOI: 10.1242/jcs.123000]

32 **Hung JH**, Su IJ, Lei HY, Wang HC, Lin WC, Chang WT, Huang W, Chang WC, Chang YS, Chen CC, Lai MD. Endoplasmic reticulum stress stimulates the expression of cyclooxygenase-2 through activation of NF-kappaB and pp38 mitogen-activated protein kinase. *J Biol Chem* 2004; **279**: 46384-46392 [PMID: 15319438 DOI: 10.1074/jbc.M403568200]

33 **Hubbard EJ**, Greenstein D. The Caenorhabditis elegans gonad: a test tube for cell and developmental biology. *Dev Dyn* 2000; **218**: 2-22 [PMID: 10822256]

34 **Lu R**, Maduro M, Li F, Li HW, Broitman-Maduro G, Li WX, Ding SW. Animal virus replication and RNAi-mediated antiviral silencing in Caenorhabditis elegans. *Nature* 2005; **436**: 1040-1043 [PMID: 16107851 DOI: 10.1038/nature03870]

35 **Jiang H**, Franz CJ, Wang D. Engineering recombinant Orsay virus directly in the metazoan host Caenorhabditis elegans. *J Virol* 2014; **88**: 11774-11781 [PMID: 25078701 DOI: 10.1128/JVI.01630-14]

36 **Franz CJ**, Renshaw H, Frezal L, Jiang Y, Félix MA, Wang D. Orsay, Santeuil and Le Blanc viruses primarily infect intestinal cells in Caenorhabditis nematodes. *Virology* 2014; **448**: 255-264 [PMID: 24314656 DOI: 10.1016/j.virol.2013.09.024]

P- Reviewer: Ghiringhelli PD, Liu ZW, Striker R **S- Editor**: Ji FF
L- Editor: A **E- Editor**: Lu YJ

Published by **Baishideng Publishing Group Inc**
8226 Regency Drive, Pleasanton, CA 94588, USA
Telephone: +1-925-223-8242
Fax: +1-925-223-8243
E-mail: bpgoffice@wjgnet.com
Help Desk: http://www.wjgnet.com/esps/helpdesk.aspx
http://www.wjgnet.com

ISSN 2220-3249 (online)

World Journal of *Virology*

World J Virol 2017 May 12; 6(2): 26-48

Published by Baishideng Publishing Group Inc

WJV World Journal of Virology

A peer-reviewed, online, open-access journal of virology

Editorial Board

2016-2019

The *World Journal of Virology* Editorial Board consists of 370 members, representing a team of worldwide experts in virology. They are from 59 countries, including Argentina (4), Australia (8), Austria (4), Barbados (1), Belgium (1), Brazil (7), Bulgaria (1), Cameroon (1), Canada (12), Chile (2), China (55), Croatia (2), Cuba (1), Czech Republic (1), Denmark (1), Egypt (3), Ethiopia (1), Finland (5), France (10), Gambia(1), Germany (11), Ghana (1), Greece (2), Hungary (1), India (13), Indonesia (1), Iran (2), Ireland (3), Israel (4), Italy (23), Japan (16), Kazakhstan (1), Kenya (1), Kosovo (1), Mexico (2), Netherlands (5), New Zealand (1), Nigeria (1), Pakistan (1), Palestine (1), Poland (1), Portugal (1), Romania (1), Russia (2), Saudi Arabia (1), Singapore (2), Slovakia (2), Slovenia (2), South Africa (2), South Korea (6), Spain (19), Sweden (4), Thailand (8), Tunisia (1), Turkey (4), United Arab Emirates (1), United Kingdom (8), United States (92), and Uruguay (1).

Eiichi N Kodama, *Sendai*
Emoto Masashi, *Gunma*
Hiromitsu Moriyama, *Tokyo*
Kenji Okuda, *Yokohama*
Nobuhiro Suzuki, *Okayama*
Takashi Suzuki, *Shizuoka*
Tetsuro Suzuki, *Hamamatsu*
Yoshiyuki Suzuki, *Nagoya-shi*
Akifumi Takaori-Kondo, *Kyoto*
Tetsuya Toyoda, *Toyohashi*

Kazakhstan

Vladimir E Berezin, *Almaty*

Kenya

George G Maina, *Nairobi*

Kosovo

Lul Raka, *Prishtina*

Mexico

Juan E Ludert, *Mexico City*
Julio Reyes-Leyva, *Mexico*

Netherlands

Kimberley SM Benschop, *Amsterdam*
Benjamin Berkhout, *Amsterdam*
Byron EE Martina, *Rotterdam*
Willem JG Melchers, *Nijmegen*
Monique Nijhuis, *Utrecht*

New Zealand

Olga S Garkavenko, *Auckland*

Nigeria

Olajide A Owolodun, *Plateau State*

Pakistan

Muhammad I Qadir, *Faisalabad*

Palestine

Ahmad Y Amro, *Jerusalem*

Poland

Brygida Knysz, *Wroclaw*

Portugal

Celso Cunha, *Lisbon*

Romania

Anda Baicus, *Bucharest*

Russia

Anton Buzdin, *Moscow*
Elena V Gavrilova, *Novosibirsk*

Saudi Arabia

Ahmed S Abdel-Moneim, *Al-Taif*

Singapore

Sophie Bellanger, *Singapore*
Ding X Liu, *Singapore*

Slovakia

Gabriela Bukovska, *Bratislava*
Julius Rajcani, *Bratislava*

Slovenia

Uros Krapez, *Ljubljana*
Andrej Steyer, *Ljubljana*

South Africa

Janusz T Paweska, *Sandringham*
Dirk Stephan, *Matieland*

South Korea

Sang Hoon Ahn, *Seoul*
Tae-Jin Choi, *Busan*
Young-Ki Choi, *Cheongju*
Kee-Jong Hong, *Cheongwon*
Bum-Joon Kim, *Seoul*
Junsoo Park, *Wonju*

Spain

Alí Alejo, *Valdeolmos*
Alfredo Berzal-Herranz, *Granada*
Rafael Blasco, *Madrid*
Julio Collazos, *Usánsolo-Galdácano*
Juan M Hernández, *Madrid*
Gómez L Jaime, *Córdoba*
Josep M Llibre, *Badalona*
Cecilio López-Galíndez, *Madrid*
F. Xavier López-Labrador, *Valencia*
JoséA Melero, *Madrid*
Luis Menéndez-Arias, *Madrid*
Andrés Moya, *València*
David R Pereda, *Sevilla*
Pilar Perez-Romero, *Sevilla*
Josep Quer, *Barcelona*
Daniel López Rodríguez, *Majadahonda*
Juan-Carlos Saiz, *Madrid*
Noemi Sevilla, *Madrid*
Natalia Soriano-Sarabia, *Madrid*

Sweden

Goran PL Bucht, *Umea*
Ali Mirazimi, *Solna*
Muhammad Munir, *Uppdala*
Bo F Oberg, *Huddinge*

Thailand

Prasert Auewarakul, *Bangkok*
Parin Chaivisuthangkura, *Bangkok*
Wasin Charerntantanakul, *Chiang Mai*
Wansika Kiatpathomchai, *Bangkok*
Sasisopin Kiertiburanakul, *Bangkok*
Winyou Mitarnun, *Chiang Mai*
Yong Poovorawan, *Bangkok*
Viroj Wiwanitkit, *Bangkok*

Tunisia

Olfa Bahri, *Tunis*

Turkey

Omer Coskun, *Ankara*
Iftihar Koksal, *Trabzon*
Aykut Ozdarendeli, *Kayseri*
Ayca A Sayiner, *Izmir*

United Arab Emirates

Tahir A Rizvi, *Al Ain*

United Kingdom

Shiu-Wan Chan, *Manchester*
Simon R Clegg, *Preston*
Chiriva I Maurizio, *Nottingham*
Iain M Morgan, *Glasgow*
Mark R Nelson, *London*
Adrian W Philbey, *Glasgow*
James P Stewart, *Liverpool*
Gavin WG Wilkinson, *Cardiff*

United States

Nafees Ahmad, *Tucson*
Ashok Aiyar, *Los Angeles*
Hizi Amnon, *Bethesda*
Judith M Ball, *Texas*
Igor M Belyakov, *Frederick*
Bradford K Berges, *Provo*
Preeti Bharaj, *Orlando*
Jay C Brown, *Charlottesville*
Victor E Buckwold, *Walkersville*
Alexander A Bukreyev, *Galveston*
Joseph J Carter, *Seattle*
Maria G Castro, *Los Angeles*
Yan-Ping Chen, *Beltsville*

World Journal of Virology

Contents

Quarterly Volume 6 Number 2 May 12, 2017

World Journal of Virology
Volume 6 Number 2 May 12, 2017

Contents

NAME OF JOURNAL
World Journal of Virology

ISSN
ISSN 2220-3249 (online)

LAUNCH DATE
February 12, 2012

FREQUENCY
Quarterly

EDITOR-IN-CHIEF
Ling Lu, MD, PhD, Department of Pathology and Laboratory Medicine, University of Kansas Medical Center, Kansas City, 3901 Rainbow Blvd, WHE 3020, KS 66160, United States

EDITORIAL BOARD MEMBERS
All editorial board members resources online at http://www.wjgnet.com/2220-3249/editorialboard.htm

EDITORIAL OFFICE
Xiu-Xia Song, Director
World Journal of Virology
Baishideng Publishing Group Inc
7901 Stoneridge Drive, Suite 501, Pleasanton, CA 94588, USA
Telephone: +1-925-2238242
Fax: +1-925-2238243
E-mail: editorialoffice@wjgnet.com
Help Desk: http://www.f6publishing.com/helpdesk
http://www.wjgnet.com

PUBLISHER
Baishideng Publishing Group Inc
7901 Stoneridge Drive, Suite 501,
Pleasanton, CA 94588, USA
Telephone: +1-925-223-8242
Fax: +1-925-223-8243
E-mail: bpgoffice@wjgnet.com
Help Desk: http://www.f6publishing.com/helpdesk
http://www.wjgnet.com

PUBLICATION DATE
May 12, 2017

INSTRUCTIONS TO AUTHORS
http://www.wjgnet.com/bpg/gerinfo/204

ONLINE SUBMISSION
http://www.f6publishing.com

World Journal of Virology

Submit a Manuscript: http://www.f6publishing.com

World J Virol 2017 May 12; 6(2): 26-35

DOI: 10.5501/wjv.v6.i2.26

ISSN 2220-3249 (online)

ORIGINAL ARTICLE

Basic Study

Structural and nucleic acid binding properties of hepatitis delta virus small antigen

Carolina Alves, Hong Cheng, João Paulo Tavanez, Ana Casaca, Severin Gudima, Heinrich Roder, Celso Cunha

Carolina Alves, João Paulo Tavanez, Ana Casaca, Celso Cunha, Global Health and Tropical Medicine, GHTM, Instituto de Higiene e Medicina Tropical, IHMT, Universidade Nova de Lisboa, 1349-008 Lisboa, Portugal

Hong Cheng, Heinrich Roder, Institute for Cancer Research, Fox Chase Cancer Center, Philadelphia, PA 19111, United States

Severin Gudima, Department of Microbiology, Molecular Genetics and Immunology, Kansas University Medical Center, Kansas City, KS 67874, United States

Author contributions: Alves C performed the majority of experiments; Cheng H performed the NMR and CD analysis; Casaca A performed production and purification of delta antigen; Tavanez JP, Gudima S and Roder H contributed to study design, provided critical discussions and wrote the manuscript; Cunha C designed and coordinated the research and wrote the manuscript.

Supported by Fundação para a Ciência e Tecnologia, FCT, to GHTM -UID/Multi/04413/2013; Carolina Alves and Ana Casaca were recipients of FCT PhD grants; João Paulo Tavanez is a recipient of a FCT post-doctoral fellowship SFRH/BPD/87494/2012.

Institutional review board statement: This study did not involve the use of any human and/or animal subjects.

Institutional animal care and use committee statement: This study did not involve the use of animal subjects.

Conflict-of-interest statement: The authors declare no conflicts of interest.

Data sharing statement: Technical appendix and dataset are available from the corresponding author at ccunha@ihmt.unl.pt.

Manuscript source: Invited manuscript

Correspondence to: Celso Cunha, Associate Professor, Global Health and Tropical Medicine, GHTM, Instituto de Higiene e Medicina Tropical, IHMT, Universidade Nova de Lisboa, Rua da Junqueira 100, 1349-008 Lisboa, Portugal. ccunha@ihmt.unl.pt
Telephone: +351-21-3652620
Fax: +351-21-3632105

Received: December 20, 2016
Peer-review started: December 25, 2016
First decision: January 16, 2017
Revised: February 8, 2017
Accepted: February 28, 2017
Article in press: March 2, 2017
Published online: May 12, 2017

Abstract

AIM

To further characterize the structure and nucleic acid binding properties of the 195 amino acid small delta antigen, S-HDAg, a study was made of a truncated form of S-HDAg, comprising amino acids 61-195 (Δ60HDAg), thus lacking the domain considered necessary for dimerization and higher order multimerization.

METHODS

Circular dichroism, and nuclear magnetic resonance experiments were used to assess the structure of Δ 60HDAg. Nucleic acid binding properties were investigated by gel retardation assays.

RESULTS

Results showed that the truncated Δ60HDAg protein is intrinsically disordered but compact, whereas the RNA

binding domain, comprising residues 94-146, adopts a dynamic helical conformation. We also found that Δ 60HDAg fails to multimerize but still contains nucleic acid binding activity, indicating that multimerization is not essential for nucleic acid binding. Moreover, in agreement with what has been previously reported for full-length protein, no apparent specificity was found for the truncated protein regarding nucleic acid binding.

CONCLUSION

Taken together these results allowed concluding that Δ60HDAg is intrinsically disordered but compact; Δ 60HDAg is not a multimer but is still capable of nucleic acid binding albeit without apparent specificity.

Key words: Hepatitis delta virus; Delta antigen; Nuclear magnetic resonance; Circular dichroism; Intrinsically disordered protein

Core tip: The characterization of a truncated form of S-HDAg lacking amino acids 1-60, Δ60HDAg is reported. Structure of Δ60HDAg was assessed by circular dichroism and nuclear magnetic resonance and its nucleic acid binding properties were investigated using gel retardation assays. This study demonstrates for the first time that Δ60HDAg is intrinsically disordered and a monomer. Furthermore, Δ60HDAg can bind a wide variety of nucleic acids without apparent specificity.

Alves C, Cheng H, Tavanez JP, Casaca A, Gudima S, Roder H, Cunha C. Structural and nucleic acid binding properties of hepatitis delta virus small antigen. *World J Virol* 2017; 6(2): 26-35 Available from: URL: http://www.wjgnet.com/2220-3249/full/v6/i2/26.htm DOI: http://dx.doi.org/10.5501/wjv.v6.i2.26

INTRODUCTION

Hepatitis delta virus (HDV) is the human pathogen with the smallest genome known to date. It is a defective virus that requires the presence of hepatitis B virus (HBV) to propagate infection, since the envelope is provided by the HBV surface antigens. HDV co-infection with HBV or super-infection of hepatitis B patients increases the severity of acute and chronic liver disease[1]. The HDV genome consists of a 1.7 kb single-stranded closed circular RNA of negative polarity. Replication of HDV genome results in the production of an intermediate complementary strand in which a single open reading frame coding for the delta antigen (HDAg) has been identified. During the replication cycle, site-specific editing of the antigenomic RNA by a host adenosine deaminase (ADAR 1) results in the expression of a second form of the HDAg. The mRNA for the original small delta antigen (S-HDAg), corresponding to a 195 amino acids long protein, has its stop codon changed to a tryptophan codon, giving rise to a 19 amino acid extension. This results in the translation of the large delta antigen (L-HDAg) with 214 amino acids. None of the HDAg forms have any known enzymatic activity and, although both antigens share most of their sequence and therefore functional domains, they display some different functions in the HDV replication cycle. S-HDAg is essential for HDV RNA accumulation while L-HDAg acts as a trans-dominant inhibitor of replication and is essential for virus assembly[1].

S-HDAg is considered an "intrinsically disordered protein" (IDP) as revealed by a meta-predictor as well as circular dichroism (CD) measurements[2]. In fact, S-HDAg has several characteristics commonly attributed to IDPs: They rarely display enzymatic activity and are commonly involved in nucleic acid binding and/or interactions with other proteins[3]. S-HDAg is a nucleic acid-binding protein, with multiple host protein partners identified over the years by different approaches[4-7]. S-HDAg is also a basic protein with a predicted net charge of +12 at neutral pH[8]. This is common for IDPs and may play an important role in the ability of the protein to bind negatively charged nucleic acids. Post-translational modification (PTM) sites are also a common feature to IDPs. S-HDAg is modified by phosphorylation, methylation, acetylation, and sumoylation, and distinct functions have been attributed to the different modified forms of the antigen[9-13]. The evidence showing that S-HDAg is an IDP can explain the difficulty in solving its 3-D structure. Despite several attempts it has not yet been possible to obtain crystals of the full-length antigen. However, crystals were readily obtained for a truncated form spanning amino acids 12 to 60 corresponding to a more ordered region of the protein[2,14]. This segment is involved in S-HDAg dimerization and was designated a coiled-coil domain (CCD) as dimers form an anti-parallel coiled-coil structure[14].

In the present study, we address the role of the C-terminal regions of S-HDAg in determining its conformational properties, multimerization and nucleic acid binding. A truncated form of S-HDAg lacking the first 60 amino acids (Δ60HDAg) was generated and purified. We characterized the structural conformation of purified Δ60HDAg using CD and nuclear magnetic resonance (NMR). Additionally, we also investigated the multimerization and nucleic acid binding properties of Δ 60HDAg.

MATERIALS AND METHODS

Plasmids and cloning

Plasmid pR5δV5 was used to express full-length S-HDAg in *Escherichia coli* (*E. coli*) as previously described[15]. This plasmid was also used as template to amplify by PCR the region encoding amino acids 61-195 (forward primer: 5′-TTTCAATTGCCAAAGATAAAGATGGCG-3′, reverse primer: 5′-TTTCTCGAGTTACGGAAAGCC-3′). The amplified sequence was cloned into the *Eco*RI-*Xho*I

cloning site of pGEX-6P-2 (GE Healthcare). The resulting plasmid, designated pGEX-6P-2-Δ60S-HDAg, allowed further expression of the fusion protein GST-Δ60HDAg.

Bacterial expression and purification of recombinant proteins

Expression and purification of full-length S-HDAg was performed as described[6]. Expression of GST-Δ60HDAg was performed in BL21 (DE3) codon plus competent cells (Novagen) and protein purification was performed as follows. Cells expressing GST-Δ 60HDAg were resuspended in PBS supplemented with protease inhibitors (cOmplete, Roche). Cell lysis was achieved by four freeze-thaw cycles after the addition of 0.1 mg/mL lysozyme. Lysates were treated with DNase 1 (Roche), sonicated, and centrifuged at 14000 × g for 10 min. Supernatants were analyzed by SDS-PAGE followed by western blot to detect the presence of recombinant protein. Total protein extracts were then used to purify recombinant GST-tagged protein as previously reported[6]. The GST tag was removed by PreScission protease (GE Healthcare) digestion following manufacturer's instructions. Finally, purified Δ60HDAg was concentrated using the protein concentrating solution and dialysis cassettes (Pierce) using the protocol suggested by the manufacturer.

RNA synthesis

Plasmid pDL542 containing a T7 promoter, was used to express full-length antigenomic HDV RNA[16]. The plasmid was transcribed *in vitro* using a T7 RiboMax transcription system (Promega) following protocols provided by the manufacturer.

Gel electrophoresis and mobility shift assays

Protein samples were analyzed by electrophoresis in 12% SDS-PAGE gels and detected by Coomassie blue staining. In cross-linking experiments, protein samples were treated with 0.01% or 0.1% glutaraldehyde for 10 min at room temperature. Glutaraldehyde was inactivated by the addition of 100 mmol/L ammonium acetate and samples were analyzed by SDS-PAGE.

Regarding protein-nucleic acid interactions *in vitro*, protein samples were diluted in a standard binding buffer containing 150 mmol/L NaCl and 10 mmol/L Tris-HCl (pH 7.5) unless stated otherwise. Nucleic acids were then added, the mix was incubated for 10 min at room temperature and resolved by electrophoretic mobility shift assays. For the study of DNA-protein interactions we used the PCR product obtained in the cloning of the truncated protein. For the study of RNA-protein interactions we used full-length antigenomic HDV RNA. Mobility shift assays were performed in non-denaturing 1 × TBE 1.5% agarose gels stained with ethidium bromide.

CD analysis

The far-UV CD spectrum of approximately 10 μmol/L protein solution (in 20 mmol/L potassium phosphate buffer, pH 6.3) was acquired at 25 ℃ on an Aviv 62A spectropolarimeter (Aviv, Lakewood, NJ), using a 1 mm quartz cuvette. The CD spectrum was the average of five scans recorded in the far-UV region (195-250 nm) with a band pass of 2 nm. The temperature dependence was studied at a protein concentration of approximately 15 μmol/L by following the change in ellipticity at 225 nm upon increasing the temperature from 5 ℃ to 85 ℃ in 2 ℃ intervals, using a 2 nm bandwidth and a 2 mm quartz cuvette. Data average and temperature equilibrate times were 1 s and 12 s, respectively. The CD thermal scans were analyzed by nonlinear least squares analysis based on the Gibbs-Helmholtz equation. The fitting model used in this case assumes two-state transition with a temperature-independent heat enthalpy, $\Delta C_p = 0$. The enthalpy of unfolding, ΔH, and the midpoint temperature of unfolding, T_m, were derived from:

$$\Delta G(T_m) = \Delta H(T_m)(1-T/T_m) - \Delta C_p[T_m - T + T\ln(T/T_m)] \quad (1)$$

where T is the sample temperature, T_m is the midpoint temperature of unfolding. ΔH is the enthalpy of unfolding at T_m, and ΔC_p is the heat capacity change.

Thermal unfolding curves monitored *via* the ellipticity at 225 nm, $\in_{255}$, were calculated as follows:

$$\in_{225} = f_N \in_N + f_U \in_U \quad (2)$$

where f_N and f_U are the fractional populations of the native and unfolded state, respectively, and $\in_N$ and $\in_U$ are the corresponding ellipticity values. The temperature dependence of $\in_N$ and $\in_U$ is given by $\in_N$

$$\in_N = \in + N_s T \quad (3)$$

$$\in_U = \in_u^i + N_U T \quad (4)$$

where $\in_N^i$ and $\in_u^i$ designate the initial ellipticity of the native and unfolded states, and N_s and U_s are slopes in the pre- and post-transition regions. For a two-state equilibrium f_N and f_U depend on ΔG as follows:

$$f_N = \frac{1}{1+e^{-\Delta G/RT}} \quad (5)$$

$$f_U = \frac{e^{-\Delta G/RT}}{1+e^{-\Delta G/RT}} \quad (6)$$

NMR sample preparation and NMR analysis

For NMR sample preparation, the DNA sequence encoding residues 61-195 of S-HDAg (Δ60HDAg) was commercially synthesized (LifeTechnology, GeneArt). The truncated gene was subcloned into the expression vector pET49b (Novagen) between BamHI and Hind Ⅲ sites. Uniformly ^{15}N-labeled fusion protein was prepared by growing previously transformed *E. coli* cells in M9 medium supplemented with 1 g/L of ^{15}N NH_4Cl. After removing GST by digestion with HRV 3C protease, the purified protein contained extra residues with the sequence GPGYNDP at its N-terminus. The protein

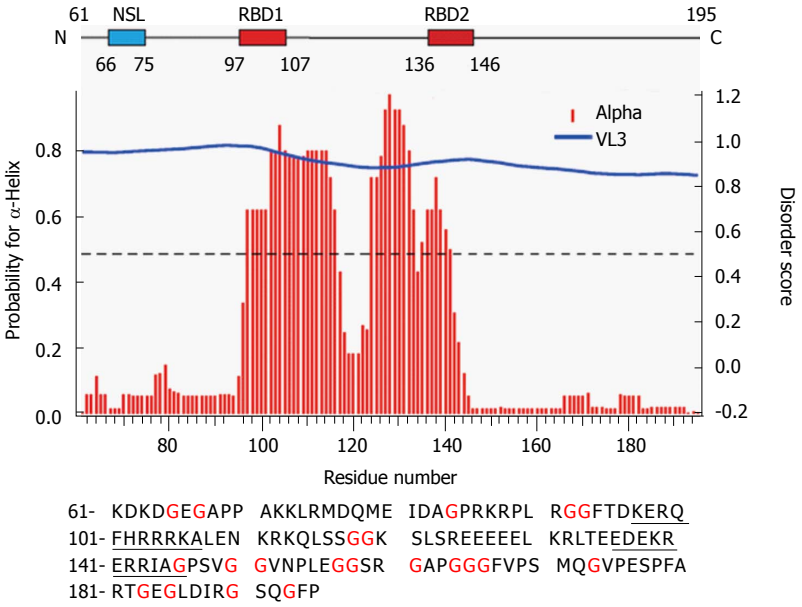

Figure 1 Primary and secondary structure features of Δ60HDAg. Upper panel displays a schematic representation of Δ60HDAg. NLS is the nuclear localization signal from amino acids 66 to 75 (Alves *et al*, 2008); RBD corresponds to the RNA binding domain comprised within amino acids 97 and 146 (Lazinski and Taylor, 1993). Middle panel shows the secondary structure prediction and disorder prediction using the meta-predictor PONDR-Fit (http://www.disprot.org/predictors.php), and one of its component programs (VL3) as indicated. The blue line corresponds to the estimated disorder score and red bars indicate the probability of acquisition of α-helix conformation. Bottom panel is the amino acid sequence of Δ60HDAg. The underlined amino acid residues correspond to the RBD. Isoelectric point of Δ60HDAg's is 9.8 and molecular weight is 14.8 kDa, estimated by using Expasy (www.expasy.org).

(approximately 1 mmol/L) was dissolved in 50 mmol/L sodium phosphate and 50 mmol/L sodium chloride buffer, pH 6.3.

All NMR data were collected on a Bruker Avance Ⅱ 600 MHz spectrometer equipped with a TCI cryoprobe. The spectra were recorded at 25 ℃, processed using the Felix 2007 NMR software (www.felixnmr.com) and analyzed with the Sparky NMR assignment and integration software (www.cgl.ucsf.edu/home/sparky/).

NMR diffusion measurements were carried out with an NMR sample (300 μL and approximately 1 mmol/L containing 3 μL of 1% 4,4-dimethyl-4-silapentane-1-sulfonic acid, DSS, used as an internal standard) by using 1D ^{1}H pulse gradient stimulated echo longitudinal encode-decode (PG-SLED) experiment with saturation of the water signal during relaxation delay[17]. A spin echo delay of 5 ms and a STE delay of 135 ms were used. The data were analyzed using TopSpin 3.2 (Bruker, MA, United States). Fitting the signal integrations from amide and aromatic ring protons (approximately 6.4-9.4 ppm) and DSS(i) as a function of gradient strength (g) to

$$i(g) = Ae^{-dg^2}$$

allowed to extraction the decay rates (d), which are proportional to the diffusion coefficients D. The protein hydrodynamic radius (R_h^{prot}) was calculated according to the equation:

$$R_h^{prot} = d_{ref}(R_h^{ref})/d_{prot} \quad (7)$$

where d_{ref} and R_h^{ref} are the decay rate and hydrodynamic radius of a reference compound (DSS in the present case), and d_{prot} is the measured decay rate (diffusion constant) of the protein. The hydrodynamic radii of native or denatured proteins are estimated from the number of residues, N, according to[18]:

$$R_{h,i} = AN_i^{\alpha} \quad (8)$$

with A = 4.75 and 2.21, and α = 0.29 and 0.57 for a compactly folded and a completely denatured protein, respectively. The effective hydrodynamic radius (R_h) of DSS was calculated as 3.38 Å from R_h: 18.4 Å of cytochrome c from the previous NMR PFG diffusion measurements (see Results).

RESULTS

Δ60HDAg is a monomer

We have previously reported that full-length S-HDAg is able to form multimers *in vitro*, similar to the behavior of S-HDAg present in viral particles[2]. Furthermore, using PONDR-Fit, a Meta predictor of protein order that combines six neural network programs we found that, with the exception of the amino acid fragment 12-60, S-HDAg is intrinsically disordered. To address the possibility that the disordered regions of the antigen contribute to S-HDAg oligomerization, we focused here on a construct that lacks the previously characterized dimerization domain, Δ60HDAg (Figure 1).

To determine whether the truncated antigen has a tendency to oligomerize, Δ60HDAg was analyzed by SDS-PAGE with and without prior glutaraldehyde crosslinking. The non-crosslinked protein displayed a well-defined single band and no changes in mobility were observed when the recombinant protein was pre-incubated with increasing amounts of glutaraldehyde (Figure 2A), indicating that Δ60HDAg is monomeric in solution. Although the truncated form of S-HDAg has an estimated weight of 15 kDa, in SDS-PAGE analysis the monomer appears to be a approximately 19 kDa protein. The difference in molecular weight relates with the reported observation that SDS-PAGE over estimates the size of full-length S-HDAg[19,20].

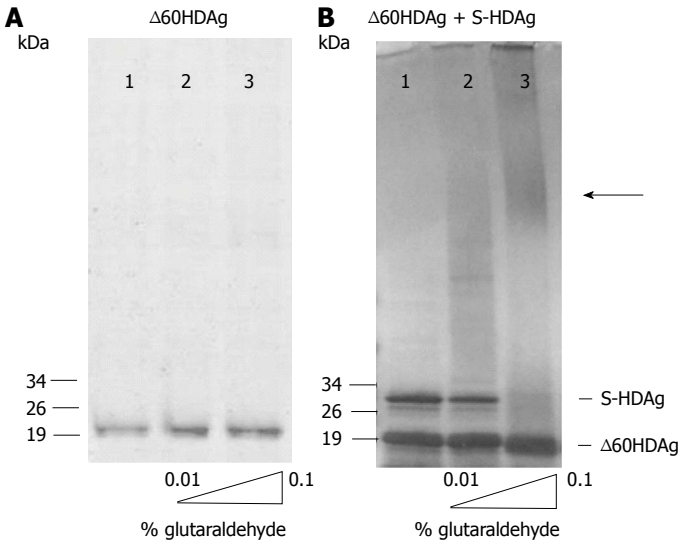

Figure 2 S-HDAg and Δ60HDAg multimerization ability. In panels A and B, purified recombinant protein was cross-linked with increasing concentrations of glutaraldehyde (0%, 0.01% and 0.1%) prior to SDS-PAGE. Proteins were detected by Coomassie blue staining. In panel A, only purified Δ60HDAg was present at 2 μmol/L and in panel B both S-HDAg and Δ60HDAg were present at 2 μmol/L each. The arrow indicates the presence high molecular weight oligomers.

To investigate whether the truncated protein can form oligomers in the presence of full-length HDAg, we combined both forms at a 1:1 molar ratio and analyzed the mixture by SDS-PAGE, with and without prior crosslinking. In the absence of crosslinking (Figure 2B, lane 1) both proteins are readily detected, one with an apparent molecular weight of approximately 19 kDa and another with an apparent molecular weight of approximately 28 kDa, corresponding to the truncated and the full-length antigens, respectively. When the protein mixture was crosslinked, levels of monomeric full-length S-HDAg were reduced, forming oligomers with higher molecular weight as increasing concentrations of glutaraldehyde were present in the mixture (Figure 2B, lanes 2-3). In contrast, levels of monomeric truncated Δ60HDAg remained unchanged, with no oligomerization observed. This result shows that the intermolecular interaction occurs through the first 60 residues of S-HDAg, which includes the CCD, essential for the oligomerization of the full-length protein.

CD analysis of Δ60HDAg

It is thought that IDPs may confer evolutionary advantages by allowing more flexible and diverse interactions with other proteins and nucleic acids. Using PONDR-Fit we have previously shown that, with the exception of portions of the N-terminal CCD, S-HDAg is a largely disordered protein[2]. The structured CCD domain is involved in the formation of dimers and higher order multimers that are believed to play important roles in the HDV replication cycle. Indeed, by using program VL3, the truncated version Δ60HDAg is also predicted to be disordered. As shown in Figure 1 (middle panel), disorder prediction of the truncated protein showed a high disorder score of approximately 0.8[21].

To investigate conformational preferences of the C-terminal S-HDAg for residues 61-195 (Δ60HDAg), we evaluated its secondary structure using CD spectroscopy. This technique allows determination of the average secondary structure content of a protein in solution[22]. Figure 3A shows the spectrum of the truncated recombinant protein exhibiting a strong negative peak around 208 nm and a weaker negative peak around 222 nm, very similar to that of the full-length protein[2]. A strong negative CD peak at 222 nm is characteristic of α-helical conformation and can be used to estimate the helix content. However, the lack of reliable protein concentration (there are no tryptophan and tyrosine residues in this peptide) made this estimate inaccurate. Nevertheless, the CD spectrum in Figure 3A clearly indicates that the truncated Δ60HDAg is at least partially helical rather than being fully disordered, as previously predicted.

To determine the thermostability of the helical conformation, we studied the thermal unfolding of Δ60HDAg by monitoring the CD signal at 225 nm as a function of temperature. As shown in Figure 3B, the negative CD peak at 225 nm became less pronounced with increasing temperature (10 ℃-85 ℃), indicating that the protein undergoes thermal melting transition. The signal measured upon cooling of the sample followed a very similar trend with only slightly more positive ellipticity at 225 nm, indicating that the transition is almost completely reversible (> 98%). In contrast to α-helical model peptides, which generally undergo a gradual helix-coil transition upon heating, the melting curve observed for Δ60HDAg has a clear sigmoidal character consistent with a cooperative (two-state) thermal unfolding transition. Indeed, we were able to quantitatively fit the data using the Gibbs-Helmholtz equation, which parametrizes a two-state thermal unfolding transition in terms of melting temperature, T_m, enthalpy change at T_m, ΔH, and heat capacity change, ΔC_p (see Materials and Methods). The value obtained for ΔH, 26 kcal/mol, is almost half of that obtained for the small globular protein erythropoietin, which has a similar amino acid length and is known to undergo cooperative (two-state) unfolding transition.

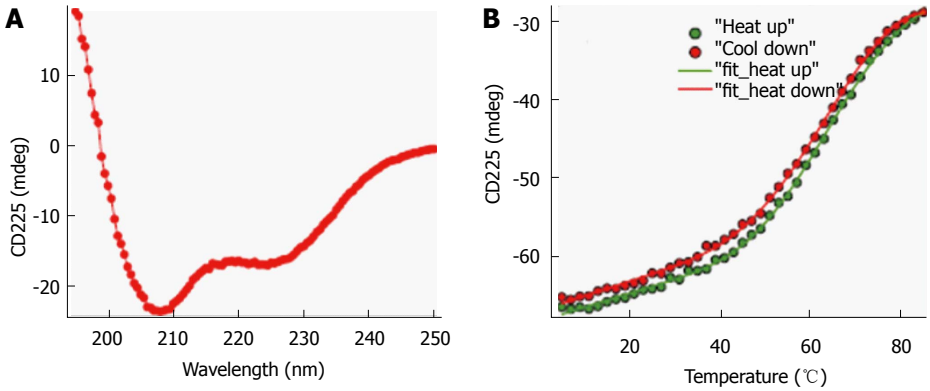

Figure 3 Circular dichroism spectrum and protein thermal stability measurement of Δ60HDAg. A: Far-UV CD spectrum of approximately 10 μmol/L protein in 20 mmol/L potassium phosphate buffer, pH 6.3 at 25 ℃. A quartz cuvette with 1 mm pathlength was used. The spectrum is an average of five scans recorded in the far-UV region (195-250 nm) with a band pass of 2 nm; B: Temperature dependence of Δ60HDAg at approximately 15 μmol/L. Change in ellipticity at 225 nm upon increasing the temperature from 5 ℃ to 85 ℃ in 2 ℃ intervals was recorded. Two nanometer band width and a 2 mm quartz cuvette were used. Data average and temperature equilibrate times were 1 s and 12 s, respectively. Solid lines are the nonlinear least squares fitting the experiment data (solid circles) to the Gibbs-Helmholtz equation (see Materials and Methods). CD: Circular dichroism.

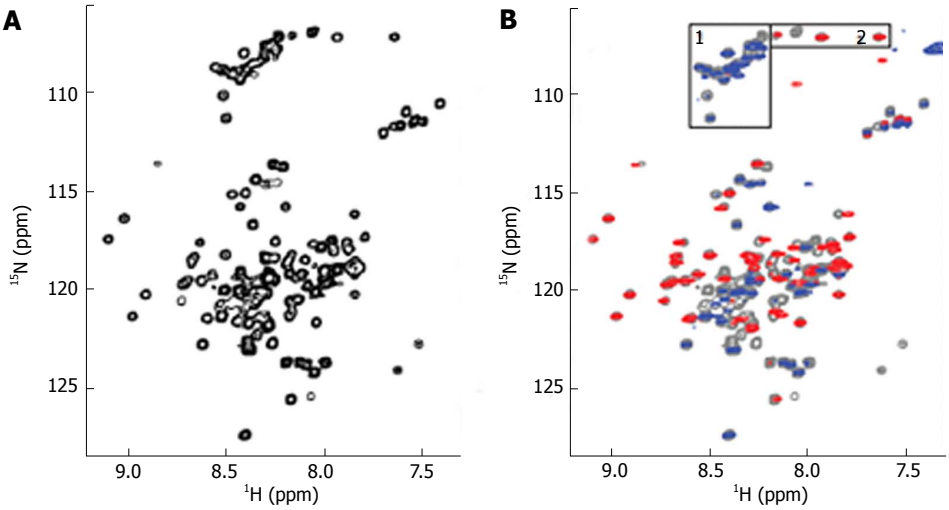

Figure 4 Nuclear magnetic resonance spectra of ^{15}N labeled Δ60HDAg. A: ^{1}H-^{15}N HSQC of Δ60HDAg recorded on a Bruker 600 MHz Avance II NMR instrument at 25 ℃ with the standard Bruker pulse sequence: hsqcetfpf3gpsi. Four thousand and ninety-eight data points in ^{1}H dimension and 256 increments in ^{15}N dimension were acquired; B: ^{1}H and ^{15}N heteronuclear NOE spectrum of Δ60HDAg, superimposed on the normal ^{1}H-^{15}N HSQC spectrum (gray contours). Heteronuclear NOE spectrum was recorded with the Bruker pulse sequence: Hsqcnoef3gpsi. Positives and negatives are displayed in red and blue contours, respectively. Peaks from glycines (boxed and labeled as 1 and 2 in the top of the spectra) are grouped.

NMR analysis of Δ60HDAg

The Δ60HDAg was also analysed by NMR. A ^{1}H-^{15}N heteronuclear single quantum coherence (HSQC) spectrum of purified Δ60HDAg is shown in Figure 4A.

This spectrum served as a "fingerprint" of the protein as it contains a unique cross peak for the backbone NH of each non-proline residue. A peak count revealed that 124 out of a total of 131 non-proline residues (142 residues minus 11 proline residues) gave rise to resolved cross peaks in the HSQC spectrum. However, in contrast to the spectrum of a totally disordered protein, these cross-peaks are distributed over a relatively broad range (7.2-9.2 ppm in ^{1}H and 106-128 ppm in ^{15}N) being consistent with those of a typical globular protein with a dominated helical conformation. Taken together, the results from both CD and NMR suggest that Δ60HDAg is not totally disordered and adopts a non-random, dynamic, ensemble of interconverting conformations.

Furthermore, we used a pulsed-field gradient (PFG) diffusion NMR approach to determine the overall dimension of the polypeptide chain. These experiments yield translational diffusion coefficients and, indirectly, the hydrodynamic radius (R_h) of a protein. Figure 5A shows the intensity of a resolved methyl resonance of Δ 60HDAg measured in a series of 1D NMR spectra as a function of gradient strength. The chemical shift marker DSS was used as an internal reference.

The effective hydrodynamic radius of DSS was measured in a separate control experiment relative to that of cytochrome c for which an R_h of 17.8 Å has been reported[18]. A similar R_h, 18.4 Å, was measured

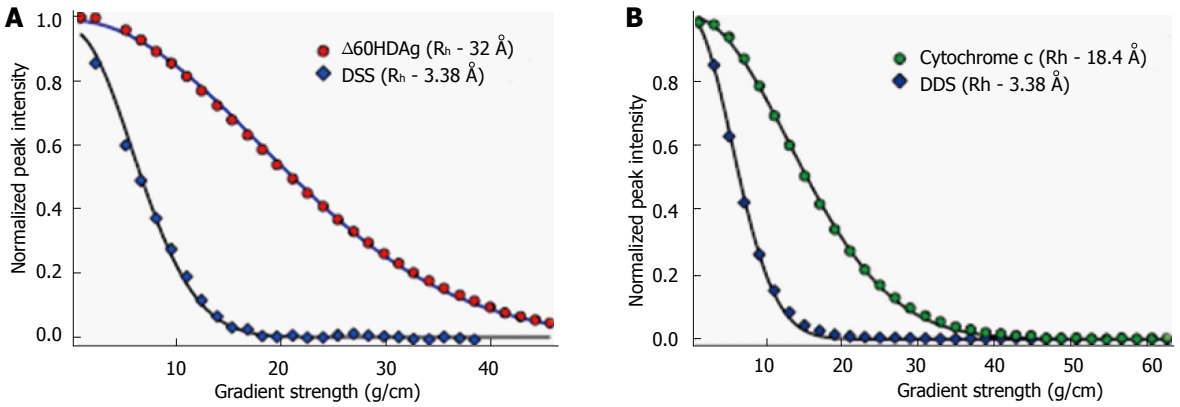

Figure 5 Nuclear magnetic resonance pulsed-field gradient diffusion measurements. A: NMR PFG diffusion measurements of Δ60HDAg, performed on a Bruker 600 MHz Avance II. DSS (4,4-dimethyl-4-silapentane-1-sulfonic acid) was used as a reference. ^{1}H pulse gradient stimulated echo longitudinal encode-decode (PG-SLED) experiment with saturation of the water signal during the relaxation delay was used with a Bruker pulse sequence: Ledbpgppr2s, at 25 ℃. A 14-ppm ^{1}H spectral width was used. Gradient strength varied linearly from 0.963-45.7 g/cm. Solid line represents the result of fitting the experimental data to the diffusion equation (see methods); B: NMR PFG diffusion measurements of cytochrome c, previously measured on a Bruker DMX 600 MHz at 25 ℃. NMR: Nuclear magnetic resonance; PFG: Pulsed-field gradient.

by dynamic light scattering (data not shown). The R_h we obtained for Δ60HDAg, 32.0 Å, is larger than that expected for a globular (folded) 142-residue protein (20.0 Å), but significantly smaller than the R_h of 37.2 Å expected for a fully unfolded protein of this size.

To identify any (partially) ordered regions within Δ60HDAg, we recorded a steady-state ^{1}H-^{15}N (heteronuclear) Nuclear Overhauser Effect (NOE) spectrum. Heteronuclear NOEs typically are strongly positive for a folded protein and weak or negative for a fully disordered protein[23]. If the protein is partially structured, however, the residues in disordered regions such as flexible loops or chain termini, undergo faster motion than the overall tumbling of the molecules (picosecond to nanosecond time scale). Thus, we expected the NOE peaks for residues in disordered regions to be less intense or of the opposite sign compared to those in structured regions of the protein. The heteronuclear NOE spectrum of Δ60HDAg (Figure 4B) shows 53 positive peaks with chemical shifts distributed over the range from 7.7 to 9.2 ppm in the amide proton dimension, which we assigned to relatively ordered regions of the protein (red contours). Of the remaining 71 residues with resolved peaks in the control HSQC spectrum (gray contours), 50 had negative ^{1}H-^{15}N NOEs (blue contours) and 21 were undetectable. These residues undergo local motion on a time scale that is fast relative to the rotational correlation time that characterizes overall tumbling of the molecule. The NH chemical shifts of these peaks fall within a relative narrow range (7.8-8.6 ppm), and can thus be assigned to residues in relatively disordered regions of the protein. The sequence of Δ60HDAg contains 23 glycines, which are expected to exhibit cross peaks near 8.33 ppm in the proton dimension and 109.1 ppm in the nitrogen dimension of the ^{1}H-^{15}N HSQC spectrum. Interestingly, in the heteronuclear NOE spectrum of Δ60HDAg (Figure 4B), the majority of glycine residues (approximately 20) gave rise to weak or negative peaks (gray or blue contours in box 1) while only three glycine cross-peaks were positive (red contours in box 2). This result indicates that most glycine residues are in disordered regions of the molecule while only three glycines are located in relatively ordered regions. The sequence of Δ60HDAg is especially rich in glycine residues in segments outside the RNA binding domain (RBD, residues 97-146, Figure 1 bottom). The RBD comprises two potential RNA binding motifs, residues 97-107 (KERQDHRRRKA) and 136-146 (EDERRERRIAG). Only 3 out of approximately 53 residues in the RBD are glycines. When Agadir (http://agadir.crg.es/agadir.jsp), an empirical algorithm based on the helix-forming tendencies of peptides, was applied to Δ60HDAg it provided a helix content of 62.2% at pH 7.0 and 5 ℃ for the sequence containing residues 94-146. The predicted helix content was highly temperature dependent, dropping to 44.7% at 26 ℃. After removing the first three residues from the N-terminus, so that the sequence only contained the two RNA binding motifs and the linker (97-146), the estimated helix content dropped to 48.84% at pH 7.0 and 5 ℃, and to 34.19% at 25 ℃, indicating that the first three residues, FTD, are important for stabilizing the helical conformation.

We also used NetSurf1.1 (http://www.cbs.dtu.dk/services/NetSurfP/) to predict the protein secondary structure. The result showed that the RBD has a high propensity for α-helix formation while random coil structure predominated in all other regions (Figure 1 middle). Furthermore, NetSurf1.1 calculation shows that the RBD contains two helical segments, residues 96-117 and 124-142, respectively, with 30%-90% probability for α-helical structure. The two helical segments are linked by a six-residue, GGKSLS (positions 118-123), loop with low (< 30%) helix propensity.

Nucleic acid binding ability of Δ60HDAg

In a previous work we have shown that full-length S-HDAg can bind a variety of nucleic acids as a multimer[2]. We reported no binding specificity in *in vitro*

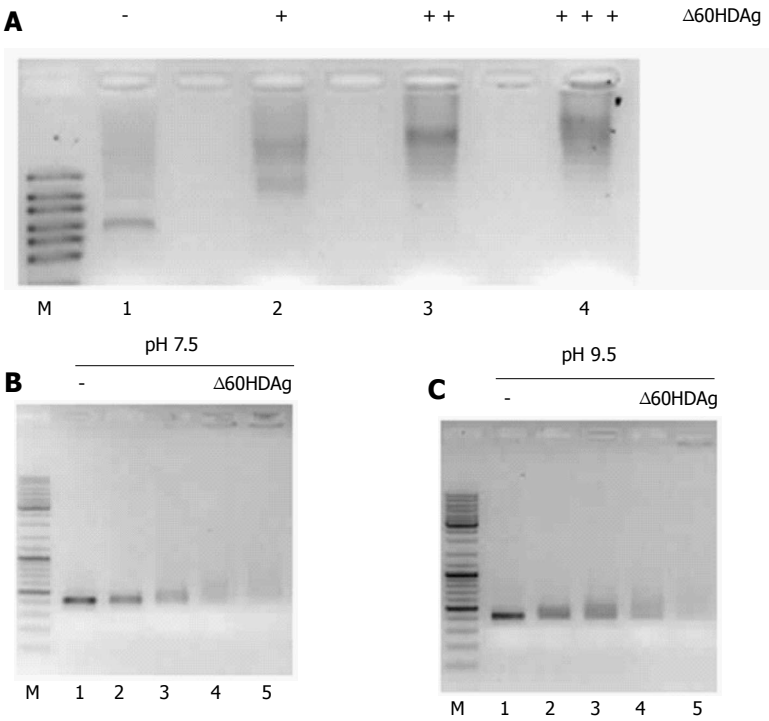

Figure 6 Gel retardation assay. A: Binding of Δ60HDAg to HDV RNA. Purified recombinant Δ60HDAg was incubated, in standard pH 7.5 binding buffer, with 100 ng of HDV RNA at increasing concentrations (0, 0.5, 1.5, and 3 μmol/L, respectively). Left in each panel is a RNA marker (RiboRuler High Range RNA Ladder, Fermentas); B and C: Δ60HDAg binding to DNA and HDV RNA, respectively. In panel B, 100 ng of dsDNA were incubated in standard pH 7.5 binding buffer, with increasing concentrations of purified recombinant Δ60HDAg (0, 2, 4, 6, 8, 10, and 12 μmol/L). Panel C shows the assay in binding buffer at pH 9.5. Recombinant Δ60HDAg was incubated with 100 ng of dsDNA, at different concentrations (0, 2, 4, 6, 8, 10, and 12 μmol/L). In panel C, 100 ng of HDV RNA was incubated, in standard pH 9.5 binding buffer, with increasing concentrations of purified recombinant Δ60HDAg (0, 0.5, 1, 1.5, and 2 μmol/L). HDV: Hepatitis delta virus.

conditions, as the full-length S-HDAg was able to bind HDV RNA, non-HDV RNA and DNA from different sources. In the present study we analyzed whether Δ60HDAg is still capable of binding nucleic acids despite of the absence of the N-terminal CCD domain, which is responsible for antigen oligomerization.

We first assessed binding of Δ60HDAg to RNA. *In vitro* synthetized HDV RNA was incubated with increasing amounts of recombinant Δ60HDAg and samples were resolved in gel retardation assays. Change in mobility of the complexes was readily observed even with the lowest concentration of Δ60HDAg used and responsive to increasing amounts of recombinant truncated protein (Figure 6A), indicating that Δ60HDAg retains the capacity of binding to RNA.

Then, we analyzed binding of Δ60HDAg to DNA. A 400-nucleotide PCR product was incubated with increasing amounts of recombinant Δ60HDAg and samples were resolved in gel retardation assays. Since Δ60HDAg has an estimated pI of 9.84 based on its amino acid composition, we performed this assay at pH 7.5 but also at pH 9.5, closer to Δ60HDAg pI. Thus, it is expected that at higher pH the net charge of S-HDAg is closer to neutral than at pH 7.5. Increasing amounts of Δ60HDAg led to a marked decrease in the amount of free dsDNA molecules in both conditions (Figure 6B and C), indicative of Δ60HDAg-dsDNA complexes formation. We conclude that, similarly to what was observed with RNA, Δ60HDAg has also the capacity to bind dsDNA molecules and that binding is not dependent on the charge of the antigen.

DISCUSSION

S-HDAg is essential for HDV genomic RNA accumulation in infected cells and plays a crucial role in the replication cycle of the virus. This 195 amino acid protein is highly promiscuous as it not only binds to HDV RNA to form viral ribonucleoproteins, but also interacts with a myriad of host factors[4-6]. S-HDAg is predicted to be an IDP, being consistent with many of its known characteristics, such as high net positive charge, ability to bind several partners and lack of enzymatic activity[2]. The high level of intrinsic disorder found in S-HDAg can explain the difficulties encountered to determine its structure. So far, only a peptide spanning the first 60 amino acids has been crystallized and its structure determined[14]. Here, we focused on a truncated version of S-HDAg, consisting of amino acids 61 through 195, lacking the CCD involved in S-HDAg multimerization. Surprisingly, our structural studies show that rather than being fully disordered, Δ60HDAg adopts a relatively compact ensemble of interconverting conformations with a partially ordered RBD. Our results show that it is possible to discriminate between ordered and disordered regions of the protein by using CD, NMR, and secondary structure prediction, without the need for laborious sequence-specific NMR resonance assignments. We show that the RNA binding domain of S-HDAg adopts a dynamic helical conformation.

The N-terminal CCD motif of S-HDAg is involved in oligomerization of the full-length protein. Consistently, cross-linking experiments with Δ60HDAg show that the truncated protein is unable to form homomultimers *in vitro*. We also show that Δ60HDAg does not interfere with multimerization of full-length S-HDAg and that multimerization of Δ60HDAg is not enhanced by the presence of full-length S-HDAg. Results from cross-linking, and specially NMR PFG diffusion measurements, show that overall dimensions are larger than those

expected for a globular protein but smaller than those of fully unfolded (random coil) protein of this size. Thus, Δ60HDAg is a monomer under the experimental conditions used.

Similar to what has been previously shown for full-length S-HDAg, nucleic acid binding results show that Δ60HDAg can bind not only RNA but also dsDNA. Incubation of Δ60HDAg with *in vitro* transcribed RNA and dsDNA and further analysis of complex formation followed by electrophoretic mobility shift assays shows that this truncated protein, although failing to oligomerize, still displays nucleic acid binding activity. *In vitro* nucleic acid binding seems to be largely unspecific as it binds RNA and DNA molecules used in this study and RNA and DNA from other sources with unrelated sequences (data not shown). Noteworthy, when analyzing nucleic acid interactions with full-length S-HDAg, there was a clear shift from the unbound to the fully-bound state without any intermediate positions[2], which most likely reflects binding of S-HDAg multimers covering the whole sequence.

Earlier reported findings, using a different approach, suggested that S-HDAg specifically binds HDV RNAs with rod-like folding[24]. Moreover, S-HDAg RNA-binding specificity has also been recently reported when a C-terminal deletion mutant of the antigen was used and with requirements that the RNA must have a minimum of approximately 300 nt of rod-like folding for binding to occur[25]. Interestingly, this report also cited that in studies with full length S-HDAg no specificity for nucleic acid binding was found. Thus, one could suggest that some level of intrinsic disorder in the C-terminus may compromise specific binding to HDV RNAs. Furthermore, more recently it was shown that binding of HDAg to HDV RNA is not sequence specific but rather depends on secondary structure features, internal loops and bulges of the nucleic acid[26].

To get a deeper insight into the non-specific nucleic acid binding ability of the protein, structural information is also required. We used CD and NMR to characterize measurable structural features in Δ60HDAg. Disordered protein regions with a measured propensity for helical secondary structure have been found to act as pre-formed molecular recognition elements. Although Δ 60HDAg is predicted to be extensively disordered, the relative large chemical shift dispersion in both proton and nitrogen in NMR HSQC spectrum indicates that this is not the case. Moreover, the CD spectrum further showed that Δ60HDAg has a measurable helical content. In conjunction with the sequence analysis, the heteronuclear NOE NMR experiment showed that the RBD domain contained a dynamic helical conformation, which is consistent with secondary structure prediction of a helix-turn-helix RNA binding motif. In addition, our study shows that qualitative NMR analysis such as ^{1}H-^{15}N HSQC, heteronuclear NOE, and PFG diffusion measurements, without need for laborious sequence-specific resonance assignments, can provide insight into structural and dynamic properties, even for disordered proteins. Such sequence-specific resonance assignments are usually a challenge as a consequence of peak overlap and live-width broadening due to conformational exchange observed in the spectra.

Accumulated data indicate that disordered regions in proteins are a common feature and may give rise to important properties as plasticity and reversibility in regulatory intermolecular interactions with their targets, such as proteins and nucleic acids. The mediation of IDR to binding can be achieved through interaction with binding domains and stabilizing their dynamic local structure upon interaction with their targets. Such regulatory functions are frequently modulated by post-translational modification in IDRs. These PTMs, namely phosphorylation, methylation, acetylation, and sumoylation, were reported for S-HDAg in different motifs, including in disordered regions of the protein[9-13]. Furthermore, modifications of S-HDAg are known to mediate the subcellular localization of S-HDAg thus facilitating its interaction with a broad number of cellular targets including the enzymatic machinery involved in the different steps of virus replication. Some of these modifications, namely phosphorylation, were reported to play important roles in the virus replication cycle, including in the accumulation of virus RNAs[11,12]. In addition, the plasticity of S-HDAg may form the basis of interaction with a vast number of cellular partners, inhibiting, redirecting or accelerating host metabolic functions contributing to promote more acute and adverse forms of the liver disease caused by HDV.

In conclusion, the information obtained in this study provides structural basis for future understanding of the non-selective nucleic acid binding property of S-HDAg.

The present *in vitro* studies show that a truncated form of the Delta antigen no longer multimerizes but still binds nucleic acids, although without specificity for HDV rodlike RNA. The lack of specificity may partially be due to an electrostatic interaction between the positively charged protein and the negatively charged nucleic acids, and mediated by the disordered regions. However, the antigen is extensively phosphorylated *in vivo*, which likely reduces its high net charge, limiting the ability to be involved in non-specific electrostatic interactions[9].

These results pave the way for more detailed future studies of structural properties of S-HDAg and its interactions with nucleic acids and other cellular partners.

COMMENTS

Background

Hepatitis delta virus small antigen (S-HDAg) is predicted to be an intrinsically disordered protein that interacts with multiple cellular targets and plays a crucial role in the virus replication cycle.

Research frontiers

Intrinsically disordered proteins exhibit high plasticity, and like S-HDAg, rarely

display enzymatic activity and are often involved in nucleic acid binding. It is well established that S-HDAg is necessary for accumulation of virus RNAs in infected cells, but its structure and precise role in hepatitis delta virus (HDV) replication cycle are still largely unknown.

Innovations and breakthroughs

The authors made use of circular dichroism and nuclear magnetic resonance NMR, as well as gel retardation assays to study a truncated form of S-HDAg, lacking the first 60 amino acids, that contain the dimerization and higher order multimerization domain (Δ60HDAg). The authors concluded that Δ60HDAg is intrinsically disordered but compact and is not a multimer under the experimental conditions used in this study. Moreover, Δ60HDAg is still capable of nucleic acid binding although without apparent specificity.

Applications

This study provides a structural basis for future understanding of the non-selective nucleic acid binding property of S-HDAg. Furthermore, it opens the way for more in-depth future investigations of structural properties of S-HDAg and its interactions with nucleic acids and other cellular partners.

Terminology

IDP: Intrinsically disordered proteins lack an ordered conformation. They may range from fully unstructured to partially structured including some well characterized domains like random coils.

Peer-review

The manuscript by Alves *et al* describes the characteristics of the C-terminal region of S-HDAg using a truncated form of this protein. The methods used in this paper are straightforward.

REFERENCES

1 **Rizzetto M**. Hepatitis D: thirty years after. *J Hepatol* 2009; **50**: 1043-1050 [PMID: 19285743 DOI: 10.1016/j.jhep.2009.01.004]

2 **Alves C**, Cheng H, Roder H, Taylor J. Intrinsic disorder and oligomerization of the hepatitis delta virus antigen. *Virology* 2010; **407**: 333-340 [PMID: 20855099 DOI: 10.1016/j.virol.2010.08.019]

3 **Uversky VN**. Intrinsically disordered proteins from A to Z. *Int J Biochem Cell Biol* 2011; **43**: 1090-1103 [PMID: 21501695 DOI: 10.1016/j.biocel.2011.04.001]

4 **Chang MF**, Baker SC, Soe LH, Kamahora T, Keck JG, Makino S, Govindarajan S, Lai MM. Human hepatitis delta antigen is a nuclear phosphoprotein with RNA-binding activity. *J Virol* 1988; **62**: 2403-2410 [PMID: 3373572]

5 **Greco-Stewart V**, Pelchat M. Interaction of host cellular proteins with components of the hepatitis delta virus. *Viruses* 2010; **2**: 189-212 [PMID: 21994607 DOI: 10.3390/v2010189]

6 **Casaca A**, Fardilha M, da Cruz e Silva E, Cunha C. The heterogeneous ribonuclear protein C interacts with the hepatitis delta virus small antigen. *Virol J* 2011; **8**: 358 [PMID: 21774814 DOI: 10.1186/1743-422X-8-358]

7 **Cao D**, Haussecker D, Huang Y, Kay MA. Combined proteomic-RNAi screen for host factors involved in human hepatitis delta virus replication. *RNA* 2009; **15**: 1971-1979 [PMID: 19776158 DOI: 10.1261/rna.1782209]

8 **Kuo MY**, Goldberg J, Coates L, Mason W, Gerin J, Taylor J. Molecular cloning of hepatitis delta virus RNA from an infected woodchuck liver: sequence, structure, and applications. *J Virol* 1988; **62**: 1855-1861 [PMID: 3367426]

9 **Mu JJ**, Wu HL, Chiang BL, Chang RP, Chen DS, Chen PJ. Characterization of the phosphorylated forms and the phosphorylated residues of hepatitis delta virus delta antigens. *J Virol* 1999; **73**: 10540-10545 [PMID: 10559375]

10 **Chen YS**, Huang WH, Hong SY, Tsay YG, Chen PJ. ERK1/2-mediated phosphorylation of small hepatitis delta antigen at serine 177 enhances hepatitis delta virus antigenomic RNA replication. *J Virol* 2008; **82**: 9345-9358 [PMID: 18632853 DOI: 10.1128/JVI.00656-08]

11 **Tseng CH**, Jeng KS, Lai MM. Transcription of subgenomic mRNA of hepatitis delta virus requires a modified hepatitis delta antigen that is distinct from antigenomic RNA synthesis. *J Virol* 2008; **82**: 9409-9416 [PMID: 18653455 DOI: 10.1128/JVI.00428-08]

12 **Mu JJ**, Tsay YG, Juan LJ, Fu TF, Huang WH, Chen DS, Chen PJ. The small delta antigen of hepatitis delta virus is an acetylated protein and acetylation of lysine 72 may influence its cellular localization and viral RNA synthesis. *Virology* 2004; **319**: 60-70 [PMID: 14967488 DOI: 10.1016/j.virol.2003.10.024]

13 **Li YJ**, Stallcup MR, Lai MM. Hepatitis delta virus antigen is methylated at arginine residues, and methylation regulates subcellular localization and RNA replication. *J Virol* 2004; **78**: 13325-13334 [PMID: 15542683 DOI: 10.1128/JVI.78.23.13325-13334.2004]

14 **Zuccola HJ**, Rozzelle JE, Lemon SM, Erickson BW, Hogle JM. Structural basis of the oligomerization of hepatitis delta antigen. *Structure* 1998; **6**: 821-830 [PMID: 9687364 DOI: 10.1016/S0969-2126(98)00084-7]

15 **Dingle K**, Bichko V, Zuccola H, Hogle J, Taylor J. Initiation of hepatitis delta virus genome replication. *J Virol* 1998; **72**: 4783-4788 [PMID: 9573243]

16 **Lazinski DW**, Taylor JM. Expression of hepatitis delta virus RNA deletions: cis and trans requirements for self-cleavage, ligation, and RNA packaging. *J Virol* 1994; **68**: 2879-2888 [PMID: 8151758]

17 **Wu DH**, Johnson CS. Diffusion-Ordered 2d Nmr in the Fringe-Field of a Superconducting Magnet. *J Magn Reson, Ser A* 1995; **116**: 270-272 [DOI: 10.1006/jmra.1995.0020]

18 **Wilkins DK**, Grimshaw SB, Receveur V, Dobson CM, Jones JA, Smith LJ. Hydrodynamic radii of native and denatured proteins measured by pulse field gradient NMR techniques. *Biochemistry* 1999; **38**: 16424-16431 [PMID: 10600103 DOI: 10.1021/bi991765q]

19 **Bergmann KF**, Pohl C, Gerin JL. Characterization of proteins of hepatitis delta virus. *Prog Clin Biol Res* 1987; **234**: 105-110 [PMID: 3628370]

20 **Gerlich WH**, Heermann KH, Ponzetto A, Crivelli O, Bonino F. Proteins of hepatitis delta virus. *Prog Clin Biol Res* 1987; **234**: 97-103 [PMID: 3628428]

21 **Obradovic Z**, Peng K, Vucetic S, Radivojac P, Brown CJ, Dunker AK. Predicting intrinsic disorder from amino acid sequence. *Proteins* 2003; **53 Suppl 6**: 566-572 [PMID: 14579347 DOI: 10.1002/prot.10532]

22 **Johnson WC**. Secondary structure of proteins through circular dichroism spectroscopy. *Annu Rev Biophys Biophys Chem* 1988; **17**: 145-166 [PMID: 3293583 DOI: 10.1146/annurev.bb.17.060188.001045]

23 **Akke M**, Carr PA, Palmer AG. Heteronuclear-correlation NMR spectroscopy with simultaneous isotope filtration, quadrature detection, and sensitivity enhancement using z rotations. *J Magn Reson B* 1994; **104**: 298-302 [PMID: 8069488 DOI: 10.1006/jmrb.1994.1090]

24 **Chao M**, Hsieh SY, Taylor J. The antigen of hepatitis delta virus: examination of in vitro RNA-binding specificity. *J Virol* 1991; **65**: 4057-4062 [PMID: 1906549]

25 **Defenbaugh DA**, Johnson M, Chen R, Zheng YY, Casey JL. Hepatitis delta antigen requires a minimum length of the hepatitis delta virus unbranched rod RNA structure for binding. *J Virol* 2009; **83**: 4548-4556 [PMID: 19244338 DOI: 10.1128/Jvi.02467-08]

26 **Griffin BL**, Chasovskikh S, Dritschilo A, Casey JL. Hepatitis delta antigen requires a flexible quasi-double-stranded RNA structure to bind and condense hepatitis delta virus RNA in a ribonucleoprotein complex. *J Virol* 2014; **88**: 7402-7411 [PMID: 24741096 DOI: 10.1128/JVI.00443-14]

P- Reviewer: Chung YH, Rodriguez-Frias F, Rossi LMG, Taylor JM
S- Editor: Ji FF **L- Editor**: A **E- Editor**: Wu HL

World Journal of Virology

Submit a Manuscript: http://www.f6publishing.com

World J Virol 2017 May 12; 6(2): 36-45

DOI: 10.5501/wjv.v6.i2.36

ISSN 2220-3249 (online)

ORIGINAL ARTICLE

Observational Study

Matrix metalloproteases and their tissue inhibitors in non-alcoholic liver fibrosis of human immunodeficiency virus-infected patients

Julio Collazos, Eulalia Valle-Garay, Tomás Suárez-Zarracina, Angel-Hugo Montes, José A Cartón, Víctor Asensi

Julio Collazos, Infectious Diseases, Hospital de Galdácano, 48960 Vizcaya, Spain

Eulalia Valle-Garay, Angel-Hugo Montes, Biochemistry and Molecular Biology, Hospital Universitario Central de Asturias, Oviedo University School of Medicine, 33006 Oviedo, Spain

Tomás Suárez-Zarracina, José A Cartón, Víctor Asensi, Infectious Diseases, Hospital Universitario Central de Asturias, Oviedo University School of Medicine, 33006 Oviedo, Spain

Author contributions: Collazos J, Suárez-Zarracina T, Cartón JA and Asensi V designed the study and contributed to the data acquisition and selection; Valle-Garay E and Montes AH performed the laboratory determinations and genotypic studies; Collazos J analyzed the data; Collazos J and Asensi V wrote the draft of the initial manuscript; Suárez-Zarracina T, Valle-Garay E, Montes AH and Cartón JA revised the article critically for important intellectual content.

Supported by the Oviedo University research grants, Nos. UNIOV-12-MA-03 and SV-PA-13-ECOEMP-57.

Institutional review board statement: The study was approved by the Principado de Asturias Research Ethic Committee.

Informed consent statement: Given the nature of the study, no formal written approval was necessary, according to our institution's regulations, being enough a verbal informed consent, which was obtained from all patients.

Conflict-of-interest statement: There is no conflict of interest related to this paper.

Data sharing statement: No additional data are available.

Manuscript source: Invited manuscript

Correspondence to: Dr. Julio Collazos, Infectious Diseases Unit, Hospital de Galdácano, Bº Labeaga s/n, 48960 Vizcaya, Spain. med003033@gmail.com
Telephone: +34-94-6032860
Fax: +34-94-6032867

Received: October 30, 2016
Peer-review started: November 3, 2016
First decision: December 1, 2016
Revised: December 20, 2016
Accepted: February 8, 2017
Article in press: February 13, 2017
Published online: May 12, 2017

Abstract

AIM

To investigate the relationships among diverse metalloproteases (MMPs) and their tissue inhibitors (TIMPs) and non-alcoholic liver fibrosis in human immunodeficiency virus (HIV)-infected patients.

METHODS

Single nucleotide polymorphisms (SNPs) in *MMPs*, *TNF-α* and *CCR5* genes, and serum levels of MMPs and TIMPs were determined in HIV-infected individuals with/out hepatitis C virus (HCV) coinfection. A total of 158 patients were included, 57 of whom were HCV-coinfected. All patients drank < 50 g ethanol/day. Diverse SNPs (*MMP-1 -1607 1G/2G*, *MMP-8 -799C/T*, *MMP-9 -1562 C/T*, *MMP-13 -77A/G*, *TNF-α -308 G/A*,

CCR5-Δ32), and serum levels of MMPs (2, 3, 8, 9 and 10) and TIMPs (1, 2 and 4) were assessed. Liver fibrosis was determined by transient elastometry, although other non-invasive markers of fibrosis were also considered. Significant liver fibrosis (F ⩾ 2) was defined by a transient elastometry value ⩾ 7.1 kPa.

RESULTS

A total of 34 patients (21.5%) had liver fibrosis ⩾ F2. MMP-2 and TIMP-2 serum levels were higher in patients with liver fibrosis ⩾ F2 (P = 0.02 and P = 0.03, respectively) and correlated positively with transient elastometry values (P = 0.02 and P = 0.0009, respectively), whereas MMP-9 values were negatively correlated with transient elastometry measurements (P = 0.01). Multivariate analyses showed that high levels of MMP-2 (OR = 2.397; 95%CI: 1.191-4.827, P = 0.014) were independently associated with liver fibrosis ⩾ F2 in the patients as a whole. MMP-2 (OR = 7.179; 95%CI: 1.210-42.581, P = 0.03) and male gender (OR = 10.040; 95%CI: 1.621-62.11, P = 0.013) were also independent predictors of fibrosis ⩾ F2 in the HCV-infected subgroup. Likewise, MMP-2, TIMP-2 and MMP-9 were independently associated with transient elastometry values and other non-invasive markers of liver fibrosis. None of the six SNPs evaluated had any significant association with liver fibrosis ⩾ F2.

CONCLUSION

Certain MMPs and TIMPs, particularly MMP-2, seems to be associated with non-alcoholic liver fibrosis in HIV-infected patients with/without HCV coinfection.

Key words: Human immunodeficiency virus; Hepatitis C virus; Liver fibrosis; Transient elastometry; Non-invasive fibrosis markers; Metalloproteases; Their tissue inhibitors; Genetic polymorphisms

Core tip: The role of matrix metalloproteases (MMPs) and their tissue inhibitors (TIMPs) in the development of liver fibrosis is uncertain. We determined some single nucleotide polymorphisms (SNPs), as well as the serum levels of diverse MMPs and TIMPs, in non-alcoholic, human immunodeficiency virus-infected patients with/out hepatitis C virus coinfection, to evaluate their possible relationship with liver fibrosis as assessed by transient elastometry. MMP-2 was independently associated with significant fibrosis. Likewise, MMP-2, TIMP-2 and MMP-9 were independent predictors of transient elastometry values and of other non-invasive tests of fibrosis. No SNP was significantly associated with liver fibrosis. Our findings support the value of these markers in the evaluation of fibrosis.

Collazos J, Valle-Garay E, Suárez-Zarracina T, Montes AH, Cartón JA, Asensi V. Matrix metalloproteases and their tissue inhibitors in non-alcoholic liver fibrosis of human immunodeficiency virus-infected patients. *World J Virol* 2017; 6(2): 36-45 Available from: URL: http://www.wjgnet.com/2220-3249/full/v6/i2/36.htm DOI: http://dx.doi.org/10.5501/wjv.v6.i2.36

INTRODUCTION

Liver fibrosis is characterized by a pathological accumulation of extracellular matrix (ECM), reflecting an imbalance between enhanced matrix synthesis and reduced breakdown of connective tissue proteins. ECM degradation is mediated by matrix metalloproteases (MMPs), a large family of zinc-dependent endopeptidases. Different levels of MMP regulation ensure the constant remodeling of the ECM, including regulation at the gene expression level, cleavage of the pro-enzyme to an active form, and specific inhibition of activated forms by tissue inhibitors (TIMPs)[1,2]. The relevance of MMPs for liver ECM remodeling is shown by the fact that pro-MMP-2 and pro-MMP-9 are activated during rat liver regeneration following hepatectomy and both MMPs contribute to priming hepatocyte proliferation[3]. Different genetic polymorphisms (SNPs) of MMPs and TIMPs have been described. Some of them such as the *MMP-1 -1607 1G/2G* , *MMP-3 -1612 5A/6A, MMP-9-1562 C/T* and *MMP-13 -77 A/G* are located in the MMPs genes promoter region and induce changes in MMPs genes mRNA and protein expression. These functional *MMPs* SNPs are associated mostly with cardiovascular diseases, but also with cancer and osteomyelitis susceptibility[4,5]. *MMP-1*, *MMP-3* and *MMP-9* SNPs have been associated with progression of liver disease in hepatitis C virus (HCV)-mono-infected Japanese patients[6]. Carriage of the *MMP-3 -1612 5A/6* SNP *6A* allele has been associated with increased albumin-globulin ratios in HCV-infected Mexican patients with advanced LF[7]. A *MMP14* SNP has also been associated with hepatocellular carcinoma[8].

Different studies have shown a correlation between TIMP-1, MMP-2 and MMP-9 serum levels and increased LF in HCV-monoinfected and human immunodeficiency virus (HIV)-HCV-coinfected individuals[9-13]. The Fibrocheck, a combination of direct and indirect markers for LF stages in chronic hepatitis C, is constructed combining collagen Ⅲ and its degrading enzyme MMP-1[14].

The aim of this study was to investigate the relationships among diverse *MMPs* SNPs, MMPs and TIMPs serum levels and non-alcoholic LF, evaluated by means of different non-invasive markers, in HIV-infected patients with and without HCV coinfection.

MATERIALS AND METHODS

Study patients and data collection

A total of 158 patients from the Infectious Diseases Outpatient Clinic of the Hospital Universitario Central de Asturias, a third-level 1500-bed University Hospital at Oviedo, Northwestern Spain, were included in the study. Patients older than 18 years with active HIV or HIV-HCV

coinfection, demonstrated by positive serology and viral RNA plasma detection, were enrolled. Demographic, analytical and clinical data, including ethanol and drug consumption, were obtained from patients and their medical charts at enrollment. In addition, we did transient elastometry (TE) to determine the degree of LF. Patients with alcohol abuse, defined as an ethanol intake of ⩾ 50 g/d for > 5 years, were excluded. Many patients were not aware of how long they were HCV infected. In such cases, it was assumed that the patients acquired HCV-infection one year after starting intravenous drugs, as previously reported[15]. All patients were receiving antiretroviral therapy (ART) at the time of inclusion. All patients underwent standard care, including routine non-invasive procedures. Patients were members of a homogeneous Caucasian population, and were residents in the same region (Asturias, Northern Spain) that has a small foreign immigrant population (less than 5%).

Exclusion criteria

Pregnant women and those individuals in whom there were technical difficulties for obtaining reliable TE readings were excluded from the study. In addition, patients with an acute episode of cytolysis or cholestasis, ascitis or spontaneous bacterial peritonitis were excluded because TE reading could be altered by these factors[15]. We also excluded patients who currently or previously were treated with anti-HCV therapy and those who had resolved their HCV infections spontaneously (defined as positive serology but with undetectable HCV RNA). Patients with ART adherence < 75% were also excluded. To avoid other confounding factors, patients with HBV coinfection with/out delta virus coinfection, ethanol consumption ⩾ 50 g/d for > 5 years, alcoholic hepatopathy, other liver diseases, or treatment with immunosuppressant drugs, were excluded from the study as well.

Laboratory methods

HIV and HCV serologies were determined by enzyme immunoassay (MEIA AxSYM; Abbott Diagnostics, Abbott Park, IL, United States). HIV and HCV RNA by quantitative PCR (Cobas TaqMan; Roche Diagnostics, Branchburg, NJ, United States) and HCV genotypes by a line probe assay (Versant HCV, Siemens). Routine laboratory methods were used to calculate LF indexes: AST and platelets for APRI index[16], age, platelet counts, total cholesterol and GGT for calculating the Forns index[17], and age, AST, ALT and platelet counts for FIB-4[18]. In addition, the Yearly Fibrosis Progression Index (YFPI) was also calculated in HCV-infected patients as follows: YFPI = TE value/years of estimated HCV infection.

Transient elastometry

LF was assessed by TE using Fibroscan (EchoSens, Paris, France) following pre-established methods[15,19]. Patients were divided into four groups according to TE measurements, reflecting the progressive stage of LF and analogous to the F0-1, F2, F3 and F4 histological stages of the Metavir scoring system. The TE cut-offs used for this purpose were those described by Castéra *et al*[20]: F0-1: < 7.1 kPa, F = 2: 7.1-9.4 kPa, F = 3: 9.5-12.4 kPa and F = 4 ⩾ 12.5 kPa.

MMPs and TIMPs serum levels assessment

Ten millilitres of whole blood were drawn in siliconized glass tubes, and centrifuged at 1800 × g for 5 min. The obtained serum was aliquoted in Eppendorf tubes and stored at -70 ℃ until further use. MMPs (-2, -3, -8, -9, -10) and TIMPs (-1,-2,-4) were measured by the Quantibody™ Human MMP Array 1 (RayBiotech, Parkway Lane, Norcross, GA, United States), according to the manufacturer's instructions and as previously published by our group[21].

MMPs SNPs genotyping

DNA was obtained from peripheral white blood cells and stored at -20 ℃ before use. The following SNPs of MMPs were genotyped by PCR: *MMP-1 (-1607 1G/2G,* rs 11292517), *MMP-8 (-799 C/T*, rs 11225395), *MMP-9 (-1562 C/T,* rs 34016235), and *MMP-13 (-77 A/G,* rs 2252070). In addition the *TNF-α* (*-308 G/A*, rs 1800629) and the *CCR5 Δ32* (rs 333) SNPs were also genotyped. Oligonucleotide primer sequences, PCR conditions and restriction enzymes used for genotyping and sequencing of the different SNPs studied have been described elsewhere[5,21-23].

Statistical analysis

As MMPs and TIMPs serum levels presented a markedly non-Gaussian distribution, original values were logarithmically transformed for analysis. The reported values are the result of back-transformation into the original units (ng/mL). Continuous variables are presented as mean (95%CI). Proportions were compared with the χ^2 test, whereas *t* test and one-way analysis of variance were used for the comparison of continuous variables in two or more than two groups, respectively. Correlations between MMPs, TIMPs and LF indexes were assessed with the Pearson's correlation coefficient. Stepwise logistic regression analyses were carried out to find the factors independently associated with significant LF, and stepwise multiple regressions were performed to detect the parameters independently predictive of the different LF indexes. SPSS v.22 software was used for statistical calculations. A *P* value < 0.05 for a two-tailed test was considered statistically significant.

RESULTS

The study population was composed of 158 HIV-infected patients, 57 (36.1%) of whom were coinfected with HCV. The mean age was 44.6 years, 65.8% were

male, the mean CD4 counts were 581.5 cells/μL and 85.4% of them had undetectable HIV viral load. Thirty-four patients (21.5%) had significant LF (⩾ F2).

Table 1 shows the demographic, clinical and laboratory data of the patients with and without LF ⩾ F2, as well as the comparison between the two groups. As expected, HCV infection and IDU were associated with LF, but the estimated duration of HCV infection was not. Regarding the HIV-related parameters, both nadir and current CD4 counts were lower, and the duration of HIV infection and time on ART higher in patients with LF ⩾ F2 than in patients without LF. There were no statistically significant differences in HIV or HCV viral loads between the two groups, although there was a trend towards higher HCV viral load and lower rates of undetectable HIV viral load in the patients with LF. The different HCV genotypes were similarly represented in the two groups and there were no significant associations between TE values and HCV genotypes (P = 0.5).

Not surprisingly, the laboratory parameters used for the calculations of the LF indexes, such as platelet count, cholesterol, AST, and GGT, differed significantly between the LF groups. Regarding MMPs and TIMPs, MMP-2 and TIMP-2 serum levels were significantly higher in LF than in patients without LF.

Table 2 shows the genotypic frequencies of the SNPs evaluated according to LF and HCV status. No genotype or SNPs was significantly associated with any of the two conditions.

The relationships of the SNPs and the LF markers are detailed in Table 3. No statistically significant association was found between the different SNPs and the LF indexes, including TE, although patients carrying the heterozygous *CT* genotype of the *MMP-9 -1562 C/T* SNP had consistently higher values of all LF indexes than those with the homozygous *CC* genotype. Table 4 shows the comparisons of the MMPs and TIMPs serum levels according to the different SNPs. Statistically significant differences were observed only between *MMP-8 -799C/T* SNP and TIMP-2 (P = 0.01), *MMP-9-77A/G* SNP and MMP-2 (P = 0.02) and *TNF-α-308 G/A* SNP and TIMP-4 levels (P = 0.02).

Table 5 summarizes the correlations between the different MMPs, TIMPs and LF indexes. There was a good positive correlation among the different LF indexes (P < 0.0001 for all comparisons). Likewise, the diverse fibrosis indexes correlated positively with MMP-2 (P = 0.02 to P = 0.06) and TIMP-2 (P = 0.08 to P < 0.0001) and negatively with MMP-9 (P = 0.2 to P = 0.01). Also, the different MMPs and TIMPs correlated among them. There were strong correlations between MMP-8 levels and levels of MMP-9 and TIMP-1, and between MMP-9 and TIMP-1 levels (P < 0.0001 for each comparison), which explained about a half of the variability of their values.

Multivariate analyses

The variables with a P ⩽ 0.2 significance level in the univariate analyses were entered into the different multivariate models for LF evaluation, excluding the parameters directly indicative of LF and the laboratory tests used for their calculations.

Stepwise logistic regression analyses revealed that high serum levels of MMP-2 (OR = 7.179; 95%CI: 1.210-42.581, P = 0.03) and male gender (OR = 10.040; 95%CI: 1.621-62.11, P = 0.013) were independent predictors of fibrosis ⩾ F2 in the HCV-infected subgroup. In the patients as a whole, only MMP-2 (OR = 2.397, 95%CI: 1.191-4.827, P = 0.014) was independently associated with LF ⩾ F2, whereas gender was close to the significance level (P = 0.08).

Multiple regression analyses were also carried out to evaluate the factors independently associated with each of the five LF indexes (TE, APRI, Forns, FIB-4, and YFPI). Among the different variables considered, only five factors (MMP-2, TIMP-2, MMP-9, CD4 counts and age) explained the diverse markers evaluated. MMP-2 was the parameter most consistently predictive of these indexes. Table 6 shows the P values corresponding to these associations, as well as the adjusted percentage of variability of each LF index accounted for by the model.

The SNPs we evaluated did not have any significant association in the multivariate analyses with either LF ⩾ F2 or any of the different LF indexes analyzed.

DISCUSSION

We found that serum MMP-2 was an independent predictor of non-alcoholic LF ⩾ F2 in HIV-infected patients, as evaluated by TE. In addition, higher serum levels of MMP-2 and TIMP-2, as well as lower levels of MMP-9, were also predictive of higher scores of the diverse laboratory-derived indexes commonly used to measure the degree of LF. Taking into account that these LF indexes are calculated by means of different parameters, the consistent association of these MMPs and TIMPs with each of them reinforces our findings and the value of these MMPs and TIMPs as additional markers of LF. Our results agree with those of Macías *et al*[13] that found an association of serum MMP-2 with LF measured by liver biopsy in 90 HIV-HCV-coinfected Spanish patients. These authors suggested that the combination of AST, platelet count and serum MMP-2 levels is a biochemical surrogate marker for LF ⩾ F2.

We did not observe any association between serum TIMP-1 and LF, or any of the multiple fibrosis indexes studied, as was reported by others studying heterogeneous aspects related to fibrosis in HCV-monoinfected or HIV-HCV-coinfected individuals[9-12]. On the contrary, we found an independent association of serum MMP-2, MMP-9 and TIMP-2 with diverse LF indexes. We did not measured serum MMP-1, which was associated with LF in HCV-mono-infected individuals in another study and was included in the Fibro-check[14].

We did not find any statistically significant association between LF and the different SNPs evaluated,

Table 1 Demographic, clinical and laboratory characteristics of the patients, according to the existence or not of significant liver fibrosis (≥ F2)

	All patients (*n* = 158)	No fibrosis (*n* = 124)	Fibrosis (*n* = 34)	*P* value
Demography, epidemiology, anthropometry and habits				
Age (yr)	44.56 (43.20-45.92)	44.50 (42.93-46.07)	44.79 (41.96-47.63)	0.9
Male, *n* (%)	104 (65.8)	78 (62.9)	26 (76.5)	0.14
Weight (kg)	65.17 (62.88-67.46)	64.46 (61.72-67.20)	67.76 (64.03-71.50)	0.24
Height (cm)	164.4 (160.6-168.2)	163.4 (158.5-168.2)	168.2 (166.2-170.2)	0.3
Body mass index (kg/m^2)	23.58 (23.10-24.05)	23.48 (22.95-24.01)	23.90 (22.75-25.0.6)	0.5
Tobacco smokers, *n* (%)	105 (66.5)	78 (62.9)	27 (79.4)	0.07
Cannabis use, *n* (%)	38 (24.1)	22 (17.7)	16 (47.1)	0.0004
Alcohol intake, *n* (%)[1]	55 (35.0)	43 (34.7)	12 (36.4)	0.9
IDU, *n* (%)	58 (36.9)	29 (23.6)	29 (85.6)	< 0.0001
Men who have sex with men, *n* (%)	28 (17.8)	27 (22.0)	1 (2.9)	0.01
Heterosexual, *n* (%)	67 (42.7)	63 (51.2)	4 (11.8)	< 0.0001
Transfusion, *n* (%)	4 (2.5)	4 (3.3)	0 (0.0)	0.3
HIV-related parameters				
Current CD4 counts (cells/μL)	581.5 (533.0-630.1)	612.3 (555.8-668.8)	469.6 (383.7-555.4)	0.017
Nadir CD4 counts (cells/μL)	201.8 (176.5-227.1)	213.4 (183.4-243.4)	159.7 (116.7-202.6)	0.04
CD4 gain (cells/μL)	379.7 (334.4-425.0)	399.0 (345.4-452.6)	309.9 (231.4-388.4)	0.11
Undetectable HIV viral load, *n* (%)	135 (85.4)	109 (87.9)	26 (76.5)	0.09
HIV viral load (log copies/mL)[2]	2.996 (2.556-3.434)	2.991 (2.407-3.575)	3.006 (2.173-3.840)	0.97
Years of HIV infection	11.93 (11.12-12.73)	11.31 (10.39-12.22)	14.19 (12.70-15.68)	0.003
Months on antiretroviral therapy	114.3 (106.8-121.8)	109.9 (101.3-118.5)	130.2 (115.0-145.3)	0.03
CDC clinical stage, *n* (%)				
A	84 (53.5)	65 (52.8)	19 (55.9)	0.07
B	23 (14.6)	22 (17.9)	1 (2.9)	
C	50 (31.8)	36 (29.3)	14 (41.2)	
HCV-related parameters				
HCV infection, *n* (%)	57 (36.1)	25 (20.2)	32 (94.1)	< 0.0001
HCV viral load (log copies/mL)	5.745 (5.504-5.985)	5.524 (5.085-5.964)	5.915 (5.649-6.181)	0.11
Years of HCV infection	22.46 (20.71-24.21)	21.84 (18.96-24.72)	22.94 (20.65-25.23)	0.5
HCV genotype, *n* (%)				
1	31 (54.4)	14 (56.0)	17 (53.1)	0.7
2	2 (1.3)	1 (4.0)	1 (3.1)	
3	15 (23.6)	5 (20.0)	10 (31.3)	
4	9 (15.8)	5 (20.0)	4 (12.5)	
Liver fibrosis parameters				
Transient elastometry (kPa)	7.53 (5.99-9.06)	4.65 (4.45-4.85)	18.02 (11.93-24.10)	< 0.0001
APRI	0.633 (0.511-0.756)	0.385 (0.346-0.423)	1.541 (1.093-1.989)	< 0.0001
Forns	4.412 (4.116-4.707)	3.990 (3.734-4.246)	5.949 (5.095-6.802)	0.0001
FIB-4	1.475 (1.249-1.700)	1.088 (0.985-1.191)	2.884 (2.031-3.736)	0.0002
YFPI[3]	0.584 (0.416-0.752)	0.281 (0.222-0.340)	0.821 (0.548-1.095)	0.0004
Degree of liver fibrosis, *n* (%)				
F0-F1	124 (78.5)	124 (100)	0 (0.0)	< 0.0001
F2	15 (9.5)	0 (0.0)	15 (44.1)	
F3	10 (6.3)	0 (0.0)	10 (29.4)	
F4	9 (5.7)	0 (0.0)	9 (26.5)	
Laboratory parameters				
Platelet count (/μL)	222570 (211690-233450)	236750 (225410-248090)	169270 (147220-191330)	< 0.0001
Glucose (mg/dL)	98.54 (95.25-101.84)	98.00 (94.62-101.38)	100.66 (90.92-110.39)	0.5
Total cholesterol (mg/dL)	195.01 (188.51-201.51)	201.0 (193.8-208.3)	173.0 (160.6-185.4)	0.0004
HDL cholesterol (mg/dL)	49.33 (46.88-51.78)	49.42 (46.95-52.29)	48.25 (42.02-54.48)	0.7
LDL cholesterol (mg/dL)	110.73 (104.68-116.77)	116.97 (110.22-123.72)	87.53 (76.91-98.16)	0.0001
Triglycerides (mg/dL)	199.79 (170.08-229.50)	189.0 (157.5-220.5)	241.7 (161.4-322.0)	0.22
AST (UI/mL)	40.89 (36.01-45.78)	30.72 (28.30-33.13)	78.00 (62.01-93.99)	< 0.0001
ALT (UI/mL)	47.82 (40.54-55.09)	36.91 (32.03-41.79)	87.59 (62.16-113.02)	0.0003
AST/ALT ratio	1.011 (0.949-1.074)	0.993 (0.927-1.059)	1.079 (0.913-1.246)	0.3
GGT (UI/mL)	83.95 (66.61-101.29)	59.73 (48.40-71.07)	174.21 (110.61-237.81)	0.001
Alkaline phosphatase (UI/mL)	91.87 (85.09-98.65)	90.72 (83.22-98.23)	98.31 (81.46-115.17)	0.4
MMP-2 (ng/mL)	0.538 (0.442-0.654)	0.482 (0.387-0.600)	0.867 (0.579-1.300)	0.02
MMP-3 (ng/mL)	15.00 (13.24-17.01)	14.36 (12.47-16.54)	17.77 (14.45-23.49)	0.18
MMP-8 (ng/mL)	0.031 (0.023-0.041)	0.029 (0.021-0.039)	0.040 (0.020-0.078)	0.4
MMP-9 (ng/mL)	22.49 (18.81-26.90)	23.19 (19.00-28.31)	19.94 (13.01-30.58)	0.5
MMP-10 (ng/mL)	2.50 (1.66-3.75)	2.163 (1.487-3.145)	5.077 (0.938-27.469)	0.12
TIMP-1 (ng/mL)	50.56 (45.58-56.08)	50.84 (45.43-56.88)	49.49 (37.71-64.94)	0.8
TIMP-2 (ng/mL)	8.23 (7.16-9.46)	7.62 (6.59-8.80)	11.15 (7.55-16.45)	0.03
TIMP-4 (ng/mL)	0.040 (0.030-0.054)	0.037 (0.027-0.051)	0.054 (0.026-0.110)	0. 3

[1]Less than 50 g/d; [2]Only if detectable; [3]YFPI: Yearly fibrosis progression index (only in HCV-infected patients), calculated as transient elastometry value divided into the years of estimated HCV infection. Values are expressed as mean (95%CI) or *n* (%) as appropriate. IDU: Intravenous drug use. MMP: Matrix metalloprotease; HCV: Hepatitis C virus; AST: Aspartate aminotransferase; ALT: Alanine aminotransferase; APRI: AST to Platelet Ratio Index; FIB-4: Fibrosis-4 index; HDL: High-density lipoprotein; LDL: Low-density lipoprotein; GGT: Gamma-glutamyl transpeptidase; TIMP: Tissue inhibitor of metalloprotease.

Table 2 Genotypic frequencies of different single nucleotide polymorphisms according to liver fibrosis ≥ F2 and hepatitis C virus status

SNP	Genotype	No fibrosis *n* (%)	Fibrosis *n* (%)	*P* value	HIV mono-infected *n* (%)	HIV/HCV coinfected *n* (%)	*P* value
MMP-1 -1607 1G/2G	*1G1G*	14 (20.3)	4 (16.7)	0.9	9 (16.1)	9 (24.3)	0.6
	1G2G	13 (18.8)	5 (20.8)		12 (21.4)	6 (16.2)	
	2G2G	42 (60.9)	15 (62.5)		35 (62.5)	22 (59.5)	
MMP-8 -799C/T	*CC*	30 (27.0)	6 (22.2)	0.6	25 (26.3)	11 (25.5)	1
	CT	47 (42.4)	10 (37.0)		39 (41.1)	18 (41.9)	
	TT	34 (30.6)	11 (40.8)		31 (32.6)	14 (32.6)	
MMP-9 -1562 C/T	*CC*	78 (81.2)	28 (84.8)	0.6	61 (83.6)	45 (80.4)	0.6
	CT	18 (18.8)	5 (15.2)		12 (16.4)	11 (19.6)	
	TT	0 (0.0)	0 (0.0)		0 (0.0)	0 (0.0)	
MMP-13 -77A/G	*AA*	89 (74.8)	21 (61.8)	0.14	70 (72.9)	40 (70.2)	0.7
	AG	30 (25.2)	13 (38.2)		26 (27.1)	17 (29.8)	
	GG	0 (0.0)	0 (0.0)		0 (0.0)	0 (0.0)	
TNF-α -308 G/A	*AA*	11 (11.3)	4 (11.8)	0.5	7 (9.5)	8 (14.0)	0.7
	AG	62 (63.9)	18 (52.9)		46 (62.1)	34 (59.6)	
	GG	24 (24.7)	12 (35.3)		21 (28.4)	15 (26.3)	
CCR5-⊿32	*wt/wt*	96 (80.0)	30 (88.2)	0.27	77 (79.4)	49 (86.0)	0.3
	wt/⊿32	24 (20.0)	4 (11.8)		20 (20.6)	8 (14.0)	
	⊿32/⊿32	0 (0.0)	0 (0.0)		0 (0.0)	0 (0.0)	

SNP: Single nucleotide polymorphisms; HCV: Hepatitis C virus; HIV: Human immunodeficiency virus; MMP: Matrix metalloprotease.

Table 3 Liver fibrosis indexes according to the single nucleotide polymorphisms genotypes

SNP	Genotype	Transient elastometry	YFPI[1]	APRI	Forns	FIB-4
MMP-1 -1607 1G/2G	*1G1G*	5.583 (4.600-6.567)	0.346 (0.215-0.477)	0.693 (0.192-1.195)	3.719 (2.860-4.579)	1.317 (0.723-1.911)
	1G2G	5.911 (4.649-7.174)	0.470 (0.250-0.691)	0.488 (0.307-0.670)	4.253 (3.430-5.077)	1.092 (0.859-1.324)
	2G2G	8.781 (5.585-11.977)	0.689 (0.378-1.001)	0.675 (0.453-0.897)	4.390 (3.914-4.867)	1.479 (1.097-1.862)
	P value	0.3	0.3	0.7	0.4	0.5
MMP-8 -799C/T	*CC*	6.644 (3.736-9.553)	0.633 (0.074-1.193)	0.615 (0.411-0.819)	4.510 (3.920-5.099)	1.461 (1.058-1.864)
	CT	5.628 (5.060-6.196)	0.357 (0.275-0.439)	0.453 (0.347-0.559)	4.126 (3.701-4.551)	1.145 (1.014-1.277)
	TT	7.729 (4.540-10.918)	0.671 (0.376-0.965)	0.768 (0.447-1.088)	4.407 (3.825-4.989)	1.603 (1.081-2.125)
	P value	0.4	0.19	0.1	0.5	0.15
MMP-9 -1562 C/T	*CC*	7.540 (5.810-9.269)	0.527 (0.361-0.694)	0.612 (0.475-0.749)	4.370 (4.024-4.717)	1.404 (1.163-1.645)
	CT	11.178 (4.093-18.264)	0.833 (0.229-1.437)	0.867 (0.412-1.323)	5.083 (4.024-6.142)	2.043 (1.044-3.041)
	TT	-	-	-	-	-
	P value	0.14	0.16	0.16	0.11	0.065
MMP-13 -77A/G	*AA*	7.217 (5.654-8.780)	0.535 (0.358-0.712)	0.623 (0.480-0.766)	4.352 (3.993-4.711)	1.462 (1.185-1.738)
	AG	8.721 (4.646-12.798)	0.700 (0.291-1.109)	0.698 (0.426-0.970)	4.588 (3.998-5.177)	1.553 (1.109-1.998)
	GG	-	-	-	-	-
	P value	0.4	0.4	0.6	0.5	0.7
TNF-α -308 G/A	*AA*	10.073 (1.300-18.849)	0.656 (0.132-1.180)	0.693 (0.135-1.250)	4.331 (3.280-5.383)	1.584 (0.693-2.475)
	AG	8.086 (5.779-10.394)	0.552 (0.336-0.767)	0.675 (0.495-0.855)	4.603 (4.174-5.033)	1.575 (1.210-1.940)
	GG	7.514 (4.623-10.404)	0.620 (0.228-1.012)	0.701 (0.405-0.997)	4.221 (3.513-4.929)	1.466 (1.021-1.910)
	P value	0.7	0.9	0.99	0.6	0.9
CCR5-⊿32	*wt/wt*	7.852 (5.998-9.707)	0.590 (0.399-0.783)	0.664 (0.525-0.803)	4.439 (4.102-4.775)	1.513 (1.264-1.762)
	wt/⊿32	6.521 (4.109-8.934)	0.545 (0.232-0.858)	0.539 (0.230-0.847)	4.391 (3.684-5.098)	1.335 (0.699-1.971)
	⊿32/⊿32	-	-	-	-	-
	P value	0.5	0.9	0.4	0.9	0.6

[1]YFPI: Yearly fibrosis progression index (only for HCV-infected patients); SNP: Single nucleotide polymorphisms; MMP: Matrix metalloprotease. Values are expressed as mean (95%CI) in ng/mL; APRI: AST to Platelet Ratio Index; FIB-4: Fibrosis-4 index.

although patients carrying the heterozygous *CT* genotype of the *MMP-9 -1562 C/T* SNP had consistently higher values of all LF indexes than those with the homozygous *CC* genotype. Okamoto *et al*[6] reported an association of *MMP-1- 1607 1G/2G*, *MMP-3 -1612 5A/6* and *MMP-9 -1562 C/T*, SNPs with LF progression measured by biochemical markers or liver biopsy in HCV-monoinfected Japanese patients. Sánchez-Parada *et al*[7] found that *TGBFB1* +915 C/G (rs 1800471) SNP carriage was associated with severity of hepatic necroinflammation and LF in HCV-mono-infected Mexican patients. In addition, the same authors reported an association between *MMP-3 -1612 5A/6* SNP *6A* allele carriage and an increase in the albumin-globulin ratio, as a surrogate marker of LF. The ethnic background of our patients was different from those of previous reports, and the relatively small sample size of our HIV-HCV-coinfected population could

Table 4 Metalloproteases and their tissue inhibitors according to the single nucleotide polymorphisms genotypes

SNP	Genotype	MMP-2	MMP-3	MMP-8	MMP-9	MMP-10	TIMP-1	TIMP-2	TIMP-4
MMP-1 -1607 1G/2G	*1G1G*	0.379 (0.195-0.736)	16.69 (11.00-25.33)	0.035 (0.013-0.095)	19.93 (11.59-34.28)	1.782 (0.350-9.071)	41.73 (30.87-56.42)	6.79 (4.52-10.21)	0.031 (0.010-0.091)
	1G2G	0.803 (0.409-1.575)	19.87 (15.13-26.10)	0.041 (0.012-0.134)	22.35 (13.37-37.36)	1.451 (0.417-5.047)	54.07 (39.44-74.14)	7.30 (4.49-11.87)	0.047 (0.020-0.113)
	2G2G	0.609 (0.449-0.826)	14.72 (11.57-18.73)	0.027 (0.017-0.042)	23.65 (17.07-32.76)	3.345 (1.512-7.399)	50.34 (42.16-60.10)	8.39 (6.54-10.76)	0.032 (0.019-0.053)
	P value	0.18	0.4	0.7	0.9	0.5	0.4	0.6	0.7
MMP-8 799C/T	*CC*	0.655 (0.473-0.908)	15.96 (12.94-19.68)	0.048 (0.025-0.090)	29.93 (19.94-44.94)	4.650 (1.354-15.97)	61.60 (49.94-75.99)	11.67 (8.59-15.85)	0.041 (0.023-0.073)
	CT	0.568 (0.409-0.787)	13.05 (10.22-16.65)	0.031 (0.018-0.054)	21.30 (15.50-29.28)	2.179 (1.201-3.953)	47.17 (38.80-57.34)	6.71 (5.50-8.18)	0.035 (0.021-0.058)
	TT	0.432 (0.280-0.668)	16.66 (13.35-20.81)	0.020 (0.015-0.027)	18.86 (14.03-25.37)	1.623 (0.938-2.808)	47.75 (40.75-55.94)	8.12 (5.89-11.20)	0.050 (0.030-0.084)
	P value	0.3	0.3	0.09	0.17	0.17	0.11	0.01	0.6
MMP-9 1562 C/T	*CC*	0.495 (0.385-0.637)	15.42 (13.11-18.14)	0.034 (0.024-0.049)	22.39 (17.79-28.19)	2.405 (1.462-3.957)	52.23 (46.17-59.07)	8.39 (7.18-9.80)	0.037 (0.026-0.053)
	CT	1.031 (0.853-1.246)	18.15 (13.99-23.54)	0.020 (0.008-0.047)	22.97 (14.77-35.71)	5.960 (0.666-53.34)	46.55 (33.82-64.07)	8.18 (4.40-15.21)	0.058 (0.025-0.137)
	TT	-	-	-	-	-	-	-	-
	P value	0.02	0.3	0.2	0.9	0.2	0.4	0.9	0.3
MMP-13 77A/G	*AA*	0.522 (0.419-0.650)	15.62 (13.47-18.13)	0.030 (0.022-0.041)	23.06 (18.64-28.54)	2.337 (1.380-3.957)	53.30 (47.05-60.38)	8.54 (7.21-10.12)	0.050 (0.036-0.069)
	AG	0.683 (0.458-1.017)	14.37 (11.10-18.59)	0.037 (0.019-0.071)	22.96 (16.01-32.93)	2.685 (1.215-5.931)	48.10 (39.30-58.88)	8.07 (6.09-10.68)	0.031 (0.016-0.058)
	GG	-	-	-	-	-	-	-	-
	P value	0.22	0.6	0.6	0.98	0.8	0.4	0.7	0.14
TNF-α 308 G/A	*AA*	0.730 (0.325-1.639)	21.40 (14.72-31.13)	0.039 (0.010-0.156)	17.42 (8.16-37.21)	0.804 (0.369-1.755)	57.25 (37.28-87.92)	13.14 (8.72-19.80)	0.111 (0.054-0.227)
	AG	0.558 (0.429-0.727)	14.65 (11.96-17.95)	0.031 (0.020-0.050)	23.41 (17.78-30.83)	4.460 (2.097-9.486)	51.62 (43.92-60.66)	8.39 (6.71-10.48)	0.043 (0.028-0.064)
	GG	0.453 (0.281-0.732)	16.54 (13.36-20.47)	0.027 (0.018-0.040)	23.62 (17.25-32.34)	1.998 (0.879-4.542)	46.63 (39.84-54.59)	7.04 (5.36-9.26)	0.023 (0.012-0.045)
	P value	0.4	0.24	0.8	0.7	0.065	0.6	0.1	0.02
CCR5-⊿32	*wt/wt*	0.601 (0.484-0.747)	15.75 (13.71-18.09)	0.031 (0.022-0.043)	21.55 (17.50-26.53)	2.441 (1.482-4.020)	50.72 (44.83-57.38)	8.10 (6.95-9.45)	0.041 (0.029-0.057)
	wt/⊿32	0.431 (0.286-0.652)	13.64 (9.87-18.85))	0.032 (0.020-0.051)	27.15 (18.55-39.73)	2.662 (1.222-5.801)	52.01 (42.66-63.42)	9.44 (6.49-13.72)	0.043 (0.021-0.088)
	⊿32/⊿32	-	-	-	-	-	-	-	-
	P value	0.15	0.4	0.9	0.3	0.9	0.9	0.4	0.9

SNP: Single nucleotide polymorphisms; MMP: Matrix metalloprotease. Values are expressed as mean (95%CI) in ng/mL. APRI: AST to Platelet Ratio Index; FIB-4: Fibrosis-4 index; TIMP: Tissue inhibitor of metalloprotease.

perhaps explain these discrepant findings. We did not genotype the *TGBFB1* +915 C/G nor the *MMP14* [-1658 (rs100349), +7096 (rs2236307) and + 8153 (rs3751489)] SNPs that have been associated with LF and hepatocellular carcinoma in HCV-monoinfected patients of Mexican and Chinese extraction[7,8].

We found that male gender was independently associated with LF in HIV-HCV coinfection. This association was already described by our group in another cohort of patients[24], and appears to be at least partially due to hormonal issues. In this regard, experimental studies in rats have shown the beneficial effects of estradiol administration on LF through diverse mechanisms[25-28].

Limitations to our study include those inherent to cross-sectional studies and the relatively small number of patients with LF ⩾ F2. The relatively small sample size might affect especially the genetic testing results. However, the sample size was large enough to find significant associations between LF and MMPs, TIMPs and other factors, and our findings on the independent relationships of MMPs and TIMPs with the diverse LF markers evaluated were highly consistent and support the reliability of our results.

A possible reason for the small numbers of patients with LF ⩾ 2 is the exclusion of alcoholics from this study. We used a definition of alcohol abuse based on an ethanol exposition ⩾ 50 g/d for > 5 years previously used by others and us[29,30]. This alcohol consumption equates to approximately 3.5 drinks per day using standard drinks in the United States. Other authors reduced the alcohol abuse to ⩾ 40 g/d for > 5 years[12]. We consider that this discrepancy might play a minor role in our study considering that only 34 patients (21.5% of the total) had LF ⩾ F2 and 32 of them had HIV-HCV coinfection.

We conclude that some MMPs and TIMPs, such as MMP-9, TIMP-2 and especially MMP-2, are associated

Table 5 Correlations among metalloproteases, their tissue inhibitors and liver fibrosis parameters

	MMP-3	MMP-8	MMP-9	MMP-10	TIMP-1	TIMP-2	TIMP-4	TE	YFPI	APRI	Forns	FIB-4
MMP-2	0.19 (0.04)	0.21 (0.02)	0.21 (0.02)	0.20 (0.09)	0.29 (0.002)	0.29 (0.002)	0.35 (0.0002)	0.23 (0.016)	0.30 (0.058)	0.20 (0.03)	0.19 (0.04)	0.20 (0.03)
MMP-3		0.29 (0.0006)	0.30 (0.0006)	0.15 (0.19)	0.33 (0.0001)	0.27 (0.002)	0.38 (< 0.0001)	0.09 (0.3)	0.001 (0.99)	0.16 (0.06)	0.16 (0.06)	0.10 (0.24)
MMP-8			0.69 (< 0.0001)	0.25 (0.02)	0.71 (< 0.0001)	0.40 (< 0.0001)	0.24 (0.005)	-0.02 (0.8)	-0.15 (0.3)	-0.01 (0.9)	0.03 (0.8)	-0.03 (0.7)
MMP-9				0.21 (0.06)	0.71 (< 0.0001)	0.16 (0.06)	0.21 (0.01)	-0.21 (0.01)	-0.32 (0.02)	-0.17 (0.047)	-0.11 (0.2)	-0.20 (0.02)
MMP-10					0.12 (0.3)	0.22 (0.051)	0.11 (0.3)	0.01 (0.9)	-0.09 (0.7)	0.12 (0.3)	-0.08 (0.5)	-0.03 (0.8)
TIMP-1						0.40 (< 0.0001)	0.39 (< 0.0001)	0.02 (0.8)	-0.04 (0.8)	-0.02 (0.8)	0.07 (0.4)	0.01 (0.9)
TIMP-2							0.33 (0.0001)	0.28 (0.0009)	0.25 (0.08)	0.35 (< 0.0001)	0.20 (0.018)	0.36 (< 0.0001)
TIMP-4								0.11 (0.2)	0.03 (0.8)	0.14 (0.12)	0.06 (0.5)	0.19 (0.03)
TE									0.94 (< 0.0001)	0.75 (< 0.0001)	0.59 (< 0.0001)	0.82 (< 0.0001)
YFPI										0.63 (< 0.0001)	0.51 (0.0001)	0.74 (< 0.0001)
APRI											0.55 (< 0.0001)	0.90 (< 0.0001)
Forns												0.67 (< 0.0001)

Values are expressed as *r* (*P* value). MMP: Matrix metalloprotease; HCV: Hepatitis C virus; TE: Transient elastometry; YFPI: Yearly fibrosis progression index (only for HCV-infected patients); TIMP: Tissue inhibitor of metalloprotease.

Table 6 Independent predictors of different fibrosis indexes

	TE	APRI	Forns	FIB-4	YFPI
Higher MMP-2 levels	0.001	0.0001	0.03	0.0009	0.004
Higher TIMP-2 levels	0.016	0.0001	0.024	0.0002	-
Lower MMP-9 levels	0.023	0.016	-	0.03	0.043
Lower current CD4 counts	-	0.032	0.037	0.043	-
Older age	-	-	0.004	0.05	-
% of the index accounted for by the model	20.00%	35.30%	23.30%	33.50%	20.70%

Numbers represent *P* values. HCV: Hepatitis C virus; MMP: Matrix metalloprotease; TE: Transient elastometry; YFPI: Yearly fibrosis progression index (only for HCV-infected patients); APRI: AST to Platelet Ratio Index; TIMP: Tissue inhibitor of metalloprotease.

with non-alcoholic LF and diverse fibrosis markers in HIV-infected patients with and without HCV coinfection. The determination of these parameters could be useful for the development of other laboratory-derived indexes of LF in order to improve the accuracy of the current non-invasive tests. On the contrary, the SNPs evaluated did not significantly associate with LF in our Caucasian cohort, although this aspect needs to be confirmed by other studies with larger sample sizes and, perhaps, with patients of different ethnic extraction, taking into account the trend that we observed with the *MMP-9 1562* SNP.

ACKNOWLEDGMENTS

We are indebted to Prof. Joshua Fierer, Division of Infectious Diseases, Veterans Affairs San Diego Healthcare System and University of California, San Diego School of Medicine, United States, for his editing of the manuscript and helpful comments.

COMMENTS

Background

Liver fibrosis reflects an imbalance between extracellular matrix synthesis and reduced breakdown of connective tissue proteins, which is regulated by matrix metalloproteases (MMPs) and their tissue inhibitors (TIMPs). Genetic polymorphisms (SNPs) of MMPs and TIMPs induce changes in *MMPs* genes mRNA and protein expression. However, the role of MMPs, TIMPs and their SNPs in the development of liver fibrosis and their usefulness for the evaluation of fibrosis in clinical practice are uncertain.

Research frontiers

Some studies have inconsistently found a relationship between liver fibrosis and certain MMPs, TIMPs and SNPs in hepatitis C virus (HCV)-monoinfected and human immunodeficiency virus (HIV)-HCV-coinfected individuals, although the issue is far from clear. The topic is important, not only to support a possible pathogenic role of these substances and their genetic polymorphisms in the generation of fibrosis, but also to define the possible value of these determinations in the evaluation of the degree of fibrosis, which could be useful

to clinicians involved in the care of these patients.

Innovations and breakthroughs

Excessive alcohol intake, a common habit among intravenous drug users, most of whom are also coinfected with HCV, is a cause of liver disease, and the influence of MMPs, TIMPs and their SNPs might vary according to the etiology of liver fibrosis. Consequently, the authors excluded patients with excessive alcohol intake, to minimize the possible confounding factor of multiple etiologies of fibrosis. On the other hand, non-invasive methods of measurement of liver fibrosis, mainly transient elastometry, are replacing liver biopsy in the evaluation of the degree of fibrosis. Therefore, the authors have also analyzed the relationships of these substances with multiple fibrosis indexes, in order to verify the consistence of such relationships from the perspective of different fibrosis markers. The authors found that high levels of MMP-2 were independently associated with liver fibrosis ≥ F2. Likewise, MMP-2, TIMP-2 and MMP-9 were independent and consistent predictors of transient elastometry values and of other non-invasive markers of fibrosis. On the contrary, they did not find any significant association between liver fibrosis ≥ F2 and the diverse SNPs evaluated.

Applications

This study supports the implication of these substances in the development of liver fibrosis, and their value as predictors of the degree of fibrosis in HIV-infected patients with non-alcoholic liver disease. The determination of these parameters could be useful for the development of laboratory-derived indexes of fibrosis, in order to improve the accuracy of the current non-invasive tests.

Terminology

MMPs, a family of zinc-dependent endoproteases, and their tissue inhibitors TIMPs are involved in the remodeling and degradation of the extracellular matrix and, therefore, may influence the development of liver fibrosis.

Peer-review

The results presented in this reviewed manuscript are of scientific merit and interest.

REFERENCES

1 **Parks WC**, Wilson CL, López-Boado YS. Matrix metalloproteinases as modulators of inflammation and innate immunity. *Nat Rev Immunol* 2004; **4**: 617-629 [PMID: 15286728 DOI: 10.1038/nri1418]

2 **Mastroianni CM**, Lichtner M, Mascia C, Zuccalà P, Vullo V. Molecular mechanisms of liver fibrosis in HIV/HCV coinfection. *Int J Mol Sci* 2014; **15**: 9184-9208 [PMID: 24865485 DOI: 10.3390/ijms15069184]

3 **Kim TH**, Mars WM, Stolz DB, Michalopoulos GK. Expression and activation of pro-MMP-2 and pro-MMP-9 during rat liver regeneration. *Hepatology* 2000; **31**: 75-82 [PMID: 10613731 DOI: 10.1002/hep.510310114]

4 **Ye S**. Influence of matrix metalloproteinase genotype on cardiovascular disease susceptibility and outcome. *Cardiovasc Res* 2006; **69**: 636-645 [PMID: 16122719 DOI: 10.1016/j.cardiores.2005.07.015]

5 **Montes AH**, Valle-Garay E, Alvarez V, Pevida M, García Pérez E, Paz J, Meana A, Asensi V. A functional polymorphism in MMP1 could influence osteomyelitis development. *J Bone Miner Res* 2010; **25**: 912-919 [PMID: 19821768 DOI: 10.1359/jbmr.091013]

6 **Okamoto K**, Mimura K, Murawaki Y, Yuasa I. Association of functional gene polymorphisms of matrix metalloproteinase (MMP)-1, MMP-3 and MMP-9 with the progression of chronic liver disease. *J Gastroenterol Hepatol* 2005; **20**: 1102-1108 [PMID: 15955221 DOI: 10.1111/j.1440-1746.2005.03860.x]

7 **Sánchez-Parada MG**, Alvarez-Rodríguez BA, Gómez-Meda BC, Troyo-Sanromán R, Sánchez-Orozco LV, Zamora-Perez AL, Landeros MS, Armendáriz-Borunda J. Association of genetic polymorphisms with histological grading of necroinflammation, staging of fibrosis, and liver function in Mexicans with chronic hepatitis C virus infection. *J Investig Med* 2013; **61**: 1088-1096 [PMID: 23941979 DOI: 10.2310/JIM.0b013e3182a32e24]

8 **Chen TY**, Li YC, Liu YF, Tsai CM, Hsieh YH, Lin CW, Yang SF, Weng CJ. Role of MMP14 gene polymorphisms in susceptibility and pathological development to hepatocellular carcinoma. *Ann Surg Oncol* 2011; **18**: 2348-2356 [PMID: 21298348 DOI: 10.1245/s10434-011-1574-x]

9 **Lichtinghagen R**, Huegel O, Seifert T, Haberkorn CI, Michels D, Flemming P, Bahr M, Boeker KH. Expression of matrix metalloproteinase-2 and -9 and their inhibitors in peripheral blood cells of patients with chronic hepatitis C. *Clin Chem* 2000; **46**: 183-192 [PMID: 10657374]

10 **Patel K**, Gordon SC, Jacobson I, Hézode C, Oh E, Smith KM, Pawlotsky JM, McHutchison JG. Evaluation of a panel of non-invasive serum markers to differentiate mild from moderate-to-advanced liver fibrosis in chronic hepatitis C patients. *J Hepatol* 2004; **41**: 935-942 [PMID: 15582126 DOI: 10.1016/j.jhep.2004.08.008]

11 **Fontana RJ**, Dienstag JL, Bonkovsky HL, Sterling RK, Naishadham D, Goodman ZD, Lok AS, Wright EC, Su GL. Serum fibrosis markers are associated with liver disease progression in non-responder patients with chronic hepatitis C. *Gut* 2010; **59**: 1401-1409 [PMID: 20675691 DOI: 10.1136/gut.2010.207423]

12 **Larrousse M**, Laguno M, Segarra M, De Lazzari E, Martinez E, Blanco JL, León A, Deulofeu R, Miquel R, Milinkovic A, Lonca M, Miró JM, Biglia A, Murillas J, Gatell JM, Mallolas J. Noninvasive diagnosis of hepatic fibrosis in HIV/HCV-coinfected patients. *J Acquir Immune Defic Syndr* 2007; **46**: 304-311 [PMID: 18172937 DOI: 10.1097/QAI.0b013e3181520502]

13 **Macías J**, Mira J, Gilabert I, Neukam K, Roldán C, Viloria M, Moro A, Pineda JA. Combined use of aspartate aminotransferase, platelet count and matrix metalloproteinase 2 measurements to predict liver fibrosis in HIV/hepatitis C virus-coinfected patients. *HIV Med* 2011; **12**: 14-21 [PMID: 20497249 DOI: 10.1111/j.1468-1293.2010.00836.x]

14 **Attallah AM**, El-Far M, Abdel Malak CA, Omran MM, Farid K, Hussien MA, Albannan MS, Attallah AA, Elbendary MS, Elbesh DA, Elmenier NA, Abdallah MO. Fibro-check: a combination of direct and indirect markers for liver fibrosis staging in chronic hepatitis C patients. *Ann Hepatol* 2015; **14**: 225-233 [PMID: 25671832]

15 **Cartón JA**, Collazos J, de la Fuente B, García-Alcalde ML, Suarez-Zarracina T, Rodríguez-Guardado A, Asensi V. Factors associated with liver fibrosis in intravenous drug users coinfected with HIV and HCV. *Antivir Ther* 2011; **16**: 27-35 [PMID: 21311106 DOI: 10.3851/IMP1708]

16 **Wai CT**, Greenson JK, Fontana RJ, Kalbfleisch JD, Marrero JA, Conjeevaram HS, Lok AS. A simple noninvasive index can predict both significant fibrosis and cirrhosis in patients with chronic hepatitis C. *Hepatology* 2003; **38**: 518-526 [PMID: 12883497 DOI: 10.1053/jhep.2003.50346]

17 **Forns X**, Ampurdanès S, Llovet JM, Aponte J, Quintó L, Martínez-Bauer E, Bruguera M, Sánchez-Tapias JM, Rodés J. Identification of chronic hepatitis C patients without hepatic fibrosis by a simple predictive model. *Hepatology* 2002; **36**: 986-992 [PMID: 12297848 DOI: 10.1053/jhep.2002.36128]

18 **Vallet-Pichard A**, Mallet V, Nalpas B, Verkarre V, Nalpas A, Dhalluin-Venier V, Fontaine H, Pol S. FIB-4: an inexpensive and accurate marker of fibrosis in HCV infection. comparison with liver biopsy and fibrotest. *Hepatology* 2007; **46**: 32-36 [PMID: 17567829 DOI: 10.1002/hep.21669]

19 **Sandrin L**, Fourquet B, Hasquenoph JM, Yon S, Fournier C, Mal F, Christidis C, Ziol M, Poulet B, Kazemi F, Beaugrand M, Palau R. Transient elastography: a new noninvasive method for assessment of hepatic fibrosis. *Ultrasound Med Biol* 2003; **29**: 1705-1713 [PMID: 14698338 DOI: 10.1016/j.ultrasmedbio.2003.07.001]

20 **Castéra L**, Vergniol J, Foucher J, Le Bail B, Chanteloup E, Haaser M, Darriet M, Couzigou P, De Lédinghen V. Prospective comparison of transient elastography, Fibrotest, APRI, and liver

biopsy for the assessment of fibrosis in chronic hepatitis C. *Gastroenterology* 2005; **128**: 343-350 [PMID: 15685546 DOI: 10.1053/j.gastro.2004.11.018]

21 **Martin G**, Asensi V, Montes AH, Collazos J, Alvarez V, Carton JA, Taboada F, Valle-Garay E. Role of plasma matrix-metalloproteases (MMPs) and their polymorphisms (SNPs) in sepsis development and outcome in ICU patients. *Sci Rep* 2014; **4**: 5002 [PMID: 24833564 DOI: 10.1038/srep05002]

22 **Asensi V**, Rego C, Montes AH, Collazos J, Carton JA, Castro MG, Alvarez V, Fernández C, Maradona JA, Valle-Garay E. IL-1beta (+3954C/T) polymorphism could protect human immunodeficiency virus (HIV)-infected patients on highly active antiretroviral treatment (HAART) against lipodystrophic syndrome. *Genet Med* 2008; **10**: 215-223 [PMID: 18344712 DOI: 10.1097/GIM.0b013e3181632713]

23 **Alvarez V**, López-Larrea C, Coto E. Mutational analysis of the CCR5 and CXCR4 genes (HIV-1 co-receptors) in resistance to HIV-1 infection and AIDS development among intravenous drug users. *Hum Genet* 1998; **102**: 483-486 [PMID: 9600249]

24 **Collazos J**, Cartón JA, Asensi V. Gender differences in liver fibrosis and hepatitis C virus-related parameters in patients coinfected with human immunodeficiency virus. *Curr HIV Res* 2011; **9**: 339-345 [PMID: 21827383 DOI: 10.2174/157016211797635982]

25 **Yasuda M**, Shimizu I, Shiba M, Ito S. Suppressive effects of estradiol on dimethylnitrosamine-induced fibrosis of the liver in rats. *Hepatology* 1999; **29**: 719-727 [PMID: 10051473 DOI: 10.1002/hep.510290307]

26 **Xu JW**, Gong J, Chang XM, Luo JY, Dong L, Hao ZM, Jia A, Xu GP. Estrogen reduces CCL4- induced liver fibrosis in rats. *World J Gastroenterol* 2002; **8**: 883-887 [PMID: 12378635 DOI: 10.3748/wjg.v8.i5.883]

27 **Xu JW**, Gong J, Chang XM, Luo JY, Dong L, Jia A, Xu GP. Effects of estradiol on liver estrogen receptor-alpha and its mRNA expression in hepatic fibrosis in rats. *World J Gastroenterol* 2004; **10**: 250-254 [PMID: 14716833 DOI: 10.3748/wjg.v10.i2.250]

28 **Liu QH**, Li DG, Huang X, Zong CH, Xu QF, Lu HM. Suppressive effects of 17beta-estradiol on hepatic fibrosis in CCl4-induced rat model. *World J Gastroenterol* 2004; **10**: 1315-1320 [PMID: 15112349 DOI: 10.3748/wjg.v10.i9.1315]

29 **Merchante N**, Pérez-Camacho I, Mira JA, Rivero A, Macías J, Camacho A, Gómez-Mateos J, García-Lázaro M, Torre-Cisneros J, Pineda JA. Prevalence and risk factors for abnormal liver stiffness in HIV-infected patients without viral hepatitis coinfection: role of didanosine. *Antivir Ther* 2010; **15**: 753-763 [PMID: 20710057 DOI: 10.3851/IMP1612]

30 **Suárez-Zarracina T**, Valle-Garay E, Collazos J, Montes AH, Cárcaba V, Carton JA, Asensi V. Didanosine (ddI) associates with increased liver fibrosis in adult HIV-HCV coinfected patients. *J Viral Hepat* 2012; **19**: 685-693 [PMID: 22967099 DOI: 10.1111/j.1365-2893.2012.01596.x]

P- Reviewer: Davis DA, Hirt-Minkowski P, Kamal SA
S- Editor: Qi Y **L- Editor**: A **E- Editor**: Wu HL

World Journal of Virology

Submit a Manuscript: http://www.f6publishing.com

World J Virol 2017 May 12; 6(2): 46-48

DOI: 10.5501/wjv.v6.i2.46

ISSN 2220-3249 (online)

LETTERS TO THE EDITOR

Pakistan needs to speed up its human immunodeficiency virus control strategy to achieve targets in fast-track acquired immune deficiency syndrome response

Yasir Waheed, Hasnain Waheed

Yasir Waheed, Foundation University Medical College, Foundation University Islamabad, Islamabad 46000, Pakistan

Hasnain Waheed, Bridging Health Foundation, Rawalpindi 44000, Pakistan

Author contributions: Waheed Y designed study, did literature search, wrote and revised manuscript; Waheed H did literature search, wrote and revised manuscript.

Conflict-of-interest statement: The authors do not have any conflict of interest in publication of this manuscript.

Manuscript source: Unsolicited manuscript

Correspondence to: Yasir Waheed, PhD, Foundation University Medical College, Foundation University Islamabad, DHA Phase I, Islamabad 46000,
Pakistan. yasir_waheed_199@hotmail.com
Telephone: +92-300-5338171

Received: November 8, 2016
Peer-review started: November 10, 2016
First decision: March 8, 2017
Revised: March 17, 2017
Accepted: April 6, 2017
Article in press: April 10, 2017
Published online: May 12, 2017

Abstract

In last fifteen years remarkable success in the fight against human immunodeficiency virus (HIV) is achieved globally. The number of HIV infections has decreased and the number of people on antiretroviral therapy is increased. This all is possible by strong political commitments and heavy investments in the fight against HIV. Pakistan is among few Asian countries in which HIV cases are increasing year by year since 1990. There are 94000 cases of HIV in Pakistan and only 14000 are registered with government. The main source of HIV infection in Pakistan is the use of contaminated injection equipment among people who inject drugs (PWID). The overall prevalence of HIV among PWID in Pakistan is 27.2%. There are five cities in Pakistan in which HIV prevalence is above 40% in PWIDs. In June 2016, United Nations political declaration on acquired immune deficiency syndrome (AIDS) provided a global mandate to fast-track the AIDS response over the next five years to achieve the targets in Sustainable Development Goals. To achieve the targets in fast-track AIDS response, the global leaders showed strong commitments to invest $ 26 billion per year by 2020. Pakistan needs to speed up its HIV control program. There is a dire need to locate all HIV positive people and enroll them in the treatment program. Pakistan also needs to calculate exact number of people living with HIV, increase HIV treatment centers and increase HIV awareness. Recently, Global Fund invested handsome money in the fight against HIV. Let's hope the country will have effective HIV control strategy to achieve the HIV elimination target by 2030.

Key words: Human immunodeficiency virus; People who inject drugs; Fast-track; Antiretroviral therapy

Core tip: Human immunodeficiency virus (HIV) cases are increasing day by day in Pakistan. Currently, the prevalence of HIV is less than 0.1% in general population

while the scenario is totally different in people who inject drugs, having prevalence of 27.2%. Approximately 15% of HIV positive cases are enrolled with government for treatment. United Nations political declaration on acquired immune deficiency syndrome (AIDS) provided a global mandate to fast-track the AIDS response over the next five years to achieve the targets in Sustainable Development Goals. Pakistan needs to speed up its HIV treatment program to achieve the targets in fast-track AIDS response.

Waheed Y, Waheed H. Pakistan needs to speed up its human immunodeficiency virus control strategy to achieve targets in fast-track acquired immune deficiency syndrome response. *World J Virol* 2017; 6(2): 46-48 Available from: URL: http://www.wjgnet.com/2220-3249/full/v6/i2/46.htm DOI: http://dx.doi.org/10.5501/wjv.v6.i2.46

TO THE EDITOR

Fifteen years ago acquired immune deficiency syndrome (AIDS) epidemic was affecting families, communities and entire nations. The epidemic united the global community and the efforts were initiated to decrease the AIDS death toll and increase human immunodeficiency virus (HIV) drugs accessibility. Millennium development goal (MDG) six played a key role in the success against AIDS epidemic[1].

From the year 2000, the number of new HIV infections around the globe has decreased from 3.1 million to 2.0 million and the number of HIV-positive people on antiretroviral therapy has increased from 1 million to 15 million. Similarly, the AIDS-related deaths decrease from 2.0 million to 1.2 million. All this is possible by the inclusion in the MDGs and increase in AIDS funding from $4.9 billion to $21.7 billion[1]. The AIDS epidemic is halted and reversed. If the efforts are stopped here the AIDS linked morbidity and mortality will again start growing.

Pakistan is among few countries in Asia in which new HIV cases are increasing year by year since 1990. There are 94000 cases of HIV in Pakistan and only 14000 are registered with government[1]. The government has no idea where are the rest of 80000 HIV cases.

The government is expected to complete the Integrated Biological and Behavioral Surveillance survey in 2016; the survey will determine the actual number of people living with HIV in Pakistan including sex workers and drug addicts.

Currently, there are 21 HIV treatment centers and 20 community-based care and support centers for HIV patients across the country. The government is planning to increase the treatment centers from 21 to 25 till 2017.

The main source of HIV infection in Pakistan is the use of contaminated injection equipment among people who inject drugs (PWID). The overall prevalence of HIV among PWID in Pakistan is 27.2%[1]. There are five cities in Pakistan in which HIV prevalence is above 40% in PWIDs. These cities include Sargodha (40.6%), Karachi (42.2%), Gujrat (46.2%), D.G. Khan (49.6%) and Faisalabad (52.5%)[2]. HIV positive PWIDs are also transmitting HIV infection to their spouses.

Pakistan shares a long porous border with Afghanistan, the leading producer of Opium. Approximately 40% of Afghan Opium is transported and sold through trafficking routes passing from major cities of Pakistan. There is an increase in shift from inhalator to injectable drugs during the last few years. In Pakistan 430000 injecting drug users are present and 70% of them are sharing needles[3].

In June 2016, United Nations political declaration on AIDS provided a global mandate to fast-track the AIDS response over the next five years to achieve the targets in Sustainable Development Goals. The declaration calls on countries to reduce new HIV infections to 500K, reduce AIDS related deaths to 500K and eliminate HIV related Stigma and discrimination by 2020[4].

The political declaration also stresses that the 90% of people living with HIV should know their positive disease status, 90% of HIV positive people who know their status have access to HIV treatment and 90% of HIV positive people getting treatment have suppressed viral load by 2020[4].

The global leaders also pledge to provide HIV prevention to both general and high risk populations, including people who inject drugs, sex workers and prisoners. The targets also include a 95% reduction in new HIV infections among children in next five years. To achieve the targets in fast-track AIDS response, the global leaders showed strong commitments to invest $ 26 billion per year by 2020[4].

In order to achieve the targets in the Fast-Track AIDs response, Pakistan needs to speed up its HIV control program. There is a dire need to locate all HIV positive people and enroll them in the treatment program. The PWIDs needs special attention, they are bridging the epidemic between other key populations including sex workers. All the PWIDs should be provided with enough syringes so that they avoid sharing the syringe. The mother to child transmission also needs special attention. Currently, 3% of HIV positive pregnant women are taking antiretroviral therapy[1]. Thailand is the only country in the Asia who halted the mother to child transmission of HIV by covering all the HIV positive pregnant women into effective HIV treatment program.

Pakistan needs to calculate the exact number of people living with HIV. The HIV awareness program also needs attention. There is hardly any HIV awareness program on electronic, print and social media. There is a need to increase the HIV treatment centers in the country; only 21 HIV treatment centers are not enough to cover a population of 180 million people. There is a need to increase HIV screening so that the 90% of HIV positive people know about their positive disease

condition and enroll 90% of HIV positive people in the treatment program.

It was also observed that the slower HIV program in Pakistan was due to lack of the financial resources. Recently, Global Fund invested handsome money in the fight against HIV. Let's hope that the Pakistan will have effective HIV control strategy by the recent investments and we will be able to achieve the targets in the Fast-Track AIDS response which will eventually lead to HIV elimination by 2030.

REFERENCES

1 **UNAIDS**. How AIDS changed everything. MDG6: 15 years, 15 lessons of hope from the AIDS response [accessed 2016 Jun 4]. Available from: URL: http: //www.unaids.org/sites/default/files/media_asset/MDG6Report_en.pdf

2 **Melesse D**, Blanchard J. The Future of HIV in Pakistan: Modeled Projections of Pakistan's Epidemic. National Dissemination of Results of Round IV. National AIDS Control Program and Canada-Pakistan HIV AIDS Surveillance Project. Pakistan: Islamabad, 2011

3 **United Nations Office on Drugs and Crime**. Drug use in Pakistan 2013. [accessed 2016 May 11]. Available from: URL: https: //www.unodc.org/documents/pakistan/Survey_Report_Final_2013.pdf

4 **UNAIDS**. 2016 United Nations political declaration on ending AIDS set world on the Fast-Track to end the epidemic by 2030 [published 2016 Jun 8; accessed 2016 Jun 9]. Available from: URL: http: //www.unaids.org/en/resources/presscentre/pressreleaseandstatementarchive/2016/june/20160608_PS_HLM_PoliticalDeclaration

P- Reviewer: Monforte AA, Panduro A **S- Editor**: Song XX
L- Editor: A **E- Editor**: Wu HL

Published by **Baishideng Publishing Group Inc**
7901 Stoneridge Drive, Suite 501, Pleasanton, CA 94588, USA
Telephone: +1-925-223-8242
Fax: +1-925-223-8243
E-mail: bpgoffice@wjgnet.com
Help Desk: http://www.f6publishing.com/helpdesk
http://www.wjgnet.com

ISSN 2220-3249 (online)

World Journal of *Virology*

World J Virol 2017 August 12; 6(3): 49-58

Published by Baishideng Publishing Group Inc

WJV World Journal of Virology

A peer-reviewed, online, open-access journal of virology

Editorial Board

2016-2019

The *World Journal of Virology* Editorial Board consists of 370 members, representing a team of worldwide experts in virology. They are from 59 countries, including Argentina (4), Australia (8), Austria (4), Barbados (1), Belgium (1), Brazil (7), Bulgaria (1), Cameroon (1), Canada (12), Chile (2), China (55), Croatia (2), Cuba (1), Czech Republic (1), Denmark (1), Egypt (3), Ethiopia (1), Finland (5), France (10), Gambia(1), Germany (11), Ghana (1), Greece (2), Hungary (1), India (13), Indonesia (1), Iran (2), Ireland (3), Israel (4), Italy (23), Japan (16), Kazakhstan (1), Kenya (1), Kosovo (1), Mexico (2), Netherlands (5), New Zealand (1), Nigeria (1), Pakistan (1), Palestine (1), Poland (1), Portugal (1), Romania (1), Russia (2), Saudi Arabia (1), Singapore (2), Slovakia (2), Slovenia (2), South Africa (2), South Korea (6), Spain (19), Sweden (4), Thailand (8), Tunisia (1), Turkey (4), United Arab Emirates (1), United Kingdom (8), United States (92), and Uruguay (1).

Eiichi N Kodama, *Sendai*
Emoto Masashi, *Gunma*
Hiromitsu Moriyama, *Tokyo*
Kenji Okuda, *Yokohama*
Nobuhiro Suzuki, *Okayama*
Takashi Suzuki, *Shizuoka*
Tetsuro Suzuki, *Hamamatsu*
Yoshiyuki Suzuki, *Nagoya-shi*
Akifumi Takaori-Kondo, *Kyoto*
Tetsuya Toyoda, *Toyohashi*

Kazakhstan

Vladimir E Berezin, *Almaty*

Kenya

George G Maina, *Nairobi*

Kosovo

Lul Raka, *Prishtina*

Mexico

Juan E Ludert, *Mexico City*
Julio Reyes-Leyva, *Mexico*

Netherlands

Kimberley SM Benschop, *Amsterdam*
Benjamin Berkhout, *Amsterdam*
Byron EE Martina, *Rotterdam*
Willem JG Melchers, *Nijmegen*
Monique Nijhuis, *Utrecht*

New Zealand

Olga S Garkavenko, *Auckland*

Nigeria

Olajide A Owolodun, *Plateau State*

Pakistan

Muhammad I Qadir, *Faisalabad*

Palestine

Ahmad Y Amro, *Jerusalem*

Poland

Brygida Knysz, *Wroclaw*

Portugal

Celso Cunha, *Lisbon*

Romania

Anda Baicus, *Bucharest*

Russia

Anton Buzdin, *Moscow*
Elena V Gavrilova, *Novosibirsk*

Saudi Arabia

Ahmed S Abdel-Moneim, *Al-Taif*

Singapore

Sophie Bellanger, *Singapore*
Ding X Liu, *Singapore*

Slovakia

Gabriela Bukovska, *Bratislava*
Julius Rajcani, *Bratislava*

Slovenia

Uros Krapez, *Ljubljana*
Andrej Steyer, *Ljubljana*

South Africa

Janusz T Paweska, *Sandringham*
Dirk Stephan, *Matieland*

South Korea

Sang Hoon Ahn, *Seoul*
Tae-Jin Choi, *Busan*
Young-Ki Choi, *Cheongju*
Kee-Jong Hong, *Cheongwon*
Bum-Joon Kim, *Seoul*
Junsoo Park, *Wonju*

Spain

Alí Alejo, *Valdeolmos*
Alfredo Berzal-Herranz, *Granada*
Rafael Blasco, *Madrid*
Julio Collazos, *Usánsolo-Galdácano*
Juan M Hernández, *Madrid*
Gómez L Jaime, *Córdoba*
Josep M Llibre, *Badalona*
Cecilio López-Galíndez, *Madrid*
F. Xavier López-Labrador, *Valencia*
JoséA Melero, *Madrid*
Luis Menéndez-Arias, *Madrid*
Andrés Moya, *València*
David R Pereda, *Sevilla*
Pilar Perez-Romero, *Sevilla*
Josep Quer, *Barcelona*
Daniel López Rodríguez, *Majadahonda*
Juan-Carlos Saiz, *Madrid*
Noemi Sevilla, *Madrid*
Natalia Soriano-Sarabia, *Madrid*

Sweden

Goran PL Bucht, *Umea*
Ali Mirazimi, *Solna*
Muhammad Munir, *Uppdala*
Bo F Oberg, *Huddinge*

Thailand

Prasert Auewarakul, *Bangkok*
Parin Chaivisuthangkura, *Bangkok*
Wasin Charerntantanakul, *Chiang Mai*
Wansika Kiatpathomchai, *Bangkok*
Sasisopin Kiertiburanakul, *Bangkok*
Winyou Mitarnun, *Chiang Mai*
Yong Poovorawan, *Bangkok*
Viroj Wiwanitkit, *Bangkok*

Tunisia

Olfa Bahri, *Tunis*

Turkey

Omer Coskun, *Ankara*
Iftihar Koksal, *Trabzon*
Aykut Ozdarendeli, *Kayseri*
Ayca A Sayiner, *Izmir*

United Arab Emirates

Tahir A Rizvi, *Al Ain*

United Kingdom

Shiu-Wan Chan, *Manchester*
Simon R Clegg, *Preston*
Chiriva I Maurizio, *Nottingham*
Iain M Morgan, *Glasgow*
Mark R Nelson, *London*
Adrian W Philbey, *Glasgow*
James P Stewart, *Liverpool*
Gavin WG Wilkinson, *Cardiff*

United States

Nafees Ahmad, *Tucson*
Ashok Aiyar, *Los Angeles*
Hizi Amnon, *Bethesda*
Judith M Ball, *Texas*
Igor M Belyakov, *Frederick*
Bradford K Berges, *Provo*
Preeti Bharaj, *Orlando*
Jay C Brown, *Charlottesville*
Victor E Buckwold, *Walkersville*
Alexander A Bukreyev, *Galveston*
Joseph J Carter, *Seattle*
Maria G Castro, *Los Angeles*
Yan-Ping Chen, *Beltsville*

World Journal of Virology

Contents

Quarterly Volume 6 Number 3 August 12, 2017

World Journal of Virology
Volume 6 Number 3 August 12, 2017

Contents

NAME OF JOURNAL
World Journal of Virology

ISSN
ISSN 2220-3249 (online)

LAUNCH DATE
February 12, 2012

FREQUENCY
Quarterly

EDITOR-IN-CHIEF
Ling Lu, MD, PhD, Department of Pathology and Laboratory Medicine, University of Kansas Medical Center, Kansas City, 3901 Rainbow Blvd, WHE 3020, KS 66160, United States

EDITORIAL BOARD MEMBERS
All editorial board members resources online at http://www.wjgnet.com/2220-3249/editorialboard.htm

EDITORIAL OFFICE
Xiu-Xia Song, Director
World Journal of Virology
Baishideng Publishing Group Inc
7901 Stoneridge Drive, Suite 501, Pleasanton, CA 94588, USA
Telephone: +1-925-2238242
Fax: +1-925-2238243
E-mail: editorialoffice@wjgnet.com
Help Desk: http://www.f6publishing.com/helpdesk
http://www.wjgnet.com

PUBLISHER
Baishideng Publishing Group Inc
7901 Stoneridge Drive, Suite 501, Pleasanton, CA 94588, USA
Telephone: +1-925-2238242
Fax: +1-925-2238243
E-mail: editorialoffice@wjgnet.com
Help Desk: http://www.f6publishing.com/helpdesk
http://www.wjgnet.com

PUBLICATION DATE
August 12, 2017

INSTRUCTIONS TO AUTHORS
http://www.wjgnet.com/bpg/gerinfo/204

ONLINE SUBMISSION
http://www.f6publishing.com

World Journal of Virology

Submit a Manuscript: http://www.f6publishing.com

World J Virol 2017 August 12; 6(3): 49-52

DOI: 10.5501/wjv.v6.i3.49

ISSN 2220-3249 (online)

FIELD OF VISION

Additional attention to combination antiretroviral therapy-related lipodystrophy

Norihiko Kobayashi, Masako Nakahara, Masako Oka, Kumiko Saeki

Norihiko Kobayashi, Masako Nakahara, Masako Oka, Kumiko Saeki, Department of Disease Control, Research Institute, National Center for Global Health and Medicine, Tokyo 162-8655, Japan

Author contributions: Kobayashi N, Nakahara M and Oka M collected the materials and wrote the manuscript; Saeki K supervised the publication of this commentary.

Conflict-of-interest statement: None.

Manuscript source: Invited manuscript

Correspondence to: Kumiko Saeki, MD, PhD, Department of Disease Control, Research Institute, National Center for Global Health and Medicine, 1-21-1, Toyama, Shinjuku-ku, Tokyo 162-8655, Japan. saeki@ri.ncgm.go.jp
Telephone: +81-3-32027181
Fax: +81-3-32071038

Received: March 23, 2017
Peer-review started: March 24, 2017
First decision: May 19, 2017
Revised: July 21, 2017
Accepted: August 3, 2017
Article in press: August 5, 2017
Published online: August 12, 2017

Abstract

The occurrence of lipodystrophy in patients taking anti-human immunodeficiency virus (HIV) medications is a serious problem as it is irreversible even after drug withdrawal. Although it was first recognized in patients taking proteinase inhibitors, other types of anti-HIV agents can also cause lipodystrophy. In a recent publication by Jones *et al* entitled "Highly active antiretroviral therapy dysregulates proliferation and differentiation of human pre-adipocytes" in *World Journal of Virology*, it was reported that simultaneous treatment of human subcutaneous adipocytes with anti-HIV drugs with different mechanisms of action synergistically exerted anti-adipogenesis effects *in vitro*, warning us to take utmost care in every case receiving combination antiretroviral therapy (cART). For elucidation of the molecular basis for cART-related lipodystrophy, multi-faceted approaches should be taken, based on a deeper understanding of the development and organization of adipose tissues.

Key words: Combination antiretroviral therapy; Lipodystrophy; Protease inhibitor; Reverse transcriptase inhibitor; Human immunodeficiency virus

Core tip: Development of lipodystrophy in patients receiving combination antiretroviral therapy (cART) has been a serious problem. Although it was first reported in patients taking proteinase inhibitors, other types of anti-human immunodeficiency virus (HIV) agents also cause lipodystrophy. A recent publication in *World Journal of Virology* reported unexpected synergism among anti-HIV drugs with different mechanisms of action in inhibiting adipogenesis *in vitro*. To elucidate the molecular basis for cART-related lipodystrophy, multi-faceted approaches should be taken with a deeper understanding of the development and organization of adipose tissues.

Kobayashi N, Nakahara M, Oka M, Saeki K. Additional attention to combination antiretroviral therapy-related lipodystrophy. *World J Virol* 2017; 6(3): 49-52 Available from: URL: http://www.wjgnet.com/2220-3249/full/v6/i3/49.htm DOI: http://dx.doi.

org/10.5501/wjv.v6.i3.49

COMMENTARY ON A RECENT ARTICLE ON COMBINATION ANTIRETROVIRAL THERAPY-RELATED LIPODYSTROPHY

Lipodystrophy is a serious problem in patients receiving combination antiretroviral therapy

The development of combination antiretroviral therapy (cART), where more than two types of anti-human immunodeficiency virus (HIV) agents with different mechanisms of action are used, has greatly improved the prognosis of acquired immune deficiency syndrome (AIDS) by reducing mortality rates and suppressing opportunistic infections. With the extension of the administration period, however, it has becoming increasingly important to take effective measures to control the side effects of cART. The major adverse conditions caused by anti-HIV agents are lipodystrophy, atherosclerosis, eruption, osteoporosis and lactic acidosis. Since the pathophysiology of cART-related lipodystrophy is an irreversible process, elucidation of the mechanism how anti-HIV agents induce lipodystrophy is a matter of particular importance. In the current commentary, possible mechanisms of cART-related lipodystrophy are discussed by referring a recent paper by Jones *et al*[1] in *World Journal of Virology*, which reported an unexpected synergy among anti-HIV drugs with different mechanisms of action in inhibiting proliferation and differentiation of human preadipocytes *in vitro* (Figure 1).

Organization of adipose tissues

Adipose tissues consist of parenchymal cells (*i.e.,* adipocytes and their progenitors) and non-parenchymal cells (*i.e.,* non-adipocyte lineage cells) (Figure 2) and disorders of any of these components may result in the development of lipodystrophy. Caso *et al*[2] previously reported that two proteinase inhibitors, ritonavir (RTV) and atazanavir (ATV), inhibited the proliferation and differentiation of human subcutaneous preadipocytes *in vitro*. In a recent paper, the same group showed that protease inhibitors (RTV, ATV), nucleoside/nucleotide reverse transcriptase inhibitors [emtricitabine (FTC), tenofovir (TDF)] and a non-nucleoside reverse transcriptase inhibitor [efavirenz (EFV)] synergistically inhibited proliferation and differentiation/maturation of human preadipocytes obtained from subcutaneous fat depots[1]. It is surprising that synergism exists among drugs with completely different action mechanisms. Although the molecular basis of this synergism remains unknown, the finding has sounded the alarm about the risk of unexpected occurrence of lipodystrophy in cART-receiving patients.

In addition to affecting parenchymal cells, anti-HIV agents may impair the functions of non-parenchymal cells, which consist of mesenchymal stem cells (MSCs), vascular endothelial cells (VEC), pericytes/vascular smooth muscle cells, resident macrophages (M2) and inflammatory macrophages (M1) (Figure 2). Among these, VECs may be of most interest for the following three reasons: First, anti-HIV agents reportedly induce oxidative damage to VECs[3], which is considered to be one of the causes of development of cART-related atherosclerosis. Atherosclerosis in adipose tissue vasculatures within specific regions of subcutaneous fat depots may cause local ischemia, resulting in degeneration/loss of adipose tissues in specific areas such as the face and limbs. However, the reason why the face and limbs are commonly affected by cART-related lipodystrophy remains unknown. Secondly, VECs in adipose tissues (A-VEC) is known as one of the ancestors of adipocytes[4,5]. Recurrent damage to A-VECs by anti-HIV agents may reduce the population size of adipocyte precursors, which might, in turn, result in the occurrence of lipodystrophy after a time. Lastly, it is accepted that A-VECs have distinctive characteristics compared with VECs of other tissues; for example, VECs of white adipose tissues exhibit specific antigenicity[6]. Moreover, it was recently reported that poly(2-methacryloyloxyethyl phosphorylcholine-co-n-butyl methacrylate (PMB)-coated carbon nanotubes specifically accumulated in the capillary endothelial cells of adipose tissues[7]. Even under conditions where anti-HIV drugs do not cause oxidative damage to A-VEC, they might possibly affect specific functions of A-VEC, thus promoting the development of lipodystrophy.

Other non-parenchymal cells could also be the targets of cART. The MSCs can be precursors of preadipocytes, and pericytes/vascular smooth muscle cells are recognized as an equivalent of MSCs[8], although a recent paper by Guimarães-Camboa *et al*[9] has challenged this idea. Similarly to A-VECs, pericytes/vascular smooth muscle cells in adipose tissues are considered as one of the ancestors of adipocytes[5]. It is known that white adipose tissues are particularly rich in M2 macrophages, which provide a niche for preadipocytes[10]. On the other hand, M1 inflammatory macrophages are recruited into adipose tissues from the bone marrow when adipocytes undergo degeneration. Defects in the clearance of degenerative adipocytes may create pathological states of adipose tissues, which possibly lead to the development of lipodystrophy.

Although the critical target cells remain undetermined, the etiology of cART-related lipodystrophy should be investigated from multiple perspectives.

Possible mechanisms of cART-lipodystrophy

The incidence of lipodystrophy was first recognized in patients receiving protease inhibitors[11,12] and more than half of affected patients reportedly take these drugs[13]. In addition to suppressing growth and differentiation of preadipocytes[1], protease inhibitors reportedly exert multifactorial effects on adipocytes including impairment of mitochondrial functions[14], changes in the gene expression

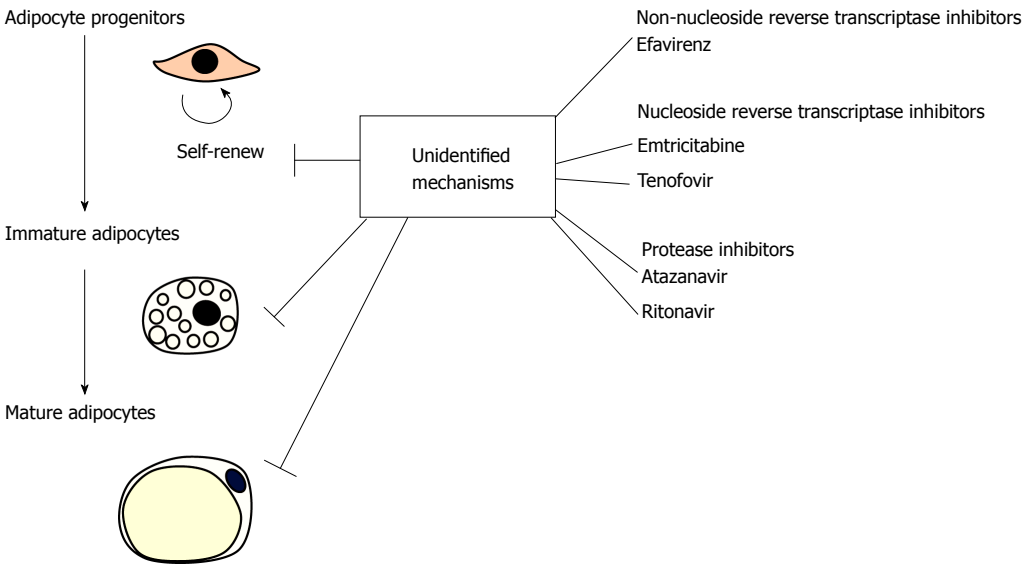

Figure 1 Diverse anti-human immunodeficiency virus agents synergistically inhibit adipogenesis *in vitro*. Although detailed processes remain elusive, anti-human immunodeficiency virus agents of different action mechanisms synergistically inhibit proliferation and differentiation of preadipocytes that are prepared from human subcutaneous fat depots as reported by Jones *et al*[1].

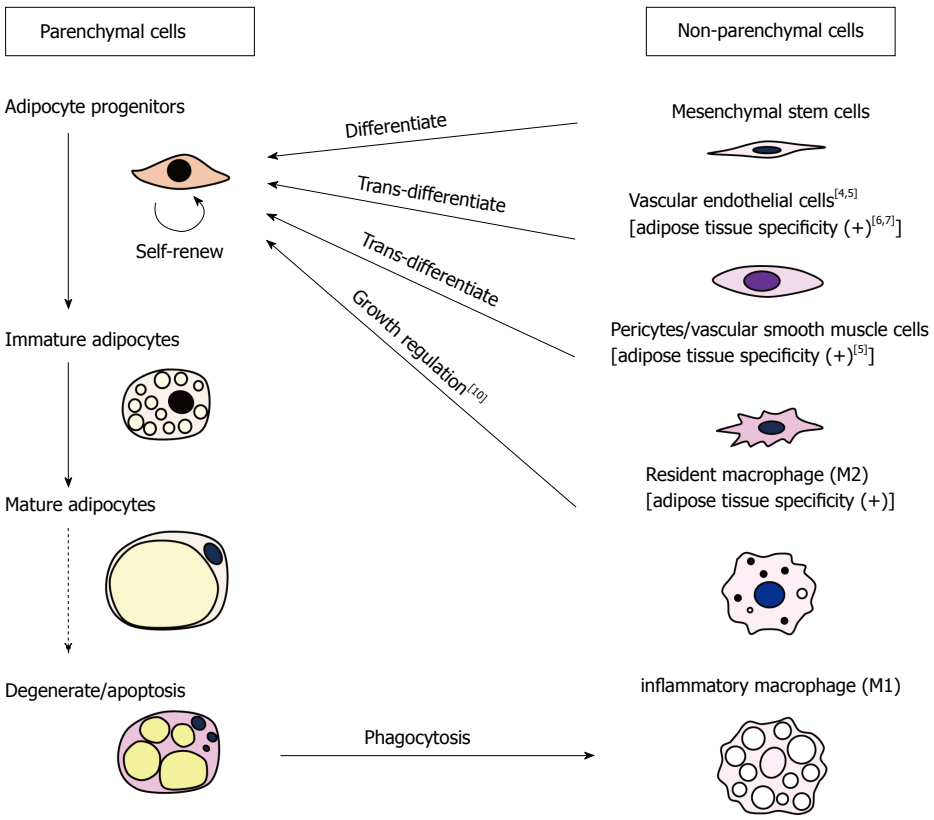

Figure 2 Organization of adipose tissues. Adipose tissues consist of parenchymal cells and non-parenchymal cells. Coordinated interactions of these two components are important for adipose tissue performance.

related to ER-stress and lipid droplet formation[14] and even an induction of mitophagy[15]. cART-related dystrophy is not restricted to protease inhibitor-receiving cases[16]. Patients with cART-related dystrophy are relatively healthy[13], although hypertriglyceridemia and insulin resistance may be present[11-13,16-19]. Nevertheless, cART-related dystrophy is a crucial issue to be addressed, since loss of fat depots frequently occurs in the face and limbs and fat wasting of the face considerably reduces quality of life. The reason why adipose tissues in the distal parts of the body are commonly affected by cART-related dystrophy remains elusive. In some cases,

subcutaneous fat depots are reciprocally accumulated in the central parts of body including the abdomen, trunk and neck. Since plasma cortisol values are reportedly within the normal range, central fat accumulation cannot be attributed to hypercortisolism[16]. Interestingly, adipose tissue-specific Dicer knockout (ADicerKO) mice reportedly exhibit a phenotype that bears a close resemblance to cART-related lipodystrophy[20]. They even show buffalo hump-like phenotypes, in which brown adipose tissues (BAT) are substantially enlarged and degenerated into white adipose tissue accumulations[20]. Since BATs are mainly located in the neck and upper back areas in mice and humans, central fat accumulation in cART-related lipodystrophy might possibly be associated with abnormal lipid accumulation in BATs.

In summary, the etiology of cART-related lipodystrophy remains largely unknown and further investigations will be required to elucidate its developmental mechanisms.

REFERENCES

1 **Jones E**, Mazirka P, McNurlan MA, Darras F, Gelato MC, Caso G. Highly active antiretroviral therapy dysregulates proliferation and differentiation of human pre-adipocytes. *World J Virol* 2017; In press

2 **Caso G**, Mileva I, McNurlan MA, Mynarcik DC, Darras F, Gelato MC. Effect of ritonavir and atazanavir on human subcutaneous preadipocyte proliferation and differentiation. *Antiviral Res* 2010; **86**: 137-143 [PMID: 20153378]

3 **Jiang B**, Hebert VY, Li Y, Mathis JM, Alexander JS, Dugas TR. HIV antiretroviral drug combination induces endothelial mitochondrial dysfunction and reactive oxygen species production, but not apoptosis. *Toxicol Appl Pharmacol* 2007; **224**: 60-71 [PMID: 17669453 DOI: 10.1016/j.taap.2007.06.010]

4 **Tran KV**, Gealekman O, Frontini A, Zingaretti MC, Morroni M, Giordano A, Smorlesi A, Perugini J, De Matteis R, Sbarbati A, Corvera S, Cinti S. The vascular endothelium of the adipose tissue gives rise to both white and brown fat cells. *Cell Metab* 2012; **15**: 222-229 [PMID: 22326223 DOI: 10.1016/j.cmet.2012.01.008]

5 **Gupta RK**, Mepani RJ, Kleiner S, Lo JC, Khandekar MJ, Cohen P, Frontini A, Bhowmick DC, Ye L, Cinti S, Spiegelman BM. Zfp423 expression identifies committed preadipocytes and localizes to adipose endothelial and perivascular cells. *Cell Metab* 2012; **15**: 230-239 [PMID: 22326224 DOI: 10.1016/j.cmet.2012.01.010]

6 **Kolonin MG**, Saha PK, Chan L, Pasqualini R, Arap W. Reversal of obesity by targeted ablation of adipose tissue. *Nat Med* 2004; **10**: 625-632 [PMID: 15133506 DOI: 10.1038/nm1048]

7 **Yudasaka M**, Yomogida Y, Zhang M, Tanaka T, Nakahara M, Kobayashi N, Okamatsu-Ogura Y, Machida K, Ishihara K, Saeki K, Kataura H. Near-Infrared Photoluminescent Carbon Nanotubes for Imaging of Brown Fat. *Sci Rep* 2017; **7**: 44760 [PMID: 28317858 DOI: 10.1038/srep44760]

8 **Crisan M**, Yap S, Casteilla L, Chen CW, Corselli M, Park TS, Andriolo G, Sun B, Zheng B, Zhang L, Norotte C, Teng PN, Traas J, Schugar R, Deasy BM, Badylak S, Buhring HJ, Giacobino JP, Lazzari L, Huard J, Péault B. A perivascular origin for mesenchymal stem cells in multiple human organs. *Cell Stem Cell* 2008; **3**: 301-313 [PMID: 18786417 DOI: 10.1016/j.stem.2008.07.003]

9 **Guimarães-Camboa N**, Cattaneo P, Sun Y, Moore-Morris T, Gu Y, Dalton ND, Rockenstein E, Masliah E, Peterson KL, Stallcup WB, Chen J, Evans SM. Pericytes of Multiple Organs Do Not Behave as Mesenchymal Stem Cells In Vivo. *Cell Stem Cell* 2017; **20**: 345-359.e5 [PMID: 28111199 DOI: 10.1016/j.stem.2016.12.006]

10 **Nawaz A**, Aminuddin A, Kado T, Takikawa A, Yamamoto S, Tsuneyama K, Igarashi Y, Ikutani M, Nishida Y, Nagai Y, Takatsu K, Imura J, Sasahara M, Mori H, Matsumoto M, Nakagawa T, Norihiko K, Saeki K, Usui I, Fujisaka S, Tobe K. CD206+ cells regulate glucose metabolism and inhibit proliferation of adipocyte progenitors through TGFβ signaling. *Nat Commun* 2017; In press

11 **Viraben R**, Aquilina C. Indinavir-associated lipodystrophy. *AIDS* 1998; **12**: F37-F39 [PMID: 9583592]

12 **Carr A**, Samaras K, Burton S, Law M, Freund J, Chisholm DJ, Cooper DA. A syndrome of peripheral lipodystrophy, hyperlipidaemia and insulin resistance in patients receiving HIV protease inhibitors. *AIDS* 1998; **12**: F51-F58 [PMID: 9619798]

13 **Garg A**. Acquired and inherited lipodystrophies. *N Engl J Med* 2004; **350**: 1220-1234 [PMID: 15028826 DOI: 10.1056/NEJMra025261]

14 **Bociąga-Jasik M**, Polus A, Góralska J, Czech U, Gruca A, Śliwa A, Garlicki A, Mach T, Dembińska-Kieć A. Metabolic effects of the HIV protease inhibitor--saquinavir in differentiating human preadipocytes. *Pharmacol Rep* 2013; **65**: 937-950 [PMID: 24145088]

15 **Gibellini L**, De Biasi S, Pinti M, Nasi M, Riccio M, Carnevale G, Cavallini GM, Sala de Oyanguren FJ, O'Connor JE, Mussini C, De Pol A, Cossarizza A. The protease inhibitor atazanavir triggers autophagy and mitophagy in human preadipocytes. *AIDS* 2012; **26**: 2017-2026 [PMID: 22948272 DOI: 10.1097/QAD.0b013e328359b8be]

16 **Lo JC**, Mulligan K, Tai VW, Algren H, Schambelan M. "Buffalo hump" in men with HIV-1 infection. *Lancet* 1998; **351**: 867-870 [PMID: 9525364 DOI: 10.1016/S0140-6736(97)11443-X]

17 **Panse I**, Vasseur E, Raffin-Sanson ML, Staroz F, Rouveix E, Saiag P. Lipodystrophy associated with protease inhibitors. *Br J Dermatol* 2000; **142**: 496-500 [PMID: 10735957]

18 **Carr A**, Samaras K, Thorisdottir A, Kaufmann GR, Chisholm DJ, Cooper DA. Diagnosis, prediction, and natural course of HIV-1 protease-inhibitor-associated lipodystrophy, hyperlipidaemia, and diabetes mellitus: a cohort study. *Lancet* 1999; **353**: 2093-2099 [PMID: 10382692 DOI: 10.1016/S0140-6736(98)08468-2]

19 **Dubé MP**, Johnson DL, Currier JS, Leedom JM. Protease inhibitor-associated hyperglycaemia. *Lancet* 1997; **350**: 713-714 [PMID: 9291911 DOI: 10.1016/S0140-6736(05)63513-1]

20 **Mori MA**, Thomou T, Boucher J, Lee KY, Lallukka S, Kim JK, Torriani M, Yki-Järvinen H, Grinspoon SK, Cypess AM, Kahn CR. Altered miRNA processing disrupts brown/white adipocyte determination and associates with lipodystrophy. *J Clin Invest* 2014; **124**: 3339-3351 [PMID: 24983316 DOI: 10.1172/JCI73468]

P- Reviewer: Arriagada GL, Chen C, Ciotti M, Menendez-Arias L
S- Editor: Kong JX **L- Editor**: A **E- Editor**: Lu YJ

World Journal of Virology

Submit a Manuscript: http://www.f6publishing.com

World J Virol 2017 August 12; 6(3): 53-58

DOI: 10.5501/wjv.v6.i3.53

ISSN 2220-3249 (online)

ORIGINAL ARTICLE

Basic Study

Highly active antiretroviral therapy dysregulates proliferation and differentiation of human pre-adipocytes

Eyone Jones, Pavel Mazirka, Margaret A McNurlan, Frank Darras, Marie C Gelato, Giuseppe Caso

Eyone Jones, Department of Surgery, Rutgers, Robert Wood Johnson Medical School, New Brunswick, NJ 08901, United States

Pavel Mazirka, Margaret A McNurlan, Giuseppe Caso, Department of Surgery, Stony Brook University Medical Center, Stony Brook, NY 11794, United States

Frank Darras, Department of Urology, Stony Brook University Medical Center, Stony Brook, NY 11794, United States

Marie C Gelato, Department of Medicine, Stony Brook University Medical Center, Stony Brook, NY 11794, United States

Author contributions: Jones E contributed to data collection; McNurlan MA contributed to study design; Darras F recruited study subjects, collected surgical samples, and contributed to drafting the manuscript; Gelato MC contributed to overall study design; Caso G contributed to study design, performed the experiments; Jones E, Mazirka P, McNurlan MA and Caso G contributed to data analysis; Jones E, Mazirka P, McNurlan MA, Gelato MC and Caso G writing of the manuscript; Jones E, McNurlan MA, Gelato MC and Caso G contributed to data interpretation; all authors approved the final version of the manuscript.

Institutional review board statement: The study was reviewed and approved by the Stony Brook University Institutional Review Board. All specimens were acquired from patients after informed consent and ethical permission was obtained for participation in the study.

Conflict-of-interest statement: The authors have no conflict of interest to disclose.

Data sharing statement: No additional data are available.

Manuscript source: Invited manuscript

Correspondence to: Giuseppe Caso, MD, PhD, Department of Surgery, Stony Brook University Medical Center, 100 Nicolls Rd, Stony Brook, NY 11794,
United States. giuseppe.caso@stonybrook.edu
Telephone: +1-631-4441790
Fax: +1-631-4448824

Received: January 28, 2017
Peer-review started: February 7, 2017
First decision: May 8, 2017
Revised: April 28, 2017
Accepted: June 6, 2017
Article in press: June 7, 2017
Published online: August 12, 2017

Abstract

AIM

To investigate the mechanism(s) by which potential effects of multi-drug highly-active antiretroviral therapy contributes to lipodystrophy syndrome.

METHODS

Preadipocytes from healthy donors were assessed for proliferation and differentiation in the presence of nucleoside reverse transcriptase inhibitors (NRTIs), nonnucleoside reverse transcriptase inhibitors (NNRTIs), and protease inhibitors (PIs) individually and in combination. Effects on proliferation were assessed with a 3-[4,5-dimethylthiazol-2-yl]-2,5-diphenyl tetrazolium bromide assay and effects on differentiation were assessed from glycerol-3-phosphate dehydrogenase (GPDH) activity and quantitation of Oil Red O staining for intracellular lipid. Data were analyzed with a randomized block ANOVA with post-hoc Fisher's Least Significant

Difference test.

RESULTS

Preadipocyte proliferation was inhibited by a combination of NNRTI + NRTI (14% at 48 h, $P < 0.001$) and PI + NRTI (19% at 48 h, $P < 0.001$) with additional suppression when ritonavir (RTV) was added (26% at 48 h). The drug combination of atazanavir (ATV) + RTV + emtricitabine (FTC) + tenofovir (TDF) had the greatest inhibitory effect on proliferation at 48 h. Preadipocyte differentiation was most significantly reduced by the efavirenz + FTC + TDF assessed either by GPDH activity (64%) or lipid accumulation (39%), $P < 0.001$. Combining NRTIs with a PI (ATV + FTC + TDF) significantly suppressed differentiation (GPDH activity reduced 29%, lipid accumulation reduced by 19%, $P < 0.01$). This effect was slightly greater when a boosting amount of RTV was added (ATV + FTC + TDF + RTV, $P < 0.001$).

CONCLUSION

Although combination antiretroviral therapy is clinically more efficacious than single drug regimens, it also has a much greater inhibitory effect on preadipocyte proliferation and differentiation.

Key words: Nucleoside reverse transcriptase inhibitors; Non-nucleoside reverse transcriptase inhibitors; Protease inhibitors; Pre-adipocytes; Highly active antiretroviral therapy; Lipodystrophy

Core tip: We demonstrated an *in vitro* system for evaluating potential antiretroviral regimens for adipose tissue toxicity. In general, combination regimens resulted in greater preadipocyte proliferation and differentiation inhibition than single therapies. The drug combination of atazanavir + emtricitabine + tenofovir had inhibitory effects on preadipocytes and adding ritonavir at levels equivalent to clinical boosting, increased toxicity still further.

Jones E, Mazirka P, McNurlan MA, Darras F, Gelato MC, Caso G. Highly active antiretroviral therapy dysregulates proliferation and differentiation of human pre-adipocytes. *World J Virol* 2017; 6(3): 53-58 Available from: URL: http://www.wjgnet.com/2220-3249/full/v6/i3/53.htm DOI: http://dx.doi.org/10.5501/wjv.v6.i3.53

INTRODUCTION

A link between highly active antiretroviral therapy (HAART) and HAART-associated lipodystrophy (HALS) has been recognized for well over a decade. HALS is associated with abnormal changes in fat distribution throughout the body, insulin resistance and altered levels of triglycerides, cholesterol and lipoproteins[1]. These changes impact the health of an individual as well as their quality of life and have reduced the impact of anti-HIV therapy development[2,3]. HAART regimens with various combinations of protease inhibitors (PI), nucleoside reverse transcriptase inhibitors (NRTI) and nonnucleoside reverse transcriptase inhibitors (NNRTI) have been associated with HALS (*e.g.*[4-6]). Previously we reported on the *in-vitro* effects of two PIs, ritonavir (RTV) and atazanavir (ATV) on preadipocyte proliferation and adipogenesis[7]. In the present study, we report the effects of common first-line combination regimens used in HIV treatment; efavirenz (EFV) + emtricitabine (FTC) + tenofovir (TDF), ATV + FTC + TDF and ATV + RTV + FTC + TDF, as well as their individual components, on *in-vitro* preadipocyte proliferation and differentiation.

MATERIALS AND METHODS

Patients and study design

Preadipocytes were obtained from abdominal subcutaneous fat tissue from healthy kidney donors undergoing nephrectomy. The samples were collected from 10 kidney donors (6 females, 4 males) who gave a written informed consent. All participants were HIV-seronegative, had an average age of 37 ± 4 years and a BMI of 29 ± 1 kg/m^2. Subjects were placed under standard general anesthesia and subcutaneous fat tissue was removed from the peri-umbilical area during nephrectomy. The specimens were then immediately placed in a sterile Hank's Buffered Salt Solution (HBSS) at pH 7.4 containing antibiotics and amphotericin. All fat samples were processed within one hour.

Once isolated, preadipocytes were tested *in vitro* for their ability to replicate and differentiate in the presence of different classes of antiretroviral drugs, which were applied individually or in combination. Fat samples from each donor were processed individually and each of the test conditions (drug combinations) were repeated with each donor sample. The selected drug combinations are recommended antiretroviral regimens for (naïve) HIV patients[8]. These included a NNRTI-based regimen consisting of a NNRTI (EFV) and 2 NRTIs (TDF and FTC) (*i.e.*, EFV + TDF + FTC); and a PI-based regimen consisting of a PI (ATV) and 2 NRTIs (TDF and FTC) (*i.e.*, ATV + TDF + FTC). The PI-based combination was tested with or without the addition of another PI, RTV (*i.e.*, ATV + RTV+ TDF + FTC), since this regimen is often recommended to boost the effects of other protease inhibitors[9]. The following drug concentrations were used in all the experiments: EFV, 20 μmol/L; FTC, 15 μmol/L; TDF, 1 μmol/L; ATV, 10 μmol/L; RTV, 2 μmol/L. These concentrations are in the range of those observed in the plasma of patients treated with the specific antiretroviral combination regimens[10-12]. The effects of antiretroviral medications were compared with control samples in which preadipocytes were cultured and stimulated to differentiate in the absence of antiretroviral medications.

Pre-adipocyte isolation and culture

Preadipocyte isolation and culture from subcutaneous fat biopsies were previously described[7]. In brief, fat tissue was digested with collagenase (3 mg/mL, type Ⅱ, Worthington, Lakewood, NJ) to obtain stromal cells that were then separated from mature adipocytes by centrifugation and incubated in erythrocyte lysing buffer (154 mmol/L NH_4Cl, 10 mmol/L K_2HPO_4, 1 mmol/L EDTA, pH 7.4) for 10 min at room temperature to eliminate red cells. Remaining debris was then removed by filtering cell suspension through a 70 μm nylon filter and then centrifuged. Pelleted preadipocytes were plated in a basal medium consisting of DMEM/F-12 (Gibco, Carlsbad, CA) supplemented with 10% Fetal Calf Serum (FCS), 2 mmol/L glutamine, 100 IU/mL penicillin and 100 μg/mL streptomycin (Gibco) and incubated for 16-18 h. After incubation, attached cells were extensively washed with warm PBS, removed from the plates with trypsin, suspended and counted. Preadipocytes were then seeded at a density of $5 \times 10^3/cm^2$.

To assess cell replication, cultures were incubated in untreated growth medium for 48 h after which the medium was exchanged for fresh medium (control) or medium containing drugs. Cell numbers were assessed over a 72 h period. For the assessment of differentiation, cultures were grown to confluence and differentiation was induced with serum-free medium (control) or the same medium containing antiretroviral drugs as previously described[7,13]. Since some drugs (*i.e.*, EFV) are tightly bound to plasma albumin, 2 g/L bovine serum albumin (Sigma, St. Loius, MO) was added to differentiation medium in all control and treated groups. Medium was replaced every 72 h and differentiation assessed after 12 d.

Assessment of preadipocyte proliferation

The effect of antiretroviral drugs on preadipocyte proliferation was assessed by measuring the cell number in cultures exposed to the drugs for 48 and 72 h. Viable cell number was assessed with a 3-[4,5-dimethylthiazol-2-yl]-2,5-diphenyl tetrazolium bromide based assay, as previously described[7,14]. Since all cultures were plated at the same initial cell number, an increase or decrease in viable cells at 48 and 72 h was assumed to represents a change in the potential of cells to increase in number, *i.e.*, proliferate.

Assessment of preadipocyte differentiation

The differentiation of preadipocytes into mature adipocytes was estimated after 12 d by measuring the activity of the lipogenic marker enzyme glycerol-3-phosphate dehydrogenase (GPDH) and by quantifying the intracellular lipid accumulation after staining with Oil Red O.

GPDH assay: Determination of GPDH activity was based on the oxidation of NADH and reported as mU where 1 mU corresponded to the amount of enzyme needed to oxidize 1 nmol of NADH/min as reported previously[7].

Oil Red O staining: Cells fixed in a 10% formaldehyde solution were stained with Oil Red O, extracted with isopropanol and assessed for absorbance at 500 nm[7].

Statistical analysis

Results are expressed as means ± SEM. Differences between control and treated groups and among the treated groups were analyzed with a randomized block ANOVA with post-hoc Fisher's Least Significant Difference (LSD) test. P values < 0.05 were considered statistically significant.

RESULTS

The effect of anti-retroviral drugs, individually and in combination, was assessed for two distinct aspects of preadipocyte metabolism; namely the proliferation of preadipocytes and the ability of preadipocytes to differentiate into adipocytes.

Preadipocyte proliferation in the presence of NRTIs, NNRTIs and PIs

All individual antiretroviral drugs inhibited the proliferation of preadipocytes incubated in concentrations of the drugs comparable to the levels seen in the plasma of treated patients compared with untreated cells (control). This effect was statistically significant at 72 h (Figure 1; $P < 0.02$). The inhibition of proliferation in FTC-treated cells was apparent even at 48 h of incubation ($P < 0.01$).

All drug combinations tested significantly suppressed preadipocyte proliferation. In the presence of EFV + FTC + TDF (NNRTI + NRTIs) preadipocyte proliferation was inhibited by 14% and 26% respectively after 48 and 72 h compared to controls. Similarly, therapeutic combinations with ATV + FTC + TDF (PI + NRTIs) showed a reduction in preadipocyte growth of 19 % at 48 h, and of 30% at 72 h (Figure 1, $P < 0.001$). When RTV was added to ATV + FTC + TDF, as it is clinically known to boost other PIs, the inhibitory effect was more noticeable, with a suppression in proliferation of 26% and 37% respectively after 48 and 72 h compared to controls (Figure 1, $P < 0.001$).

The inhibition of proliferative activity of preadipocytes in multi-drug combinations was more severe than the inhibition of proliferation observed with the individual component drugs in some cases, but not all. In the combination EFV + FTC + TDF, suppression of proliferation was greater than the suppression observed when EFV and TDF were used individually ($P < 0.02$), but there was not an additional effect when EFV + FTC + TDF combination was compared to FTC treatment alone (P = NS). Combining ATV + FTC + TDF or ATV + RTV + FTC + TDF increased the inhibition of adipocyte proliferation to a greater extent than treatment with the same concentration of the individual drugs both at 48 ($P < 0.05$) and 72 h ($P < 0.01$).

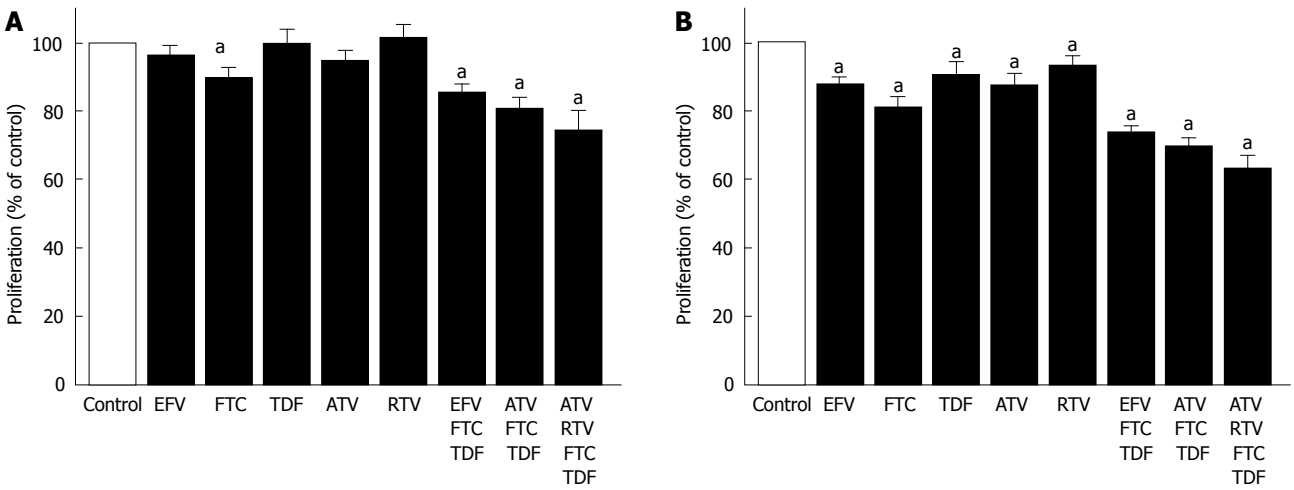

Figure 1 Pre-adipocyte proliferation in the presence of individual drugs or drug combinations for 48 h (A) and 72 h (B) (MTT test). The results are expressed as percent values of control cultures. Mean ± SEM, n = 7. Significantly different from control, $^aP \leqslant 0.05$. EFV: Efavirenz; FTC: Emtricitabine; TDF: Tenofovir; ATV: Atazanavir.

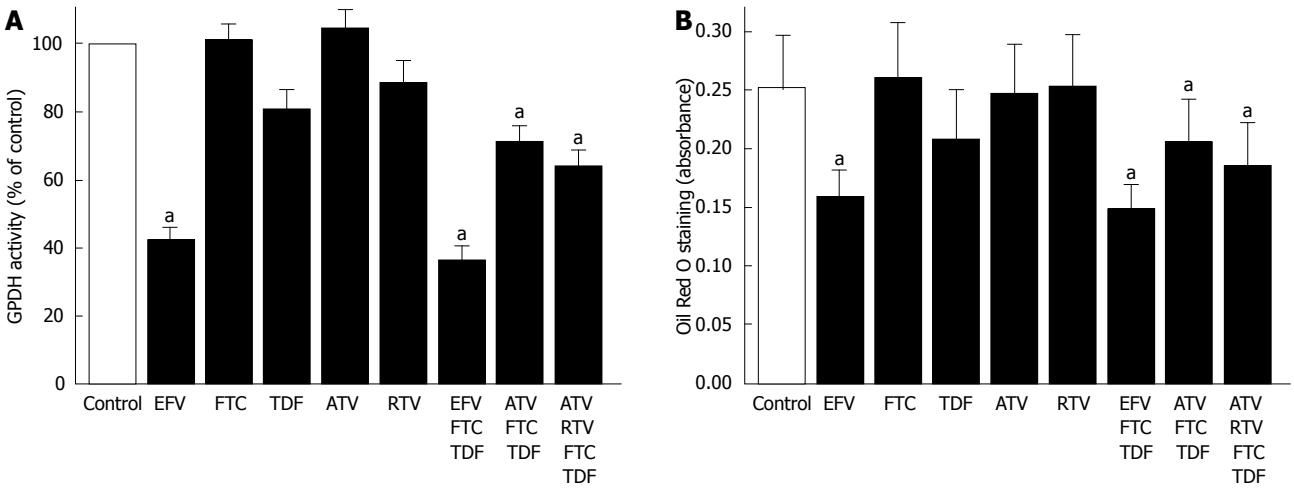

Figure 2 Effect of individual drugs or drug combinations on differentiation of human preadipocytes. Differentiation was assessed after 12 d by measuring the glycerol-3-phosphate dehydrogenase activity (A), and Oil Red O staining (B). All results are expressed as percent values of control cultures. Mean ± SEM, n = 9. Significantly different from control, $^aP \leqslant 0.05$. EFV: Efavirenz; FTC: Emtricitabine; TDF: Tenofovir; ATV: Atazanavir.

Of the three multi-drug regimens, the drug combination ATV + RTV + FTC + TDF had a more suppressive effect on proliferation of preadipocytes than the other multi-drug regimens at 48 h (P < 0.02). At 72 h, the combination, ATV + RTV + FTC + TDF, was not statistically significantly different from ATV + FTC + TDF but was significantly different from EFV + FTC + TDF (P = 0.05).

Preadipocyte differentiation in the presence of NRTIs, NNRTIs and PIs

Preadipocyte differentiation, in the presence of anti-retroviral drugs, was assessed by 2 different techniques, one involved measuring the enzymatic activity of GPDH and the other involved quantifying intracellular lipid accumulation after staining with Oil Red O. The two techniques produced comparable results (Figure 2).

EFV had a profound inhibitory effect on preadipocyte differentiation (Figure 2). Both GPDH activity and lipid accumulation were greatly reduced in cells treated with EFV compared to controls (Figure 2, P < 0.001). Of the other anti-retroviral drugs tested, only TDF appeared to have an effect on intracellular lipid accumulation, which tended to be lower when cells were treated with TDF (P = 0.06). Preadipocyte differentiation in the presence of remaining individual drugs did not differ from controls (Figure 2).

Figure 2 demonstrates that, preadipocyte differentiation was significantly reduced when the anti-retroviral drugs were used in combination compared to untreated cultures. Compared to control cells, the EFV + FTC + TDF (NNRTI + NRTIs) combination showed the most suppressive effect on differentiation with GPDH activity and lipid accumulation 64% and 39% lower respectively (Figure 2, P < 0.001). Combining NRTIs with a PI (ATV + FTC + TDF) inhibited GPDH activity by 29% and lipid accumulation by 19% compared to controls (Figure 2, P < 0.01). This effect was slightly

greater when a boosting amount of RTV was added (ATV + FTC + TDF + RTV, Figure 2, $P < 0.001$).

The inhibitory effect of a multi-drug combination NNRTI and NRTI (EFV + FTC + TDF) was also compared to the suppression in differentiation observed with the anti-retroviral medications individually. Suppression with the combination resulted in a greater reduction in preadipocyte differentiation than either FTC or TDF alone ($P < 0.001$). However, suppression of differentiation with the combination of EFV + FTC + TDF was comparable in magnitude to treatment with EFV alone suggesting EFV was accountable for most of the reduction in differentiation observed with the combination regimen (Figure 2). The two multi-drug regimens containing PI + NRTI were also examined relative to the incubations with the individual medications. The multi-drug combinations containing PIs had greater inhibitory effects on differentiation than treatment with the same concentration of each individual drug (Figure 2, $P < 0.003$), with the exception of TDF.

The multi-drug regimens have also been compared with each other. The combination with NNRT and NRTI (EFV, FTC, TDF) reduced differentiation to a greater extent than either of the two regimens with PI + NRTI, whether assessed as either GPDH activity ($P < 0.001$) or intracellular lipid accumulation ($P < 0.02$).

DISCUSSION

There is no doubt that the etiology of HIV/HAART-associated lipodystrophy syndrome is multi-factorial, but antiretroviral medications contribute to the condition. This *in vitro* technique, with primary cultures of pre-adipocytes isolated from healthy subjects, provides a way of assessing effects of single and combination drug regimens on preadipocyte proliferation and differentiation; and consequently, on the potential of drug regimens to contribute to HALS. The antiretroviral medications currently in use have profound effects on both preadipocyte proliferation and differentiation.

All of the antiretroviral agents tested inhibited pre-adipocyte proliferation. Individually, the NRTI, FTC, had a more pronounced effect on preadipocyte proliferation than the NRTI, TDF; the NNRTI, EFV; or the PIs ATV or RTV (Figure 1). While in general combinations of anti-retroviral drugs were more toxic than the individual drugs, this was not true for combinations containing FTC. The addition of TDF (another NRTI) and EFV (a NNRTI) to emtricitabine did not produce any greater toxicity than was observed with EFV alone. However, multidrug regimens containing PIs in combination with NRTI (ATV + FTC + TDF and ATV + RTV + FTC + TDF) resulted in further suppression of proliferation. Having previously demonstrated that RTV does not suppress preadipocyte proliferation at levels comparable to those used for boosting[7], this study indicates that adding RTV to a combination of ATV, TDF and FTC does increase toxicity (Figure 1). Clearly, the toxicity of individual antiretrovirals can be affected by concurrent antiretroviral administration.

In contrast to preadipocyte proliferation, it is the NNRT EFV that has the most profound effect on pre-adipocyte differentiation, an effect that has been reported previously[15,16]. Combining EFV with NRTIs (EFV + FTC + TDF) does not result in any greater suppression. Regimens containing PIs and NRTIs (ATV + FTC + TDF and ATV + RTV + FTC + TDF) are not as toxic as those containing EFV. However, the multi-drug combinations containing PIs suppressed differentiation to a greater extent than the use of any drug individually. This study highlights the importance of assessing both the effects on the proliferation of preadipocytes and the differentiation of preadipocytes into mature adipocytes since multi-drug regimens affect them differently.

In conclusion, antiretroviral medications affect not only the differentiation of preadipocyte into mature adipocytes, these drugs also affect the proliferation of preadipocytes and can, therefore, impact on the number of preadipocytes that are available. While FTC has the most profound effect on preadipocyte proliferation, it is EFV that has the greatest impact on differentiation. Combinations of antiretroviral medications, which have no impact when used individually, increase the toxicity for preadipocytes.

COMMENTS

Background

Highly active antiretroviral therapy (HAART) regimens with various combinations of protease inhibitors (PI), nucleoside reverse transcriptase inhibitors (NRTI) and nonnucleoside reverse transcriptase inhibitors (NNRTI) have long been linked to HAART-associated lipodystrophy syndrome (HALS). Once HALS is manifest, it is difficult to reverse. There is a need to develop ways of assessing drug combinations for the potential to contribute to HALS.

Research frontiers

The effect of individual anti-retroviral drugs have been studied *in vitro*, but this is the first report of the effect of drug combinations assessed at clinically relevant concentrations. The differential effects on preadipocyte proliferation and differentiation were also assessed, providing important mechanistic information.

Innovations and breakthroughs

The study demonstrates that replacing ritonavir-based regimens with the clinically more acceptable protease inhibitor, atazanavir, does not eliminate the potential for toxic effects on adipose tissue. In addition, adding ritonavir at "boosting" levels to regimens containing nucleoside reverse transcriptase inhibitors and non-reverse transcriptase inhibitors also increases the lipo-toxic potential of these antiretroviral combinations.

Applications

Although combination antiretroviral therapy is clinically more efficacious than single drug regimens, the combination regimens also have the potential to contribute to adipose tissue toxicity through effects of preadipocyte replication and differentiation. The study also illustrates the value of an *in vitro* system for screening drug combinations for potential adipose tissue toxicity.

Terminology

HALS is a condition that is characterized by loss of subcutaneous fat, particularly in the face, buttocks, arms and legs. Antiretroviral therapy typically includes a combination of drugs with different mechanisms of action including NRTIs, NNRTIs, and PIs. These drug classes have the potential for differential effects on adipose tissue and the effect of combination therapy may be greater than the individual drugs alone. This study also investigated the mechanisms by which antiretroviral drugs can contribute to the loss of adipose tissue;

an inability of preadipocytes to proliferate reduces the potential number of precursor cells for the formation of adipose tissue, the inability of pre-adipocytes to differentiation reduces the formation of adipose tissue by arresting precursor cells in an undifferentiated state.

Peer-review

This manuscript is worth publishing, reporting the synergistic or cooperative effects of anti-HIV agents on inhibiting adipogenesis by performing *in vitro* experiments using human materials. It will help us to recognize the importance to take extra caution in executing HAART.

REFERENCES

1 **Guaraldi G**, Stentarelli C, Zona S, Santoro A. HIV-associated lipodystrophy: impact of antiretroviral therapy. *Drugs* 2013; **73**: 1431-1450 [PMID: 24002702 DOI: 10.1007/s40265-013-0108-1]

2 **Lake JE**, Wohl D, Scherzer R, Grunfeld C, Tien PC, Sidney S, Currier JS. Regional fat deposition and cardiovascular risk in HIV infection: the FRAM study. *AIDS Care* 2011; **23**: 929-938 [PMID: 21767228 DOI: 10.1080/09540121.2010.543885]

3 **Quintas RC**, de França ER, de Petribú KC, Ximenes RA, Quintas LF, Cavalcanti EL, Kitamura MA, Magalhães KA, Paiva KC, Filho DB. Treatment of facial lipoatrophy with polymethylmethacrylate among patients with human immunodeficiency virus/acquired immunodeficiency syndrome (HIV/AIDS): impact on the quality of life. *Int J Dermatol* 2014; **53**: 497-502 [PMID: 24602032 DOI: 10.1111/ijd.12400]

4 **Domingo P**, Estrada V, López-Aldeguer J, Villaroya F, Martínez E. Fat redistribution syndromes associated with HIV-1 infection and combination antiretroviral therapy. *AIDS Rev* 2012; **14**: 112-123 [PMID: 22627607]

5 **Martin A**, Moore CL, Mallon PW, Hoy JF, Emery S, Belloso WH, Phanuphak P, Ferret S, Cooper DA, Boyd MA; Second-Line Study Team. HIV lipodystrophy in participants randomised to lopinavir/ritonavir (LPV/r) +2-3 nucleoside/nucleotide reverse transcriptase inhibitors (N(t)RTI) or LPV/r + raltegravir as second-line antiretroviral therapy. *PLoS One* 2013; **8**: e77138 [PMID: 24204757 DOI: 10.1371/journal.pone.0077138]

6 **Minami R**, Yamamoto M, Takahama S, Ando H, Miyamura T, Suematsu E. Comparison of the influence of four classes of HIV antiretrovirals on adipogenic differentiation: the minimal effect of raltegravir and atazanavir. *J Infect Chemother* 2011; **17**: 183-188 [PMID: 20706762 DOI: 10.1007/s10156-010-0101-5]

7 **Caso G**, Mileva I, McNurlan MA, Mynarcik DC, Darras F, Gelato MC. Effect of ritonavir and atazanavir on human subcutaneous preadipocyte proliferation and differentiation. *Antiviral Res* 2010; **86**: 137-143 [PMID: 20153378]

8 **Panel on Antiretroviral Guidelines for Adults and Adolescents**. Guidelines for the use of antiretroviral agents in HIV-1-infected adults and adolescents. Department of Health and Human Services. Section accessed on March 18, 2015 (Table 6). Available from: URL: http://aidsinfo.nih.gov/contentfiles/lvguidelines/AdultandAdolescentGL.pdf

9 **Zeldin RK**, Petruschke RA. Pharmacological and therapeutic properties of ritonavir-boosted protease inhibitor therapy in HIV-infected patients. *J Antimicrob Chemother* 2004; **53**: 4-9 [PMID: 14657084 DOI: 10.1093/jac/dkh029]

10 **Clay PG**, Taylor TA, Glaros AG, McRae M, Williams C, McCandless D, Oelklaus M. "One pill, once daily": what clinicians need to know about Atriplatrade mark. *Ther Clin Risk Manag* 2008; **4**: 291-302 [PMID: 18728842]

11 **Kiser JJ**, Fletcher CV, Flynn PM, Cunningham CK, Wilson CM, Kapogiannis BG, Major-Wilson H, Viani RM, Liu NX, Muenz LR, Harris DR, Havens PL; Adolescent Trials Network for HIV/AIDS Interventions. Pharmacokinetics of antiretroviral regimens containing tenofovir disoproxil fumarate and atazanavir-ritonavir in adolescents and young adults with human immunodeficiency virus infection. *Antimicrob Agents Chemother* 2008; **52**: 631-637 [PMID: 18025112 DOI: 10.1128/AAC.00761-07]

12 **von Hentig N**, Dauer B, Haberl A, Klauke S, Lutz T, Staszewski S, Harder S. Tenofovir comedication does not impair the steady-state pharmacokinetics of ritonavir-boosted atazanavir in HIV-1-infected adults. *Eur J Clin Pharmacol* 2007; **63**: 935-940 [PMID: 17665183 DOI: 10.1007/s00228-007-0344-y]

13 **Tchkonia T**, Giorgadze N, Pirtskhalava T, Tchoukalova Y, Karagiannides I, Forse RA, DePonte M, Stevenson M, Guo W, Han J, Waloga G, Lash TL, Jensen MD, Kirkland JL. Fat depot origin affects adipogenesis in primary cultured and cloned human preadipocytes. *Am J Physiol Regul Integr Comp Physiol* 2002; **282**: R1286-R1296 [PMID: 11959668]

14 **Caso G**, McNurlan MA, McMillan ND, Eremin O, Garlick PJ. Tumour cell growth in culture: dependence on arginine. *Clin Sci* (Lond) 2004; **107**: 371-379 [PMID: 15157183]

15 **El Hadri K**, Glorian M, Monsempes C, Dieudonné MN, Pecquery R, Giudicelli Y, Andreani M, Dugail I, Fève B. In vitro suppression of the lipogenic pathway by the nonnucleoside reverse transcriptase inhibitor efavirenz in 3T3 and human preadipocytes or adipocytes. *J Biol Chem* 2004; **279**: 15130-15141 [PMID: 14722061 DOI: 10.1074/jbc.M312875200]

16 **Gallego-Escuredo JM**, Del Mar Gutierrez M, Diaz-Delfin J, Domingo JC, Mateo MG, Domingo P, Giralt M, Villarroya F. Differential effects of efavirenz and lopinavir/ritonavir on human adipocyte differentiation, gene expression and release of adipokines and pro-inflammatory cytokines. *Curr HIV Res* 2010; **8**: 545-553 [PMID: 21073442]

P- Reviewer: Saeki K, Shen WJ **S- Editor**: Song XX **L- Editor**: A
E- Editor: Lu YJ

Published by **Baishideng Publishing Group Inc**
7901 Stoneridge Drive, Suite 501, Pleasanton, CA 94588, USA
Telephone: +1-925-223-8242
Fax: +1-925-223-8243
E-mail: bpgoffice@wjgnet.com
Help Desk: http://www.f6publishing.com/helpdesk
http://www.wjgnet.com

ISSN 2220-3249 (online)

World Journal of *Virology*

World J Virol 2017 November 12; 6(4): 59-72

Published by Baishideng Publishing Group Inc

WJV World Journal of Virology

A peer-reviewed, online, open-access journal of virology

Editorial Board

2016-2019

The *World Journal of Virology* Editorial Board consists of 370 members, representing a team of worldwide experts in virology. They are from 59 countries, including Argentina (4), Australia (8), Austria (4), Barbados (1), Belgium (1), Brazil (7), Bulgaria (1), Cameroon (1), Canada (12), Chile (2), China (55), Croatia (2), Cuba (1), Czech Republic (1), Denmark (1), Egypt (3), Ethiopia (1), Finland (5), France (10), Gambia(1), Germany (11), Ghana (1), Greece (2), Hungary (1), India (13), Indonesia (1), Iran (2), Ireland (3), Israel (4), Italy (23), Japan (16), Kazakhstan (1), Kenya (1), Kosovo (1), Mexico (2), Netherlands (5), New Zealand (1), Nigeria (1), Pakistan (1), Palestine (1), Poland (1), Portugal (1), Romania (1), Russia (2), Saudi Arabia (1), Singapore (2), Slovakia (2), Slovenia (2), South Africa (2), South Korea (6), Spain (19), Sweden (4), Thailand (8), Tunisia (1), Turkey (4), United Arab Emirates (1), United Kingdom (8), United States (92), and Uruguay (1).

Eiichi N Kodama, *Sendai*
Emoto Masashi, *Gunma*
Hiromitsu Moriyama, *Tokyo*
Kenji Okuda, *Yokohama*
Nobuhiro Suzuki, *Okayama*
Takashi Suzuki, *Shizuoka*
Tetsuro Suzuki, *Hamamatsu*
Yoshiyuki Suzuki, *Nagoya-shi*
Akifumi Takaori-Kondo, *Kyoto*
Tetsuya Toyoda, *Toyohashi*

Kazakhstan

Vladimir E Berezin, *Almaty*

Kenya

George G Maina, *Nairobi*

Kosovo

Lul Raka, *Prishtina*

Mexico

Juan E Ludert, *Mexico City*
Julio Reyes-Leyva, *Mexico*

Netherlands

Kimberley SM Benschop, *Amsterdam*
Benjamin Berkhout, *Amsterdam*
Byron EE Martina, *Rotterdam*
Willem JG Melchers, *Nijmegen*
Monique Nijhuis, *Utrecht*

New Zealand

Olga S Garkavenko, *Auckland*

Nigeria

Olajide A Owolodun, *Plateau State*

Pakistan

Muhammad I Qadir, *Faisalabad*

Palestine

Ahmad Y Amro, *Jerusalem*

Poland

Brygida Knysz, *Wroclaw*

Portugal

Celso Cunha, *Lisbon*

Romania

Anda Baicus, *Bucharest*

Russia

Anton Buzdin, *Moscow*
Elena V Gavrilova, *Novosibirsk*

Saudi Arabia

Ahmed S Abdel-Moneim, *Al-Taif*

Singapore

Sophie Bellanger, *Singapore*
Ding X Liu, *Singapore*

Slovakia

Gabriela Bukovska, *Bratislava*
Julius Rajcani, *Bratislava*

Slovenia

Uros Krapez, *Ljubljana*
Andrej Steyer, *Ljubljana*

South Africa

Janusz T Paweska, *Sandringham*
Dirk Stephan, *Matieland*

South Korea

Sang Hoon Ahn, *Seoul*
Tae-Jin Choi, *Busan*
Young-Ki Choi, *Cheongju*
Kee-Jong Hong, *Cheongwon*
Bum-Joon Kim, *Seoul*
Junsoo Park, *Wonju*

Spain

Alí Alejo, *Valdeolmos*
Alfredo Berzal-Herranz, *Granada*
Rafael Blasco, *Madrid*
Julio Collazos, *Usánsolo-Galdácano*
Juan M Hernández, *Madrid*
Gómez L Jaime, *Córdoba*
Josep M Llibre, *Badalona*
Cecilio López-Galíndez, *Madrid*
F. Xavier López-Labrador, *Valencia*
JoséA Melero, *Madrid*
Luis Menéndez-Arias, *Madrid*
Andrés Moya, *València*
David R Pereda, *Sevilla*
Pilar Perez-Romero, *Sevilla*
Josep Quer, *Barcelona*
Daniel López Rodríguez, *Majadahonda*
Juan-Carlos Saiz, *Madrid*
Noemi Sevilla, *Madrid*
Natalia Soriano-Sarabia, *Madrid*

Sweden

Goran PL Bucht, *Umea*
Ali Mirazimi, *Solna*
Muhammad Munir, *Uppdala*
Bo F Oberg, *Huddinge*

Thailand

Prasert Auewarakul, *Bangkok*
Parin Chaivisuthangkura, *Bangkok*
Wasin Charerntantanakul, *Chiang Mai*
Wansika Kiatpathomchai, *Bangkok*
Sasisopin Kiertiburanakul, *Bangkok*
Winyou Mitarnun, *Chiang Mai*
Yong Poovorawan, *Bangkok*
Viroj Wiwanitkit, *Bangkok*

Tunisia

Olfa Bahri, *Tunis*

Turkey

Omer Coskun, *Ankara*
Iftihar Koksal, *Trabzon*
Aykut Ozdarendeli, *Kayseri*
Ayca A Sayiner, *Izmir*

United Arab Emirates

Tahir A Rizvi, *Al Ain*

United Kingdom

Shiu-Wan Chan, *Manchester*
Simon R Clegg, *Preston*
Chiriva I Maurizio, *Nottingham*
Iain M Morgan, *Glasgow*
Mark R Nelson, *London*
Adrian W Philbey, *Glasgow*
James P Stewart, *Liverpool*
Gavin WG Wilkinson, *Cardiff*

United States

Nafees Ahmad, *Tucson*
Ashok Aiyar, *Los Angeles*
Hizi Amnon, *Bethesda*
Judith M Ball, *Texas*
Igor M Belyakov, *Frederick*
Bradford K Berges, *Provo*
Preeti Bharaj, *Orlando*
Jay C Brown, *Charlottesville*
Victor E Buckwold, *Walkersville*
Alexander A Bukreyev, *Galveston*
Joseph J Carter, *Seattle*
Maria G Castro, *Los Angeles*
Yan-Ping Chen, *Beltsville*

World Journal of Virology

Contents

Quarterly Volume 6 Number 4 November 12, 2017

World Journal of Virology
Volume 6 Number 4 November 12, 2017

Contents

NAME OF JOURNAL
World Journal of Virology

ISSN
ISSN 2220-3249 (online)

LAUNCH DATE
February 12, 2012

FREQUENCY
Quarterly

EDITOR-IN-CHIEF
Ling Lu, MD, PhD, Department of Pathology and Laboratory Medicine, University of Kansas Medical Center, Kansas City, 3901 Rainbow Blvd, WHE 3020, KS 66160, United States

EDITORIAL BOARD MEMBERS
All editorial board members resources online at http://www.wjgnet.com/2220-3249/editorialboard.htm

EDITORIAL OFFICE
Xiu-Xia Song, Director
World Journal of Virology
Baishideng Publishing Group Inc
7901 Stoneridge Drive, Suite 501, Pleasanton, CA 94588, USA
Telephone: +1-925-2238242
Fax: +1-925-2238243
E-mail: editorialoffice@wjgnet.com
Help Desk: http://www.f6publishing.com/helpdesk
http://www.wjgnet.com

PUBLISHER
Baishideng Publishing Group Inc
7901 Stoneridge Drive, Suite 501, Pleasanton, CA 94588, USA
Telephone: +1-925-2238242
Fax: +1-925-2238243
E-mail: editorialoffice@wjgnet.com
Help Desk: http://www.f6publishing.com/helpdesk
http://www.wjgnet.com

PUBLICATION DATE
November 12, 2017

INSTRUCTIONS TO AUTHORS
http://www.wjgnet.com/bpg/gerinfo/204

ONLINE SUBMISSION
http://www.f6publishing.com

World Journal of Virology

Submit a Manuscript: http://www.f6publishing.com

World J Virol 2017 November 12; 6(4): 59-72

DOI: 10.5501/wjv.v6.i4.59

ISSN 2220-3249 (online)

ORIGINAL ARTICLE

Observational Study

Real-world cure rates for hepatitis C virus treatments that include simeprevir and/or sofosbuvir are comparable to clinical trial results

Kian Bichoupan, Neeta Tandon, James F Crismale, Joshua Hartman, David Del Bello, Neal Patel, Sweta Chekuri, Alyson Harty, Michel Ng, Keith M Sigel, Meena B Bansal, Priya Grewal, Charissa Y Chang, Jennifer Leong, Gene Y Im, Lawrence U Liu, Joseph A Odin, Nancy Bach, Scott L Friedman, Thomas D Schiano, Ponni V Perumalswami, Douglas T Dieterich, Andrea D Branch

Kian Bichoupan, James F Crismale, Joshua Hartman, David Del Bello, Neal Patel, Sweta Chekuri, Alyson Harty, Michel Ng, Meena B Bansal, Priya Grewal, Charissa Y Chang, Jennifer Leong, Gene Y Im, Lawrence U Liu, Joseph A Odin, Nancy Bach, Scott L Friedman, Thomas D Schiano, Ponni V Perumalswami, Douglas T Dieterich, Andrea D Branch, Division of Liver Diseases, Icahn School of Medicine at Mount Sinai, New York, NY 10029, United States

Neeta Tandon, Janssen Scientific Affairs, LLC, Titusville, NJ 08560, United States

Keith M Sigel, Division of General Internal Medicine, Icahn School of Medicine at Mount Sinai, New York, NY 10029, United States

ORCID number: Kian Bichoupan (0000-0002-4449-7229); Neeta Tandon (0000-0002-9474-7214); James F Crismale (0000-0002-3219-882X); Joshua Hartman (0000-0002-4169-4825); David Del Bello (0000-0002-3248-0235); Neal Patel (0000-0002-9004-6883); Sweta Chekuri (0000-0003-2123-1951); Alyson Harty (0000-0002-8979-4905); Michel Ng (0000-0002-6555-9337); Keith M Sigel (0000-0002-4051-4861); Meena B Bansal (0000-0002-7501-2191); Priya Grewal (0000-0001-7820-9769); Charissa Y Chang (0000-0002-1814-5131); Jennifer Leong (0000-0003-2386-4437); Gene Y Im (0000-0003-0009-8418); Lawrence U Liu (0000-0001-8847-841X); Joseph A Odin (0000-0003-0923-5685); Nancy Bach (0000-0003-2939-0391); Scott L Friedman (0000-0003-1178-6195); Thomas D Schiano (0000-0003-1878-5101); Ponni V Perumalswami (0000-0003-3070-3906); Douglas T Dieterich (0000-0001-7786-8594); Andrea D Branch (0000-0003-2865-3188).

Author contributions: Bichoupan K, Dieterich DT and Branch AD contributed to study conception and design; Hartman J, Del Bello D, Patel N and Chekuri S gathered and analyzed patient data; Harty A, Ng M, Sigel KM, Bansal MB, Grewal P, Chang CY, Leong J, Im GY, Liu LU, Odin JA, Bach N, Schiano TD and Perumalswami PV contributed patient data for analysis and assisted in editing the manuscript; Friedman SL assisted in editing the manuscript; Bichoupan K performed the statistical analysis; Bichoupan K, Tandon N, Crismale JF and Branch AD contributed to the final writing of the manuscript; all authors had final approval of the article to be published.

Supported by Janssen Scientific Affairs and National Institutes of Health, Nos. DA031095 and DK090317.

Institutional review board statement: The study was conducted in accordance with the Helsinki agreement, with approval of the Mount Sinai Institutional Review Board (GCO 10-0032).

Informed consent statement: Study participants did not provide informed consent prior to study enrollment as the Icahn School of Medicine at Mount Sinai Institutional Review Board provided a waiver of authorization to release de-identified patient data for research purposes.

Conflict-of-interest statement: Dr. Kian Bichoupan is a paid consultant for Gilead Sciences and Janssen Pharmaceuticals, Inc. Neeta Tandon is an employee of Johnson and Johnson. Dr. Andrea D Branch received research support from Gilead Sciences and Janssen Pharmaceuticals, Inc. Dr. Douglas T Dieterich serves as a paid lecturer, consultant and is a member on scientific advisory boards of companies which either develop or assess medicines used for the treatment of viral hepatitis. These companies include Gilead Sciences, Abbvie, Achillion, Bristol-Myers Squibb, Merck, and Janssen Pharmaceuticals, Inc. Dr. Thomas D Schiano is a paid consultant for Salix, Merck, Gilead, BMS, Novartis and Janssen and received research support from Mass biologics, Gilead, Merck, Biotest and Genentech. Michel Ng is a paid member of AbbVie's Speakers bureau. Dr. Ponni V Perumalswami receives research support from Gilead Sciences. Dr. Keith M Sigel has served on an advisory board for Gilead Sciences. Dr. James Crismale, Dr Meena B Bansal, Dr. Joshua Hartman, Dr. Sweta Chekuri, Alyson Harty, Dr. Joseph A Odin,

Dr. Priya Grewal, Dr. Nancy Bach, Dr. Lawrence Liu, Dr. Charissa Y Chang, Dr. Gene Y Im, Dr. Jennifer Leong, Dr. David Del Bello, Dr. Neal M Patel and Dr. Scott L Friedman do not have any relevant disclosures.

Data sharing statement: Technical appendix, statistical code, and dataset available from the corresponding author at andrea.branch@mssm.edu. Consent was not obtained but the presented data are anonymized and risk of identification is low.

Manuscript source: Invited Manuscript

Correspondence to: Andrea D Branch, PhD, Professor of Medicine, Division of Liver Diseases, Icahn School of Medicine at Mount Sinai, One Gustave L. Levy Place, New York, NY 10029, United States. andrea.branch@mssm.edu
Telephone: +1-212-6598371
Fax: +1-212-3483517

Received: June 11, 2017
Peer-review started: June 12, 2017
First decision: July 20, 2017
Revised: August 3, 2017
Accepted: September 16, 2017
Article in press: September 17, 2017
Published online: November 12, 2017

Abstract

AIM

To assess the real-world effectiveness and cost of simeprevir (SMV), and/or sofosbuvir (SOF)-based therapy for chronic hepatitis C virus (HCV) infection.

METHODS

The real-world performance of patients treated with SMV/SOF ± ribavirin (RBV), SOF/RBV, and SOF/RBV with pegylated-interferon (PEG) were analyzed in a consecutive series of 508 patients with chronic HCV infection treated at a single academic medical center. Patients with genotypes 1 through 4 were included. Rates of sustained virological response - the absence of a detectable serum HCV RNA 12 wk after the end of treatment [sustained virological response (SVR) 12] - were calculated on an intention-to-treat basis. Costs were calculated from the payer's perspective using Medicare/Medicaid fees and Redbook Wholesale Acquisition Costs. Patient-related factors associated with SVR12 were identified using multivariable logistic regression.

RESULTS

SVR12 rates were as follows: 86% (95%CI: 80%-91%) among 178 patients on SMV/SOF ± RBV; 62% (95%CI: 55%-68%) among 234 patients on SOF/RBV; and 78% (95%CI: 68%-86%) among 96 patients on SOF/PEG/RBV. Mean costs-per-SVR12 were $174442 (standard deviation: ± $18588) for SMV/SOF ± RBV; $223003 (± $77946) for SOF/RBV; and $126496 (± $31052) for SOF/PEG/RBV. Among patients on SMV/SOF ± RBV, SVR12 was less likely in patients previously treated with a protease inhibitor [odds ratio (OR): 0.20, 95%CI: 0.06-0.56]. Higher bilirubin (OR: 0.47, 95%CI: 0.30-0.69) reduced the likelihood of SVR12 among patients on SOF/RBV, while FIB-4 score ⩾ 3.25 reduced the likelihood of SVR12 (OR: 0.18, 95%CI: 0.05-0.59) among those on SOF/PEG/RBV.

CONCLUSION

SVR12 rates for SMV and/or SOF-based regimens in a diverse real-world population are comparable to those in clinical trials. Treatment failure accounts for 27% of costs.

Key words: Cirrhosis; Cost; Sustained virological response; Protease inhibitor; Polymerase inhibitor

Core tip: To our knowledge, this study is the largest real-world investigation of outcomes in patients with chronic hepatitis C virus infection with genotypes 1-4 being treated with simeprevir and/or sofosbuvir-containing regimens that has been conducted in a single center. We provide compelling real-world data in a large (*n* = 508), diverse population of patients, showing that the effectiveness of these regimens is comparable to that seen in multicenter clinical trials. Further, our unique cost analysis reveals that the cost-per-sustained virological response of simeprevir- and/or sofosbuvir-based therapy is lower than telaprevir-based triple therapy, likely due to higher rates of cure and lower rates of adverse events.

Bichoupan K, Tandon N, Crismale JF, Hartman J, Del Bello D, Patel N, Chekuri S, Harty A, Ng M, Sigel KM, Bansal MB, Grewal P, Chang CY, Leong J, Im GY, Liu LU, Odin JA, Bach N, Friedman SL, Schiano TD, Perumalswami PV, Dieterich DT, Branch AD. Real-world cure rates for hepatitis C virus treatments that include simeprevir and/or sofosbuvir are comparable to clinical trial results. *World J Virol* 2017; 6(4): 59-72 Available from: URL: http://www.wjgnet.com/2220-3249/full/v6/i4/59.htm
DOI: http://dx.doi.org/10.5501/wjv.v6.i4.59

INTRODUCTION

Treatment options for patients with chronic hepatitis C virus (HCV) infection are expanding rapidly. Data from clinical trials indicate that newer regimens have reduced side effects compared to dual therapy with pegylated interferon (PEG) and ribavirin (RBV) and higher sustained virological response (SVR) rates[1-10].

SVR is equivalent to a virological cure, and is currently defined as the absence of detectable HCV RNA in blood 12 wk after the end-of-treatment (EOT). SVR at 12 wk (SVR12) has supplanted SVR at 24 wk as the standard endpoint[11]. SVR12 is associated with reduced rates of liver-related and all-cause mortality, even among patients with advanced liver disease[12-14]. Additional benefits include improvements in quality of life, as well as decreased healthcare utilization[15].

As most patients can be treated safely with newer interferon-free direct-acting antiviral (DAA) regimens, current AASLD/IDSA guidelines recommend treating all patients with chronic HCV, except those with life expectancies too short for HCV cure to be considered beneficial[16]. These recommendations, along with birth cohort screening of baby boomers and direct-to-consumer advertising, have created a significant public demand for treatment[17]. Comparative data about the clinical and economic effectiveness of new regimens are needed to inform discussions about costs and to allow selection of the best option for each patient.

The first HCV NS3/4A protease inhibitors (PIs), telaprevir (TVR) and boceprevir (BOC), were used in combination with PEG and RBV. These triple therapy regimens had a high burden of adverse events and high costs-per-SVR, as well as cumbersome dosing regimens[2-5,18,19]. Simeprevir (SMV) was approved by the United States Food and Drug Administration (United States FDA) in 2013 for the treatment of genotype (GT) 1 HCV. Used in combination with PEG and RBV, it was at least as effective in achieving SVR as TVR and BOC in large randomized trials, but it reduced the pill burden and improved tolerability[9,10,20]. In 2014, the United States FDA approved sofosbuvir (SOF), a nucleotide analog NS5B polymerase inhibitor with activity against GT 1-6. Depending upon GT and prior treatment history, it was initially used either in combination with PEG/RBV, with SMV ± RBV, or with RBV alone. SVR rates with these SOF-containing regimens ranged from 56% to over 90% in registration trials[6-8]. SOF is now used most commonly in fixed-dose combination with NS5A inhibitors, including ledipasvir and velpatasvir[21].

We previously established that the cost-per-SVR of TVR-based triple therapy in clinical practice approached $200000-far higher than projections based on results of randomized clinical trials[19]. In the present study, we examine the clinical and economic performance of regimens containing SMV and/or SOF in a consecutive series of 508 patients and identify risk factors associated with treatment success (SVR12) or failure. SMV remains an important option for patients with resistance associated substitutions (RASs) to NS5A inhibitors, and in liver transplantation recipients[22-24]. Prior studies assessing outcomes of SMV- and/or SOF-containing regimens in clinical practice were limited to patients with GT 1 HCV[25-29]. Other recent studies assessing real-world outcomes of SOF-based dual- or triple-therapy have focused on patients with a single genotype[30,31]. Here we offer a comprehensive examination of real-world outcomes of three different treatment regimens across genotypes 1-4.

MATERIALS AND METHODS

Identification of a cohort of patients initiating treatment with SMV and/or SOF December 2013-June 2014

Data were collected on a consecutive series of 508 patients with chronic HCV infection who started treatment with a SMV- and/or SOF-containing regimen between December 2013 and June 2014 at the Mount Sinai Medical Center in New York City. Patients with HCV GT 1, 2, 3, and 4 were included in the study. Subjects were identified using two complementary methods: (1) healthcare providers compiled lists of patients meeting inclusion criteria; and (2) the Mount Sinai Data Warehouse, a database integrating multiple electronic health record platforms, was queried to identify all patients with any history of International Classification of Diseases, Ninth Revision (ICD-9) diagnostic codes for chronic HCV infection (070.54) and a prescription order for SMV or SOF. The combined list was validated by manual chart review. Patients on the following regimens were included: SMV/SOF ± RBV, SOF/RBV, and SOF/PEG/RBV. All patients received at least one dose of SMV and/or SOF. Patients who had undergone liver transplantation or who had HIV/HCV co-infection were excluded from this study; however, data on HIV/HCV co-infected patients are published elsewhere[32]. Choice of the HCV treatment regimen, duration of treatment, and adverse event (AE) management, including the use of erythropoietin, were at the discretion of the provider. Data on demographics, HCV kinetics, clinical laboratory tests, office visits, medications, AE management, and other aspects of medical care, including past use of PIs (TVR or BOC) were collected. Providers were notified of patients who were lost to follow-up (LFU), but there was no systematic method for contacting patients who did not complete SVR12 testing.

HCV viral load was measured using a real-time polymerase chain reaction assay (COBAS AmpliPrepCOBAS Taqman HCV Test version 2.0; Roche Molecular Diagnostics, Pleasanton, CA), which defines a HCV viral load below 15 IU/mL as "undetectable". Breakthrough and relapse were defined as the achievement of undetectable HCV RNA during treatment, followed by the detection of HCV RNA during treatment, or after treatment was completed or stopped, respectively. Advanced fibrosis/cirrhosis was defined as a FIB-4 score $\geqslant$ 3.25 (24). SVR12 was defined as an undetectable HCV RNA at least 12 wk after the EOT. The study was conducted in accordance with the Helsinki agreement, with approval of the Mount Sinai Institutional Review Board (GCO 10-0032).

Use of resources and costs

The cost of care was calculated for each patient based on Medicare and Medicaid fee schedules as described in our previous study[19], and included laboratory tests, physician fees, and AE management. Costs of HCV medications were derived from the Red Book Wholesale Acquisition Costs, accessed in December 2014: SOF,

$1000/d; SMV, $790/d; RBV, $15.56/d; PEG, $672/wk. Costs are expressed in 2014 United States dollars.

Statistical analysis

Descriptive statistics were used to analyze the baseline characteristics of the cohort of 508 patients who initiated SMV- and/or SOF-based therapy and to compare these characteristics to those of a cohort of patients who initiated treatment with TVR- or BOC-based regimens at the Mount Sinai Medical Center[19].

SVR12 rates and costs were calculated on an intention-to-treat (ITT) basis for the entire population of 508 patients who initiated SMV- and/or SOF-based therapy and for patients on each of the three treatment regimens. Treatment outcome (SVR12 or non-SVR12) was imputed for 14/508 (2.75%) patients (3 on SMV/SOF ± RBV, 5 patients on SOF/RBV, and 6 on SOF/PEG/RBV) who lacked SVR12 data, but who had an undetectable viral load at EOT and/or at 4 wk after EOT, based on the average SVR12 rate for patients on the same regimen. For patients receiving SOF/RBV, each genotype was analyzed separately because of the varying SVR12 rates of different genotypes[6,33]. A subgroup analysis was carried out on 130 patients receiving SMV/SOF ± RBV who had no prior exposure to PI therapy and did not have Childs-Pugh B or C cirrhosis, similar to the study group in the COSMOS trial[34].

Costs were calculated as mean and standard deviation (SD). The cost-per-SVR12 and its SD were calculated by determining the mean and SD of total cost of care (medications, adverse event costs, laboratory fees, and care provider fees) and dividing it by the SVR12 rate. A one-way sensitivity analysis was conducted to determine the impact of the costs of medications on the cost-per-SVR12, with the prices of HCV medications varied from 50% to 100% to reflect possible drug discount rates.

For the 470 patients with confirmed SVR12 data, univariable and multivariable logistic regression were used to identify factors associated with SVR12 and generate forest plots. Unless otherwise indicated, multivariable models retained variables with a P-value < 0.05. In a fully-adjusted model, all variables were included except those that exhibited collinearity.

To compare values between groups, t-tests were used for normally distributed continuous variables and Mann-Whitney U tests for non-normally distributed variables or costs. χ^2 or Fisher's exact tests were used for categorical variables. A P-value < 0.05 was considered significant. R software and Microsoft Excel were used for statistical analysis.

RESULTS

Characteristics of the patients initiating treatment December 2013-June 2014

Table 1 shows the characteristics of all 508 patients and those of patients on each regimen: 178 (35%) received SMV/SOF ± RBV, 234 (46%) received SOF/RBV, and 96 (19%) received SOF/PEG/RBV. Of patents treated with SMV/SOF ± RBV, 99% were GT 1, compared with 87% of patients treated with PEG/RBV/SOF and 44% treated with SOF/RBV. The remaining distribution of HCV GTs in each treatment group is displayed in Table 1. The median age was 60 years [interquartile range (IQR): 54-64], 71 (14%) were black, 183 (37%) were female, and 204 (40%) were naïve to previous HCV treatment, while 18% had failed TVR or BOC treatment in the past. Over half (54%) had a FIB-4 score ⩾ 3.25, indicating advanced fibrosis/cirrhosis (METAVIR F3-F4). The median FIB-4 score was 3.54 (IQR: 1.73-6.72), consistent with the likelihood that most patients had advanced fibrosis/cirrhosis.

To investigate how the real-world population of patients seeking and receiving treatment may be changing, characteristics of 508 patients initiating treatment with SMV- and/or SOF-based regimens (December 2013 until June 2014) were compared to those of 223 patients who initiated treatment with BOC- and TVR-based regimens during the previous era, May 2011 until December 2011 (Table 2). The group treated with SMV- and/or SOF-based regimens was significantly older (P < 0.01), had a higher percentage with a FIB-4 score ⩾ 3.25 (P = 0.02), and lower hemoglobin levels (P < 0.01). A subset analysis of treatment naïve patients indicated that patients on a SMV- or SOF-based treatment regimen had significantly lower albumin than treatment naïve patients receiving BOC and/or TVR (P = 0.04, Supplementary Table 1). The greater age and more advanced liver disease of the cohort on SMV- and SOF-based regimens likely reflects both the aging of HCV-infected population and the higher potency and tolerability of the newer regimens, which allow patients with advanced liver disease to be treated with a greater probability of success.

Real-world SVR12 rates

Of the 508 patients who started treatment, the outcome (SVR12 or non-SVR12) was known with certainty for 470 patients who completed SVR12 testing, and it was imputed for 14 patients who completed EOT or SVR4 testing (see Methods and Figure 1). Twenty-four patients (5%) initiated treatment but lacked EOT data. Their baseline characteristics were compared to those of the other 484 patients, and no significant differences were found (Supplementary Table 2). In the ITT analysis of SVR12 rates, 136 (27%) patients were considered to fail treatment. This number included 16 patients with a null response to treatment, 91 who relapsed after an EOT response (including 61 patients treated with SOF/RBV, 15 treated with SMV/SOF ± RBV, and 15 treated with SOF/PEG/RBV), one patient with a virological breakthrough (treated with SOF/RBV), three who died, two with imputed failure, and 24 who were LFU. SVR12 rates and corresponding 95% confidence intervals (CIs) are presented in Table 3. The overall SVR12 rate was 73% (95%CI: 69%-77%). It was 86% (95%CI: 80%-91%) among patients on SMV/SOF ± RBV, 62%

Table 1 Baseline characteristics of 508 patients who initiated simeprevir- and/or sofosbuvir-based therapy

	Total	SMV/SOF ± RBV	SOF/RBV	SOF/PEG/RBV
		Continuous: median (IQR)/categorical: *n* (%)		
n	508	178	234	96
Age, yr	60 (54-64)	61 (57-65)	60 (54-65)	56 (50-62)
Race, black, *n* (%)	71 (14)	27 (15)	23 (10)	21 (22)
HCV genotype, *n* (%)				
1	362 (71)	177 (99.4)	102 (44)	83 (87)
2	69 (14)	0 (0)	69 (29)	0 (0)
3	52 (10)	0 (0)	52 (22)	0 (0)
4	25 (5)	1 (0.6)	11 (5)	13 (14)
Gender, female	183 (37)	67 (39)	87 (39)	29 (31)
BMI, kg/m^2	27.7 (24.7-30.8)	27.5 (24.5-30.2)	27.9 (2.6-31.0)	27.7 (25.1-31.1)
Diabetes, *n* (%)	111 (22)	29 (16)	59 (25)	23 (24)
Naïve to treatment, *n* (%)	204 (40)	51 (29)	114 (49)	39 (41)
PI failure, *n* (%)	89 (18)	48 (27)	18 (8)	23 (24)
HCV viral load, log U/mL	6.15 (5.61-6.58)	6.28 (5.78-6.74)	6.05 (5.43-6.50)	6.13 (5.63-6.53)
Hemoglobin, g/dL	13.8 (12.6-15.1)	13.9 (12.8-15.1)	13.5 (12.4-14.7)	14.7 (13.3-15.4)
Platelet, x 10^3/μL	143 (90-195)	146 (94-193)	125 (71-183)	180 (125-209)
ALT, U/L	63 (39-105)	72 (45-119)	59 (37-99)	60 (37-101)
AST, U/L	62 (38-99)	70 (40-113)	63 (38-101)	48 (33-83)
Total Bilirubin, mg/L	0.70 (0.50-1.10)	0.70 (0.50-1.00)	0.8 (0.5-1.5)	0.60 (0.40-0.83)
Albumin, g/dL	4.0 (3.5-4.4)	4.10 (3.70-4.40)	3.8 (3.2-4.3)	4.20 (3.80-4.45)
FIB-4 score	3.54 (1.73-6.72)	3.66 (1.90-5.99)	4.74 (1.91-9.89)	2.09 (1.46-3.85)
FIB-4 ⩾ 3.25, *n* (%)	267 (54)	97 (56)	137 (61)	33 (34)

SMV: Simeprevir; SOF: Sofosbuvir; RBV: Ribavirin; PEG: Pegylated interferon; IQR: Interquartile range; BMI: Body mass index; PI: Protease inhibitor; HCV: Hepatitis C virus; ALT: Alanine transaminase; AST: Aspartate transaminase.

Table 2 Comparison of the baseline characteristics of patients on simeprevir- and/or sofosbuvir-based regimens and patients on telaprevir- or boceprevir-based regimens

	SMV- and/or SOF-containing regimens	TVR- or BOC-containing regimens	*P*-value
	Continuous: median (IQR)/categorical: *n* (%)		
n	508	223	
Age, yr	60 (54-64)	57 (51-61)	< 0.01[1]
Race, black, *n* (%)	71/508 (14)	41/223 (18)	0.13[2]
Gender, female, *n* (%)	183/508 (37)	79/223 (35)	0.89[2]
BMI, kg/m^2	27.7 (24.7-30.8)	27.1 (24.5-30.7)	0.65[1]
Diabetes, *n* (%)	111/508 (22)	48/223 (22)	0.89[2]
Naïve to treatment, *n* (%)	204/508 (40)	68/223 (31)	0.01[2]
HCV viral load, log IU/mL	6.15 (5.61-6.58)	6.31 (5.89-6.66)	< 0.01[3]
Hemoglobin, g/dL	13.8 (12.6-15.1)	14.3 (13.1-15.3)	< 0.01[1]
Platelet, x 10^3/μL	143 (90-195)	152 (107-195)	0.19[3]
ALT, U/L	63 (39-105)	67 (44-106)	0.13[3]
AST, U/L	62 (38-99)	62 (39-104)	0.75[3]
Albumin, g/dL	4.0 (3.5-4.4)	4.2 (3.9-45)	< 0.01[1]
FIB-4 score	3.54 (1.73-6.72)	2.65 (1.77-5.60)	0.06[3]
FIB-4 ⩾ 3.25, *n* (%)	267/508 (54)	98/221 (44)	0.03[2]

[1]*T*-test; [2]χ^2; [3]Mann-Whitney. SMV: Simeprevir; SOF: Sofosbuvir; TVR: Telaprevir; BOC: Boceprevir; IQR: Interquartile range; BMI: Body mass index; HCV: Hepatitis C virus; ALT: Alanine transaminase; AST: Aspartate transaminase.

(95%CI: 55%-68%) among patients on SOF/RBV, and 78% (95%CI: 68%-86%) among patients on SOF/PEG/RBV. Among patients treated with SMV/SOF ± RBV in the "COSMOS-like" cohort (which excluded patients who had previously failed a PI and/or had Child-Pugh class B or C cirrhosis), the SVR12 rate was 90% (95%CI: 83%-94%). This is similar to the SVR12 rate in the COSMOS study, which was 92% for patients with METAVIR scores F0-2 and 94% for patients with METAVIR scores F3-4[34]. SVR12 rates varied by GT for patients treated with SOF/RBV, and ranged from 44% (95%CI: 34%-54%) for GT 1 to 83% (95%CI: 71%-90%) for GT 2 (Table 3). A comparison between SVR12 rates with regards to GT was not statistically feasible in the group receiving SMV/SOF ± RBV as only one patient in this group was infected with GT 4. SVR12 rates did not differ significantly between patients with GT 1 and GT 4 HCV in the group treated with SOF/PEG/RBV.

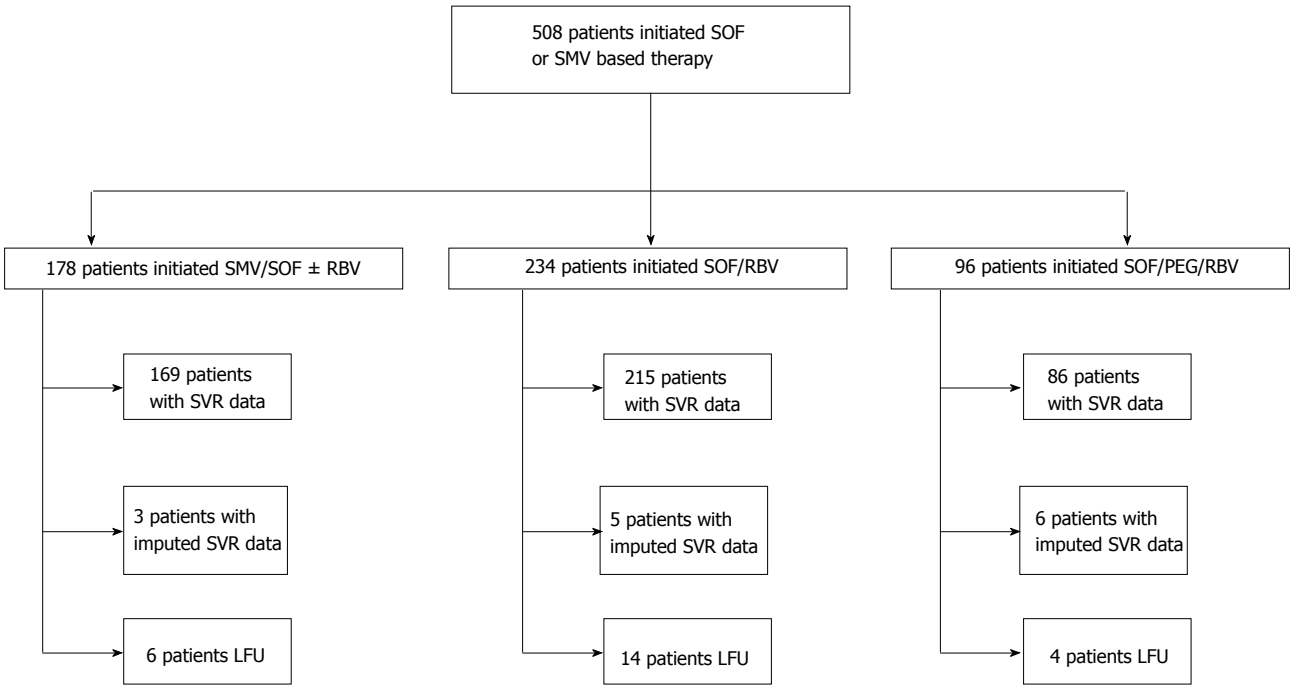

Figure 1 Outline of the study cohort. Five hundred and eight patients initiated treatment. The number of patients with confirmed outcomes [sustained virological response (SVR) 12 or non-SVR12], the number with imputed outcomes, and the number who were lost to follow-up on each of three regimens are indicated. SVR: Sustained virological response; SMV: Simeprevir; SOF: Sofosbuvir; RBV: Ribavirin; PEG: Pegylated interferon.

Table 3 SVR12 rates for 508 patients who initiated therapy with simeprevir- and/or sofosbuvir-based treatment regimens, calculated on an intention-to-treat basis, with imputed data on 14 patients

	SVR12 rates	
	SVR/total, (%)	95%CI, %
All treatments	372/508 (73)	69-77
SMV/SOF ± RBV	153/178 (86)	80-91
"COSMOS-like" cohort	117/130 (90)	83-94
SOF/RBV	144/234 (62)	55-68
Genotype		
1	45/102 (44)	34-54
2	57/69 (83)	71-90
3	35/52 (67)	53-79
4	7/11 (64)	32-88
SOF/PEG/RBV	75/96 (78)	68-86

SVR: Sustained virological response; SMV: Simeprevir; SOF: Sofosbuvir; RBV: Ribavirin; PEG: Pegylated interferon.

Costs

The total cost of care from the payer's perspective was determined for all 508 patients (including the 24 LFU patients). The analysis included costs of HCV medications, laboratory tests, physician fees, and adverse event management. Table 4 presents the total costs as well as costs-per-SVR for each regimen. The total cost of care for the 508 patients was $68.29 million. Treatment of the 136/508 (27%) patients who failed therapy accounted for $18.23 million (27%) of these costs. Adverse event management accounted for only about $289371 (0.4%) of costs[19].

Costs-per-SVR were calculated on an ITT basis by dividing the total costs by the SVR12 rate. As shown in Table 4, the cost-per-SVR was $174442 (SD ± $18588) for SMV/SOF ± RBV; $223003 (± $77946) for SOF/RBV; and $126469 (± $31052) for SOF/PEG/RBV. The cost-per-SVR when drug costs were discounted by 50% were $88,233 (± $9188), $113223 (± $39282), and $64657 (± $16002) for SMV/SOF ± RBV, SOF/RBV, and SOF/PEG/RBV, respectively. The cost-per-SVR for SMV/SOF ± RBV was compared to the cost-per-SVR for patients treated with TVR-based regimens at our center. The median cost-per-SVR for TVR-based regimens was $189322 (IQR: $143558-$211296) and the median cost-per-SVR for SMV/SOF ± RBV was $177975 (IQR: $176455-$178138), which was significantly different (P = 0.02) according to the Mann-Whitney U test.

Factors associated with SVR12

Univariable and multivariable logistic regression were used to identify factors associated with SVR12 for the 470 patients with confirmed SVR12 test results. Data are presented separately for the 3 regimens: SMV/SOF ± RBV (Table 5), SOF/RBV (Table 6), and SOF/PEG/RBV (Table 7). Among patients on SMV/SOF ± RBV, in a multivariable model that retained variables with a P-value below 0.05, SVR12 was less likely in patients with a history of failed PI treatment (OR: 0.20, 95%CI: 0.06-0.56, P = 0.01). Factors associated with SVR12 in patients treated with SMV/SOF ± RBV were also examined in a fully-adjusted model that retained all variables except those that exhibited collinearity with other variables (Table 8). In this model, SVR12 was less

Table 4 Cost of care and cost-per-sustained virological response by treatment for 508 patients in study

	HCV medications ($)	Adverse Event costs ($)	Lab fees ($)	Provider fees ($)	Total cost of care ($)	[1]SVR12 rate (%)	Cost-per-SVR ($)
SMV/SOF ± RBV	26379909	65231	89947	154488	26689574	153/178 (86)	174442 (18588)
SOF/RBV genotype	31616725	143770	136353	215584	32112432	144/234 (62)	223003 (77946)
1	15723055	106274	59942	94435	15983705	45/102 (44)	355193 (98493)
2	5736955	32477	37540	61136	5868109	57/69 (83)	102949 (21346)
3	8279942	5019	31914	49381	8366257	35/52 (67)	239036 (48831)
4	1876773		6956	10633	1894362	7/11 (64)	270623 (124)
SOF/PEG/RBV	9275858	80370	48929	82045	9487202	75/96 (78)	126469 (31052)

[1]SVR12 rate was calculated with imputations for 14 patients with an EOT response based on the average SVR12 rate for other patients on the same regimen. SMV: Simeprevir; SOF: Sofosbuvir; RBV: Ribavirin; PEG: Pegylated interferon; SVR: Sustained virological response; HCV: Hepatitis C virus.

Table 5 Univariable and multivariable logistic regression analysis of factors associated with SVR12 for 169 patients treated with simeprevir/sofosbuvir ± ribavirin and a confirmed outcome

SMV/SOF ± RBV	Univariable			Multivariable		
	OR	95%CI	*P* value	OR	95%CI	*P* value
Age, per yr	1.01	0.96-1.06	0.73			
Race, black	0.43	0.15-1.45	0.14			
Gender, female	1.69	0.61-5.44	0.34			
BMI, per kg/m^2	0.97	0.87-1.08	0.55			
Diabetes, *n* (%)	0.64	0.21-2.42	0.47			
Naïve to treatment	7.96	1.57-145.37	0.04			
PI Failure	0.23	0.08-0.61	< 0.01	0.2	0.06-0.56	< 0.01
Ribavirin	0.78	0.29-2.03	0.61			
HCV viral load, per log IU/mL	0.61	0.26-1.26	0.22			
Hemoglobin, per g/dL	1.17	0.92-1.48	0.18			
Platelets, per 103/μL	1	0.99-1.01	0.19			
ALT, per U/L	1	0.99-1.01	0.37			
AST, per U/L	1	0.99-1.01	0.89			
Total bilirubin, per mg/dL	0.56	0.29-1.06	0.06	0.52	0.28-1.02	0.06
Albumin, per g/dL	1.82	0.72-4.45	0.19			
FIB-4 ⩾ 3.25	0.66	0.22-1.83	0.44			

SMV: Simeprevir; SOF: Sofosbuvir; RBV: Ribavirin; OR: Odds ratio; CI: Confidence interval; BMI: Body mass index; PI: Protease inhibitor; HCV: Hepatitis C virus; ALT: Alanine transaminase; AST: Aspartate transaminase.

likely among patients with a history of PI failure (OR: 0.12, 95%CI: 0.02-0.52, $P < 0.01$), higher baseline bilirubin (OR: 0.31, 95%CI: 0.08-0.86, $P = 0.04$), and a higher viral load (OR: 0.21, 95%CI: 0.05-0.70, $P = 0.04$). RBV use was not significantly associated with SVR12 (OR: 0.64, 95%CI: 0.09-3.78, $P = 0.63$); however, patients treated with SMV/SOF with RBV were more likely to have a history of PI failure ($P < 0.01$), reflecting a tendency to prescribe RBV for patients with less favorable treatment characteristics (Supplementary Table 3).

Among patients on SOF/RBV, SVR12 was less likely among patients with a higher baseline total bilirubin level (OR: 0.37, 95%CI: 0.24-0.55, $P < 0.01$) and more likely among patients infected by GT 2 HCV (OR: 4.66, 95% CI: 2.06-11.42, $P < 0.01$) or GT 3 HCV (OR: 2.76, 95%CI: 1.22-6.59, $P = 0.02$) compared to GT 1. There was no difference between GT 4 and GT 1 (Table 6). Among patients on SOF/PEG/RBV, SVR12 was more likely among patients who were naïve to treatment (OR: 7.01, 95%CI: 1.69-48.27, $P = 0.02$) and less likely among patients with a FIB-4 score ⩾ 3.25 (OR: 0.18, 95%CI: 0.05-0.59, $P < 0.01$; Table 7).

Figure 2 presents forest plots of SVR12 rates and 95%CIs of various subgroups of the 470 patients on each of the three regimens. Of note: Among patients on SMV/SOF ± RBV, the SVR12 rate was 77% (36/47) among patients who previously failed PI treatment, compared to 93% (114/122) among patients without a history of PI failure, $P < 0.01$ (Figure 2A). SVR12 was also significantly lower among patients with advanced fibrosis/cirrhosis as noted by a FIB-4 score ≥ 3.25 who were treated with either SOF/RBV (83% *vs* 53%, $P < 0.01$, Figure 2B) or SOF/PEG/RBV (91% *vs* 61%, $P < 0.01$, Figure 2C).

DISCUSSION

HCV treatment is evolving at a rapid pace, and timely data are needed regarding the clinical and economic performance of current and emerging medical therapies. This study provides information about the largest

Table 6 Univariable and multivariable logistic regression analysis of factors associated with SVR12 for 215 patients treated with sofosbuvir/ribavirin and a confirmed outcome

SOF/RBV	Univariable			Multivariable		
	OR	95%CI	*P* value	OR	95%CI	*P* value
Age, per yr	0.98	0.95-1.01	0.14			
Race, black	0.33	0.13-0.80	0.02			
Gender, female	1.96	1.08-3.65	0.03			
BMI, per kg/m^2	0.96	0.90-1.01	0.15			
Diabetes	0.95	0.50-1.83	0.87			
Naïve to treatment	1.24	0.71-2.19	0.45			
PI failure	0.33	0.11-0.89	0.03			
HCV viral load, per log IU/mL	0.80	0.56-1.11	0.2			
HCV genotype						
1	Ref	Ref	Ref	Ref	Ref	Ref
2	7.24	0.57-1.29	< 0.01	4.66	2.06-11.42	< 0.01
3	3.29	1.55-7.37	< 0.01	2.76	1.22-6.59	0.02
4	2.03	0.57-8.21	0.28	1.91	0.51-8.06	0.35
Hemoglobin, per g/dL	1.11	0.95-1.32	0.17			
Platelet, per 10^3/μL	1.01	1.01-1.02	< 0.01			
ALT, per U/L	1	0.99-1.00	0.1			
AST, per U/L	0.99	0.99-1.00	< 0.01			
Total bilirubin, per mg/dL	0.37	0.24-0.55	< 0.01	0.47	0.30-0.69	< 0.01
Albumin, per g/dL	3.15	1.98-5.19	< 0.01			
FIB-4 ⩾ 3.25	0.23	0.12-0.45	< 0.01			

CI: Confidence interval; OR: Odds ratio; BMI: Body mass index; PI: Protease inhibitor; HCV: Hepatitis C virus; ALT: Alanine transaminase; AST: Aspartate transaminase; SOF: Sofosbuvir; RBV: Ribavirin; SVR: Sustained virological response.

Table 7 Univariable and multivariable logistic regression analysis of factors associated with SVR12 for 86 patients treated with sofosbuvir/pegylated interferon/ribavirin and a confirmed outcome

SOF/PEG/RBV	Univariable			Multivariable		
	OR	95%CI	*P* value	OR	95%CI	*P* value
Age, per yr	0.99	0.94-1.04	0.67			
Race, black	0.98	0.30-3.86	0.98			
Gender, female	2.31	0.67-10.79	0.22			
BMI, per kg/m^2	0.95	0.83-1.09	0.42			
Diabetes, *n* (%)	1.15	0.35-4.48	0.83			
Naïve to treatment	7.72	1.98-51.36	< 0.01	7.01	1.69-48.27	0.02
PI failure	1.06	0.32-4.16	0.92			
HCV viral load, log IU/mL	1.07	0.55-1.92	0.83			
HCV genotype						
1	Ref	Ref	Ref			
4	1.42	0.33-9.83	0.67			
Hemoglobin, per g/dL	1309	0.76-1.55	0.64			
Platelets, per 10^3/μL	1.01	0.99-1.02	0.14			
ALT, per U/L	0.99	0.98-1.01	0.39			
AST, per U/L	0.98	0.96-0.99	< 0.01			
Total bilirubin, per mg/dL	0.18	0.04-0.73	0.02			
Albumin, per g/dL	3.50	1.21-11.04	0.03			
FIB-4 ⩾ 3.25	0.16	0.05-0.50	< 0.01	0.18	0.05-0.59	< 0.01

PEG: Pegylated interferon; SOF: Sofosbuvir; RBV: Ribavirin; OR: Odds ratio; CI: Confidence interval; BMI: Body mass index; PI: Protease inhibitor; HCV: Hepatitis C virus; ALT: Alanine transaminase; AST: Aspartate transaminase; SVR: Sustained virological response.

consecutive series of patients treated at a single center in the United States with regimens containing SMV and/or SOF that has been reported thus far. Importantly, we examined outcomes in patients infected with GTs 1-4, while other large studies of SMV- and/or SOF-based regimens in the United States were limited to patients with single GTs[25-27,29-31]. This study provides data about the effectiveness of various regimens when used in real-world clinical practice in a diverse patient population. Fourteen percent of the cohort was African-American, over half (54%) likely had advanced fibrosis/cirrhosis as determined by FIB-4 score ≥ 3.25, and 60% had previously failed treatment, including 17% that failed prior treatment with PIs.

Compared to the group of patients treated at our center with first generation PIs, the group treated with

Table 8 Fully adjusted multivariable logistic regression model of factors associated with SVR12 among 169 patients treated with simeprevir/sofosbuvir ± ribavirin and a confirmed outcome

SMV/SOF ± RBV	Univariable			Multivariable		
	OR	95%CI	*P* value	OR	95%CI	*P* value
Age, per yr	1.01	0.96-1.06	0.73	0.97	0.87-1.06	0.55
Race, black	0.43	0.15-1.45	0.14	0.66	0.11-4.90	0.66
Gender, female	1.69	0.61-5.44	0.34	0.41	0.08-1.94	0.26
BMI, per kg/m^2	0.97	0.87-1.08	0.55	1.02	0.88-1.20	0.75
Diabetes, *n* (%)	0.64	0.21-2.42	0.47			
Naïve to treatment	7.96	1.57-145.37	0.04			
PI failure	0.23	0.08-0.61	< 0.01	0.12	0.02-0.52	< 0.01
Ribavirin	0.78	0.29-2.03	0.61	0.64	0.09-3.78	0.63
HCV viral load, per log IU/mL	0.61	0.26-1.26	0.22	0.21	0.05-0.70	0.02
Hemoglobin, g/dL	1.17	0.92-1.48	0.18			
Platelet, per 10^3/μL	1	0.99-1.01	0.19	1.01	0.99-1.02	0.35
ALT, per U/L	1	0.99-1.01	0.37	1.01	0.99-1.02	0.41
AST, per U/L	1	0.99-1.01	0.89			
Total Bili, per mg/dL	0.56	0.29-1.06	0.06	0.31	0.08-0.86	0.04
Albumin, per g/dL	1.82	0.72-4.45	0.19			
FIB-4 ⩾ 3.25	0.66	0.22-1.83	0.44	0.89	0.10-6.29	0.92

BMI: Body mass index; PI: Protease inhibitor; HCV: Hepatitis C virus; ALT: Alanine transaminase; AST: Aspartate transaminase; SVM: Simeprevir; SOF: Sofosbuvir; RBV: Ribavirin.

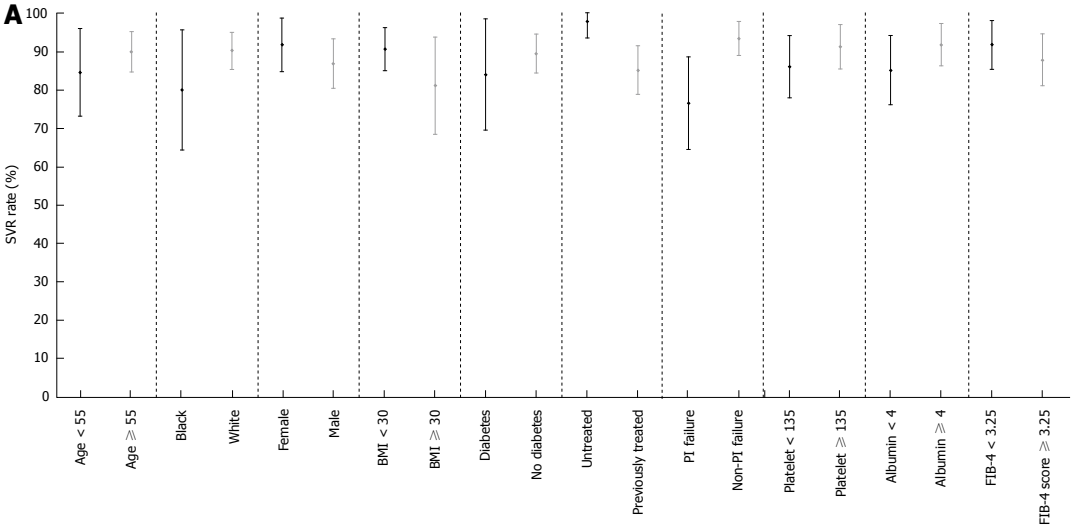

85%	90%	80%	90%	92%	87%	91%	81%	84%	90%	98%	85%	77%	93%	86%	91%	85%	92%	92%	88%
33/39	117/130	20/25	130/144	56/61	93/107	97/107	30/37	21/25	128/143	46/47	104/122	36/47	114/122	62/72	84/92	52/61	90/98	67/73	81/92
P = 0.39		*P* = 0.17		*P* = 0.34		*P* = 0.14		*P* = 0.50		*P* = 0.03		*P* < 0.01		*P* = 0.29		*P* = 0.19		*P* = 0.43	

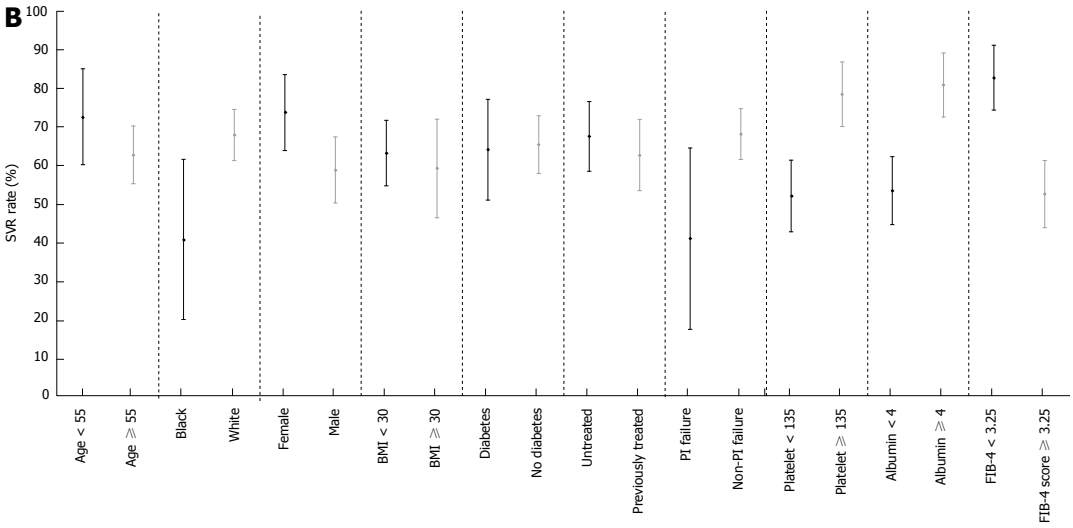

73%	63%	41%	68%	74%	59%	63%	59%	64%	65%	68%	63%	41%	68%	52%	78%	54%	81%	83%	53%
37/52	103/164	9/22	131/193	59/80	76/129	81/128	35/59	34/53	106/162	71/105	69/110	7/17	133/195	59/113	76/97	67/125	72/89	67/81	68/129
P = 0.27		*P* = 0.02		*P* = 0.04		*P* = 0.72		*P* = 0.99		*P* = 0.54		*P* = 0.03		*P* < 0.01		*P* < 0.01		*P* < 0.01	

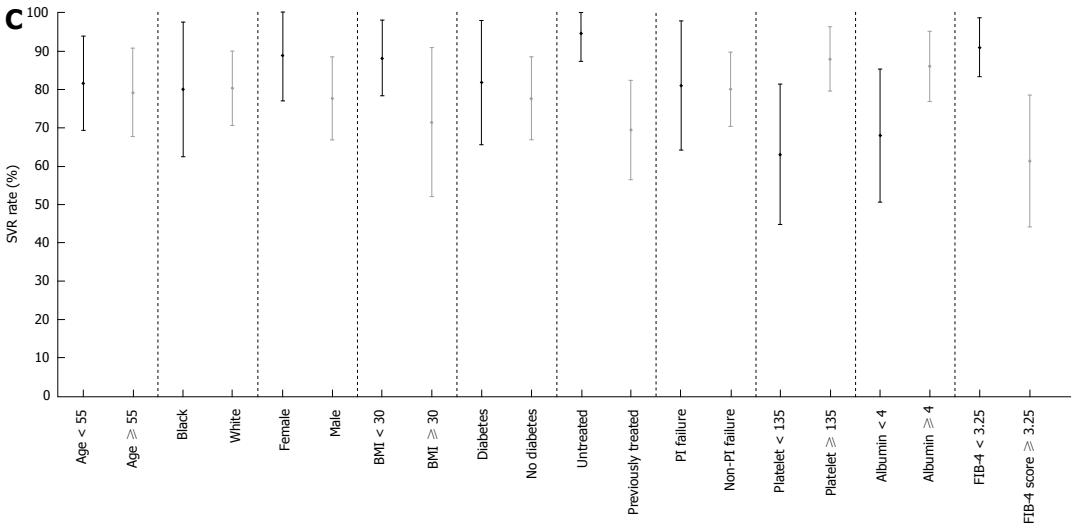

82%	79%	80%	80%	89%	78%	88%	71%	82%	78%	95%	69%	81%	80%	63%	88%	68%	86%	91%	64%
31/38	38/48	16/20	53/66	24/27	45/58	37/42	15/21	18/22	45/58	35/37	34/49	17/21	52/65	17/27	51/58	19/28	49/57	50/55	19/31
$P = 0.99$		$P = 0.99$		$P = 0.35$		$P = 0.20$		$P = 0.99$		$P < 0.01$		$P = 0.99$		$P = 0.02$		$P = 0.09$		$P < 0.01$	

Figure 2 Forest plot of sustained virological response 12 rates for 470 patients with confirmed outcomes. A: SMV/SOF ± RBV; B: SOF/RBV; C: SOF/PEG/RBV. Dotted lines represent the separation of categories. The sustained virological response 12 rate, number in each subgroup, and *P* value of the categorical comparison are shown below the graph. SMV: Simeprevir; SOF: Sofosbuvir; RBV: Ribavirin; PEG: pegylated-interferon.

SMV- and/or SOF-based regimens was significantly older and included a higher percentage of patients with advanced fibrosis/cirrhosis. These differences are consistent with the aging of the baby-boomer cohort, which comprises over 75% of patients infected with HCV in the United States[35]. The greater tolerability and effectiveness of the newer therapies allow patients with more advanced liver disease to achieve an SVR12, causing a shift in the demographic profile of patients receiving treatment. The higher probability of cure and reduced side effect profile may also may encourage a greater number of patients to seek treatment[36,37].

Whereas real-world SVR12 rates with TVR- and BOC-containing regimens were lower than in large registration trials[18,38], the SVR12 rates in this study generally accord with results obtained in formal trials. Among the 508 patients who began therapy, SVR12 rates calculated on an ITT basis were 86% for SMV/SOF ± RBV, 62% for SOF/RBV, and 78% for SOF/PEG/RBV. For comparison, in registration trials, SVR12 rates for SMV/SOF ± RBV ranged from 83%-97%[7,8]; for SOF/RBV, they ranged from 56%-97%[6]; and for SOF/PEG/RBV, they ranged from 80%-90%[6]. The relatively low overall SVR12 rate for SOF/RBV in our population likely reflects the fact that 48% (113/234) of patients treated with SOF/RBV had GT 1 or GT 4 HCV. Published data show that SVR12 rates may be lower for these genotypes, especially in the setting of advanced liver disease[33]. Patients with GT 3 HCV also had a relatively lower rate of SVR12 at 67%; this is similar to the SVR12 rate seen in another recent study assessing real-world rates of SVR12 in patients with GT3 HCV, where the SVR12 rate was 69.4%[39]. In contrast, patients in our study with GT 2 HCV who were treated with SOF/RBV had an SVR12 rate of 83% (95%CI: 71%-90%), again consistent with the high rate of response to SOF/RBV for GT 2 as published in the literature. Among patients treated with either SMV/SOF ± RBV or SOF/PEG/RBV, GT did not significantly impact SVR12 rates.

Multivariable logistic regression identified factors associated with lower SVR12 rates, helping to define patients who may benefit from alternative treatment strategies. Among all treatment regimens examined, the presence of more advanced liver disease was negatively associated with achieving an SVR12. These findings accord with another recently published study assessing treatment outcomes among patients with GT4 HCV treated with SOF/RBV or SOF/PEG/RBV, where those with advanced liver disease were less likely to achieve SVR12[31]. The observation that more advanced liver disease was associated with treatment failure across all three regimens is noteworthy because advanced liver disease is becoming increasingly prevalent in patients with HCV infection[40,41]. This underscores the urgency of efforts to screen patients for HCV infection and transition them into care in order to minimize liver disease progression and obtain the maximal benefits from HCV therapies.

Cost of HCV eradication has become a major concern for the general public and the medical community[42]. We previously analyzed costs of TVR-based triple therapy and found that TVR, which at the time cost $4606/wk, accounted for the majority of the expenses[19]. The costs of both SMV ($5530/wk) and SOF ($7000/wk) are higher than TVR. In part because of this increased drug cost, data from a recently published study suggested that cost-per-SVR was relatively constant when comparing SMV/SOF ± RBV with TVR-based triple therapy[28]. In contrast, our data suggest that the median cost-per-SVR for SMV/SOF ± RBV is significantly lower than that of TVR-

based treatment, likely because of a shorter duration of treatment, reduced adverse event management costs, and higher SVR12 rates compared with TVR-based regimens. Heterogeneity in the demographic makeup and percentage of patients with advanced fibrosis/cirrhosis in study populations may account for the discordant results.

Interestingly, SOF/RBV had the highest mean cost-per-SVR, $223003. This may be related to the reduced effectiveness of this regimen in patients with GT 1 and GT4 HCV[6,33]. Among patients with GT 2 HCV treated with SOF/RBV, the mean cost-per-SVR was the lowest for any regimen, $102949 (SD ± $21346). In addition to GT, the stage of liver fibrosis may affect the choice and duration of treatment and therefore cost. For instance, AASLD/IDSA guidelines suggest treating patients with compensated GT 1 HCV cirrhosis for 24 wk with the combination of SMV/SOF with or without RBV, compared to 12 wk for those without cirrhosis[16]. This regimen would therefore be more expensive in patients with cirrhosis than in those without.

While DAAs remain expensive, it is hoped that the increasing number of treatment options and increased competition will drive costs down. This may especially be important in emerging economies[43]. In addition to occupying a place in the global market, SMV will likely play an important role in specific settings, including the treatment of HCV after liver transplantation, where it has been used successfully without RBV with SVR12 rates ranging from 78%-88%[24,26,44,45]. SMV may also play an important role in patients with a history of failed NS5A inhibitor therapy. Approximately 5%-15% of patients may fail therapy with regimens containing NS5A inhibitors such as ledipasvir, elbasvir, or daclatasvir. These treatment failures often occur in patients with HCV RASs, some of which may confer cross-resistance for multiple drugs within this class[46]. In patients who fail NS5A therapy, treatment with SMV/SOF can result in an SVR12 rate of 88%[22]. RAS testing is becoming more common, as it is recommended by AASLD guidelines prior to initiation of therapy with elbasvir/grazoprevir[47]. While the newest NS5A inhibitor, velpatasvir (used in fixed-dose combination with SOF) may be impacted less by the presence of pretreatment RASs, this regimen remains expensive and may not be accessible to all patients[21]. More precise targeting of therapy may improve patient outcomes and reduce costs.

The strengths of this study include the large number of patients who consecutively initiated therapy, as well as the diversity of the cohort, which was comprised of a racially heterogeneous population with varying stages of liver fibrosis, treatment history, and HCV GT. Importantly, costs were based on data from individual patients, as opposed to aggregate outcomes or projections, and are thus more reflective of costs incurred by payers.

Despite these strengths, our study group was not large enough to delineate all the factors that may impact SVR12 rates. Further, ITT analyses included treatment outcomes (SVR12/non-SVR12) that were imputed in 14 (2.75%) patients; however, any minor artifactual elevation in the SVR12 rate that occurred because of this imputation was likely more than off-set by the assumption that all 24 LFU patients failed therapy. Finally, costs in this study were only calculated from the payer's perspective, rather than from a patient or societal perspective.

In conclusion, this study provides the largest single-center consecutive series of patients treated with SMV- and/or SOF-based regimens in a diverse population. Rates of SVR12 were high, and generally comparable to those seen in registration trials. Cost-per-SVR was dependent upon the drug regimen, and was influenced by patient and HCV-specific factors. Patients with more advanced liver disease were less likely to achieve SVR12.

COMMENTS

Background

Treatment options for patients with chronic hepatitis C virus (HCV) infection are expanding rapidly. The first direct-acting antiviral drugs for HCV, telaprevir (TVR) and boceprevir (BOC), were used in combination with pegylated interferon (PEG) and ribavirin (RBV). These drugs led to enhanced rates of sustained virological response (SVR), but had high rates of adverse events, cumbersome dosing regimens, and high costs-per-SVR due to low SVR rates in clinical practice. Newer regimens based on the NS5B inhibitor sofosbuvir (SOF) have greater tolerability, easier dosing, and higher SVR rates, but remain costly. Comparative data regarding the clinical and economic effectiveness of new regimens are necessary to optimize selection of a treatment regimen for each patient. This paper analyzes the clinical effectiveness and cost of simeprevir (SMV)- and/or SOF-based regimens in a large, diverse real-world patient population among patients infected with HCV genotypes 1-4.

Research frontiers

Efforts to screen patients within the baby-boomer cohort for chronic HCV infection, direct-to-consumer advertising, and an increased drive to by the World Health Organization to eliminate viral hepatitis by 2030 are allowing a greater number of patients to receive care. Understanding the real-world effectiveness and cost of various HCV treatment regimens can help providers optimize therapy for their patients, especially in resource-poor areas that may not have access to the newest and most costly treatment regimens. Prior studies have addressed these questions among patients within more homogenous populations, with respect to both ethnic diversity and HCV genotype. Here, the authors assess effectiveness and cost an ethnically and genotypically diverse patient population.

Innovations and breakthroughs

The authors offer an analysis of HCV cure rates using three treatment regimens: SMV/SOF ± RBV, SOF/RBV, and SOF/PEG/RBV. Cure rates with these regimens are comparable to those seen in clinical trials. The authors describe factors associated with a lower likelihood of SVR, which include the presence of more advanced liver disease and prior failure of TVR- or BOC-based triple therapy. Importantly, despite SMV and SOF being more expensive medications than telaprevir or boceprevir, the cost-per-SVR was significantly lower than that which was seen using TVR-based triple therapy.

Applications

These data will be useful to providers when selecting SMV- and/or SOF-based therapy for patients, especially when newer and more expensive direct-acting antiviral therapy is not available. A similar cost analysis could be performed using newer drugs, utilizing the data presented in this study as a comparator.

Terminology

Sustained virological response - the absence of detectable HCV RNA in the blood at 12 wk after completion of treatment. Direct-acting antiviral (DAA) drugs - a class of oral drugs that directly inhibit HCV viral replication, which includes

NS3/4A protease inhibitors (PIs) such as TVR, BOC, SMV, and grazoprevir; NS5B polymerase inhibitors, including SOF and dasabuvir; and NS5A inhibitors, including ledipasvir, velpatasvir elbasvir, daclatasvir, and ombitasvir.

Peer-review

From the clinical point of view, this study reports valuable results and gives clue to clinicians to properly manage chronic HCV infection in patients.

REFERENCES

1 **Asselah T**, Boyer N, Saadoun D, Martinot-Peignoux M, Marcellin P. Direct-acting antivirals for the treatment of hepatitis C virus infection: optimizing current IFN-free treatment and future perspectives. *Liver Int* 2016; **1**: 47-57 [PMID: 26725897 DOI: 10.1111/liv.13027]

2 **Jacobson IM**, McHutchison JG, Dusheiko G, Di Bisceglie AM, Reddy KR, Bzowej NH, Marcellin P, Muir AJ, Ferenci P, Flisiak R, George J, Rizzetto M, Shouval D, Sola R, Terg RA, Yoshida EM, Adda N, Bengtsson L, Sankoh AJ, Kieffer TL, George S, Kauffman RS, Zeuzem S; ADVANCE Study Team. Telaprevir for previously untreated chronic hepatitis C virus infection. *N Engl J Med* 2011; **364**: 2405-2416 [PMID: 21696307 DOI: 10.1056/NEJMoa1012912]

3 **Zeuzem S**, Andreone P, Pol S, Lawitz E, Diago M, Roberts S, Focaccia R, Younossi Z, Foster GR, Horban A, Ferenci P, Nevens F, Müllhaupt B, Pockros P, Terg R, Shouval D, van Hoek B, Weiland O, Van Heeswijk R, De Meyer S, Luo D, Boogaerts G, Polo R, Picchio G, Beumont M; REALIZE Study Team. Telaprevir for retreatment of HCV infection. *N Engl J Med* 2011; **364**: 2417-2428 [PMID: 21696308 DOI: 10.1056/NEJMoa1013086]

4 **Poordad F**, McCone J Jr, Bacon BR, Bruno S, Manns MP, Sulkowski MS, Jacobson IM, Reddy KR, Goodman ZD, Boparai N, DiNubile MJ, Sniukiene V, Brass CA, Albrecht JK, Bronowicki JP; SPRINT-2 Investigators. Boceprevir for untreated chronic HCV genotype 1 infection. *N Engl J Med* 2011; **364**: 1195-1206 [PMID: 21449783 DOI: 10.1056/NEJMoa1010494]

5 **Bacon BR**, Gordon SC, Lawitz E, Marcellin P, Vierling JM, Zeuzem S, Poordad F, Goodman ZD, Sings HL, Boparai N, Burroughs M, Brass CA, Albrecht JK, Esteban R; HCV RESPOND-2 Investigators. Boceprevir for previously treated chronic HCV genotype 1 infection. *N Engl J Med* 2011; **364**: 1207-1217 [PMID: 21449784 DOI: 10.1056/NEJMoa1009482]

6 **Lawitz E**, Mangia A, Wyles D, Rodriguez-Torres M, Hassanein T, Gordon SC, Schultz M, Davis MN, Kayali Z, Reddy KR, Jacobson IM, Kowdley KV, Nyberg L, Subramanian GM, Hyland RH, Arterburn S, Jiang D, McNally J, Brainard D, Symonds WT, McHutchison JG, Sheikh AM, Younossi Z, Gane EJ. Sofosbuvir for previously untreated chronic hepatitis C infection. *N Engl J Med* 2013; **368**: 1878-1887 [PMID: 23607594 DOI: 10.1056/NEJMoa1214853]

7 **Kwo P**, Gitlin N, Nahass R, Bernstein D, Etzkorn K, Rojter S, Schiff E, Davis M, Ruane P, Younes Z, Kalmeijer R, Sinha R, Peeters M, Lenz O, Fevery B, De La Rosa G, Scott J, Witek J. Simeprevir plus sofosbuvir (12 and 8 weeks) in hepatitis C virus genotype 1-infected patients without cirrhosis: OPTIMIST-1, a phase 3, randomized study. *Hepatology* 2016; **64**: 370-380 [PMID: 26799692 DOI: 10.1002/hep.28467]

8 **Lawitz E**, Matusow G, DeJesus E, Yoshida EM, Felizarta F, Ghalib R, Godofsky E, Herring RW, Poleynard G, Sheikh A, Tobias H, Kugelmas M, Kalmeijer R, Peeters M, Lenz O, Fevery B, De La Rosa G, Scott J, Sinha R, Witek J. Simeprevir plus sofosbuvir in patients with chronic hepatitis C virus genotype 1 infection and cirrhosis: A phase 3 study (OPTIMIST-2). *Hepatology* 2016; **64**: 360-369 [PMID: 26704148 DOI: 10.1002/hep.28422]

9 **Forns X**, Lawitz E, Zeuzem S, Gane E, Bronowicki JP, Andreone P, Horban A, Brown A, Peeters M, Lenz O, Ouwerkerk-Mahadevan S, Scott J, De La Rosa G, Kalmeijer R, Sinha R, Beumont-Mauviel M. Simeprevir with peginterferon and ribavirin leads to high rates of SVR in patients with HCV genotype 1 who relapsed after previous therapy: a phase 3 trial. *Gastroenterology* 2014; **146**: 1669-1679.e3 [PMID: 24602923 DOI: 10.1053/j.gastro.2014.02.051]

10 **Manns M**, Marcellin P, Poordad F, de Araujo ES, Buti M, Horsmans Y, Janczewska E, Villamil F, Scott J, Peeters M, Lenz O, Ouwerkerk-Mahadevan S, De La Rosa G, Kalmeijer R, Sinha R, Beumont-Mauviel M. Simeprevir with pegylated interferon alfa 2a or 2b plus ribavirin in treatment-naive patients with chronic hepatitis C virus genotype 1 infection (QUEST-2): a randomised, double-blind, placebo-controlled phase 3 trial. *Lancet* 2014; **384**: 414-426 [PMID: 24907224 DOI: 10.1016/S0140-6736(14)60538-9]

11 **Yoshida EM**, Sulkowski MS, Gane EJ, Herring RW Jr, Ratziu V, Ding X, Wang J, Chuang SM, Ma J, McNally J, Stamm LM, Brainard DM, Symonds WT, McHutchison JG, Beavers KL, Jacobson IM, Reddy KR, Lawitz E. Concordance of sustained virological response 4, 12, and 24 weeks post-treatment with sofosbuvir-containing regimens for hepatitis C virus. *Hepatology* 2015; **61**: 41-45 [PMID: 25314116 DOI: 10.1002/hep.27366]

12 **Morgan RL**, Baack B, Smith BD, Yartel A, Pitasi M, Falck-Ytter Y. Eradication of hepatitis C virus infection and the development of hepatocellular carcinoma: a meta-analysis of observational studies. *Ann Intern Med* 2013; **158**: 329-337 [PMID: 23460056 DOI: 10.7326/0003-4819-158-5-201303050-00005]

13 **Simmons B**, Saleem J, Heath K, Cooke GS, Hill A. Long-Term Treatment Outcomes of Patients Infected With Hepatitis C Virus: A Systematic Review and Meta-analysis of the Survival Benefit of Achieving a Sustained Virological Response. *Clin Infect Dis* 2015; **61**: 730-740 [PMID: 25987643 DOI: 10.1093/cid/civ396]

14 **Tada T**, Kumada T, Toyoda H, Kiriyama S, Tanikawa M, Hisanaga Y, Kanamori A, Kitabatake S, Yama T, Tanaka J. Viral eradication reduces all-cause mortality in patients with chronic hepatitis C virus infection: a propensity score analysis. *Liver Int* 2016; **36**: 817-826 [PMID: 26787002 DOI: 10.1111/liv.13071]

15 **Smith-Palmer J**, Cerri K, Valentine W. Achieving sustained virologic response in hepatitis C: a systematic review of the clinical, economic and quality of life benefits. *BMC Infect Dis* 2015; **15**: 19 [PMID: 25596623 DOI: 10.1186/s12879-015-0748-8]

16 **AASLD-IDSA**. When and in Whom to Initiate HCV Therapy. Recommendations for testing, managing, and treating hepatitis C. Available from: URL: http://www.hcvguidelines.org/full-report/when-and-whom-initiate-hcv-therapy

17 **Westergaard RP**, Stockman LJ, Hyland HA, Guilfoyle SM, Fangman JJ, Vergeront JM. Provider Workforce Assessment in a Rural Hepatitis C Epidemic: Implications for Scale-up of Antiviral Therapy. *J Prim Care Community Health* 2015; **6**: 215-217 [PMID: 25422260 DOI: 10.1177/2150131914560229]

18 **Vo KP**, Vutien P, Akiyama MJ, Vu VD, Ha NB, Piotrowski JI, Wantuck J, Roytman MM, Tsai N, Cheung R, Li J, Nguyen MH. Poor Sustained Virological Response in a Multicenter Real-Life Cohort of Chronic Hepatitis C Patients Treated with Pegylated Interferon and Ribavirin plus Telaprevir or Boceprevir. *Dig Dis Sci* 2015; **60**: 1045-1051 [PMID: 25821099 DOI: 10.1007/s10620-015-3621-0]

19 **Bichoupan K**, Martel-Laferriere V, Sachs D, Ng M, Schonfeld EA, Pappas A, Crismale J, Stivala A, Khaitova V, Gardenier D, Linderman M, Perumalswami PV, Schiano TD, Odin JA, Liu L, Moskowitz AJ, Dieterich DT, Branch AD. Costs of telaprevir-based triple therapy for hepatitis C: $189,000 per sustained virological response. *Hepatology* 2014; **60**: 1187-1195 [PMID: 25065814 DOI: 10.1002/hep.27340]

20 **Reddy KR**, Zeuzem S, Zoulim F, Weiland O, Horban A, Stanciu C, Villamil FG, Andreone P, George J, Dammers E, Fu M, Kurland D, Lenz O, Ouwerkerk-Mahadevan S, Verbinnen T, Scott J, Jessner W. Simeprevir versus telaprevir with peginterferon and ribavirin in previous null or partial responders with chronic hepatitis C virus genotype 1 infection (ATTAIN): a randomised, double-blind, non-inferiority phase 3 trial. *Lancet Infect Dis* 2015; **15**: 27-35 [PMID: 25482330 DOI: 10.1016/S1473-3099(14)71002-3]

21 **Weisberg IS**, Jacobson IM. A pangenotypic, single tablet regimen of sofosbuvir/velpatasvir for the treatment of chronic hepatitis C infection. *Expert Opin Pharmacother* 2017; **18**: 535-543 [PMID: 28092171 DOI: 10.1080/14656566.2017.1282459]

22 **Hézode C**, Chevaliez S, Scoazec G, Soulier A, Varaut A, Bouvier-Alias M, Ruiz I, Roudot-Thoraval F, Mallat A, Féray C, Pawlotsky JM. Retreatment with sofosbuvir and simeprevir of patients with hepatitis C virus genotype 1 or 4 who previously failed a daclatasvir-

containing regimen. *Hepatology* 2016; **63**: 1809-1816 [PMID: 26853230 DOI: 10.1002/hep.28491]

23 **O'Leary JG**, Fontana RJ, Brown K, Burton JR Jr, Firpi-Morell R, Muir A, O'Brien C, Rabinovitz M, Reddy R, Ryan R, Shprecher A, Villadiego S, Prabhakar A, Brown RS Jr. Efficacy and safety of simeprevir and sofosbuvir with and without ribavirin in subjects with recurrent genotype 1 hepatitis C postorthotopic liver transplant: the randomized GALAXY study. *Transpl Int* 2017; **30**: 196-208 [PMID: 27896858 DOI: 10.1111/tri.12896]

24 **Pungpapong S**, Aqel B, Leise M, Werner KT, Murphy JL, Henry TM, Ryland K, Chervenak AE, Watt KD, Vargas HE, Keaveny AP. Multicenter experience using simeprevir and sofosbuvir with or without ribavirin to treat hepatitis C genotype 1 after liver transplant. *Hepatology* 2015; **61**: 1880-1886 [PMID: 25722203 DOI: 10.1002/hep.27770]

25 **Sulkowski MS**, Vargas HE, Di Bisceglie AM, Kuo A, Reddy KR, Lim JK, Morelli G, Darling JM, Feld JJ, Brown RS, Frazier LM, Stewart TG, Fried MW, Nelson DR, Jacobson IM; HCV-TARGET Study Group. Effectiveness of Simeprevir Plus Sofosbuvir, With or Without Ribavirin, in Real-World Patients With HCV Genotype 1 Infection. *Gastroenterology* 2016; **150**: 419-429 [PMID: 26497081 DOI: 10.1053/j.gastro.2015.10.013]

26 **Pillai AA**, Wedd J, Norvell JP, Parekh S, Cheng N, Young N, Spivey JR, Ford R. Simeprevir and Sofosbuvir (SMV-SOF) for 12 Weeks for the Treatment of Chronic Hepatitis C Genotype 1 Infection: A Real World (Transplant) Hepatology Practice Experience. *Am J Gastroenterol* 2016; **111**: 250-260 [PMID: 26832650 DOI: 10.1038/ajg.2015.422]

27 **Yee BE**, Nguyen NH, Jin M, Lutchman G, Lim JK, Nguyen MH. Lower response to simeprevir and sofosbuvir in HCV genotype 1 in routine practice compared with clinical trials. *BMJ Open Gastroenterol* 2016; **3**: e000056 [PMID: 26966547 DOI: 10.1136/bmjgast-2015-000056]

28 **Langness JA**, Tabano D, Wieland A, Tise S, Pratt L, Harrington LA, Lin S, Ghuschcyan V, Nair KV, Everson GT. Curing Chronic Hepatitis C: A Cost Comparison of the Combination Simeprevir Plus Sofosbuvir vs. Protease-Inhibitor-Based Triple Therapy. *Ann Hepatol* 2017; **16**: 366-374 [PMID: 28425406 DOI: 10.5604/16652681.1235479]

29 **Dolatimehr F**, Karimi-Sari H, Rezaee-Zavareh MS, Alavian SM, Behnava B, Gholami-Fesharaki M, Sharafi H. Combination of sofosbuvir, pegylated-interferon and ribavirin for treatment of hepatitis C virus genotype 1 infection: a systematic review and meta-analysis. *Daru* 2017; **25**: 11 [PMID: 28427463 DOI: 10.1186/s40199-017-0177-x]

30 **Satsangi S**, Mehta M, Duseja A, Taneja S, Dhiman RK, Chawla Y. Dual treatment with sofosbuvir plus ribavirin is as effective as triple therapy with pegylated interferon plus sofosbuvir plus ribavirin in predominant genotype 3 patients with chronic hepatitis C. *J Gastroenterol Hepatol* 2017; **32**: 859-863 [PMID: 27624314 DOI: 10.1111/jgh.13595]

31 **Elsharkawy A**, Fouad R, El Akel W, El Raziky M, Hassany M, Shiha G, Said M, Motawea I, El Demerdash T, Seif S, Gaballah A, El Shazly Y, Makhlouf MA, Waked I, Abdelaziz AO, Yosry A, El Serafy M, Thursz M, Doss W, Esmat G. Sofosbuvir-based treatment regimens: real life results of 14 409 chronic HCV genotype 4 patients in Egypt. *Aliment Pharmacol Ther* 2017; **45**: 681-687 [PMID: 28070899 DOI: 10.1111/apt.13923]

32 **Del Bello D**, Cha A, Sorbera M, Bichoupan K, Levine C, Doyle E, Harty A, Patel N, Ng M, Gardenier D, Odin J, Schiano TD, Fierer DS, Berkowitz L, Perumalswami PV, Dieterich DT, Branch AD. Real-World Sustained Virologic Response Rates of Sofosbuvir-Containing Regimens in Patients Coinfected With Hepatitis C and HIV. *Clin Infect Dis* 2016; **62**: 1497-1504 [PMID: 26936665 DOI: 10.1093/cid/ciw119]

33 **Osinusi A**, Meissner EG, Lee YJ, Bon D, Heytens L, Nelson A, Sneller M, Kohli A, Barrett L, Proschan M, Herrmann E, Shivakumar B, Gu W, Kwan R, Teferi G, Talwani R, Silk R, Kotb C, Wroblewski S, Fishbein D, Dewar R, Highbarger H, Zhang X, Kleiner D, Wood BJ, Chavez J, Symonds WT, Subramanian M, McHutchison J, Polis MA, Fauci AS, Masur H, Kottilil S. Sofosbuvir and ribavirin for hepatitis C genotype 1 in patients with unfavorable treatment characteristics: a randomized clinical trial. *JAMA* 2013; **310**: 804-811 [PMID: 23982366 DOI: 10.1001/jama.2013.109309]

34 **Lawitz E**, Sulkowski MS, Ghalib R, Rodriguez-Torres M, Younossi ZM, Corregidor A, DeJesus E, Pearlman B, Rabinovitz M, Gitlin N, Lim JK, Pockros PJ, Scott JD, Fevery B, Lambrecht T, Ouwerkerk-Mahadevan S, Callewaert K, Symonds WT, Picchio G, Lindsay KL, Beumont M, Jacobson IM. Simeprevir plus sofosbuvir, with or without ribavirin, to treat chronic infection with hepatitis C virus genotype 1 in non-responders to pegylated interferon and ribavirin and treatment-naive patients: the COSMOS randomised study. *Lancet* 2014; **384**: 1756-1765 [PMID: 25078309 DOI: 10.1016/S0140-6736(14)61036-9]

35 **Sayiner M**, Wymer M, Golabi P, Ford J, Srishord I, Younossi ZM. Presence of hepatitis C (HCV) infection in Baby Boomers with Medicare is independently associated with mortality and resource utilisation. *Aliment Pharmacol Ther* 2016; **43**: 1060-1068 [PMID: 26991652 DOI: 10.1111/apt.13592]

36 **Norton BL**, Voils CI, Timberlake SH, Hecker EJ, Goswami ND, Huffman KM, Landgraf A, Naggie S, Stout JE. Community-based HCV screening: knowledge and attitudes in a high risk urban population. *BMC Infect Dis* 2014; **14**: 74 [PMID: 24512462 DOI: 10.1186/1471-2334-14-74]

37 **Zeremski M**, Dimova RB, Zavala R, Kritz S, Lin M, Smith BD, Zibbell JE, Talal AH. Hepatitis C virus-related knowledge and willingness to receive treatment among patients on methadone maintenance. *J Addict Med* 2014; **8**: 249-257 [PMID: 24820257 DOI: 10.1097/ADM.0000000000000041]

38 **Mauss S**, Böker K, Buggisch P, Christensen S, Hofmann WP, Schott E, Pfeiffer-Vornkahl H, Alshuth U, Hüppe D. Real-life experience with first generation HCV protease inhibitor therapy in Germany: The prospective, non-interventional PAN cohort. *Z Gastroenterol* 2015; **53**: 644-654 [PMID: 26167694 DOI: 10.1055/s-0034-1399383]

39 **Wehmeyer MH**, Ingiliz P, Christensen S, Hueppe D, Lutz T, Simon KG, Schewe K, Boesecke C, Baumgarten A, Busch H, Rockstroh J, Schmutz G, Kimhofer T, Berger F, Mauss S, Wiesch JSZ. Real-world effectiveness of sofosbuvir-based treatment regimens for chronic hepatitis C genotype 3 infection: results from the multicenter German hepatitis C cohort (GECCO-03). *J Med Virol* 2017; Epub ahead of print [PMID: 28710853 DOI: 10.1002/jmv.24903]

40 **Younossi ZM**, Otgonsuren M, Henry L, Arsalla Z, Stepnaova M, Mishra A, Venkatesan C, Hunt S. Inpatient resource utilization, disease severity, mortality and insurance coverage for patients hospitalized for hepatitis C virus in the United States. *J Viral Hepat* 2015; **22**: 137-145 [PMID: 24813350 DOI: 10.1111/jvh.12262]

41 **Galbraith JW**, Donnelly JP, Franco RA, Overton ET, Rodgers JB, Wang HE. National estimates of healthcare utilization by individuals with hepatitis C virus infection in the United States. *Clin Infect Dis* 2014; **59**: 755-764 [PMID: 24917659 DOI: 10.1093/cid/ciu427]

42 **Reau NS**, Jensen DM. Sticker shock and the price of new therapies for hepatitis C: Is it worth it? *Hepatology* 2014; **59**: 1246-1269 [PMID: 24493069 DOI: 10.1002/hep.27039]

43 **Andrieux-Meyer I**, Cohn J, de Araújo ES, Hamid SS. Disparity in market prices for hepatitis C virus direct-acting drugs. *Lancet Glob Health* 2015; **3**: e676-e677 [PMID: 26475012 DOI: 10.1016/S2214-109X(15)00156-4]

44 **Crittenden NE**, Buchanan LA, Pinkston CM, Cave B, Barve A, Marsano L, McClain CJ, Jones CM, Marvin MR, Davis EG, Kuns-Adkins CB, Gedaly R, Brock G, Shah MB, Rosenau J, Cave MC. Simeprevir and sofosbuvir with or without ribavirin to treat recurrent genotype 1 hepatitis C virus infection after orthotopic liver transplantation. *Liver Transpl* 2016; **22**: 635-643 [PMID: 26915588 DOI: 10.1002/lt.24422]

45 **Jackson WE**, Hanouneh M, Apfel T, Alkhouri N, John BV, Zervos X, Zein NN, Hanouneh IA. Sofosbuvir and simeprevir without ribavirin effectively treat hepatitis C virus genotype 1 infection after liver transplantation in a two-center experience. *Clin Transplant* 2016; **30**: 709-713 [PMID: 27019204 DOI: 10.1111/ctr.12738]

46 **Poveda E**, Wyles DL, Mena A, Pedreira JD, Castro-Iglesias A, Cachay E. Update on hepatitis C virus resistance to direct-acting antiviral agents.*Antiviral Res* 2014; **108**: 181-191 [PMID: 24911972

DOI: 10.1016/j.antiviral.2014.05.015]
47 **AASLD**. AASLD-IDSA. Recommendations for testing, managing, and treating hepatitis C. Available from: URL: http://www.hcvguidelines.org

P- Reviewer: Farshadpour F, Roohvand F **S- Editor**: Cui LJ
L- Editor: A **E- Editor**: Lu YJ

Published by **Baishideng Publishing Group Inc**
7901 Stoneridge Drive, Suite 501, Pleasanton, CA 94588, USA
Telephone: +1-925-223-8242
Fax: +1-925-223-8243
E-mail: bpgoffice@wjgnet.com
Help Desk: http://www.f6publishing.com/helpdesk
http://www.wjgnet.com